

**UNIVERSITA' DEGLI STUDI DI VERONA**

DEPARTMENT OF BIOTECHNOLOGY

*GRADUATE SCHOOL OF NATURAL SCIENCE AND ENGINEERING*

*DOCTORAL PROGRAM IN BIOTECHNOLOGY*

CYCLE XXX

PhD THESIS

**TRANSCRIPTOMIC AND BIOCHEMICAL APPROACHES TO UNRAVEL THE  
BASIS OF BACTERIAL VIRULENCE IN *Pseudomonas syringae* pv. *actinidiae***

S.S.D. AGR/12 Plant Pathology

Coordinator: Prof Massimo Delledonne

Tutor: Prof Annalisa Polverari

Co-tutor: Dr Elodie Vandelle

Co-tutor: PD Dr Ralf Heermann

Doctoral Student: Alice Regaiolo

*“Would you tell me, please, which way I ought to go from here?”*

*“That depends a good deal on where you want to get to,” said the Cat.*

*“I don’t much care where—” said Alice.*

*“Then it doesn’t matter which way you go,” said the Cat.*

*“—so long as I get SOMEWHERE,” Alice added as an explanation.*

*“Oh, you’re sure to do that,” said the Cat, “if you only walk long enough.”*

Lewis Carroll

### Dedication

This thesis is dedicated to the author's Grandmothers: Maria Mattana (1937-2015), Nonna Maria and Lucia Imoli (1932-2017), Nonna Lucia.

**UNIVERSITA' DEGLI STUDI DI VERONA**

DEPARTMENT OF BIOTECHNOLOGY

*GRADUATE SCHOOL OF NATURAL SCIENCE AND ENGINEERING*

*DOCTORAL PROGRAM IN BIOTECHNOLOGY*

CYCLE XXX

PhD THESIS

**TRANSCRIPTOMIC AND BIOCHEMICAL APPROACHES TO UNRAVEL THE  
BASIS OF BACTERIAL VIRULENCE IN *Pseudomonas syringae* pv. *actinidiae***

S.S.D. AGR/12 Plant Pathology

Coordinator: Prof Massimo Delledonne

Tutor: Prof Annalisa Polverari

Co-tutor: Dr Elodie Vandelle

Co-tutor: PD Dr Ralf Heermann

Doctoral Student: Alice Regaiolo



---

# Contents

## **Chapter 1: Introduction**

1. PLANT PATHOGEN BACTERIA
  2. THE QUORUM-SENSING MECHANISM IN GRAM NEGATIVE BACTERIA
    - 2.1 LuxR-type solo receptors
    - 2.2 QS virulence regulation network
    - 2.3 Biofilm regulation by QS
    - 2.4 Iron uptake and metabolism, a link with QS and virulence
  3. PLANT CHEMICAL SIGNAL(S) MIMIKING BACTERIAL QS SIGNALS
  4. *PSEUDOMONAS SYRINGAE PV. ACTINIDIAE*
    - 4.1 LuxR-type proteins in *Pseudomonas syringae pv. actinidiae*
- AIMS OF THE THESIS
- REFERENCES

## **Chapter 2: Microarray gene expression analysis of *Pseudomonas syringae pv. actinidiae* biovars**

1. ABSTRACT
2. INTRODUCTION
3. MATERIAL AND METHODS
  - 3.1 Chip design procedure
  - 3.2 Experimental design preparation
    - 3.2.1 Bacterial growth
    - 3.2.2 *hrp* Gene expression evaluation
  - 3.3 Evaluation of differential expressed genes by microarray analysis
4. RESULTS
  - 4.1 Evaluation for the conditions for Psa gene expression analysis
    - 4.1.1 Kinetic of bacterial growth
    - 4.1.2 *hrp* Gene expression evaluation
  - 4.2 Gene expression analysis of *Pseudomonas syringae* strains by microarray
    - 4.2.1 Statistical overview of the microarray data

---

4.2.2 Identification of differentially expressed genes among different strains and conditions: a general overview

4.2.3 Enrichment in functional categories among HIM-responsive genes in the different *Pseudomonas* strains

4.2.3.1 GO term enrichment among DEGs in CRA-FRU 8.43 (biovar 3)

4.2.3.2 GO term enrichment among DEGs in V-13 (biovar 3)

4.2.3.3 GO term enrichment among DEGs in J35 (biovar 1)

4.2.3.4 GO term enrichment among DEGs in KN2 (biovar 2)

4.2.3.5 GO term enrichment among DEGs in Pst DC3000

5. DISCUSSION

6. SUPPLEMENTAL RESOURCES

7. REFERENCES

8. ACKNOWLEDGEMENT

### **Chapter 3: The LuxR solos PsaR3 in *Pseudomonas syringae* pv. *actinidiae* biovar**

1. ABSTRACT

2. INTRODUCTION

3. MATERIAL AND METHODS

3.1 Bacterial strains

3.2 Bioinformatic analysis of PsaR3 LuxR solos

3.3 In vitro bacterial growth assay

3.4 Gene expression analysis by Real-time qPCR

3.5 Gene expression analysis by microarray

4. RESULTS

4.1 Characterization of PsaR3-encoding gene: localization and specificity

4.2 Evaluation of putative function of PsaR3 in Psa growth and in the expression of the genes belonging to its cluster

4.2.1 Psa growth kinetics

4.2.2 Targeted expression analysis of the genes belonging to PsaR3 cluster

4.2.2.1 Expression evaluation of the genes in sense orientation

4.2.2.2 Expression evaluation of the genes in antisense orientation

- 
- 4.3 Targeted expression analysis of PsaR1 and PsaR2 and genes involved in bacterial virulence
  - 4.4 Large-scale transcription profile analysis of CRA-FRU 10.22 wild type and  $\Delta$ *psaR3* mutant strains
    - 4.4.1 Statistical overview of the microarray data
    - 4.4.2 General overview of differential expressed genes in both strains
    - 4.4.3 Functional category enrichment in wild-type and  $\Delta$ *psaR3* mutant strains in the different conditions
  - 5. DISCUSSION
  - 6. SUPPLEMENTAL RESOURCES
  - 7. REFERENCES

**Chapter 4: Inter-kingdom signalling via PsaR3 between the kiwifruit pathogen *Pseudomonas syringae* pv. *actinidiae* and its host plant**

- 1. ABSTRACT
  - 2. INTRODUCTION
  - 3. MATERIAL AND METHODS
    - 3.1 Bacterial strains, culture conditions and constructs
    - 3.2 *cis*-acting elements analysis of the *citM* promoter region
    - 3.3 Luciferase assay
    - 3.4 Kiwifruit leaf extract HPLC separation and test
    - 3.5 Recombinant PsaR3 production and purification
      - 3.5.1 Cell culture
      - 3.5.2 Protein extraction
      - 3.5.3 Protein purification
    - 3.6 RNA-seq analysis to identify genes regulated by PsaR3
      - 3.6.1 Cell culture
      - 3.6.2 RNA extraction
      - 3.6.3 DNase treatment
      - 3.6.4 RNA-seq library preparation
  - 4. RESULTS
    - 4.1 Evaluation of the ability of PsaR3 to induce the *citM* promoter
-



---

4.2 Evaluation of the intergenic region as a putative bidirectional promoter and its responsiveness to PsaR3

4.3 Effect of different HPLC fraction of kiwifruit leaf extract on the activity of the “antisense” promoter region

4.4 Production and purification of the recombinant PsaR3

4.5 RNA-seq analysis to identify the transcriptomic profiles regulated by PsaR3

4.5.1 Statistical overview of the RNA-seq data

4.5.2 DEGs among the different condition tested a general overview

4.5.3 Functional enrichment analysis of the DEGs between PsaR3-dependet gene expression

4.5.4 Genomic islands, operons and *psaR3*-cluster modulation

5. DISCUSSION

6. SUPPLEMENTAL RESOURCES

7. REFERENCES

8. ACKNOWLEDGEMENT

## **Conclusions and future perspectives**

---

**List of abbreviations:**

AHLs= acyl-homoserine lactones  
DEGs= Differential expressed genes  
DFS= diffusible signal factor  
eDNA= external-DNA  
EPS= exopolysaccharides  
ETI= effector-trigger immunity  
FDR= false discovery rate  
GO= Gene ontology  
HIM= *hrp*-inducing media  
hpi= hours post inoculation  
HR= hypersensitive response  
Hrp= hypersensitive response and pathogenicity  
HTH= helix-turn-helix  
ICEs= integrative conjugative elements  
JA= jasmonic acid  
KB= King's B  
OD= optical density  
PAB= plant-associated bacteria  
PAIs= pathogenicity islands  
PCA= Principal component analysis  
Pip= proline imino-peptidase  
Psa= *Pseudomonas syringae* pv. *actinidae*  
PRRs= pattern-recognition receptors  
PTI= PAMP-trigger immunity  
QS= quorum-sensing  
SA= salicylic acid  
TCA= tricarboxylic acid  
TCS= two-component system  
TTSS= type III secretion system

# Chapter 1: Introduction

## 1. 1 PLANT PATHOGENIC BACTERIA

The main plant pathogen bacterial species belong to *Erwinia*, *Agrobacterium*, *Pseudomonas*, *Xanthomonas*, *Xylella*, *Streptomyces* genera. Phytopathogenic bacteria can enter into the host plant through natural openings such as stomata, lenticels and hydrotodes, fissures in the cuticular layer, mechanical wounding or through vectors, and can subsequently multiply in the intercellular spaces; or in the vascular tissue, causing disease, and several plant symptoms such as: leaf and fruit spots, canker, blights, vascular wilts, rots and tumours [1-4].

The pathogenicity factors developed by the plant pathogenic bacteria are: *i*) lytic enzymes such as pectinases, causing the soft rot; *ii*) phytotoxines acting in the competition with other organisms and in the pathogen fitness, *iii*) exopolysaccharides involving in the high-hygroscopic matrix development, useful during the pathogen epiphytic phase.

However, the most important feature of bacterial pathogenicity is the existence of the type three secretion system (TTSS), mainly characterised in *Pseudomonas syringae* spp. [5] and *Xanthomonas* spp.

The TTSS (Fig. 1) is involved in the elicitation of the plant defence mechanisms which lead the resistance in non-host or resistant host-plant often followed by the occurrence of the hypersensitive response (HR) which consists in a rapid cell death in the infection sites avoiding the pathogen spreads and pathogenesis in susceptible plants [6].

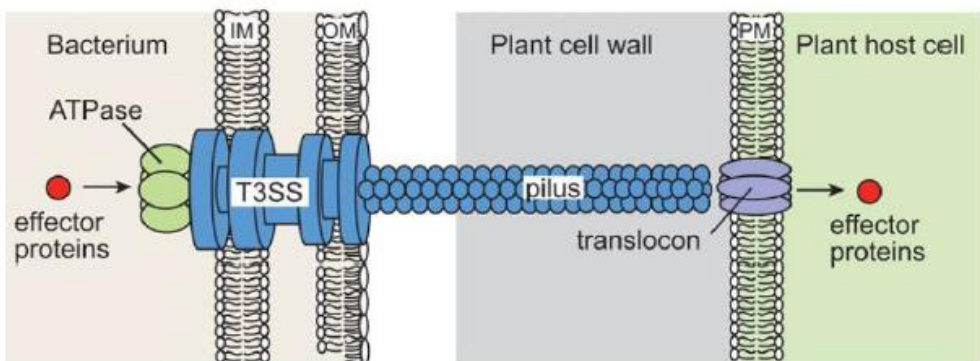


Figure 1: Representation of the type III secretion system (T3SS) [5].

TTSS is encoded by hypersensitive response and pathogenicity (*hrp*) genes and the main structural protein is encoding by *hrpA* in *Pseudomonas syringae* and *hprY* in *R. solanacearum* [7, 8].

The role of the TTSS consists in delivering effector proteins in the host which are involved in suppressing the host defence mechanism *i.e.*: PAMP-trigger immunity (PTI) and effector-triggered immunity (ETI); often mimicking or inhibiting the host cellular functions, and it has a key role in the bacterial virulence and parasitic life style [9]. Once *Pseudomonas syringae* enters in the host plant, bacterial PAMPs, such as flagellin, LPS, peptidoglycan, and elongation factor TU are recognized by pattern-recognition receptors (PRRs) eliciting the PTI. Pathogens overcome this defence by injecting effectors, through the TTSS. Plants can recognize the activity of one or more effectors via *R* genes eliciting the ETI (Fig 2).

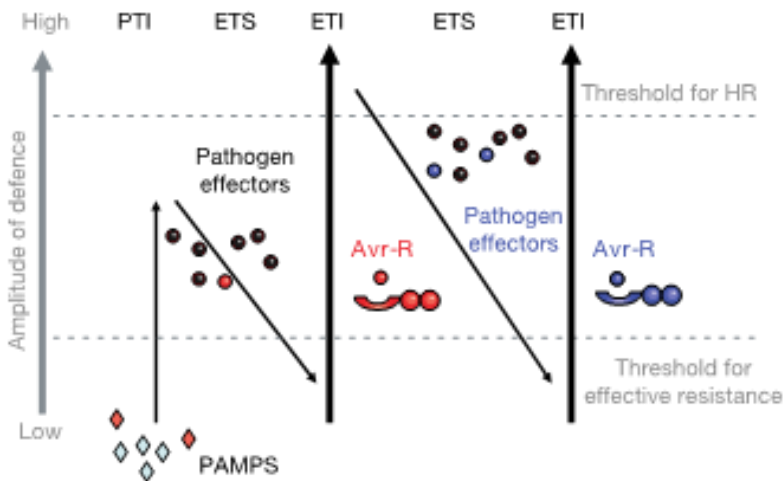


Figure 2: The “zigzag model” illustrates the quantitative output of the plant immune system. PTI= PAMP-trigger immunity, ETI= effector-triggered immunity, ETS= effector-triggered susceptibility, HR= hypersensitive response [12].

The continuous war of recognition and invasion between plants and pathogens has generated highly polymorphic repertoires of R proteins and effectors [10].

The first effectors were identified in various *Pseudomonas syringae* pathovars, as “Avr” proteins, *i.e.*: effectors specifically recognized by matching R proteins. Successively a giant repertoire of effectors was identified through bioinformatic analysis and functional screen of

Hrp promoters through a reporter gene and experimental validation tests based on their Hrp-outer protein (Hop) behaviour in translocation assays [11].

An active effector gene is associated to *cis*-acting elements containing Hrp-box in its promoter region which responds to HrpL alternative sigma factor [13].

Examples of effectors role include HopM effector of *Pseudomonas syringae* which targets the host protein involved in the vesicle transport [14] important for a successful bacterial colonization. AvrPtoB, HopE1, HoPG1, HopAM1, HopAA1 and HopN1 which enhance the growth of *Pseudomonas syringae* pv. *tomato* in *Nicotina benthamiana* and enhance the production of necrotic/clorotic disease lesion [15].

*Pseudomonas syringae* employs several virulence factors such as: HopD1, HopBB1 and HopW1 to suppress ETI [16], promote the host transcriptional repression [17] and disrupt the actin cytoskeleton of the host plant [18] respectively, to promote pathogen growth and virulence within its host.

Other virulence factors are involved in the phytotoxin production and secretion, such as the phytotoxin coronatine in *Pseudomonas syringae*, a chemical compound that mimics jasmonic acid (JA) [19] and represses the salicylic-acid (SA) resistance pathway.

Genes involved in bacterial pathogenicity are often localized in pathogenicity islands (PAIs) in the bacterial chromosome. These regions are characterized by a G+C content different from other portions of bacterial genome, suggesting an acquisition through horizontal gene transfer. Moreover, PAIs can also be localized in plasmids [20].

Plants have evolved two strategies to detect pathogens *i.e.*: a first layer of defense based on the recognition of conserved microbial elicitors, such as the bacterial flagellin, called pathogen-associated molecular patterns (PAMPs) or on perception of danger-associated molecular patterns (DAMPs) released during the pathogen infection (such as the cell wall components), through receptors proteins called pattern-recognition receptors (PRRs). The stimulation of the PRRs leads to PAMP-trigger immunity (PTI). A second layer of defense is more specifically activated by the recognition of pathogen virulence molecules called effectors through disease resistance receptors encoded by *R* genes, resulting in the effector-triggered immunity (ETI). PTI is generally involved in non-host resistance whereas ETI is effective against specific adapted pathogens [21]. A successful pathogen can suppress the PTI of the host plant, multiply and cause disease. Moreover, some environmental factors such as: high

humidity and warm temperatures are helpful for the pathogen to overcome the plant defence mechanisms [22].

## 1.2 THE QUORUM-SENSING MECHANISM IN GRAM NEGATIVE BACTERIA

The quorum-sensing (QS) is a cell-cell communication mechanism based on extracellular signalling molecules called autoinducers which enable bacteria to modify their behaviour in response to bacterial population density. Several processes are controlled by the QS such as: bioluminescence, virulence factors secretions and biofilm formation [23].

The QS in the Gram-positive bacteria is characterized by the secretion of oligopeptides sensed by a two-component system (TCS) which consists of a membrane-bound sensor kinase receptor and a cytoplasmic transcription factor that leads to gene expression [24], whereas the QS in Gram-negative bacteria is regulated by a LuxR-type receptors which detect autoinducers like acyl-homoserine lactones (AHLs) produced by LuxI-type synthase (**Fig 3**) and control the transcription of several genes or operons [25, 26].

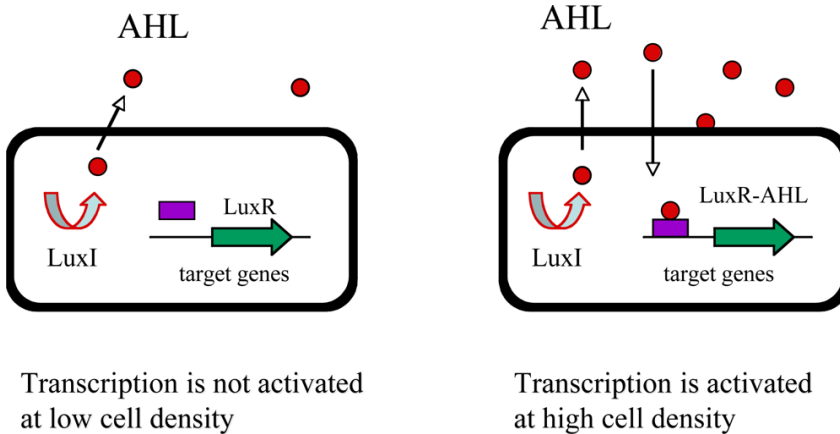


*Figure 3:* The LuxI/LuxR QS system in Gram-negative bacteria. The figure shows: LuxI synthase that synthesizes the signal molecule AHL (acyl-homoserine lactone). When AHLs reach a certain threshold, following the increase of cell density, they are sensed by the LuxR receptor, forming the complex LuxR-AHL which regulate the transcription of target genes [25].

The AHLs are the most common class of autoinducers with a *N*-homoserine lactone ring and a carbon acyl-chain that can vary in length (4-18). Some plant-associated bacteria produce atypical autoinducers such as: *cis*-11-methyl-2-dodecenoic acid from *Xanthomonas*

*campestris*, also known as a diffusible signal factor (DFS) that modulate its planktonic life style and biofilm formation [27]; 3-hydroxypalmitic-acid-methyl-ester (3-OH PAME) and (*R*)-methyl-3-hydroxymyristate ((*R*)-3-OH MAME) synthesized by PhcB a LuxI-type synthase of *Ralstonia solanacearum* [28].

The LuxR proteins are characterized by two functional domains: an amino-terminal ligand binding domain and a carboxy-terminal DNA-binding domain. LuxR receptors are generally stabilized in a dimerized form after binding to its cognate autoinducer. The complex LuxR-autoinducer recognizes and binds specific DNA-sites called *lux-box* situated up-stream of the target genes. Some LuxR proteins function as transcriptional repressors without the cognate autoinducer and release the binding with DNA following the autoinducer binding, allowing gene expression, as reported for instance for EsaR a LuxR-type protein of *Pantoea stewartii* [29]. Nowadays, four full-length LuxR-type-receptor structures have been solved: TraR from *Agrobacterium tumefaciens* [30] and *Rhizobium* spp. [31], QscR of *Pseudomonas aeruginosa* [32], CviR from *Chromobacterium violaceum* [33]. The binding pocket is often characterized by the presence of three highly conserved tryptophan residues and a combination of different amino acids that confer flexibility and allow the binding of a specific autoinducer [34]. More than half of LuxR-type proteins belong to the so called LuxR-solo class of transcription factors characterized by the absence of the cognate LuxI-type synthase and which can detect endogenous or exogenous autoinducers. One of the best characterized LuxR-solo receptor is QscR from *Pseudomonas aeruginosa*, which is involved to detect an autoinducer produced by *Burkholderia cepacia* [35].

Another class of QS regulator in Gram-negative bacteria, beside LuxR receptors, are the two-component membrane bound kinases that signal through phosphorylation to cytoplasmic transcription factors. The main studied examples are HAI-1, CAI-1 and AI-2 autoinducers detected by LuxN, CqsS, LuxQ respectively, from *Vibrio harvei* and *V. cholerae* [36].

The QS network consists in the interpretation of the extracellular chemical information and its conversion in gene expression changes is able to modify the bacterial behaviour. One of the main characterized canonical QS network is that of *Pseudomonas* spp. *Pseudomonas aeruginosa* which has two LuxI/R-type systems: LasI/LasR and RhlI/RhlR. LasR is situated at the top of the cascade, binds 3-oxo-C12-HLS and activates some downstream genes and *lasI*. The complex LasR-autoinducer activates also the expression of *rhIII* and *rhlR* which encode for a second QS pathways and *pqsR* gene which encode for the PqsR system [37].

---

QS controls the formation of the biofilm and the expression of virulence factors. For example, in *B. cenocepacia*, *cis*-2-dodecenoic acid (BDSF), a DFS-like autoinducer, binds to RpfR, a LuxR-type protein, causing a decrease of the cyclic dimeric guanosine monophosphate (c-di-GMP), a second message-signalling molecules, which affects the expression of virulence and motility genes and biofilm formation [38].

### 1.2.1 LuxR-type SOLO RECEPTORS

The LuxR-type solo receptors are LuxR-type proteins lacking the cognate LuxI-type synthase proteins. They consist of an AHLs binding site situated in the N-terminus and a DNA binding helix-turn-helix (HTH) motif at the C-terminus. Some of them respond to an exogenous AHLs or non-AHL endogenous inducer regulating some target genes. QscR, a LuxR-type solos protein of *Pseudomonas aeruginosa* respond to 3-oxo-C12-HLS, an endogenous AHLs and one of its role is preventing the premature expression of endogenous AHLs signal and virulence factors [39]. SidA of *Salmonella enterica* and *Escherichia coli* bind exogenous ALHs such as: 3-oxo-C8-HLS, 3-oxo-C4-HLs, 3-oxo-C10-HLS, and regulates some virulence factors increasing the transcription of cell division operon and increasing the resistance to diverse antibiotics [40].

Some LuxR-type solos have been found responsive to non-AHL endogenous molecules. PluR a LuxR-type protein from *Photothabdus luminescens* responds to  $\alpha$ -pyrones which are produced by an endogenous ketosynthase called PpyS regulating the cell-clumping as virulence mechanism [41].

Recently it has hypothesized that some LuxR solos derived from plant-associated bacteria (PAB) do not bind AHLs but could detect small signal molecules derived from plant [42]. These LuxR-type solo proteins differ from the LuxR-type proteins in one or two of the highly conserved amino-acids in the AHL-binding which likely leads to the binding with plant low molecular weight compound(s). Nowadays five members of this sub-family have been studied, *i.e.*: OryR from *Xanthomonas oryzae* pv. *oryzae*, XccR from *Xanthomonas campestris* pv. *campestris*, PsoR from *Pseudomonas fluorescens*, XagR from *Xanthomonas axonopodis* pv. *glycines* and NesR from *Sinorhizobium meliloti*. For OryR, there is some evidence of interaction with an uncharacterized compound(s) derived from rice macerate. Indeed, in presence of rice macerate, the recombinant OryR protein is soluble, and the quantity produced increases. Moreover, OryR regulate: the promoter of the neighbouring proline iminopeptidase



(*pip*) virulence gene, as well as swarming and swimming activities in presence of rice macerate [43]. It was observed that XccR mediates host interaction, likely recognising plant compound(s) and promoting the transcription of *pip* gene through binding in the *lux-box* present in the *pip*-promoter region facilitating the growth of the pathogen within its host [44]. PsoR was solubilized and able to activate a *luxbox*-containing promoter only in presence of plant macerate suggesting that plant compounds could be recognized by PsoR. Moreover, PsoR regulated genes that were important during the infection process like those involved in iron metabolism [45]. XagR differentially modulated the expression of genes involved in the infection process such as: proline imino-peptidase (*pip*) gene and adhesine (YapH-encoding gene), in response to plant molecule(s) [46]. The deletion mutant of NesR-encoding gene renders *S. meliloti* unable to survive under environmental and nutritional stressful conditions. Moreover, the mutant showed competitive disadvantage in nodulation compared to the wild type, suggesting a possible activity in plant-root exudate recognition [47].

### 1.2.2 QS VIRULENCE REGULATION NETWORK

Cell-cell communication systems allow the temporary expression of genes based on the bacterial density population such as those involved in the infection process, which requires a fast change in gene expression to coordinate crucial steps in pathogenesis or involved in response to diverse environmental stimuli. Several communication systems of phytopathogenic bacteria are coordinated by the LuxI/R QS [48].

In *Ralstonia solanacearum* the 3-OH-PAME system coordinate the transition from the early to late-stage of pathogenesis by controlling the activity of the PhcA-encoding gene, a global virulence regulator [28]. The 3-OH-PAME system is encoded by the *phc* operon which allows the expression of: PhcB (3-OH-PAME synthase), PhcS (membrane-bound sensor), PhcR (downstream response regulator). At low-cellular density level the expression of PhcA-encoding gene is inhibited, when the cell density reaches the concentration of about  $10^7$  cells, PhcS releases the repression on PhcA; then PhcA activate the expression of virulence factor required for the late-stage infection such as: exopolysaccharides (EPS) and cellulase production [49]. Moreover, PhcA represses the expression of the genes involved in the early-stage infection: TTSS, swimming motility and siderophore [50].

The cell-cell communication system of *Pectobacterium carotovorum* subsp. *carotovorum*, regulated by ExpI synthase and ExpR1 and ExpR2 receptors is responsible for the regulation

---

of genes encoding the TTSS-, plant-cell wall degradation enzymes- and antibiotic production [51].

*Xanthomonas campestris* possesses a cell-cell communication system that produces a diffusible signal factors (DFS) sensed by the two component RpfC/RpfG system, leading to the regulation of different mechanism such as: motility, toxin and oxidative stress resistance, aerobic respiration, biofilm formation, EPS production and iron uptake [52].

In *Pseudomonas syringae* the two-component system GacA/S controls the AhlRI/R (LuxI/R homologues) QS in combination with AefR-transcription regulator [53] (reported in Fig. 4 as example).

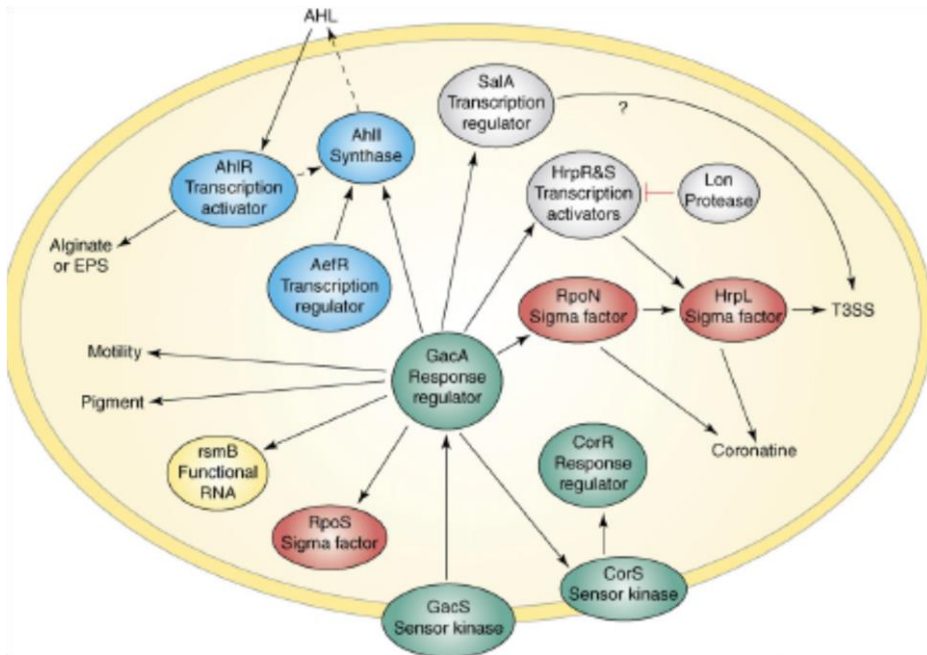


Figure 4: The global regulation system in *Pseudomonas syringae* pv. tomato is the GacA/S TCST system. GacA is known to directly or indirectly regulate QS (AhlR/AhlI system), TTSS through regulation of RpoN and HrpL sigma factors, coronatine production and pigmentation production [47].

Moreover, the GacA/S is directly or indirectly involved in the production of most known virulence factors of Ps such as: coronatine phytotoxin, EPS, expression of TTSS and its

effectors. Indeed, the GacA/S system is activated in the host apoplast by a combination of factors such as: low pH, osmolarity, sucrose or fructose sugars, and lack of complex nitrogen or carbon sources; and in turn GacA/S positively regulate the QS system which regulate the EPS-encoding gene expression [54].

### 1.2.3 BIOFILM REGULATION BY QS

The QS of *Pseudomonas aeruginosa* is involved in the regulation of biofilm formation. Indeed, the *lasI* (a LuxI-type synthase of *P. aeruginosa*) mutant showed a flat, homogenous biofilm which was sensitive to detergent treatment [55]. Moreover, the furanones, a AHL antagonist of LasR influence the biofilm production similar to that observed for the *lasI* mutant [56]. Rhamnolipid production is under the control of the QS system RhlI/R and affects the swarming and the biofilm development. Moreover, LecA and LecB, two QS-dependent carbohydrate-binding lectins could influence the biofilm formation by as a yet unclear mechanism [57]. QS of *P. aeruginosa* controls the iron-siderophore pyoverdine and mutants unable to produce this iron chelator were unable to develop biofilm [58]. PQS system (*P. aeruginosa* QS) is responsible for the production of external-DNA (eDNA) which interact with positively charged ESP-matrix (known be an important interaction for the initial scaffolding for the biofilm) [59].

The QS of *E. coli* regulates the flagellar synthesis and activity which influence the adhesion of the bacteria in different surfaces. In *Burkholderia pseudomallei* the QS regulate the biofilm attachment, structure and dispersal and accumulation of biofilm biomass [60].

There are diverse environmental parameters that influence the QS-mediated control of biofilm formation; *i.e.*: *i*) different carbon sources have dramatic effects on the QS contribution to biofilm formation in *P. aeruginosa*; *ii*) a role in played by pH: as AHLs are stable in neutral or acid pH, while at high pH the molecules can be reduced within minutes; *iii*) mass signal transfer: high flow rates allow a faster AHLs diffusion influencing the speed in of the response signal [61].

### 1.2.4 IRON UPTAKE AND METABOLISM, A LINK WITH QS AND VIRULENCE

Iron uptake is essential for bacteria as well as for many organisms and is involved as cofactor in different metabolic activities, such as the tricarboxylic acid (TCA) cycle, catalases

and cytochrome. Its uptake is strictly controlled because its high reactivity through the Fenton reaction can cause the production of dangerous reactive oxygen species.

The Gram-negative bacteria developed two strategies for iron ( $\text{Fe}^{3+}$ ) up-take under aerobic conditions: via uptake of heme or via uptake system or via siderophore [62]. It has been established that under iron limitation conditions, the plant pathogen *Pseudomonas syringae* produces pyoverdine [63] as a siderophore and that this is an important colonization factor for this pathogen. Moreover, pyoverdine is necessary for the synthesis of the toxin tabtoxin and AHLs, thus establishing a link between iron uptake, virulence and quorum sensing [64]. Another important siderophore compound recently suggested is citrate. Indeed, in the apoplast the  $\text{Fe}^{3+}$  is often associated to citrate, and it was reported that high concentration of  $\text{Fe}^{3+}$ -citrate can induce the expression of TTSS and virulence genes in *Pseudomonas syringae* pv. *tomato* [65]. Moreover, it was observed that the gene that encodes for a citrate transporter called *citN* in *Pseudomonas savastanoi* pv. *savastanoi* influenced the fitness of the pathogen within its host showing a link between iron uptake and pathogenesis [66]. Finally, it was established that under iron limiting condition alginate production and mucoidy increased in *P. aeruginosa* showing that iron availability can influence biofilm development [67].

### 1.3 PLANT CHEMICAL SIGNAL(S) MIMIKING BACTERIAL QS SIGNALS

Nowadays, there are evidences that pathogenic bacteria can recognize plant signal molecule(s) but none has been identified yet. Moreover, the identification of a communication mechanism between pathogen and its host, which trigger the pathogen virulence would be important to develop new control strategies. Plants have evolved the capacity to produce low-molecular weight compounds able to interfere with the bacterial AHLs-QS systems which interfere by acting as agonist or antagonist of the canonical bacterial AHLs [68]. Moreover, plants can recognize and respond to bacterial AHLs as indicated in *Medicago truncatula* which respond to AHLs produced by *S. meliloti* thus establish a symbiotic relationship [69].

Conversely, some bacterial AHLs are involved in plant hormone responses, especially regulating genes implicated in auxin and cytokinin synthesis, conditioning plant growth and development. Indeed, the C6-HLS decreases the concentration of cytokinin and auxin in treated *Arabidopsis thaliana* showing a developmental aberrant phenotype [70]. This mechanism seems AHLs specific because C8-HLS did not cause any alteration in the cytokinin or auxin levels [71], suggesting that plant could respond specifically and to different AHLs. Moreover,

AHLs seem to have a role in establishment of pathogenicity also when transgenically expressed in plants. Indeed, potato plants expressing *yenI*, a LuxI-type synthase of *Yersinia enterocolitica*, infected with *Pectobacterium carotovorum* (*Erwinia carotovora*) showed significantly higher disease severity than the controls, in an inoculum-concentration dependent manner [72]. Conversely, tobacco plants transformed with the same gene were less susceptible to *Pseudomonas syringae* pv. *tomato* DC3000 [73], suggesting that plants producing AHLs agonist might lead to pathogen confusion decreasing pathogenicity because they could stimulate a premature expression of virulence genes.

In *Pseudomonas syringae* pv. *syringae*, some plant molecules, not yet identified, are able to induce the biosynthesis of two lipodepsipeptide phytotoxins *i.e.*: by promote the expression of *syr* and *syp* genes which are under the control of the GacA/S two component system [74]. Other studies have shown that the *o*-coumaric acid and *t*-cinamic acid, two plant phenolic compounds, could regulate the TTSS gene of *Dickeya dadantii*, a causative agent of soft-rot, wilt and blight on several plant species [75].

#### **1.4 PSEUDOMONAS SYRINGAE PV. ACTINIDIAE**

*Pseudomonas syringae* pv. *actinidae* (Psa) is the causative agent of canker in kiwifruit. It is a Gram-negative bacterium, aerobic, that can grow epiphytically and endophytically on the plant foliage and enter into the plant through natural openings like stomata, through mechanical wounds and thought pollen dissemination [76]. Then, Psa can migrate systemically into the whole plant causing severe symptoms in kiwifruit, such as dark brown spots surrounded by yellow haloes on leaves, and cankers with copious reddish exudate on twigs and stem (Fig. 5) [77]. High humidity and cool temperature can promote the multiplication of this pathogen and increase the severity of plant disease.

Psa caused severe decline of kiwifruit production huge economic losses and even death of entire orchards [78] in the main productive countries such as China, New Zealand and Italy.

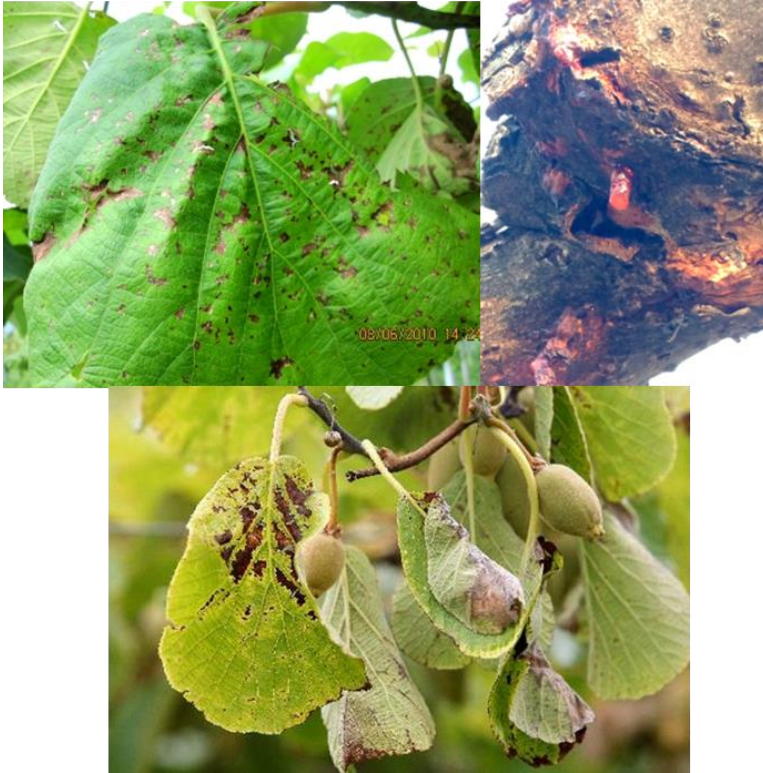


*Figure 5:* Symptoms of the canker in kiwifruit, the pictures were taken in an orchard in Verona in December 2014.

*Psa* is closely related to *Pseudomonas syringae* pv. *theae* [79] and it is divided in 5 different clades or biovars based on the country of origins, period of spread, biochemical characteristics and genomic evidence. The Biovar 1 includes strains isolated in Japan (1984) and Italy (1992). This biovar can synthesize phaseolotoxin thanks to the *argK-tox* gene cluster. Biovar 2 was isolated in South Korea in 1990 and can produce coronatine. Biovar 3 is responsible for the last world-wide outbreak occurred in New Zealand, Italy, Chile and Asia in 2010. The strains belonging to biovar 3 cannot produce phaseolotoxin or coronatine but they possess four putative clade-specific TTSS effectors: hop-H1, hop-Z5, hopAM1-2 and hopAA1-2. Biovar 4 was recently re-classified as a new pathovar *actinidifoliorum* (Pfm) on the basis of phenotypic

and phylogenetic differences [80]. Biovar 5 and 6 were found in specific and limited areas in Japan in 2015 and 2016 [81] (Fig. 6).

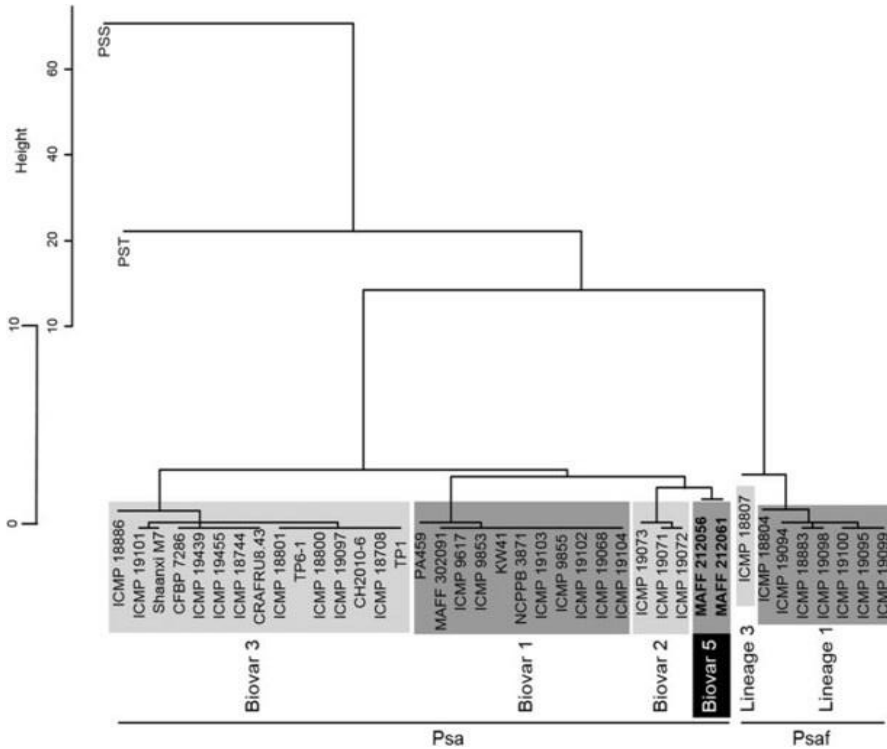


*Figure 6:* Phylogenetic tree of the five *Ps. actinidiae* biovars. *Psa* “biovar 4” has been transferred to the new pathovar *actinidifoliorum* (*Psaf*) with 3 lineages (1 to 3). *Ps. syringae* B728a (*PSS*) and *Ps. tomato* DC3000 (*PST*) were used as outgroups [80].

The *Psa* genome includes a set of genes useful for the fitness of the pathogen within its host and for the competition with other microorganisms, such as a pyoverdine-encoding gene, an efficient system for iron up-take, considered an important virulence factor. *Psa* also contains genes involved in detoxification of nitric oxide in the host plant, an important signal of plant defence [82, 83, 84]. Moreover, the different biovars contain important genomic variations such as the presence or not of plasmids, carrying pathogenicity islands (PAIs), considered

important determinants of pathogen virulence. The biovar 3, as opposite to the biovar 1 and 2, does not contain the genomic cluster encoding phaseolotoxin and coronatine, but has acquired a plasmid of 160 kb, probably involved in Psa pathogenicity on different Actinidia species [84].

The identification of biovar-specific set of genes could explain the different Actinidia specificity of the different Psa biovars. The three principal Psa biovars, *i.e.*: biovar 1, 2 and 3 despite their genomic differences are able to infect and growth in the Actinidia species assuming that there is a genomic core shared among the biovars which is responsible for the bacterial pathogenicity [82]. However, the biovar 3 which is characterized by a higher virulence.

#### **1.4.1 LuxR-type PROTEINS IN *Pseudomonas syringae* pv. *actinidiae***

QS plays an important role in gene and virulence regulation in plant pathogenic bacteria. However, Psa does not produce AHLs as autoinducer and the complete LuxI/R QS is absent in Psa strains [85]. It was established that Psa possesses three putative LuxR-type solos protein namely: PsaR1, PsaR2 and PsaR3 that could detect exogenous signals. Moreover, a bioinformatics analysis revealed that PsaR2 likely belongs to the subfamily of LuxR-type solos found in the plant-associated bacteria (PAB) which have some evidence to bind an uncharacterized plant signal(s) [85].

PsaR1 and PsaR3 are similar to LuxR-type protein associated to QS in other species, suggesting that these two putative receptors could detect also AHLs signal.

Preliminary studies on PsaR solos were performed through *psaR* mutant characterization. Mutants of PsaR-encoding genes showed a decreased growth *in planta* in comparison to the wild-type (**Fig. 7**) suggesting a possible role of these putative LuxR solos in the growth and multiplication of the pathogen within its host, probably mediating pathogen virulence. Moreover, the PsaR3-encoding gene seems involved in the regulation of bacterial motility and lipase production, as the corresponding mutant showed either a reduced lipase secretion or motility in comparison to the wild-type or the *psaR2* or *psaR1* mutants [85].



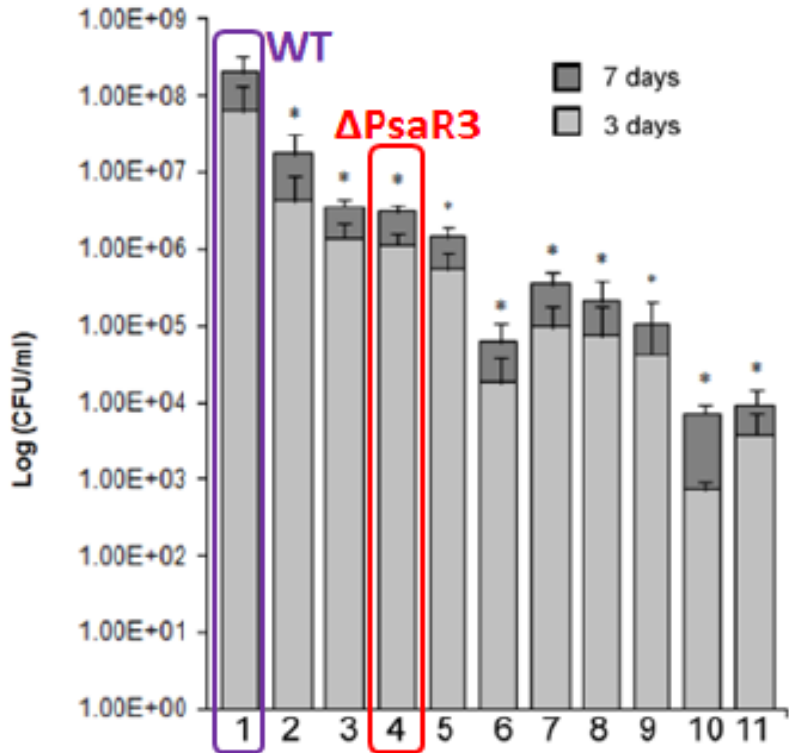


*Figure 7: Psa growth in planta. In position 1 and 4 are highlighted the wild-type and the  $\Delta psar3$  mutant, while the  $\Delta psar1$  and  $\Delta psar2$  mutant are in position 2 and 3, respectively. More in detail: 1= Psa wild-type, 2= Psa mutR1, 3= Psa mutR2, 4= Psa mutR3, 5= Psa mutR1+pBBR-*psaR1*, 6= Psa mutR2+pBBR-*psaR2*, 7= Psa mutR3+pBBR-*psaR3*, 8= Psa mutR1+Psa mutR3, 9= Psa mutR2+Psa mutR3, 10= Psa mutR1+Psa mutR3+p*cospsaR3*+pBBR-*psaR1*, 11= Psa mutR2+Psa mutR3+p*cospsaR3*+pBBR-*psaR2* [85].*

**AIMS OF THE THESIS**

The aims of the PhD research project were: i) identification of Psa genes and pathways involved in Psa aggressiveness. To this aim, we evaluated gene expression profiles of three different Psa biovars (biovar 1, 2 and 3), grown in two different conditions *i.e.*: a rich medium and a minimal medium mimicking in planta conditions, using the microarray technique; ii) a targeted study of the role of LuxR solo PsaR3 in Psa communication, in particular with the kiwifruit plant.

To this aim, the first objective was the identification of the transcripts regulated by PsaR3 through a comparative gene expression analysis between the Psa biovar 3 wild type strain and the  $\Delta psar3$  mutant. The experiment was performed using the microarray technique in different growing conditions. Moreover, to elucidate better the transcriptional regulation role of this protein and the pathway(s) influenced by PsaR3, we performed a RNA-seq analysis on a strain of Psa over-expressing *psar3*.

The last objective was to identify possible PsaR3-responding promoters, in particular of genes located, within the identified PsaR3 cluster, to elucidate if PsaR3 could promote the transcription of the genes in the cluster in both orientations and moreover, if PsaR3 could be involved in the responsiveness of Psa to the perception of the host plant. Finally, we used a PsaR3-responsive promoter as a marker in the attempt to identify the kiwifruit signal molecule(s) possibly recognized or transduced through PsaR3, to promote or repress the transcription of target genes.

---

**REFERENCES**

- 1** Hirano, S. S. and Upper, D. C. (2000) Bacteria in the leaf ecosystem with emphasis on *Pseudomonas syringae* a pathogen, ice nucleus, and epiphyte. *MMBR*, doi: 10.1128/MMBR.64.3.624-653.2000
- 2** Mansvelt, E. L. and Hattingh, M. J. (1987) Scanning electron microscopy of colonization of pear leaves by *Pseudomonas syringae* pv. *syringae*. *Can. J. Bot.* 65:2517–22
- 3** van der Wolf, J. M. *et al.* (2013) Flower infection of *Brassica oleracea* with *Xanthomonas campestris* pv. *campestris* results in high levels of seed infection. *Eur. J. Plant Pathol* 136:103–11
- 4** Chatterjee, S. *et al.* (2008). Living in two worlds: the plant and insect lifestyles of *Xylella fastidiosa*. *Annu. Rev. Phytopathol*, doi: 10.1146/annurev.phyto.45.062806.094342
- 5** Crabill, E. (2012). The *Pseudomonas syringae* type III secretion system: the translocator proteins, their secretion, and the restriction of translocation by the plant immune system. Dissertations and Theses in Biological Sciences. Retrieved from <http://digitalcommons.unl.edu/bioscidiss>
- 6** Chang, J. H. *et al.* (2003) Wake of the flood: ascribing functions to the wave of type III effector proteins of phytopathogenic
- 9** Wei, W. *et al.* (2000) The gene coding for the Hrp pilus structural protein is required for type III secretion of Hrp and Avr proteins in *Pseudomonas syringae* pv. *tomato*. *PNAS*, doi: 10.1073/pnas.040570097
- 10** Valls, M. *et al.* (2006) Integrated Regulation of the Type III Secretion System and Other Virulence Determinants in *Ralstonia solanacearum*. *Plos Pathogen*, doi: 10.1371/journal.ppat.0020082
- 11** Grant, R. S. *et al.* (2006) Subterfuge and manipulation: Type III effector Proteins of phytopathogenic bacteria. *Annual Review of Microbiology*, doi: 10.1146/annurev.micro.60.080805.142251
- 12** Jones, J. D. G. and Dangl, J. L. (2006) The plant immune system. *Nature Reviews*, doi: 10.1038/nature05286
- 13** Lindeberg, M. *et al.* (2006) Closing the circle on the discovery of genes encoding Hrp regulon members and type III secretion system effectors in the genomes of three model *Pseudomonas syringae* strains. *Mol Plant Microbe Interact*, doi: 10.1094/MPMI-19-1151

- 14** Lindeberg, M. *et. al* (2012) *Pseudomonas syringae* type III effector repertoires: last word in endless argument. *Cell Press*, doi: 10.1016/j.tim.2012.01.003
- 15** Ferreira, A.O. *et al.* (2006) Whole-genome expression profiling defines the HrpL regulon of *Pseudomonas syringae* pv. *tomato* DC3000, allows de novo reconstruction of the Hrp cis element, and identifies novel co-regulated gene. *Mol Plant Microbe Interact*, doi: 10.1094/MPMI-19-1167
- 16** Mackey, D. *et. al.* (2003) Arabidopsis RIN4 is a target of the type III virulence effector AvrRpt2 and modulates RPS2-mediated resistance. *Cell*, doi: 10.1016/S0092-8674(03)00040-0
- 17** Kay, S. *et. al* (2007) A bacterial effector acts as a plant transcription factor and Induces a cell size regulator. *Science*, doi: 10.1126/science.1144956
- 18** Block, A. *et. al.* (2014) The *Pseudomonas syringae* type III effector HopD1 suppresses effector-triggered immunity, localizes to the endoplasmic reticulum, and targets the Arabidopsis transcription factor NTL9. *New Phytol*, doi: 10.1111/nph.12626
- 19** Yang, L. *et. al.* (2017) *Pseudomonas syringae* Type III Effector HopBB1 promotes host transcriptional repressor degradation to regulate phytohormone responses and virulence. *Cell Host Microbe*, doi: 10.1016/j.chom.2017.01.003
- 20** Kang, Y. *et. al.* (2014) HopW1 from *Pseudomonas syringae* disrupts the actin cytoskeleton to promote virulence in Arabidopsis. *Plos Patho*, doi: 10.1371/journal.ppat.1004232
- 21** Zheng X. *et. al.* (2012) Coronatine promotes *Pseudomonas syringae* virulence in plants by activating a signaling cascade that inhibits salicylic acid accumulation. *Cell Host Microbe*, doi: 10.1016/j.chom.2012.04.014
- 21** Büttner, D. and Bonas, U. (2002) Getting across—bacterial type III effector proteins on their way to the plant cell. *EMBO*, doi: 10.1093/emboj/cdf536
- 22** Dodds, P. N. and Rathjen, J. P. (2010) Plant immunity: towards an integrated view of plant–pathogen interactions. *Nature review*, doi: 10.1038/nrg2812
- 23** Rutherford, S. T. and Bassler, B. L. (2012) Bacterial quorum sensing: its role in virulence and possibilities for its control, CSH perspectives, doi: 10.1101/cshperspect.a012427
- 24** Bassler, B. L. and Losick, R. (2006) Bacterially speaking. *Cell*, doi: 10.1016/j.cell.2006.04.001
- 25** Fuqua, C. & Greenberg, E. P. (2002). Listening in on bacteria: acylhomoserine lactone signalling. *Nat Rev Mol Cell Biol*, doi: 10.1038/nrm907

- 26** Li, Y. and Tian, X. (2012) Quorum sensing and bacterial interaction in biofilms. *Sensors*, doi: 10.3390/s120302519
- 27** Tao, F. *et al.* (2010) Quorum sensing modulation of a putative glycosyltransferase gene cluster essential for *Xanthomonas campestris* biofilm formation. *Environ Microbiol*, doi: 10.1111/j.1462-2920.2010.02288.x
- 28** Flavier, A. B. *et al.* (1997) Identification of 3-hydroxypalmitic acid methyl ester as a novel autoregulator controlling virulence in *Ralstonia solanacearum*. *Mol Microbiol*, doi: 10.1046/j.1365-2958.1997.5661945.x
- 29** von Bodman, S. B. *et al.* (1998) A negative regulator mediates quorum-sensing control of exopolysaccharide production in *Pantoea stewartii* subsp. *stewartii*. *PNAS*, doi: Vol. 95, pp. 7687–7692
- 30** Zhang, R. G. *et al.* (2002) Structure of a bacterial quorum-sensing transcription factor complexed with pheromone and DNA. *Nature*, doi: 10.1038/nature00833
- 31** Chen, G. *et al.* (2007) Structural basis for antiactivation in bacterial quorum sensing. *PNAS*, doi: 10.1073/pnas.0704843104
- 32** Lintz, M. J. *et al.* (2011) Crystal structure of QscR, a *Pseudomonas aeruginosa* quorum sensing signal receptor. *PNAS*, doi: 10.1073/pnas.1112398108
- 33** Chen G, *et al.* (2011) A strategy for antagonizing quorum sensing. *Mol Cell*, doi: 10.1016/j.molcel.2011.04.003
- 34** Li, Z. and Nair, S. K. (2012) Quorum sensing: how bacteria can coordinate activity and synchronize their response to external signals? *Protein Sci* doi: 10.1002/pro.2132
- 35** Riedel, K. *et al.* (2001) N-acylhomoserine-lactone-mediated communication between *Pseudomonas aeruginosa* and *Burkholderia cepacia* in mixed biofilms. *Microbiology*, doi: 10.1099/00221287-147-12-3249
- 36** Ng, W. L. and Bassler B. L. (2009) Bacterial quorum-sensing network architectures. *Annu Rev Genet*. doi: 10.1146/annurev-genet-102108-134304
- 37** Winson, M. K. *et al.* (1995) Multiple N-acyl-L-homoserine lactone signal molecules regulate production of virulence determinants and secondary metabolites in *Pseudomonas aeruginosa*. *PNAS*, 92(20): 9427–9431
- 38** Deng, Y. *et al.* (2012) Cis-2-dodecenoic acid receptor RpfR links quorum-sensing signal perception with regulation of virulence through cyclic dimeric guanosine monophosphate turnover. *PNAS*, doi: 10.1073/pnas.1205037109
-

- 39** Lequette, Y. et. al. (2006). A distinct QscR regulon in the *Pseudomonas aeruginosa* quorum-sensing circuit. *J Bacteriol*, doi: 10.1128/JB.188.9.3365-3370.2006
- 40** Lindsay, A. and Ahmer, B. M. (2005). Effect of sdiA on biosensors of N-acylhomoserine lactones. *J Bacteriol*, doi: 10.1128/JB.187.14.5054-5058.2005
- 41** Brameyer S. et al. (2014) Dialkylresorcinols as bacterial signaling molecules. *PNAS*, doi: 10.1073/pnas.1417685112
- 42** Gonzalez, J. E. and Marketon, M. M.(2003). Quorum sensing in nitrogen-fixing rhizobia. *Microbiol.Mol.Biol.Rev.* doi:10.1128/MMBR.67.4.574-592.2003
- 43** Ferluga, S. et. al. (2007). A LuxR homologue of *Xanthomonas oryzae* pv. *oryzae* is required for optimal rice virulence. *Mol. Plant Pathol.*, doi:10.1111/j.1364-3703.2007.00415.x
- 44** Zhang, L. et. al. (2007). A proline iminopeptidase gene up-regulated in planta by a LuxR homologue is essential for pathogenicity of *Xanthomonas campestris* pv. *campestris*. *Mol.Microbiol*, doi:10.1111/j.1365-2958.2007.05775.x
- 45** Subramoni, S. et al. (2011) Bacterial subfamily of LuxR regulators that respond to plant compounds. *Appl.Environ.Microbiol*, doi:10.1128/AEM.00183-11
- 46** Chatnapat, T. et. al. (2012) XagR, a LuxR homolog, contributes to the virulence of *Xanthomonas axonopodis* pv. *glycines* to Soybean. *Mol. Plant Microbe Interact.* doi:10.1094/MPMI-01-12-0008-R
- 47** Patankar, A.V. and Gonzalez, J. E. (2009) An orphan LuxR homolog of *Sinorhizobium meliloti* affects stress adaptation and competition for nodulation. *Appl. Environ. Microbiol.*, doi:10.1128/AEM.01692-08
- 48** Grant, S. R et. al (2007) Global virulence regulation networks in phytopathogenic bacteria. *Trends in Microbiology*, doi: 10.1016/j.tim.2007.06.005
- 49** Huang, J. et al. (1998) Joint transcriptional control of xpsR, the unusual signal integrator of the *Ralstonia solanacearum* virulence gene regulatory network, by a response regulator and a LysR-type transcriptional activator. *J. Bacteriol.* 180, 2736–2743
- 50** Genin, S. et al. (2005) Control of the *Ralstonia solanacearum* Type III secretion system (Hrp) genes by the global virulence regulator PhcA. *FEBS Lett.* doi: 10.1016/j.febslet.2005.02.058
- 51** Sjoblom, S. et al. (2006) Cooperation of two distinct ExpR regulators controls quorum sensing specificity and virulence in the plant pathogen *Erwinia carotovora*. *Mol. Microbiol*, doi: 10.1111/j.1365-2958.2006.05210.x

- 52** Romling, U. and Amikam, D. (2006) Cyclic di-GMP as a second messenger. *Curr. Opin. Microbiol*, doi: 10.1016/j.mib.2006.02.010
- 53** Quinones, B. *et al.* (2005) Quorum sensing regulates exopolysaccharide production, motility, and virulence in *Pseudomonas syringae*. *Mol. Plant Microbe Interact.* doi: 10.1094/MPMI-18-0682
- 54** Chatterjee, A. *et al.* (2003) GacA, the response regulator of a two component system, acts as a master regulator in *Pseudomonas syringae* pv. *tomato* DC3000 by controlling regulatory RNA, transcriptional activators, and alternate sigma factors. *Mol. Plant Microbe Interact.* doi: 10.1094/MPMI.2003.16.12.1106
- 54** Davies, D. G. *et al.* (1998) The involvement of cell-to-cell signals in the development of a bacterial biofilm. *Science*, Apr 10;280(5361):295-8
- 55** Davey, M. E. *et al.* (2003) Rhamnolipid surfactant production affects biofilm architecture in *Pseudomonas aeruginosa* PAO1. *J. Bacteriol*, doi: 10.1128/JB.185.3.1027-1036.2003
- 56** Tielker, D. *et al.* (2005) *Pseudomonas aeruginosa* lectin LecB is located in the outer membrane and is involved in biofilm formation. *Microbiology*, doi: 10.1099/mic.0.27701-0
- 57** Allesen-Holm, M. *et al.* (2006) Tolker-Nielsen, T. A characterization of DNA release in *Pseudomonas aeruginosa* cultures and biofilms. *Mol. Microbiol*, doi: 10.1111/j.1365-2958.2005.05008.x
- 59** Jennings, L. K. *et al.* (2015) Pel is a cationic exopolysaccharide that cross-links extracellular DNA in the *Pseudomonas aeruginosa* biofilm matrix. *PNAS*, doi: 10.1073/pnas.1503058112
- 60** Gamage, A. M. *et al.* (2011) N-octanoylhomoserine lactone signalling mediated by the bpsI-bpsR quorum sensing system plays a major role in biofilm formation of *Burkholderia pseudomallei*. *Microbiology*, doi: 10.1099/mic.0.046540-0
- 61** Passos da Silva, D. *et al.* (2017) An update on the sociomicrobiology of Quorum Sensing in Gram-negative biofilm development. *Pathogens*, doi: 10.3390/pathogens6040051
- 62** Cornelis, P. (2010) Iron uptake and methabolism in pseudomonads. *Appl Microbiol Biotechnol* (2010) 86: 1637 doi: org/10.1007/s00253-010-2550-2
- 63** Loper, J. E. and Buyer, J. S. (1991) Siderophores in microbial interaction on plant surfaces. *Molec. Plant. Microb. Inter.*, vol.4 n.1 pp-5-13
-

- 64** Taquichi, F. et. al. (2010) The siderophore pyoverdine of *Pseudomonas syringae* pv. *tabaci* 6605 is an intrinsic virulence factor in host tobacco infection. *J. Bacteriol*, doi: 10.1128/JB.00689-09
- 65** Jones, A. M, and Wildermuth M. C. (2011), The phytopathogen *Pseudomonas syringae* pv. *tomato* DC3000 has three high-affinity iron-scavenging systems functional under iron limitation conditions but dispensable for pathogenesis. *J. Bacteriol*, doi: 10.1128/JB.00069-10
- 66** Matas, M. I. et. al. (2012) Identification of novel virulence genes and metabolic pathways required for full fitness of *Pseudomonas savastanoi* pv. *savastanoi* in olive (*Olea europaea*) knots. *New Phytologist*, DOI: 10.1111/j.1469-8137.2012.04357.x
- 67** Banin, E. et. al. (2005), Iron and *Pseudomonas aeruginosa* biofilm formation. *PNAS*, doi: 10.1073/pnas.0504266102
- 68** Patel, H. K. et. al. (2013), Bacterial LuxR solos have evolved to respond to different molecules including signals from plants. *Front. Plant Sci.*, doi: 10.3389/fpls.2013.00447
- 69** Mathesius, U. et. al. (2003) Extensive and specific responses of a eukaryote to bacterial quorum-sensing signals. *PNAS*, doi: 10.1073/pnas.262672599
- 70** von Rad, U. et. al. (2008) Response of *Arabidopsis thaliana* to N-hexanoyl-DL-homoserine-lactone, a bacterial quorum sensing molecule produced in the rhizosphere. *Planta*, doi: 10.1007/s00425-008-0811-4
- 71** You, Y. S. et. al. (2006) Use of bacterial quorum-sensing components to regulate gene expression in plants. *Plant Physiol*, doi: 10.1104/pp.105.074666
- 72** Toth, I. K. et. al. (2004) Potato plants genetically modified to produce N-acylhomoserine lactones increase susceptibility to soft rot erwiniae. *Mol. Plant-Microbe Interact*, doi: 10.1094/MPMI.2004.17.8.880
- 73** Shaw, P. D. et. al. (1997) Detecting and characterizing N-acylhomoserine lactone signal molecules by thin-layer chromatography. *PNAS*, Vol. 94, pp. 6036 – 604
- 74** Wang, N. et. al. (2006) The expression of genes encoding lipodepsipeptide phytotoxins by *Pseudomonas syringae* pv. *syringae* is coordinated in response to plant signal molecules. *Mol. Plant-Microbe Interact*, doi; 10.1094/MPMI-19-0257
- 75** Yang, S. et. al. (2008) Type III secretion system genes of *Dickeya dadantii* 3937 are induced by plant phenolic acids. *PLoS ONE*, doi: 0.1371/annotation/91170966-226f-4678-999e-22f2c4a6bb8d



- 76** Balestra, G. M. *et al.* (2009) Current status of bacterial spread on kiwifruit in Italy. *CSIRO*, 4, 34–36
- 77** Scorichini, M. *et al.* (2012) *Pseudomonas syringae* pv. *actinidiae*: a re-emerging, multi-faceted, pandemic pathogen. *Molecular Plant Pathology*, doi: 10.1111/j.1364-3703.2012.00788.x
- 78** Vanneste, J. L. (2012) *Pseudomonas syringae* pv. *actinidiae* (Psa): a threat to the New Zealand and global kiwifruit industry. *New Zealand Journal of Crop and Horticultural Science*, doi: 10.1080/01140671.2012.736084
- 79** Mazzaglia, A. (2012) *Pseudomonas syringae* pv. *actinidiae* (PSA) Isolates from Recent Bacterial Canker of Kiwifruit Outbreaks Belong to the Same Genetic Lineage. *PLoS ONE*, doi: 10.1371/journal.pone.0036518
- 80** Zupeng, W. *et al.* (2017) Whole transcriptome sequencing of *Pseudomonas syringae* pv. *actinidiae*-infected kiwifruit plants reveals species-specific interaction between long non coding RNA and coding genes. *Scientific Report*, 7: 4910, doi: 10.1038/s41598-017-05377-y
- 81** Takashi, F. and Hiroyuki, S. (2106) Genome analysis of the kiwifruit canker pathogen *Pseudomona syringae* pv. *actinidiae* biovar 5. *Scientific Report*, 6:21399, doi: 10.1038/srep21399
- 82** Marcelletti, S. *et al.* (2011) *Pseudomonas syringae* pv. *actinidiae* draft genomes comparison reveal strain-specific features involved in adaptation and virulence to *Actinidia* species. *PLoS ONE*, doi: 10.1371/journal.pone.0027297
- 83** Delledonne, M. *et al.* (1998) Nitric oxide functions as a signal in plant disease resistance. *Nature*, doi: 10.1038/29087
- 84** McCann, H. C. *et al.* (2013) Genomic Analysis of the Kiwifruit Pathogen *Pseudomonas syringae* pv. *actinidiae* Provides Insight into the Origins of an Emergent Plant Disease. *PLoS Pathogens*, doi: 10.1371/journal.ppat.1003503
- 85** Patel, H. K. *et al.* (2014), The Kiwifruit Emerging Pathogen *Pseudomonas syringae* pv. *actinidiae* Does Not Produce AHLs but Possesses Three LuxR Solos. *Plos One*, DOI: 10.1371/journal.pone.0087862

# **Chapter 2: Microarray gene expression analysis of *Pseudomonas syringae* pv. *actinidiae* biovars**

## **1. ABSTRACT**

In 2010 a world-wide spread of *Pseudomonas syringae* pv *actinidiae* (Psa) was recorded. In particular, New Zealand and Italy, the two most productive countries for kiwifruit, reported huge economic losses. Knowledge of the pathogen population and its characteristics is necessary to better understand the disease and to develop new control strategies. Psa strains are divided into 5 different biovars detected in various countries of origin based on genetic and biological traits, and out-breaks period. Genomic information about this pathogen increased during the last 5 years thanks to a massive sequencing effort on different Psa strains collected around the world, thus allowing a better understanding of the origin of both the pathogen and the disease.

To investigate the molecular bases of Psa virulence in the different biovars, we performed a gene expression analysis, using a multi-strain custom microarray chip encompassing on the three main known biovars (1, 2 and 3) designed in our laboratory and manufactured by Agilent (Design ID: 078853). The microarray was used to compare gene expression profiles across different strains grown in rich medium or in minimal medium, mimicking the apoplastic conditions, and assayed after 4 and 8 hours of growth. This analysis can help clarifying the differences in virulence observed among the biovars and to assisting the design of new control strategies.

## **2. INTRODUCTION**

Actinidia is an economically important crop cultivated worldwide. Its fruit, the kiwifruit, is highly appreciated for its high nutritional properties, it is rich in vitamins of the C, K and E groups, in fibres, and in important salts such as: manganese and potassium. However, the worldwide spread of the kiwifruit canker disease caused huge economic losses, in particular in Italy and New Zealand which are among the largest producer countries. The present sever outbreaks of the disease are caused by *Pseudomonas syringae* pv. *actinidiae* (Psa) a Gram-negative phythopathogenic bacterium diffused in all growing areas. Psa strains

are classified into 5 different biovars based on genetic and biological traits, including virulence diversity and toxin production. In particular, the biovar 1, includes the first identified strain, found in Japan in 1984 and it is characterized by the phaseolotoxin production; the biovar 2 identified in Korea in 1997, it can produce coronatin; the biovar 3, whose strains are responsible for the worldwide out-breaks in Italy, New Zealand, Chile and China in 2010, is the most virulent one despite lacking production of any known toxin. However, it has been reported that the strains belonging to the biovar 3 contain four putative type III secretion system effector proteins namely hopH1, hopZ5, hopAM1-2 and hopAA1-2, not present in the other strains from the other biovars. The biovar 4 identified in Australia and New Zealand was initially classified as a “low virulent” Psa strain, but it has been subsequently reclassified as belonging to a different pathovar, the *actinidifoliorum* (Psaf); the biovars 5 and 6, still poorly characterized, were found in small areas in Japan in 2012 and 2015, respectively [1, 2]. Psa can enter into the kiwifruit plant by natural openings such as stomata and hydrotodes or by mechanical wounding or by pollen dissemination [3] and then spread systematically to the whole plant by multiplication in the apoplast. Apoplast colonization is the primary phase of the disease cycle of phytopathogenic bacteria including *Pseudomonas* species [4]. The ability to colonize the apoplast is due to the Type III protein Secretion System (TTSS) which delivers various effector proteins into the host to promote development of the disease and alter host cellular processes. The TTSS is encoded by hypersensitive reaction and pathogenicity genes (*hrp*) discovered in *Pseudomonas syringae* pv *phaseolicola* [5]. *hrp* genes are present in almost all plant pathogenic bacteria including Psa, as reported in available Psa-genomic-resources [6]. Expression of *hrp* genes, one of the most important transcriptional reprogramming in phytopathogenic bacteria during the infection, is induced only in plant tissues or in *hrp*-inducing media (HIM) [7]. The latter, mimic apoplastic conditions, such as poorness of nutrients, glucose or fructose as available carbon sources and low pH.

In order to identify Psa genes and pathways associated with the activation of virulence and to highlight the peculiar characteristics responsible for the highly virulence of biovar 3, we performed a transcriptomic analysis on different Psa strains belonging to biovar 1, 2 and 3 grown in rich medium and the above mentioned minimal medium (HIM). To this end, thanks to recent collection of extensive Psa genome resources [8, 9, 10], we first designed a custom multi-strain microarray chip covering the complete pan-genome of the Psa biovars considered in this study that is been manufactured by Agilent and it is now available to the plant

community (Design ID: 078853). The present study might help to draw hypotheses about molecular bases supporting different degrees of aggressiveness in the different strains as well as about virulence mechanisms activated in the plant apoplast.

### 3. MATERIALS AND METHODS

#### 3.1 CHIP DESIGN PROCEDURE

In order to highlight the transcriptomic differences among the different Psa biovars our group designed a multi-strain microarray chip (in collaboration with Dr Teresa Colombo, CNR, Rome) containing whole set of annotated sequences from four Psa strains belonging to the three main biovars, the strain J35 (NCPPB3739) belonging to biovar 1, the strain KN2 (ICMP19073) belonging to biovar 2, and the strains V-13 (ICMP18884) and CRA-FRU8.43 belonging to biovar 3. Moreover, the genome of *Pseudomonas syringae* pv. *tomato* DC3000 (Pst DC3000) a widely used phytopathogenic bacterial model, has been also included in the microarray chip design to help discriminating Psa-specific transcriptomic features. Finally, annotated transcripts from 3 integrative conjugative elements (ICEs) are also covered by our custom microarray chip. Annotated transcripts represented on the multi-strain chip (*i.e.*: for all *Pseudomonas syringae* strains and 3 ICEs) were collected from different public genome annotation sources (summarized in the **Table 1**) on July 2015. Additional genome annotation related to CRA-FRU 8.43 Psa strain were received and from the University of Udine (Dr Giuseppe Firrao, personal communication).

Strain	Type of genomic data	Strain description	GenBank assembly	Ref. seq assembly	Lenght
CRAFRU 8.43	Whole-genome sequence	Psa	GCA_000233815.2 (ASM23381v2)	GCF_000233815.1 (ASM23381v2)	6,143,194
ICMP18884 (V-13)	Whole-genome sequence	Psa	GCA_000648735.3 (ASM64873v3)	GCF_000648735.3 (ASM64873v3)	6,538,260
NCPPB3739 (J35)	Whole-genome sequence	Psa	GCA_000233835.2 (ASM23383v2)	GCF_000233835.1 (ASM23383v2)	6,538,053
ICMP19073 (KN2)	Whole-genome sequence	Psa	GCA_000416505.1 (ASM41650v1)	GCF_000416505.1 (ASM41650v1)	5,974,547
DC3000	Whole-genome sequence	Pst	GCA_000007805.1 (ASM780v1)	GCF_000007805.1 (ASM780v1)	5,927,897
M7	Pac_ICE1_cn, complete sequence	Psa	KC148185		102,575
ICMP18744	Pac_ICE2_cn, complete sequence	Psa	KC148186.1		108,802
ICMP19455	Pac_ICE3_cn, complete sequence	Psa	KC148188.1		100,782

*Table 1:* Summary of the *Pseudomonas* strain used in this study, and the genomic annotation resources used for the microarray chip design.

For those strains with multiple resources of genome annotation available, a unique reference transcriptome has been first created by merging of the different annotation data so to avoid introducing artificial redundancy in the chip design. These merged transcriptome datasets were created by retaining a single representative for any annotated transcript, with annotation source priority: RefSeq > GeneBank > University of Udine.

Collections of unique annotated sequences for each strain were then used to perform all-against-all transcriptome comparisons at the nucleotidic level across strains included in the chip design by using the well-established BLAST software (NCBI: <https://blast.ncbi.nlm.nih.gov/Blast.cgi>). These comparisons allowed identification of genes shared by all strains (the *core-genome*) as well as partially shared and strain-specific genes (the *dispensable-genome*).

The procedure adopted to design the *Pseudomonas* multi-strain microarray is summarized in **Fig. 1** (Supplemental Resources). Altogether, the multi-strain chip designed created by using the Agilent eArray platform (<https://earray.chem.agilent.com/earray/>) yielded 18,598 best probes (*i.e.*: with lowest possible target ambiguity) interrogating 20,554 CDS sequences, of which 14,457 have a unique match (unambiguous probes) (Agilent Design ID: 078853).

The Agilent eArray web tool was used to design probes with the following parameters:

**Method:** Tm Matching Methodology;

**Method:** Best Distribution Methodology;

**Probe length:** 60 bp;

**Number of probe per target:** 3;

**Transcriptome detail:** “use a target file as transcriptome”;

**Probe design:** “design without 3'-bias”.

Moreover, eleven human housekeeping genes were included in the microarray design, namely: *C1orf43*, *chmp2A*, *emc7*, *gpi*, *psmb2*, *psmb4*, *rab7A*, *reep5*, *snrpd3*, *vcp* and *vps29* as negative controls.

The microarray chip designed by Agilent contains the following features:

**SurePrint G3 Custom GE 8x60K** (Tot features: 62,976; Available features: 61,657; Used: 55,997 or 91%):

**experimental (replicate probes):** 17 probes for 17 ORFs of *Pseudomonas* species (x 10 replicates each = 170 features)

**experimental:** 18,581 probes for 20,537 ORFs of *Pseudomonas* species (x 3 replicates = 55,743 features)

**negative controls:** 28 probes for 11 housekeeping genes of *Homo sapiens* (x 3 replicates = 84 features)

**Agilent controls:** 1,319 probes

Finally, gene sequences were functionally annotated using Blast2GO suite (release 4.1.9) after mapping against the NCBI non-redundant database with the BLASTX tool (release 2.6.0).

### 3.2 EXPERIMENTAL DESIGN PREPARATION

The growth rate of the 5 *Pseudomonas* strains under investigation was analysed to determine the suitable harvest-time points for the microarray analysis, in two different growing conditions, a rich medium (King's B) and a minimal medium (*hrp*-inducing medium HIM) [11]. The composition of the two media is reposted in **Tables 2** and **3**.

*Table 2: King's B (KB) composition*

**KING'S B**

PEPTONE	20 gr
GLYCEROL	10 ml
K <sub>2</sub> HPO <sub>4</sub>	1.5 gr
MgSO <sub>4</sub>	1.5 gr
WATER	Up to 1L
pH	7.2

*Table 3: hrp-inducing medium (HIM) composition*

**HIM**

K <sub>2</sub> HPO <sub>4</sub>	1.5 gr
KH <sub>2</sub> PO <sub>4</sub>	5.5 gr
MgCl <sub>2</sub>	0.34 gr
(NH <sub>4</sub> )SO <sub>4</sub>	1 gr
NaCl	0.1 gr
GLYCEROL	2 ml
WATER	Up to 1L
pH	5.5

### 3.2.1 BACTERIAL GROWTH

Single colonies of the 5 *Pseudomonas* strains: CRA-FRU 8.43, V-13 (ICMP18884), J35 (NCPB3739) KN2 (ICMP19073) and Pst DC3000 grown on KB agar were used to inoculate KB broth cultures, incubated with shaking (200 rpm) over-night at 28°C. Then 3 ml aliquots of cell suspension were centrifuged and washed three times in KB or HIM

respectively. Then the bacterial suspensions were adjusted to an  $OD_{600} = 0.2$  for HIM and 0.02 for KB a final volume of 20 ml in 100 ml flasks, incubated at 28°C with shaking (200 rpm). The  $OD_{600}$  was measured every 4 hours over 48 hours. Three independent experiments were performed.

### 3.2.2 *hrp* GENE EXPRESSION EVALUATION

To determine the suitable early-harvest time point for the microarray gene expression analysis, the expression of virulence early genes *hrpC* and *hrpW* [12] was evaluated in Psa CRA-FRU 8.43 as a representative strain. In particular, the bacteria were grown in KB and HIM media as described previously and sampled at 4, 8 and 24 hours ( $2.4 \times 10^9$  cells). The RNA from the bacterial culture was extracted using the Spectrum Plant Total RNA Kit (Sigma Aldrich), and quantified by Nanodrop (Thermo Fischer) measurement. Then 2 µg of total RNA was treated with TURBO DNase (Ambion) to remove the contaminant DNA and 10 µl of treated RNA was retro-transcribed by SuperScript III Reverse Transcriptase (Invitrogen). Then the cDNA obtained was diluted to obtain a final amount of 20 ng. The primers, specific for each selected gene, were diluted to 200 mM and the reaction was performed using the GoTaq PCR Master MIX (Promega) in the Proflex PCR System (Applied Bio-system) instrument. A gene, encoding the sigma factor RpoD, was used as internal reference genes [13]. Specific primer were designed to amplify a small portion of the cDNA of interest using the NCBI primer blast tool (<https://www.ncbi.nlm.nih.gov/tools/primer-blast/>) and the quality of the primers was evaluated using Melting DNA Hybrid project PCR tool and DNA-hybridization program ([http://promix.cribi.unipd.it/cgi-bin/promix/melting/melting\\_main.exe?GRUP=0](http://promix.cribi.unipd.it/cgi-bin/promix/melting/melting_main.exe?GRUP=0)). The Real-time qPCR reaction cycle was set up as following:

50°C x 2 minutes	
95°C x 5 minutes	
95°C x 30 seconds	}
60°C x 30 seconds	
	40 cycles
72°C x 20 seconds	

The Proflex software (Applied Bio-system) automatically set up a threshold for the amplification curve and gives back the Ct for each sample. The relative expression values (Mean Normalized Expression, MNE) of the target genes and the standard errors were



calculated using Pfaffl and Simon equation [13, 14]. The LingRegPCR program (<http://www.hartfaalcentrum.nl/index.php?main=files&fileName=LinRegPCR.zip&description=LinRegPCR:%20qPCR%20data%20analysis&sub=LinRegPCR>) [15] was used to calculate the efficiency of the amplification reaction from the fluorescence data.

### 3.3 EVALUATION OF DIFFERENTIAL EXPRESSED GENES BY MICROARRAY ANALYSIS

The differentially expressed genes among the *Pseudomonas syringae* (Ps) strains were evaluated at early-time points of growth, that is 4 and 8 hours-post inoculation (hpi); in order to elucidate the earliest virulence mechanism. In particular, to clarify the peculiar virulence mechanism of the *Pseudomonas syringae* pv. *actinidae* strains and moreover the virulence mechanism specific to the most virulent biovar, the biovar 3.

The 5 strains of *Pseudomonas syringae*, CRA-FRU 8.43, V-13, J35, KN2 and Pst DC3000, were grown in KB and HIM, as described in section 3.2.1, and harvested at 4 and 8 hpi ( $2.4 \times 10^9$  cells). Three biological replicates for each strain at each condition were harvested and used for the microarray analysis. The RNA was extracted from using the Spectrum Plant Total RNA Kit (Sigma Aldrich), quantified by Nanodrop (Thermo Fischer), and the RNA quality was evaluated through Bioanalyser (Agilent RNA 6000 Nano Kit). Then the RNA was processed for microarray analysis using the One-Color Microarray-Based Gene Expression Analysis Low Input Quick Amp WT Labeling kit (Agilent Technologies, August 2015), according to manufacturer's instructions. Results of the hybridizations were analysed by Agilent G4900DA SureScan Microarray Scanner System with the Agilent Scan Control software and the data extrapolated using the Agilent Feature Extraction software (2010).

The raw data obtained were normalized, statistically evaluated and processed in collaboration with Dr Nicola Vitulo (University of Verona). Briefly, we calculated the average and the standard deviation value of the triplicates-probe present in the microarray, then the data were normalized using the non-parametric tests.

Normalized data were submitted for the Differential Expressed Genes (DEGs) identification. The DEGs list was created using  $P$ -value  $P < 0.05$  and absolute  $\log_2$ -fold-change  $> 1$ . Functional enrichment analysis was performed using BinGo (<http://apps.cytoscape.org/apps/bin-go>, [16]). The comparison of DEGs across different strains and/or conditions was performed using the online software Calculate and Draw Custom Venn Diagrams

(<http://bioinformatics.psb.ugent.be/webtools/Venn/>, 2017). The bar charts based on the enrichment in Gene Ontology (GO) terms of the DEGs was generated using Blast2GO suite (release 4.1.9, March 2017) by filtering for False Discovery Rate(FDR)<0.01.

## 4. RESULTS

### 4.1 EVALUATION OF THE CONDITIONS FOR Psa GENE EXPRESSION ANALYSIS

Microarray analysis represents a well-established and powerful tool for gene expression evaluation. However, a well-planned experimental design is required in order to produce the most informative data. To this end, preliminary experiments were carried out to evaluate the kinetic of bacterial growth for the different *Pseudomonas syringae* (Ps) strains and to identify the specific time points at which early pathogenesis genes (*hrp*) were expressed in minimal medium (HIM)

#### 4.1.1 KINETIC OF BACTERIAL GROWTH

The primary aims of this experiment was to establish the best suitable harvesting time-points for the microarray analysis by assessing the ability of Ps strains to grow in rich and in minimal medium and by then comparing the two kinetics of growth.

The four Psa strains belonging to the three different biovars, namely, J35 (biovar 1), KN2 (biovar 2), CRA-FRU 8.43 and V-13 (biovar 3), as well as a strain of *Ps pv. tomato* (DC3000) used as an external term of comparison, showed a similar growing pattern in the rich medium, featuring an exponential phase between 8 and 24 hpi followed by a plateau phase (**Fig. 2, a**).

Conversely, the growth was slower in the *hrp*-inducing minimal medium, where the different strains hardly reached the optical density  $OD_{600}=1$  (**Fig. 2, b**). Moreover, the optical density drastically (for CRA-FRU 8.43, V-13 and J35) or more gradually (for KN2) decreased for all Psa strains after reaching its maximum value at 24 hpi, different from the Pst strain that continued to increase in optical density until the end of the measurements (and reaching the maximum at 36 hpi). The different optical density curves may be explained by the formation of large cell aggregates clearly visible at the late growth phases only in the Psa strains exhibiting abrupt drop in optical density. Conversely, the KN2, where optical density values dropped more gradually, showed formation of smaller cell aggregates after 36 hpi, while Pst-DC3000 cell density decreased slightly only after 48 hpi (**Fig. 2, b**).

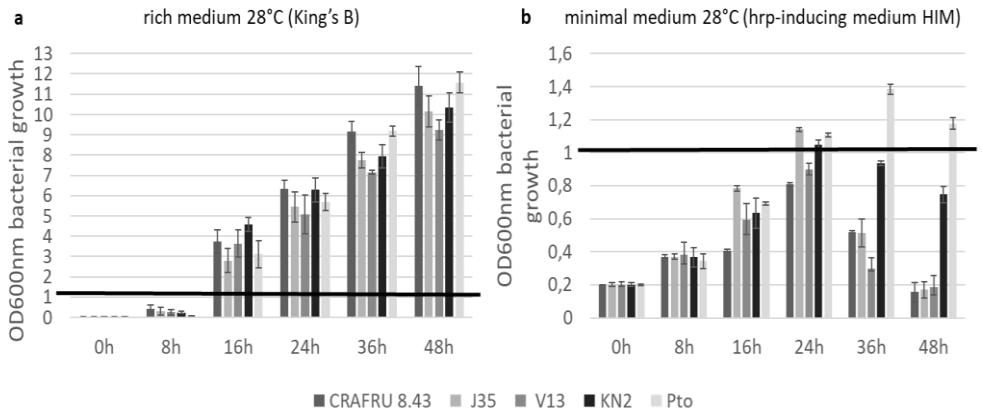


**Figure 2:** Growth kinetic of the Ps strains in rich medium (a) and minimal medium (b), at 28°C. The y-axis reports the OD<sub>600</sub> values and the x-axis reports the time of analysis. The black line indicates the OD<sub>600</sub>=1.

#### 4.1.2 *hrp* GENE EXPRESSION EVALUATION

The infection process causes a fast transcriptomic reprogramming in phytopathogenic bacteria. Therefore, a massive transcriptomic analysis considering two early-time points could help to understand the pathways involved and elucidate the virulence differences observed among the Psa biovars. Thus, a gene expression evaluation of few virulence genes involved in the TTSS formation, considered one of the primary pathogenesis mechanism that occurs during the infection process, could be useful for the choice of suitable harvesting-time points for the microarray gene expression analysis.

For this purpose, we performed a Real-time qPCR to evaluate the expression of two *hrp* genes, *i.e.*: *hrpC* and *hrpW* at 4, 8 and 24 hpi in KB and HIM media using CRA-FRU 8.43, as the experimental model strain and the *rpoD*, as reference gene. The plots in **Fig. 3** report gene expression values, expressed as Mean Normalized Expression (MNE). The two genes considered in the analysis show a similar expression pattern, a high expression level at 4 and 8 hpi in the apoplastic-mimic HIM medium, which decreases at 24 hpi. Conversely, in the rich medium the *hrp* were not expressed at 4 and 8 hpi, while their expression level slight increased at 24 hpi, especially for *hrpC* (**Fig. 3, a**) showing a possible shift to a pathogenicity-like behaviour possibly due to the decrease of nutrient in the medium.

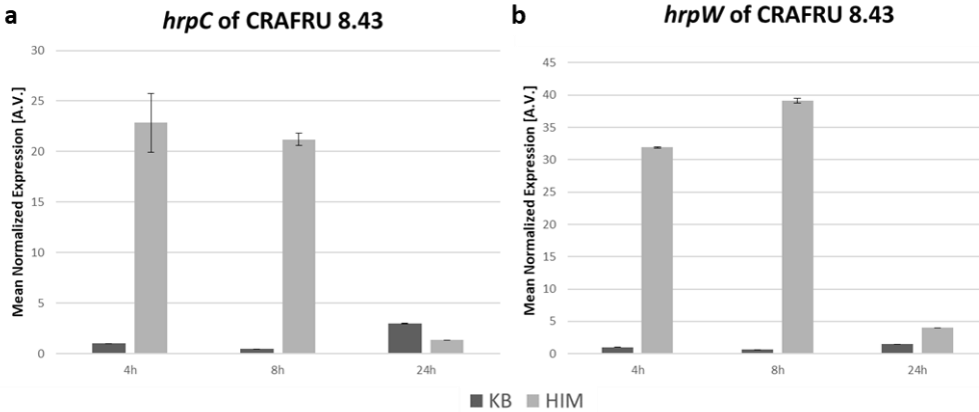


*Figure 3:* Gene expression evaluation by Real-time qPCR of the *hrpC* (a) and *hrpW* (b) genes in rich medium (KB) and minimal medium (HIM), at 4, 8 and 24 hpi.

## 4.2 GENE EXPRESSION ANALYSIS OF *PSEUDOMONAS SYRINGAE* STRAINS BY MICROARRAY

### 4.2.1 STATISTICAL OVERVIEW OF THE MICROARRAY DATA

Considering the previous results, the microarray gene expression analysis was performed in the Psa strains: CRA-FRU 8.43, V-13, J35, KN2 and Pst DC3000 grown in rich and minimal medium and harvested at 4 and 8 hpi. The statistical analysis of samples expressed using a dendrogram, **Fig. 4**, shows a good biological reproducibility among the biological replicates which cluster together. More in detail, we could observe a first clustering based on the pathovar, indeed Pst and Psa clustered separately, a second clustering based on the Psa biovars, as the biovars 3 strains, CRA-FRU 8.43 and V-13 formed a unique cluster separated from biovar 1 (J35) and biovar 2 (KN2). Finally, the biovar 1 and 2 further clustered into two distinct groups. The growth conditions and the time points of the analysis played a minor role in the clustering of the gene expression profiles, as we could observe a separation between HIM and KB growing conditions only for Pst DC3000.

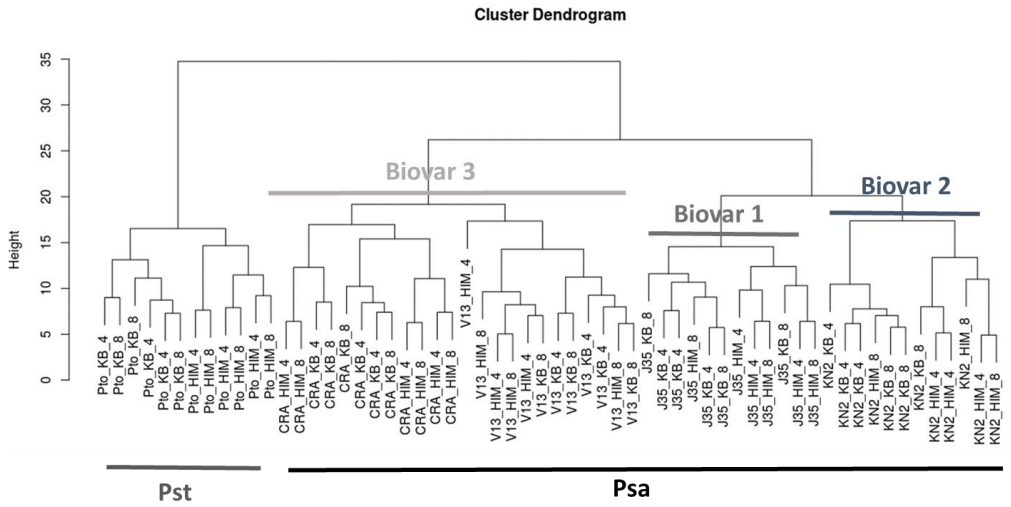


**Figure 4:** Cluster dendrogram of the microarray experiment, the different clusters are highlighted. The first letter represents the strains used, i.e. Pto= Pst DC3000, CRA= CRA-FRU 8.43, V13= ICMP18884, J35= NCPPB3739, KN2= ICMP19073; the second letters represent the growth conditions i.e. KB= King's B and HIM= *hrp*-inducing medium, the number represents the harvest time point, i.e. 4= 4hpi, 8= 8hpi.

The Principal Component Analysis (PCA) confirmed the clustering observed in the dendrogram, **Fig. 5**. The PCA analysis based on the strains (**Fig. 5, a**) showed as the first principal component the pathovars, then the second and the third components were based on the biovars, with the biovar 3 clustering separately from the biovars 1 and 2.

The PCA analysis based on the experimental conditions (**Fig. 5, b**) showed a clustering based on the media considered i.e.: KB and HIM and confirmed the minor role played by the time of growth in the clustering. The results thus indicated that microarray data extrapolated from the experiment are suitable for identify the genes differentially expressed among the different biovars and the different media tested. Therefore, the different analyses could elucidate the possible behaviour within the host based on the genes expression observed in the apoplastic-mimic medium (HIM).

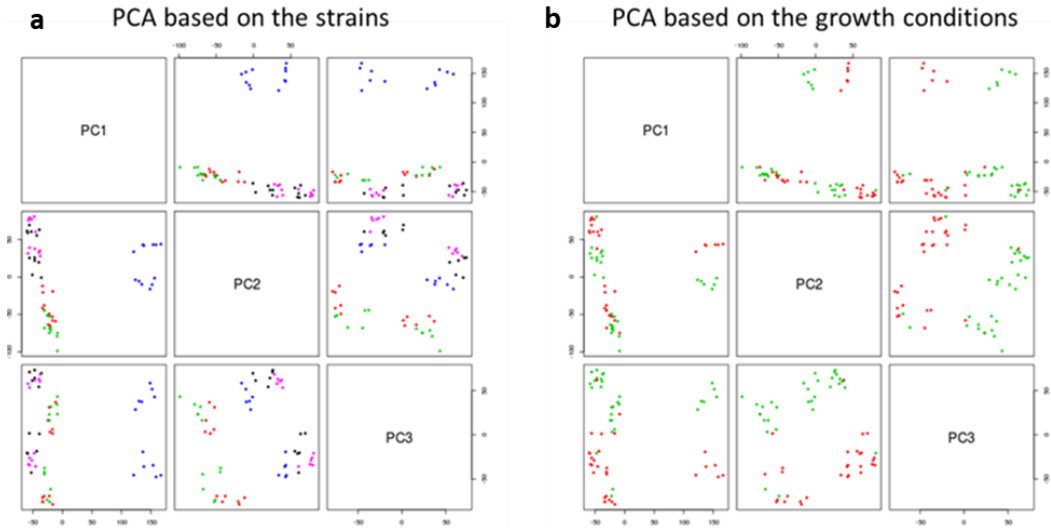


*Figure 5:* PCA analysis based on the strains (a), and on the growth conditions, (b). In (a) strains are indicated in colours. Blue= Pst DC3000, purple= V13, black=CRA-FRU 8.43, red= J35 and green= KN2. In the PCA based on the growth conditions, (b), red= KB and green= HIM.

#### 4.2.2 IDENTIFICATION OF DIFFERENTIALLY EXPRESSED GENES AMONG DIFFERENT STRAINS AND CONDITIONS: A GENERAL OVERVIEW

Gene expression experiments, such as the microarray analysis, provide a fast tool to systematically identify the Differentially Expressed Genes (DEGs) among different conditions tested. This large body of information can be used to generate hypothesis for future experiments and suggested which physiological and molecular pathways should be further characterized. The microarray gene expression analysis performed among the different pathovars of *P. syringae* and the different Psa biovars provided us an overview of strain specific and common transcriptional changes, while the DEGs between growing media provided the hypothesis about the genes potentially involved in pathogenicity (minimal medium) in comparison with the saprophytic life-style.

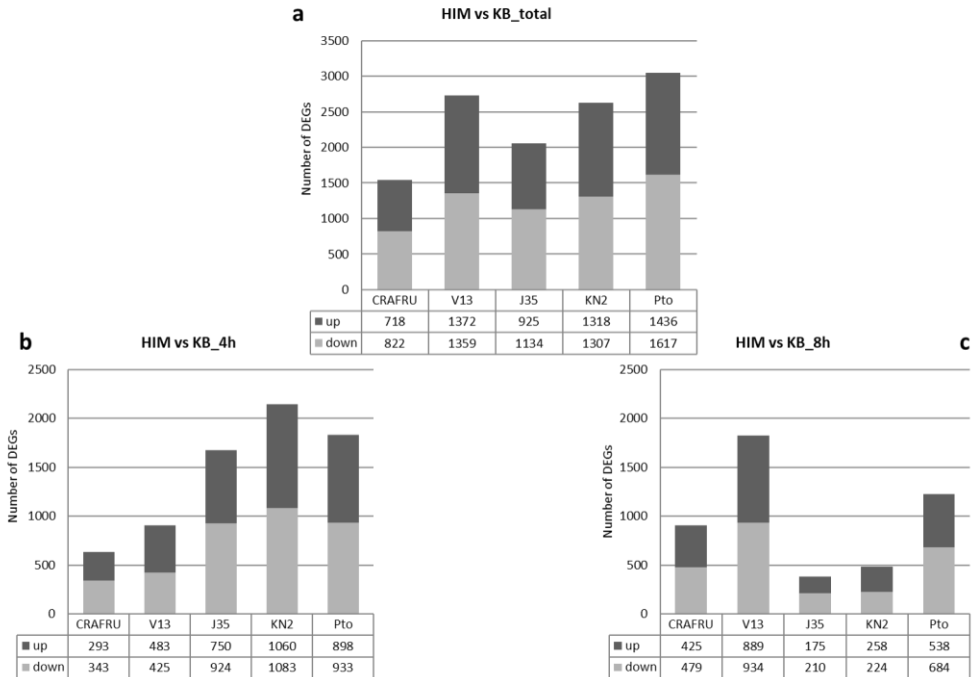


**Figure 6:** Number of DEGs in the different strains considered in the experiment at the different condition tested i.e.: minimal medium (HIM) and rich medium (KB). a) number of DEGs between HIM and KB considering both time point of the analysis i.e.: 4 and 8 hpi; b) number of DEGs between HIM and KB at 4hpi; c) number of DEGs between HIM and KB at 8 hpi. up= up-regulated genes; down= down regulated genes;

For instance, we noticed a relatively smaller transcriptomic modulation in CRA-FRU 8.43 in comparison to all the other strains, including the strain V-13 belonging to the same biovar 3 as testified by a consistently lower number of DEGs ( $FDR < 0.05$  and absolute  $\log_2\text{-fold-change} > 1$ ) identified both at 4 and 8 hpi when comparing the growth in minimal *versus* rich medium (**Fig. 6, a**).

When considering the number of the DEGs between the minimal medium and rich medium at the two time points separately (4 and 8 hpi), we could observe a somewhat similar behaviour of the strains belonging to biovar 3 (**Fig. 6, b-c**) which both seem to react to minimal medium later than the other strains, while J35, KN2 and Pst DC3000 modulated a higher number of genes already at 4 hpi.



Considering the number DEGs, between minimal and rich medium at 4 and 8 hpi (using the same filter parameter used previously *i.e.*:  $FDR < 0.05$  and  $\log_2FC > 1$ ), involved in the primary mechanism of pathogenesis, such as the genes encoding for the TTSS formation and the genes involved in the regulation of the bacterial flagellum we can observe that the two strains belonging to the biovar 3 modulate a higher number of DEGs involved in the TTSS regulation than the strains belonging to the biovar 1 and 2 (**Fig. 7, a**) and the rate is similar to those modulated in Pto. Conversely, the number of DEGs involved in the bacterial flagellum regulation (**Fig. 7, b**) is higher in the strains belonging to the biovars 1 and 2 and in Pst DC3000 in comparison with the Psa stains of the biovar 3, in which only, 2 and 1 genes were modulated in CRA-FRU 8.43 and V-13 respectively. These data suggest that the Psa strains activate either the TTSS or the bacterial flagellum in a biovar-specific way.

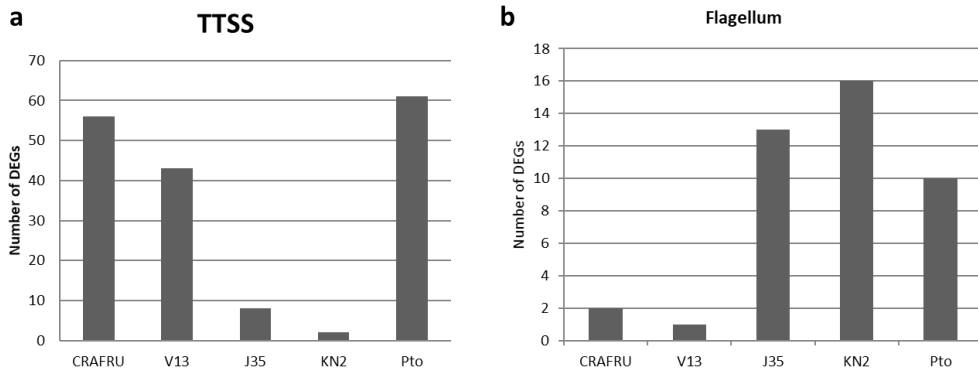


**Figure 7:** Number of DEGs specifically modulated in the different strains at 4 and 8 h and annotated as involved in TTSS (a) or flagellum (b) activity or regulation.

Considering the DEGs, between minimal and rich media at 4 and 8 hpi, specific only of the Psa strains we could observe that the strains belonging to the biovar 3, shared 306 DEGs, while the specific DEGs were 171 and 594 for CRA-FRU 8.43 and V-13 respectively (**Fig. 8**). Considering the pull of the common DEGs specific of the strains belonging to the biovar 3, we could observe as the strain belonging to the biovar 1, J35, shared a higher number of DEGs than the KN2, which is the representative strain of the biovar 2. Moreover, KN2 modulated more DEGs than the other Psa strains.

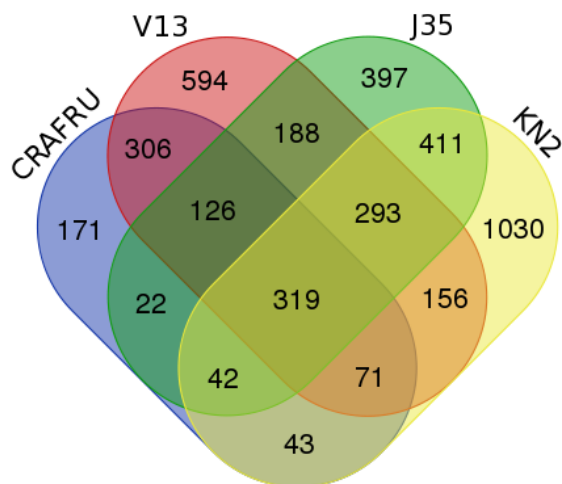


*Figure 8:* The Venn diagram shows the number of DEGs commonly and specifically modulated in the different Psa strains at 4 and 8 h.

Considering the DEGs, between minimal and rich media at 4 and 8 hpi, specific only of the Psa strains up-regulated in minimal medium we could observe that the strains belonging to the biovar 3 shared 304 DEGs, and 123 were CRA-FRU 8.43 specific, while 653 were V-13 specific (**Fig. 9**). KN2 showed the higher number of the up-regulated DEGs. Moreover, considering the pull of the common DEGs specific of the strains belonging to the biovar 3, we could observe as the stain belonging to the biovar 2, KN2, shared a higher number of up-regulated DEGs than the J35.

Conversely the strains belonging to the biovar 3, shared only 143 down-regulated DEGs, while 104 were CRA-FRU 8.43 and 787 V-13 specific (**Fig. 10**). Considering the pull of the common DEGs specific of the strains belonging to the biovar 3, we could observe as the stain belonging to biovar 1, J35, shared a higher number of DEGs than the KN2, which is the representative strain of the biovar 2.

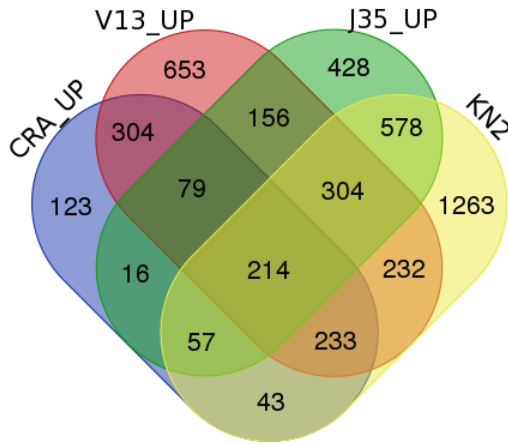


*Figure 9:* The Venn diagram shows the number of DEGs commonly and specifically up-regulated in the different Psa strains (CRA= CRAFRU-8.43, V13, J35 and KN2) at 4 and 8 h.

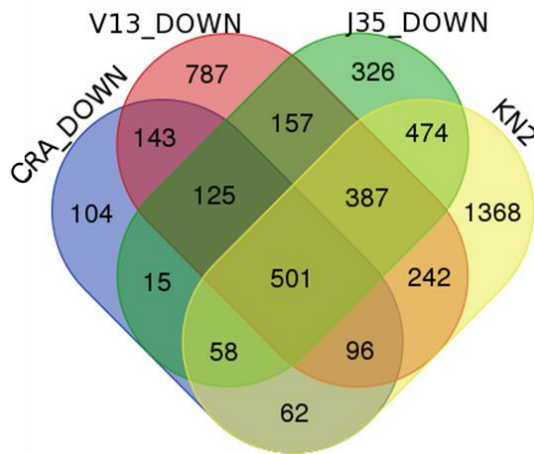


*Figure 10:* The Venn diagram shows the number of DEGs commonly and specifically down-regulated in the different Psa strains (CRA= CRAFRU-8.43, V13, J35 and KN2) at 4 and 8 h.

### **4.2.3 ENRICHMENT IN FUNCTIONAL CATEGORIES AMONG HIM-RESPONSIVE GENES IN THE DIFFERENT *PSEUDOMONAS* STRAINS**

To provide hypothesis about the pathways regulated by perception of the minimal medium and highlight the transcriptomic differences among the different strains, we performed a functional enrichment in *Gene Ontology* (GO) terms using the BinGo (Cytoscape) software on the DEGs between minimal medium (HIM) and rich medium (KB). The different plots were represented using Blast2GO tool (version 4.1 March 2017).

#### **4.2.3.1 GO TERM ENRICHMENT AMONG DEGs IN CRA-FRU 8.43 (BIOVAR 3)**

The GO terms enriched among DEGs between HIM and KB of CRA-FRU 8.43 at both time points (4 and 8 hpi) (**Fig. 11**) showed that the main enriched classes were related to pathogenesis, TTSS protein secretion, interaction with host, and the energetic metabolic processes, such as: tricarboxylic acid cycle (TCA), and electron chain reactions. When considering the two time points separately, we could observe at 4 hpi (**Fig. 12**) enriched classes belonging to the motility process, catabolic process, and sugar metabolic processes, such as: fructose, mannose and other carbohydrates and the biosynthesis of alginic-acid.

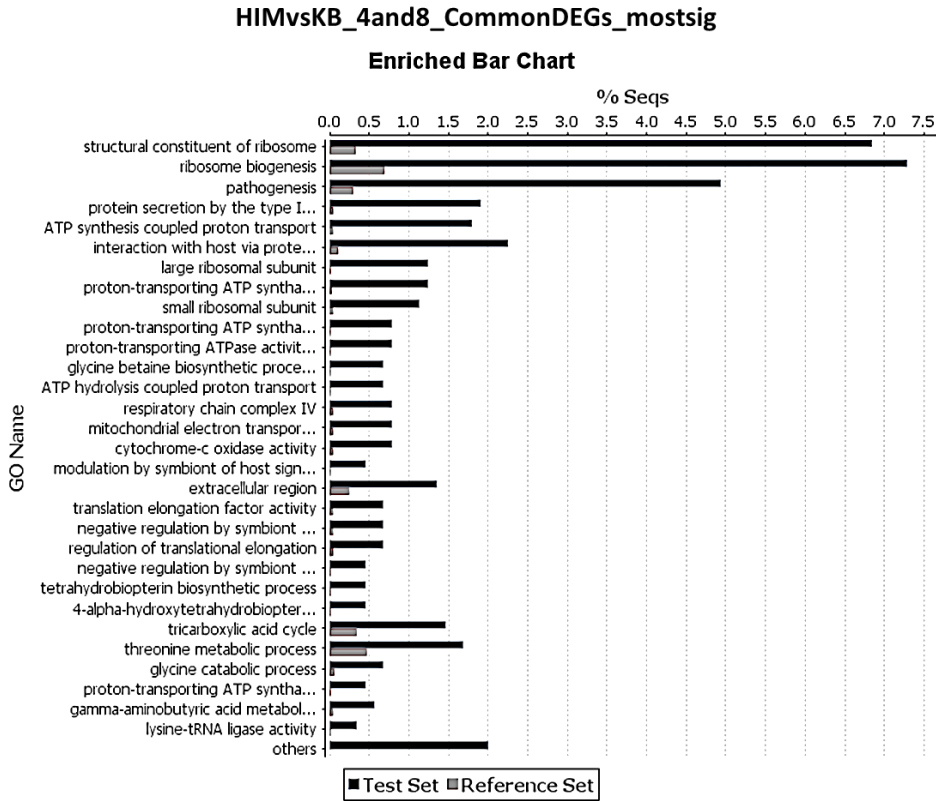


*Figure 11:* Functional enrichment analysis considering the GO term of the DEGs between HIM and KB at both time points tested (4 and 8 h). The Test Set represents the percentage of the DEGs of CRA-FRU 8.43, annotated with the select GO term, while, the Reference Set is the percentage of genes represented in the microarray chip.

The same comparison, at 8 hpi (**Fig. 13**), showed functional enrichments in metal ion transport, iron ion transport and siderophore/iron chelation activity, together with process correlated to the cellular respiration and transcriptional regulation.

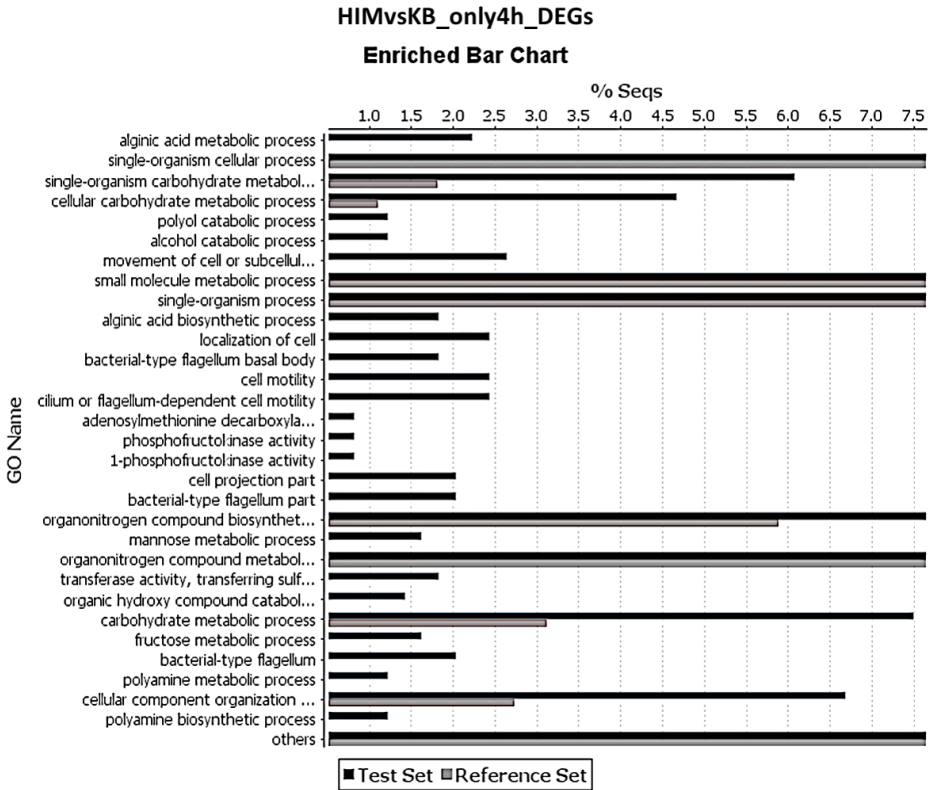


*Figure 12:* Functional enrichment analysis considering the GO term of the DEGs between HIM and KB at 4h. The Test Set represents the percentage of the DEGs of CRA-FRU 8.43, annotated with the select GO term, while, the Reference Set is the percentage of genes represented in the microarray chip.

The same analysis was repeated considering only the up- or the down-regulated groups of DEGs at both time point. Among the up-regulated transcripts (**Fig. 14**), we could observe enriched classes belonging to pathogenesis process, and TTSS protein secretion, mechanism involved in bacteria-host interaction and transcription regulation activity.

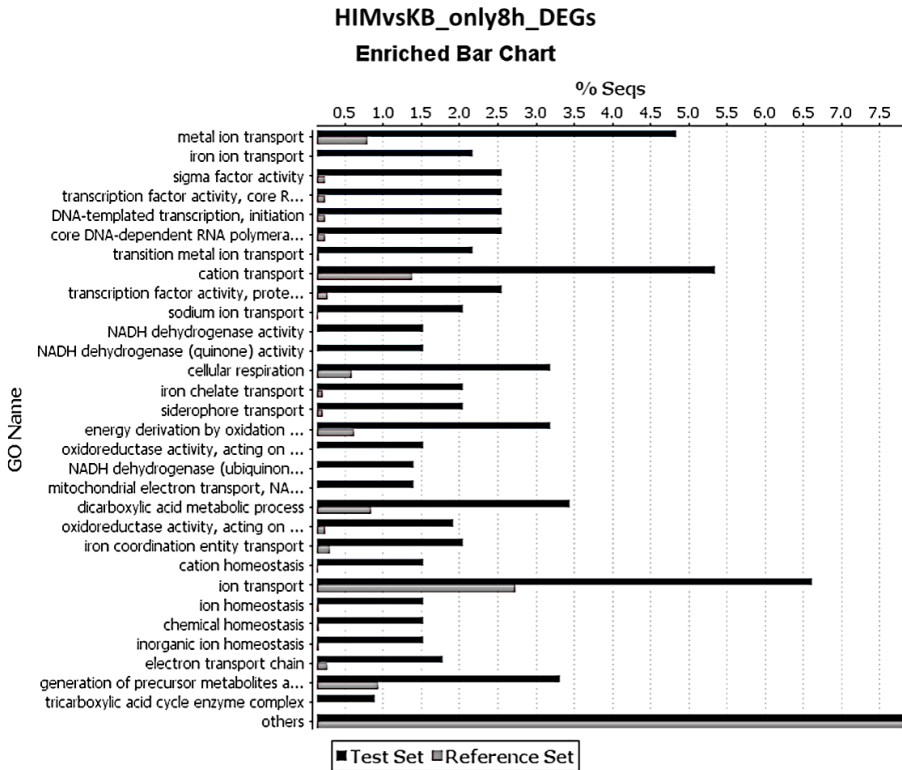


*Figure 13:* Functional enrichment analysis considering the GO term of the DEGs between HIM and KB at 8h. The Test Set represents the percentage of the DEGs of CRA-FRU 8.43, annotated with the select GO term, while, the Reference Set is the percentage of genes represented in the microarray chip.

Moreover, if we select the DEGs up-regulated in HIM which showed an  $p$ -value $<0.01$ , to perform the GO terms enrichment (**Fig. 15**), we could observe also other enriched classes belonging to ferric ion transport, iron permease complex, motor activity, tryptophan synthase activity CoA-transferase activity and cyclic-di-GMP binding, the last one involved in biofilm formation, switching between planktonic and sessile life-style and regulator of virulence factor.

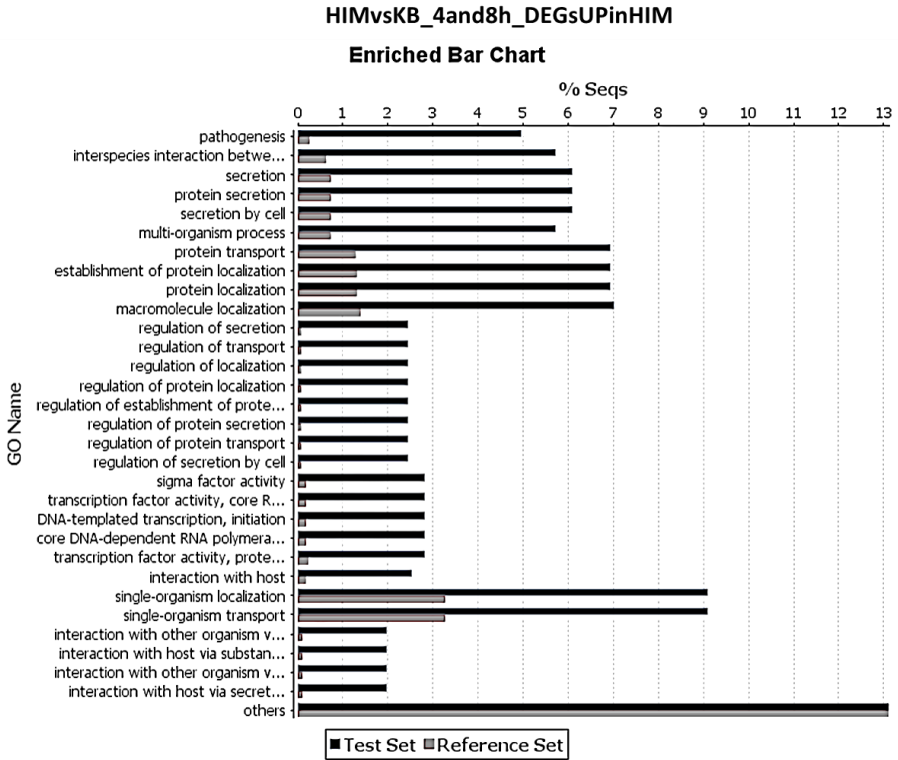


*Figure 14:* Functional enrichment analysis considering the GO term of the DEGs between HIM and KB at 4 and 8 hpi considering the DEGs up-regulated in HIM. The Test Set represents the percentage of the DEGs of CRA-FRU 8.43, annotated with the select GO term, while, the Reference Set is the percentage of genes represented in the microarray chip.

Conversely, the functional enrichment on DEGs down-regulated in HIM showed (**Fig. 16**) GO terms mainly related to different metabolic processes, such as nitrogen and the peptide metabolisms.



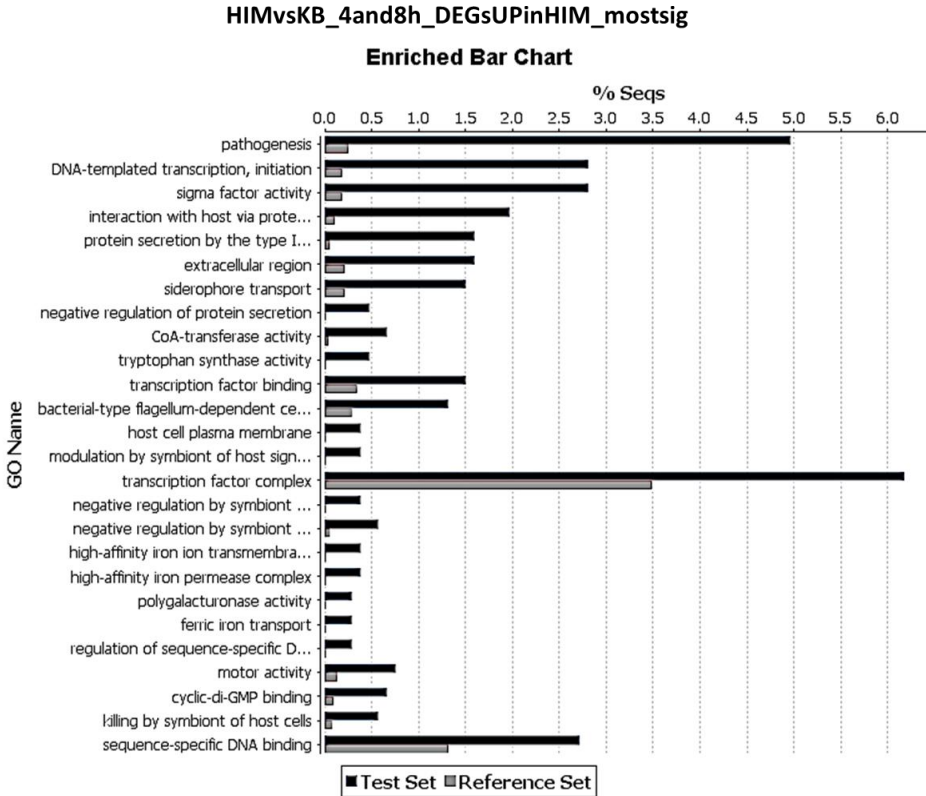


*Figure 15:* Functional enrichment analysis considering the GO term of the DEGs between HIM and KB at 4 and 8 hpi considering the DEGs up-regulated in HIM which showed a  $p$ -value < 0.01. The Test Set represents the percentage of the DEGs of CRA-FRU 8.43, annotated with the select GO term, while, the Reference Set is the percentage of genes represented in the microarray chip.

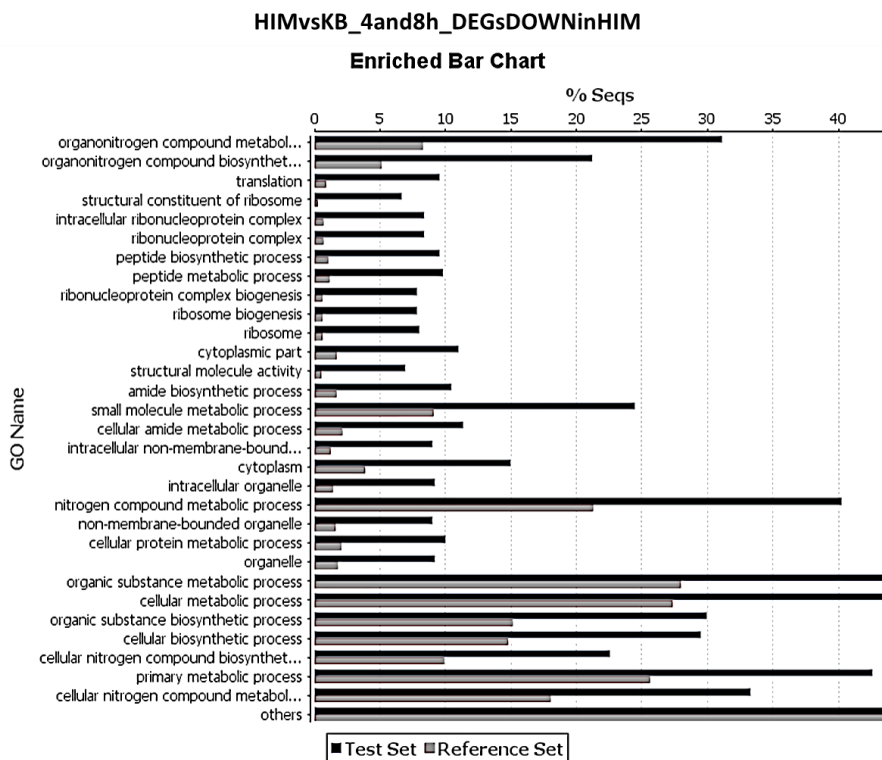


*Figure 16:* Functional enrichment analysis considering the GO term of the DEGs between HIM and KB at 4 and 8 hpi considering the DEGs down-regulated in HIM. The Test Set represents the percentage of the DEGs of CRA-FRU 8.43, annotated with the select GO term, while, the Reference Set is the percentage of genes represented in the microarray chip.

#### 4.2.3.2 GO TERM ENRICHMENT AMONG DEGs IN V-13 (BIOVAR 3)

The GO terms enriched among DEGs between HIM and KB of V-13 at both time points (4 and 8 hpi) (**Fig. 17**) showed enriched classes related to translation regulation, biosynthesis process, and to pathogenesis. When considering the two time points separately,

we could observe at 4 hpi (**Fig. 18**) enriched classes belonging to transport process, catalytic and lipid metabolisms such as: acyl-CoA and acetyl-CoA biosynthesis processes and CoA-ligase activity.

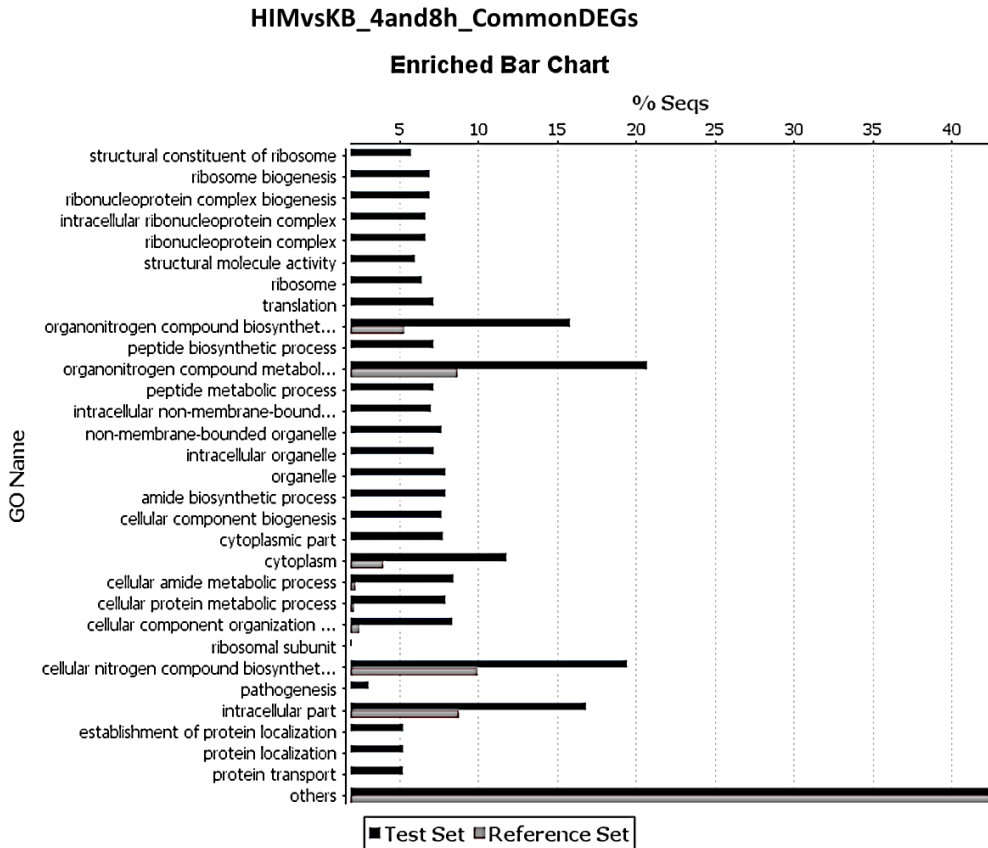


*Figure 17:* Functional enrichment analysis considering the GO term of the DEGs between HIM and KB at both time points tested (4 and 8 h). The Test Set represents the percentage of the DEGs of V-13, annotated with the select GO term, while, the Reference Set is the percentage of genes represented in the microarray chip.

The same comparison, at 8 hpi (**Fig. 19**), showed functional enrichments in cell motility, iron ion transport, ferroxidase complex, metal ion transport and, processes involved in the transcriptional regulation and vitamin binding.

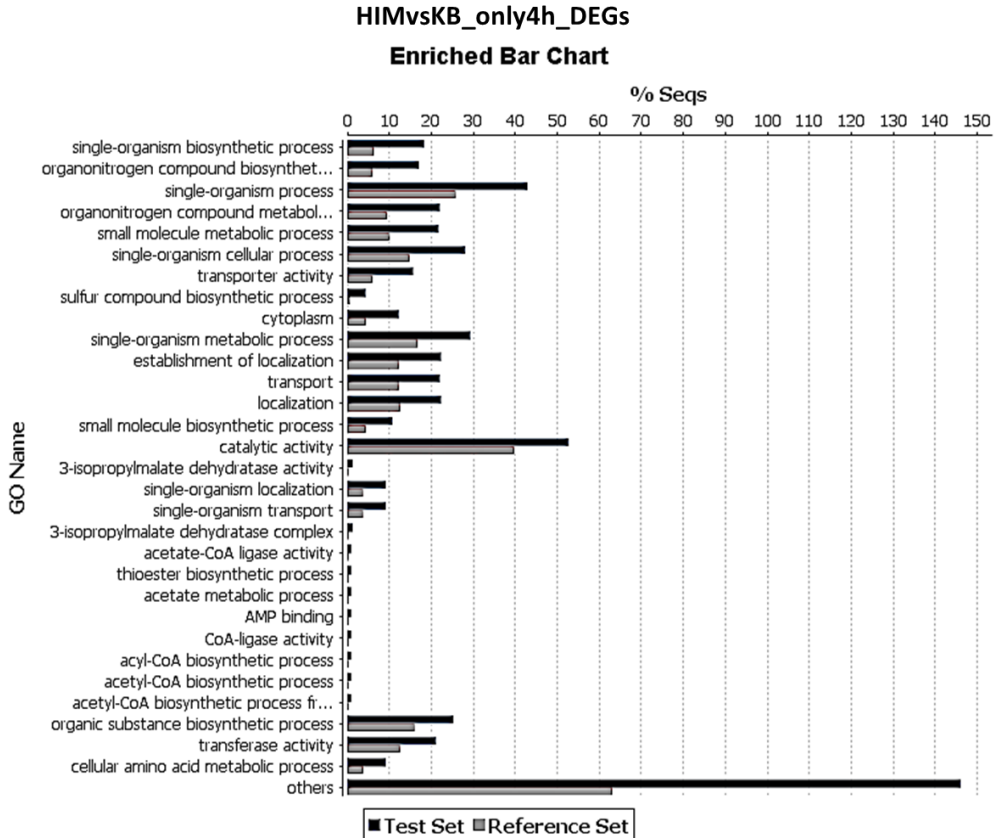


*Figure 18:* Functional enrichment analysis considering the GO term of the DEGs between HIM and KB at 4h. The Test Set represents the percentage of the DEGs of V-13, annotated with the select GO term, while, the Reference Set is the percentage of genes represented in the microarray chip.

The same analysis was repeated considering only the up- or the down-regulated groups of DEGs at both time point. Among the up-regulated transcripts (**Fig. 20**), we could observe enriched classes belonging to flagella regulation and motility, transcription regulation activity, pathogenesis and TTSS secretion protein.

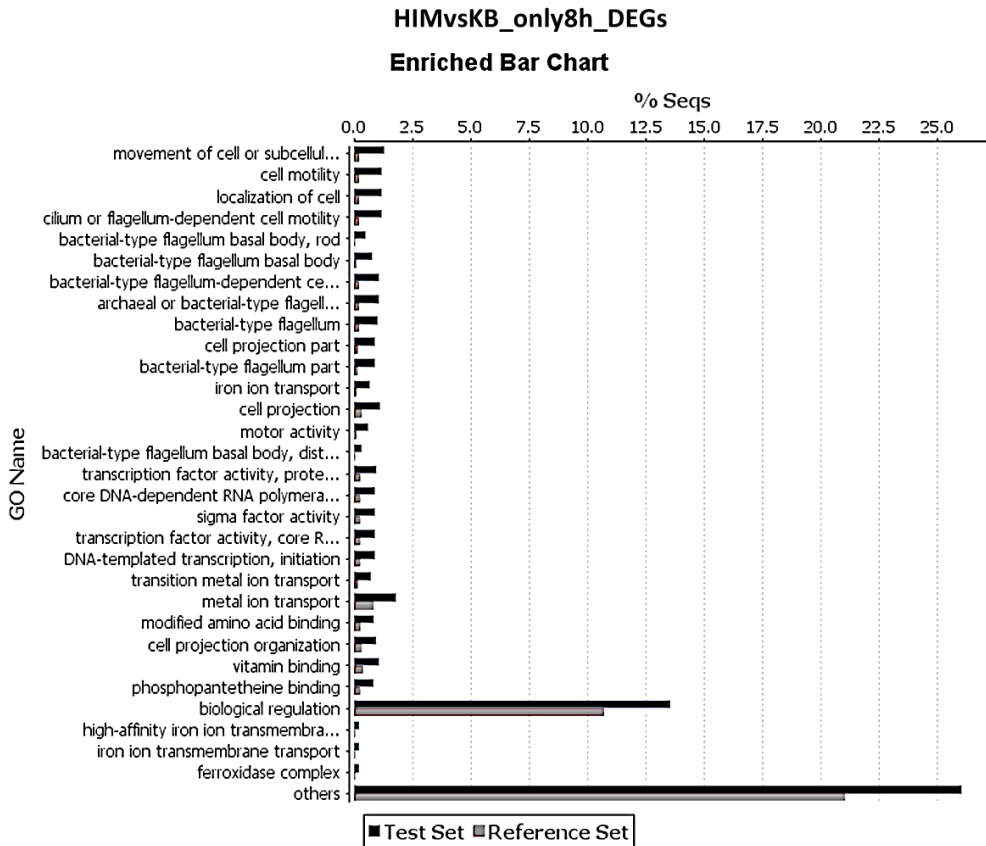


*Figure 19:* Functional enrichment analysis considering the GO term of the DEGs between HIM and KB at 8h. The Test Set represents the percentage of the DEGs of V-13, annotated with the select GO term, while, the Reference Set is the percentage of genes represented in the microarray chip.

Conversely, the functional enrichment on DEGs down-regulated in HIM showed (**Fig. 21**) GO terms mainly related to different metabolic processes, such as: nitrogen and the peptide biosynthesis and metabolisms and translational process.

HIMvsKB\_4and8h\_DEGsUPinHIM

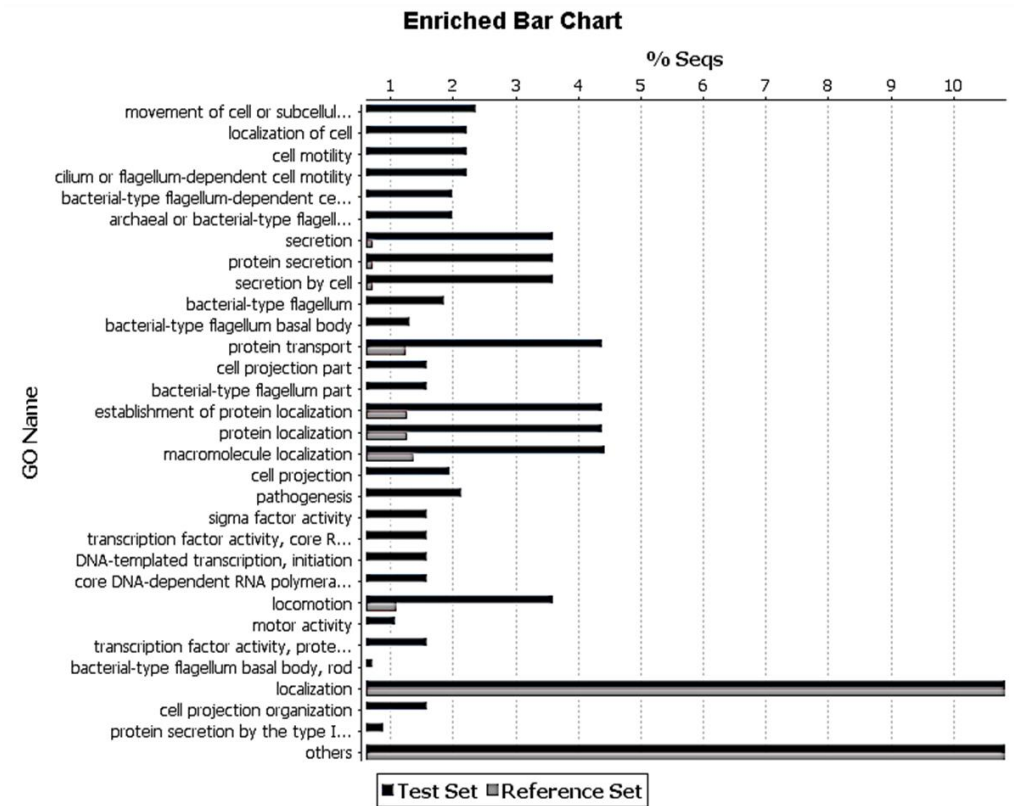


*Figure 20:* Functional enrichment analysis considering the GO term of the DEGs between HIM and KB at 4 and 8 hpi considering the DEGs up-regulated in HIM. The Test Set represents the percentage of the DEGs of V-13, annotated with the select GO term, while, the Reference Set is the percentage of genes represented in the microarray chip.

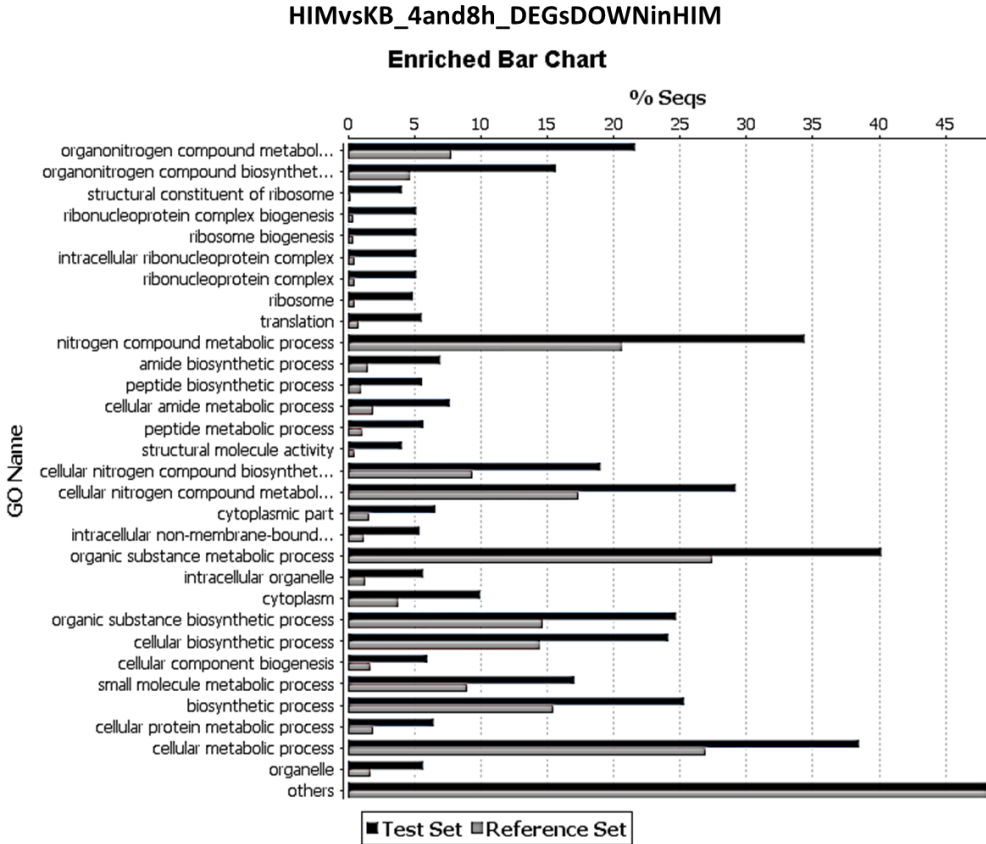


*Figure 21:* Functional enrichment analysis considering the GO term of the DEGs between HIM and KB at 4 and 8 hpi considering the DEGs down-regulated in HIM. The Test Set represents the percentage of the DEGs of V-13, annotated with the select GO term, while, the Reference Set is the percentage of genes represented in the microarray chip.

### 4.2.3.3 GO TERM ENRICHMENT AMONG DEGs IN J35 (BIOVAR 1)

The GO terms enriched among DEGs between HIM and KB of J35 at both time points (4 and 8 hpi) (**Fig. 22**) showed that the enriched classes were related to chemotaxis, locomotion, signal transduction activity and process linked to the membrane biosynthesis.

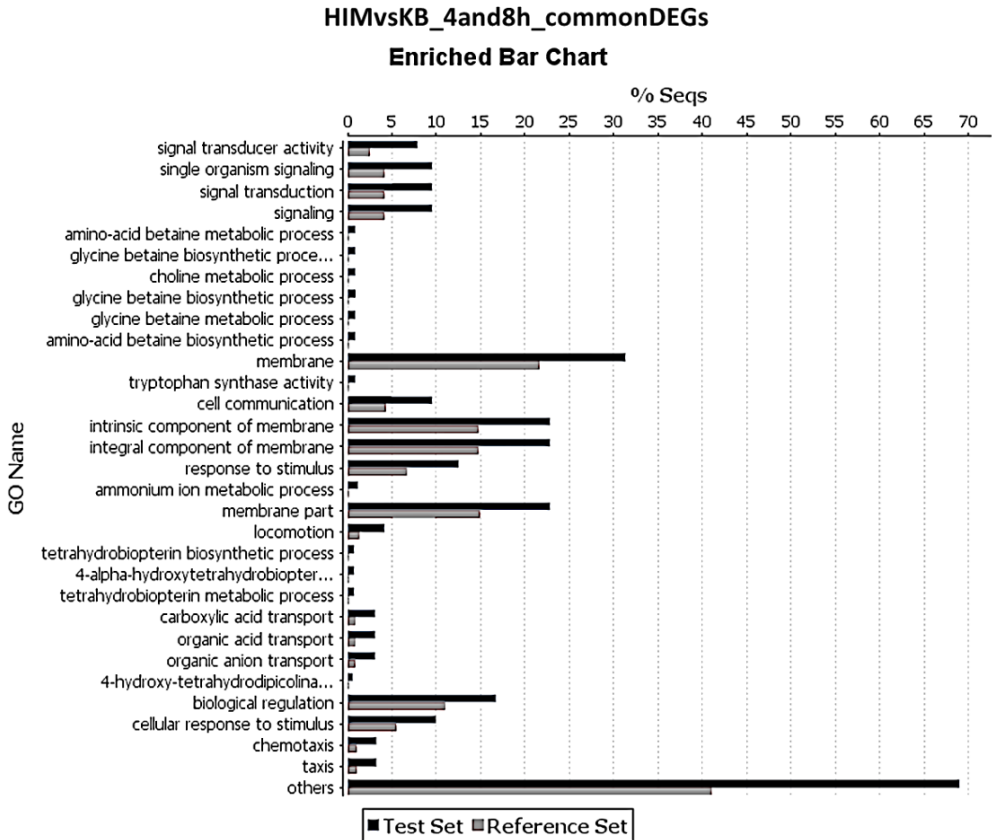


*Figure 22:* Functional enrichment analysis considering the GO term of the DEGs between HIM and KB at both time points tested (4 and 8 h). The Test Set represents the percentage of the DEGs of J35, annotated with the select GO term, while, the Reference Set is the percentage of genes represented in the microarray chip.



When considering the two time points separately, we can observe at 4 hpi (**Fig. 23**) enriched classes belonging to translation processes, and processes linked to the peptide and cellular metabolisms.

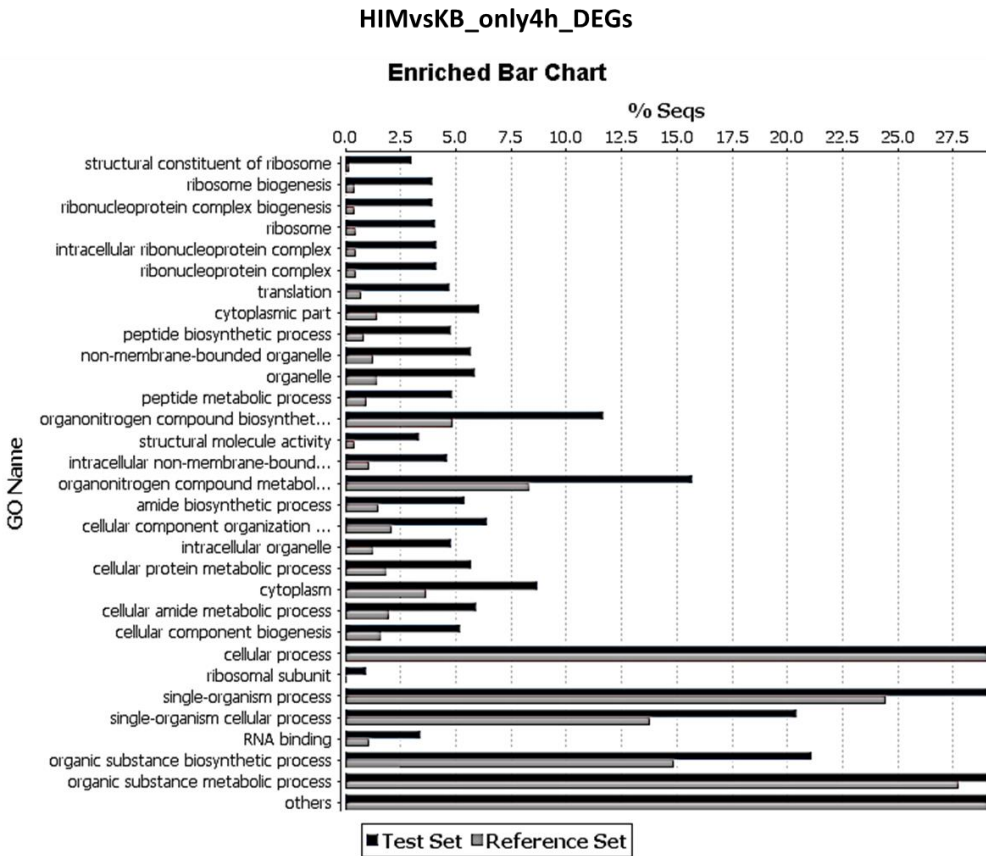


*Figure 23:* Functional enrichment analysis considering the GO term of the DEGs between HIM and KB at 4h. The Test Set represents the percentage of the DEGs of J35, annotated with the select GO term, while, the Reference Set is the percentage of genes represented in the microarray chip.

The same comparison, at 8 hpi (**Fig. 24**), showed functional enrichments in transcription, amino acid, biological regulation and small molecules catabolic processes; but also metal ion transport and iron ion transport activity.

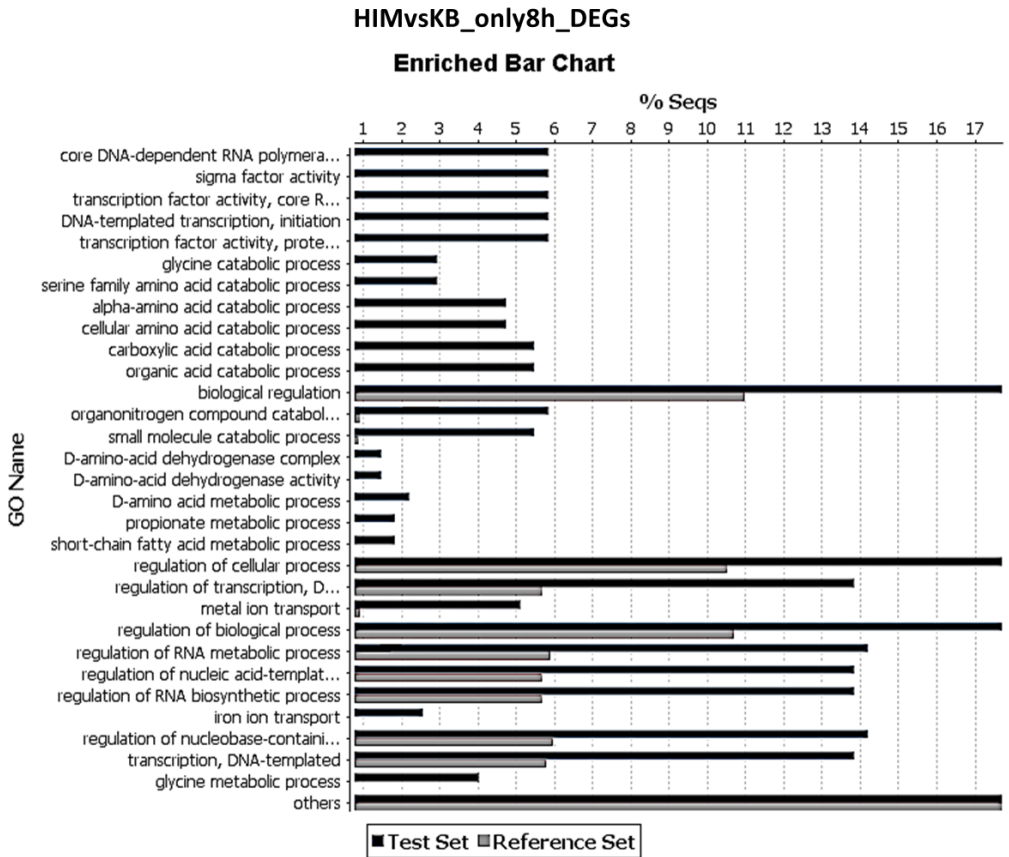


*Figure 24:* Functional enrichment analysis considering the GO term of the DEGs between HIM and KB at 8h. The Test Set represents the percentage of the DEGs of J35, annotated with the select GO term, while, the Reference Set is the percentage of genes represented in the microarray chip.

The same analysis was repeated considering only the up- or the down-regulated groups of DEGs at both time point. Among the up-regulated transcripts (**Fig. 25**), we could observe enriched classes belonging to cell motility such as: flagella, locomotion and motor activity; signalling, chemotaxis, and transcriptional regulation processes.

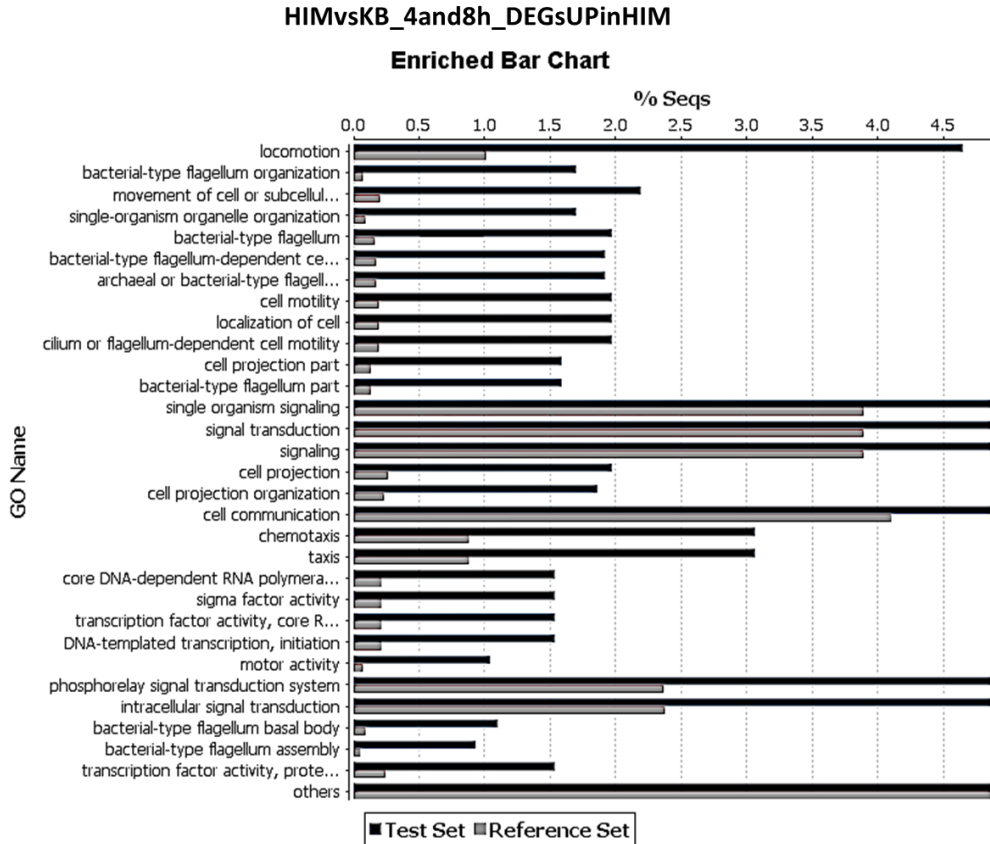


*Figure 25:* Functional enrichment analysis considering the GO term of the DEGs between HIM and KB at 4 and 8 hpi considering the DEGs up-regulated in HIM. The Test Set represents the percentage of the DEGs of J35, annotated with the select GO term, while, the Reference Set is the percentage of genes represented in the microarray chip.

Conversely, the functional enrichment on DEGs down-regulated in HIM showed (Fig. 26) classes mainly related to translation and ribosomal biogenesis, small molecule metabolic process and nitrogen compound metabolic process.

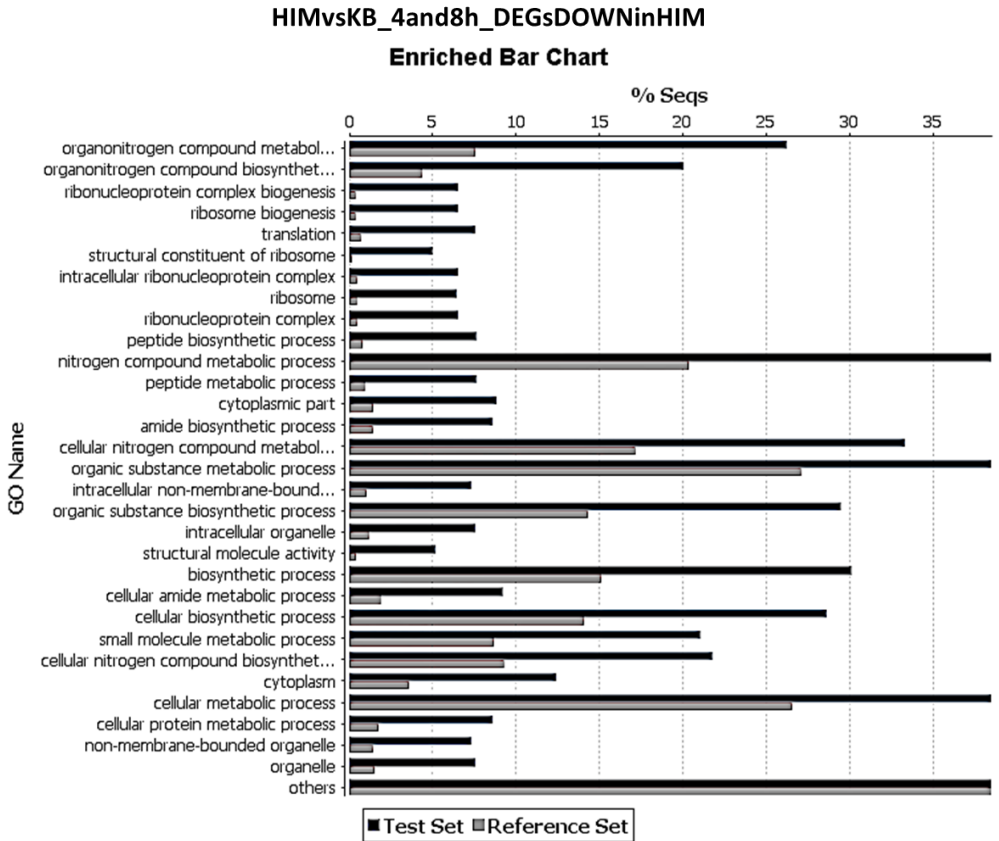


*Figure 26:* Functional enrichment analysis considering the GO term of the DEGs between HIM and KB at 4 and 8 hpi considering the DEGs down-regulated in HIM. The Test Set represents the percentage of the DEGs of J35, annotated with the select GO term, while, the Reference Set is the percentage of genes represented in the microarray chip.

#### 4.2.3.4 GO TERM ENRICHMENT AMONG DEGs IN KN2 (BIOVAR 2)

The GO terms enriched among DEGs between HIM and KB of KN2 at both time points (4 and 8 hpi) (**Fig. 27**) showed that the main enriched classes were related to the organic substances metabolic processes, primary metabolic, small molecule metabolic and nitrogen compound metabolic processes; catalytic activity, transporter activity, ion transmembrane transport and biosynthesis processes of alpha-amino acids and tryptophan.

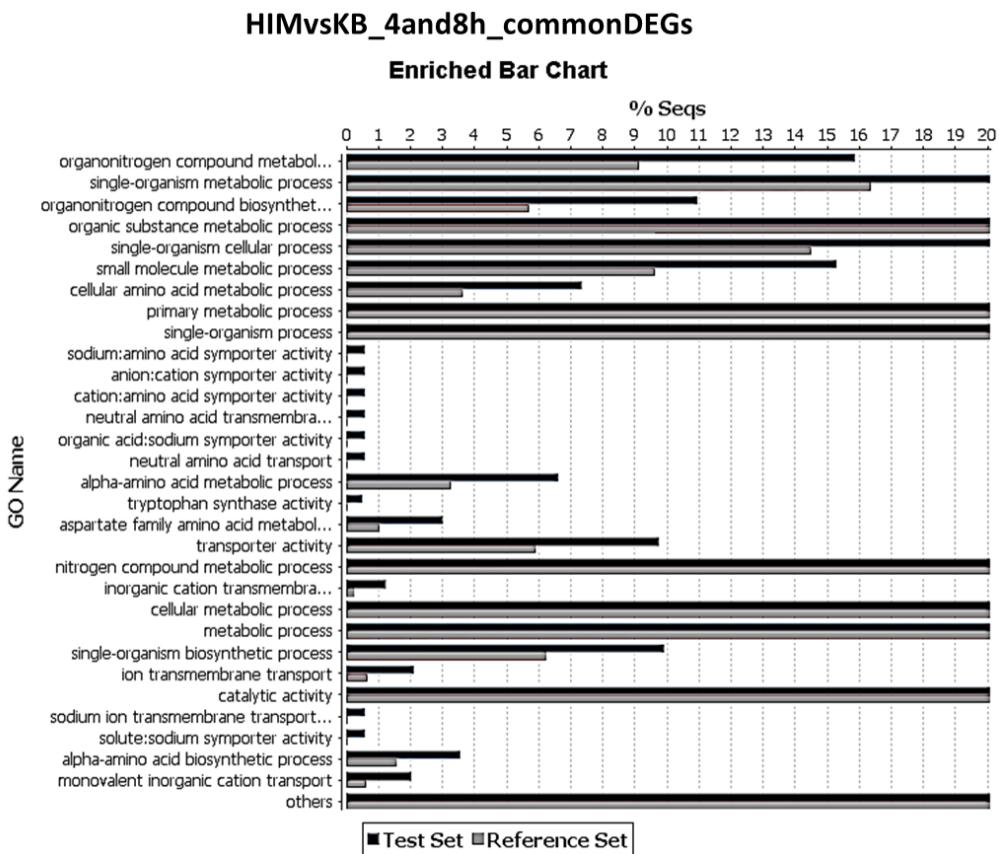


*Figure 27:* Functional enrichment analysis considering the GO term of the DEGs between HIM and KB at both time points tested (4 and 8 h). The Test Set represents the percentage of the DEGs of KN2, annotated with the select GO term, while, the Reference Set is the percentage of genes represented in the microarray chip.

When considering the two time points separately, we could observe at 4 hpi (**Fig. 28**) enriched classes belonging to organonitrogen compound metabolism, ribosome activity, peptide biosynthesis and translation processes.

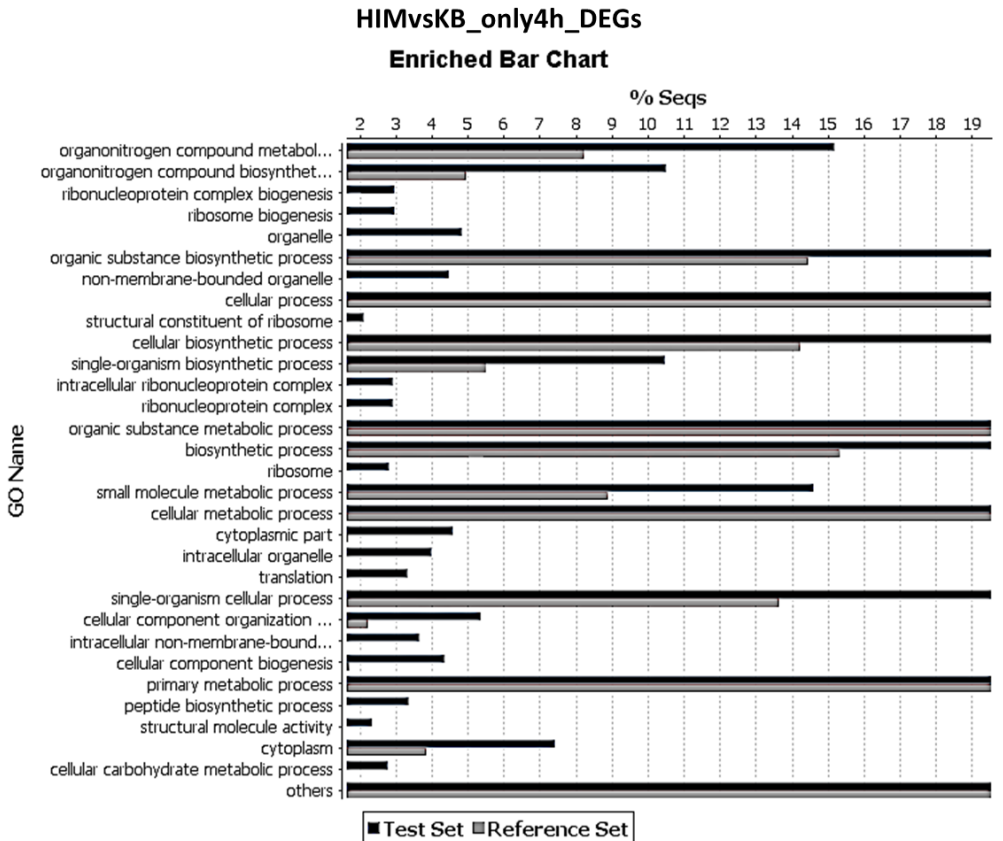


*Figure 28:* Functional enrichment analysis considering the GO term of the DEGs between HIM and KB at 4h. The Test Set represents the percentage of the DEGs of KN2, annotated with the select GO term, while, the Reference Set is the percentage of genes represented in the microarray chip.

The same comparison, at 8 hpi (**Fig. 29**), showed functional enrichments in alginic acid metabolic and biosynthesis processes.

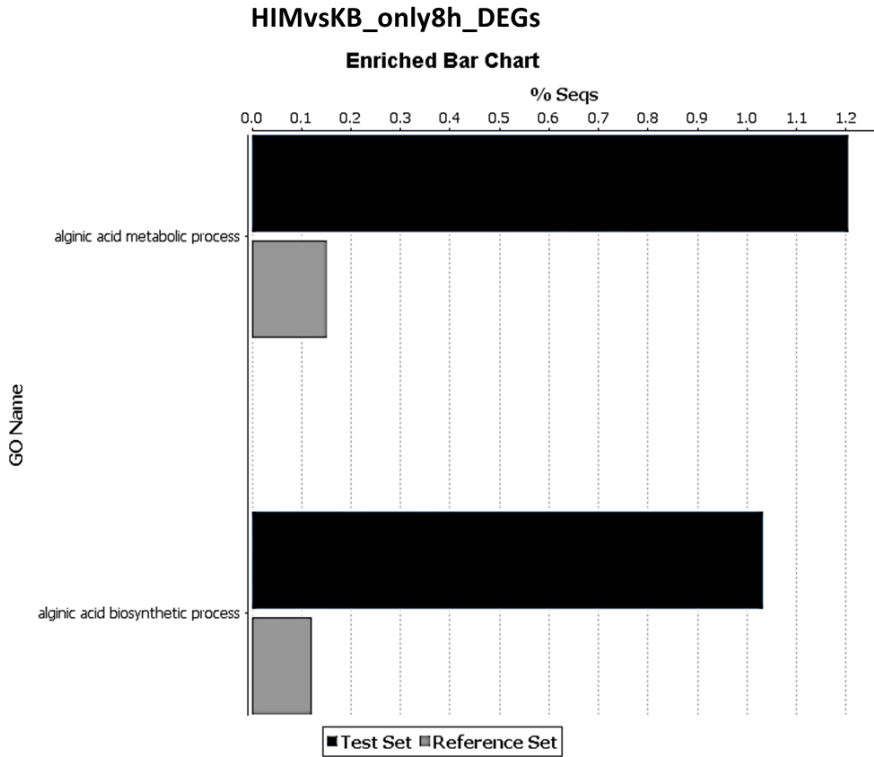


*Figure 29:* Functional enrichment analysis considering the GO term of the DEGs between HIM and KB at 8h. The Test Set represents the percentage of the DEGs of KN2, annotated with the select GO term, while, the Reference Set is the percentage of genes represented in the microarray chip.

The same analysis was repeated considering only the up- or the down-regulated groups of DEGs at both time point. Among the up-regulated transcripts (**Fig. 30**), we could observe enriched classes belonging to cellular carbohydrate metabolic processes, cell motility, signalling, CoA-transferase activity and transcription regulation processes.

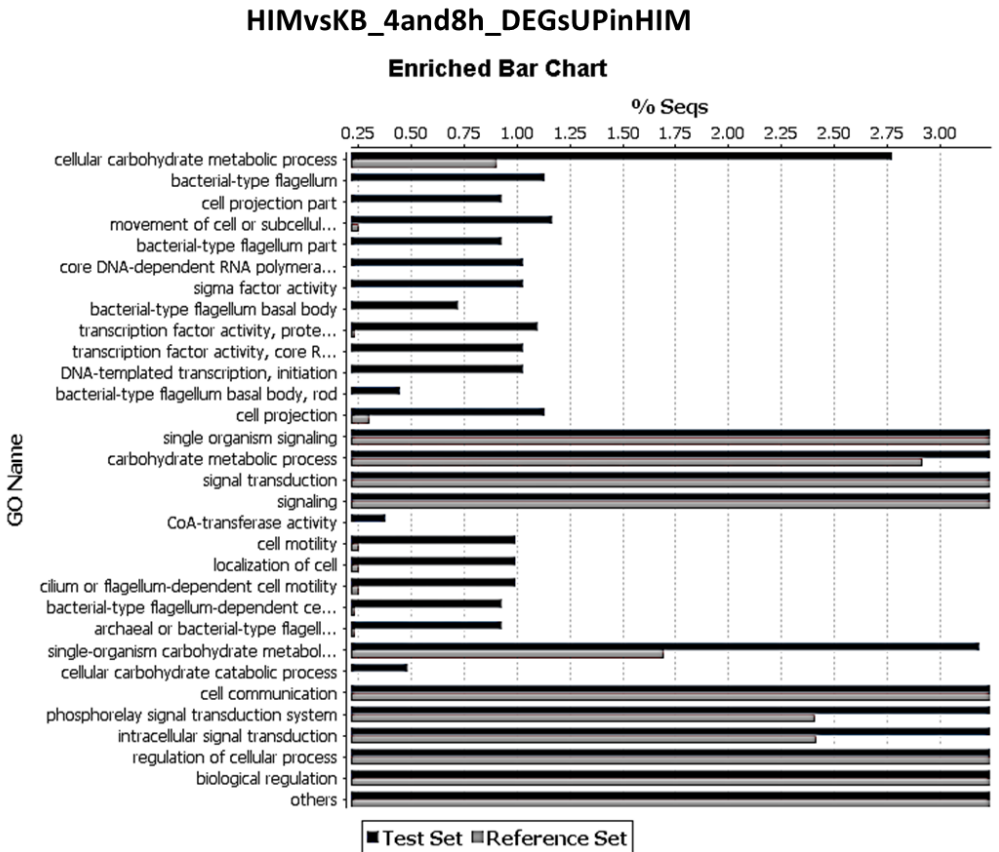


*Figure 30:* Functional enrichment analysis considering the GO term of the DEGs between HIM and KB at 4 and 8 hpi considering the DEGs up-regulated in HIM. The Test Set represents the percentage of the DEGs of KN2, annotated with the select GO term, while, the Reference Set is the percentage of genes represented in the microarray chip.

Conversely the down-regulated transcripts (**Fig. 31**) showed enriched classes belonging to the organonitrogen compound biosynthesis, small molecule metabolic process, catalytic activity, translation activity, carbohydrate derivative metabolism.



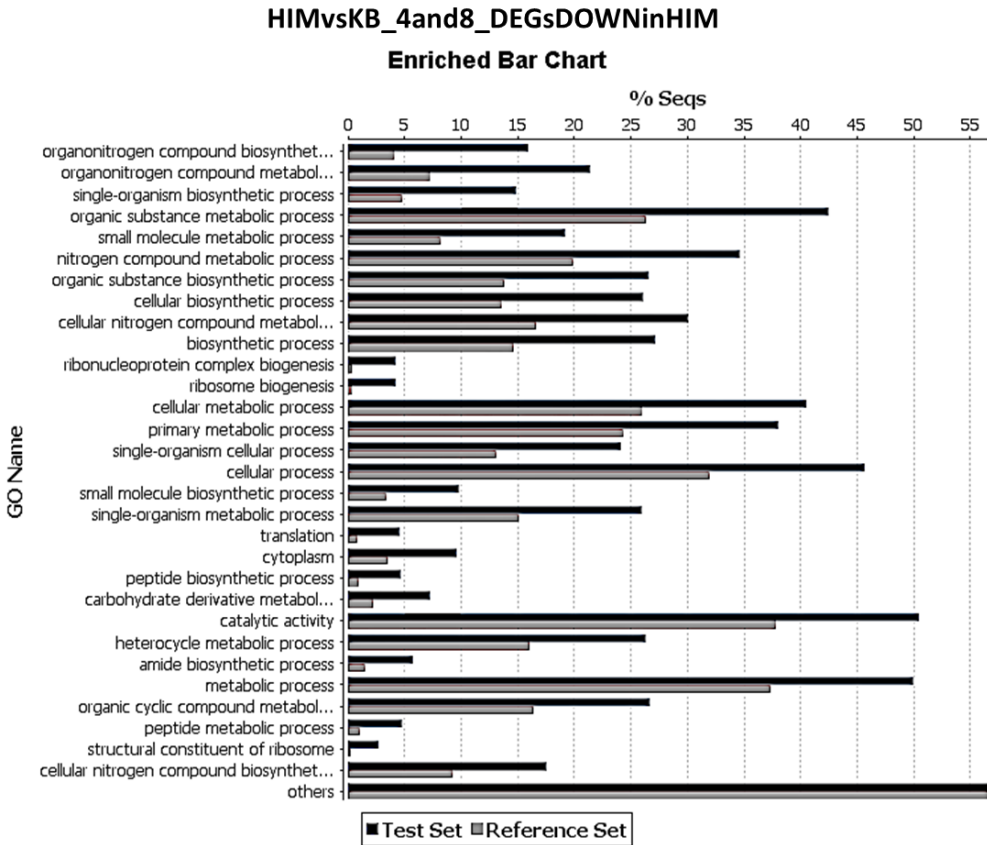


*Figure 31:* Functional enrichment analysis considering the GO term of the DEGs between HIM and KB at 4 and 8 hpi considering the DEGs down-regulated in HIM. The Test Set represents the percentage of the DEGs of KN2, annotated with the select GO term, while, the Reference Set is the percentage of genes represented in the microarray chip.

#### 4.2.3.5 GO TERM ENRICHMENT AMONG DEGs IN Pst DC3000

The GO terms enriched among DEGs between HIM and KB of Pst DC3000 at both time points (4 and 8 hpi) (**Fig. 32**) shows that the main enriched classes are related to organonitrogen compound metabolism, pathogenesis, interaction with host via TTSS, proton and hydrogen transport, cellular amino acids metabolic and morphology modification processes.

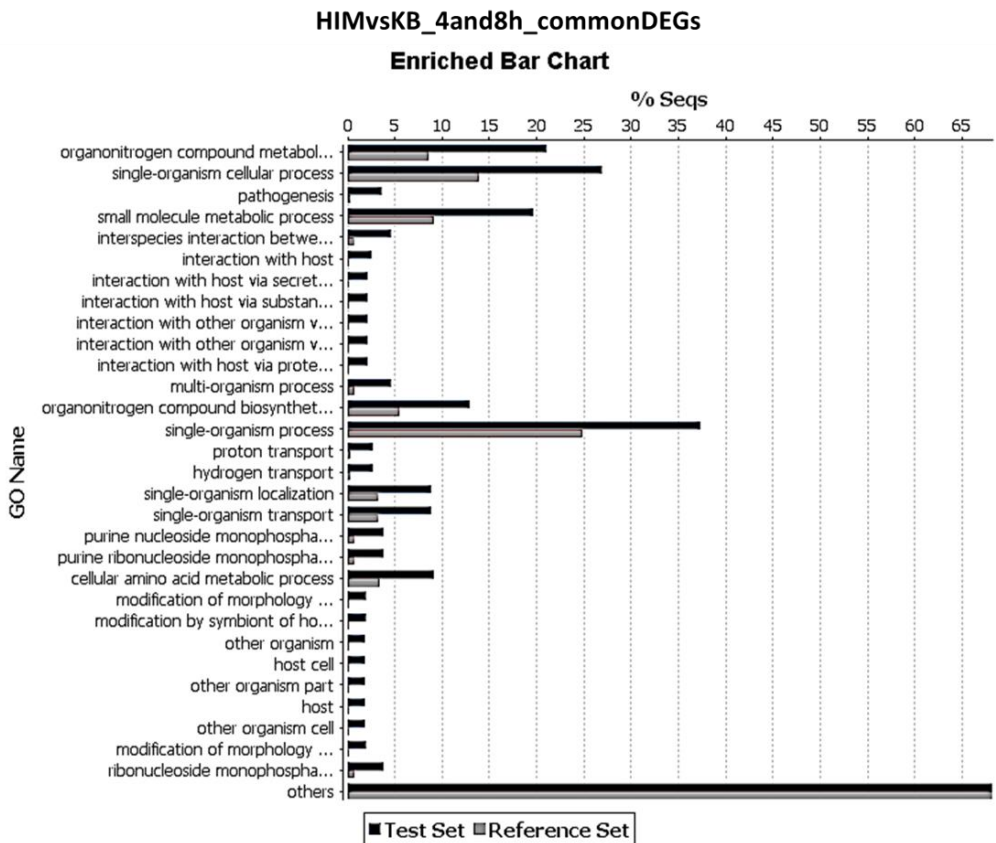


*Figure 32:* Functional enrichment analysis considering the GO term of the DEGs between HIM and KB at both time points tested (4 and 8 h). The Test Set represents the percentage of the DEGs of Pst DC3000, annotated with the select GO term, while, the Reference Set is the percentage of genes represented in the microarray chip.

When considering the two time points separately, we could observe at 4 hpi (**Fig. 33**) enriched classes belonging to organonitrogen compound biosynthesis and metabolism, catalytic activity, small molecule metabolic process, transferase activity, translation process and post-transcriptional modification activity.

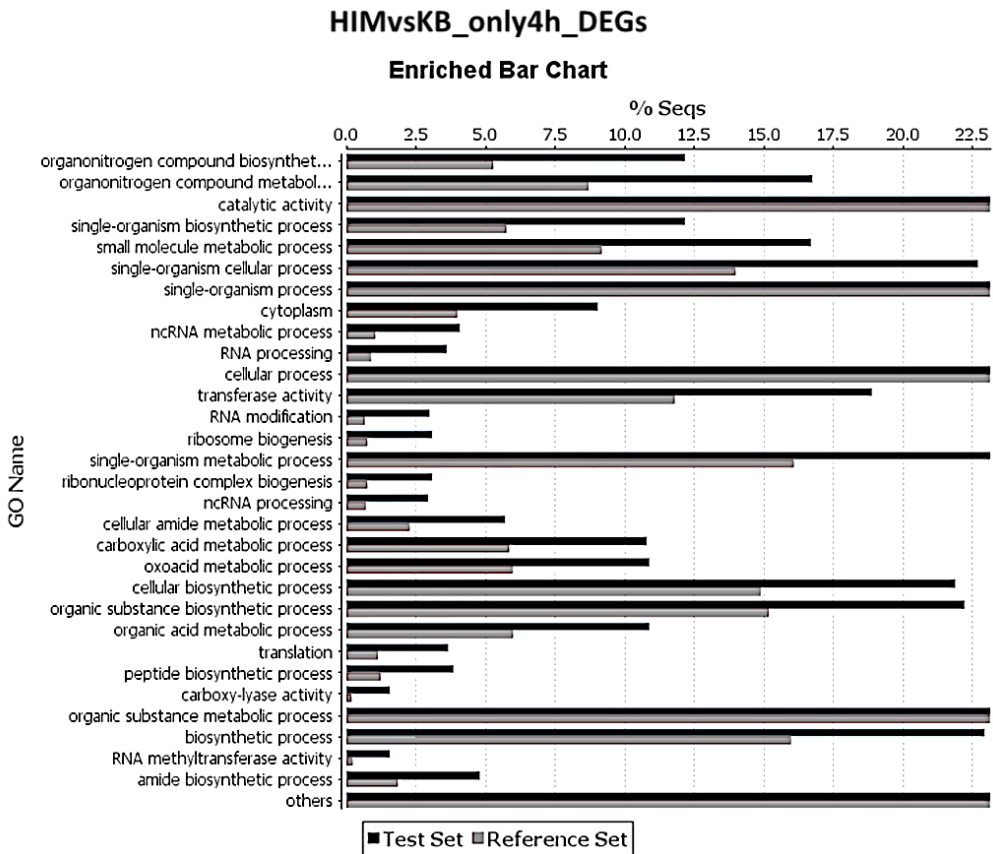


*Figure 33:* Functional enrichment analysis considering the GO term of the DEGs between HIM and KB at 4h. The Test Set represents the percentage of the DEGs of Pst DC3000, annotated with the select GO term, while, the Reference Set is the percentage of genes represented in the microarray chip.

At 8 hpi (**Fig. 34**) we could instead observe enriched classes belonging to metabolic processes, cation and vitamin binding, catalytic activity, metal ion and ion binding, cofactor biosynthesis process, oxidation-reduction activity and arsenite transport.

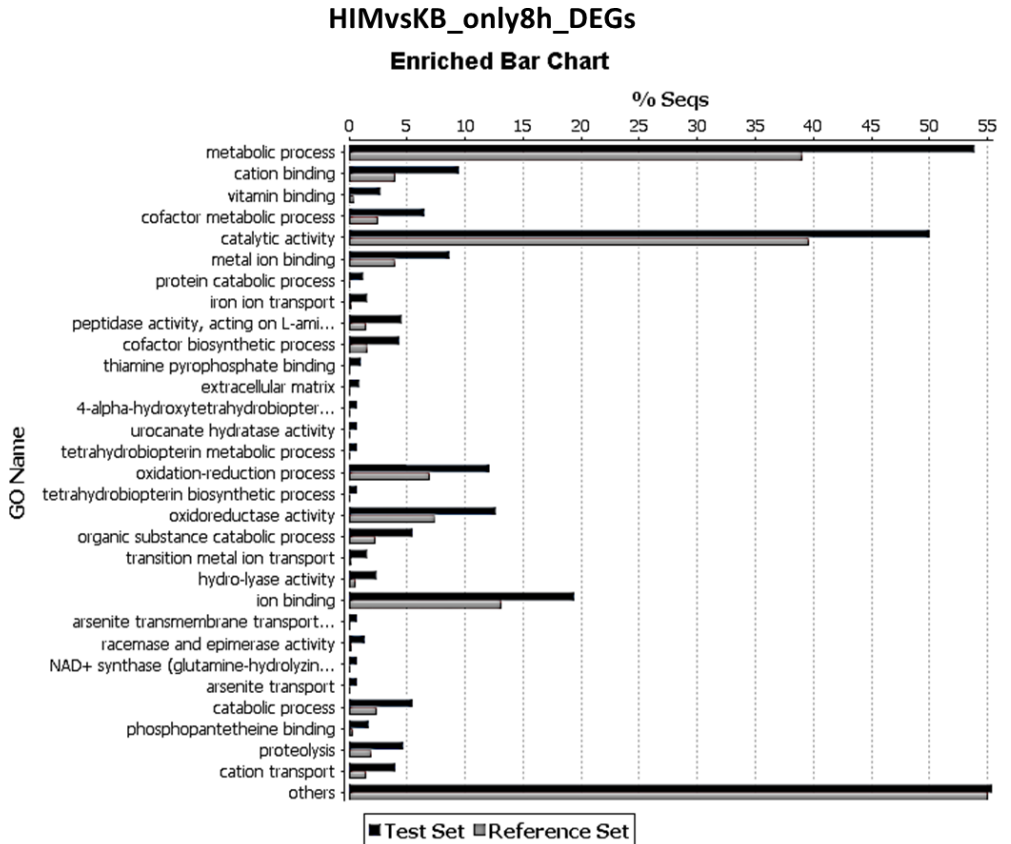


*Figure 34:* Functional enrichment analysis considering the GO term of the DEGs between HIM and KB at 8h. The Test Set represents the percentage of the DEGs of Pst DC3000, annotated with the select GO term, while, the Reference Set is the percentage of genes represented in the microarray chip.

The same analysis was repeated considering only the up- or the down-regulated groups of DEGs at both time point. Among the up-regulated transcripts (**Fig. 35**), we could observe enriched classes belonging to pathogenesis, interaction with host mediated by the TTSS, morphology modification and response to host activities and regulation of programmed cell death.

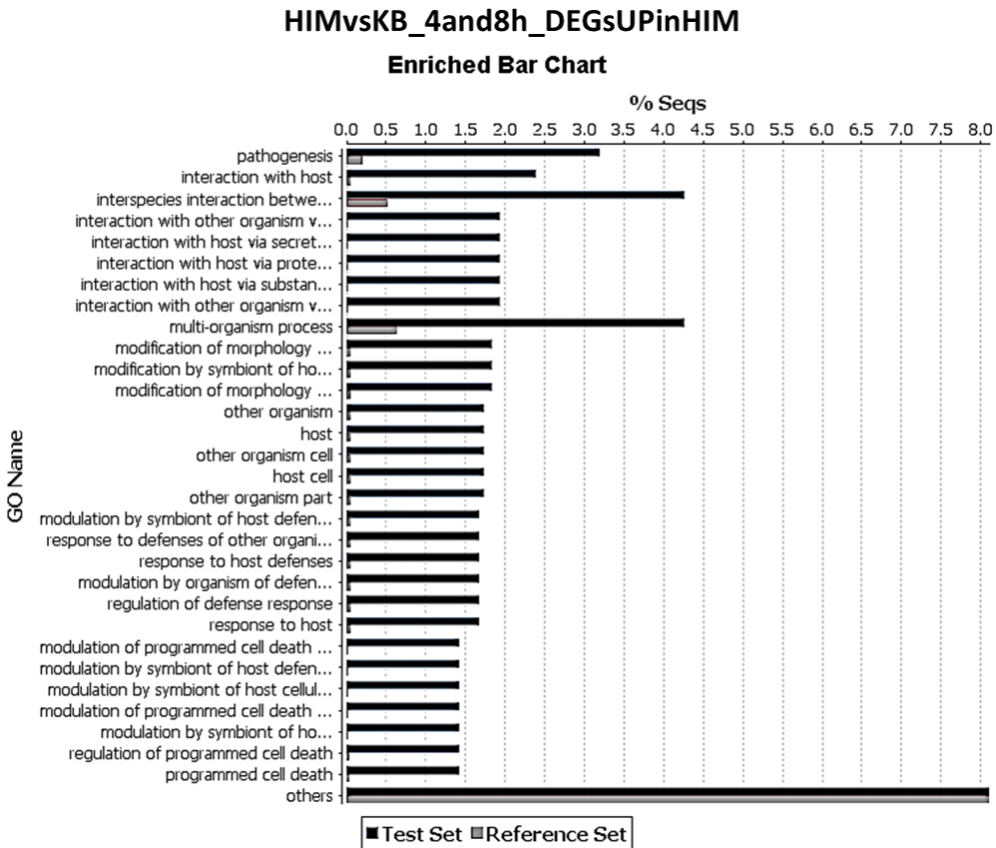


*Figure 35:* Functional enrichment analysis considering the GO term of the DEGs between HIM and KB at 4 and 8 hpi considering the DEGs up-regulated in HIM. The Test Set represents the percentage of the DEGs of Pst DC3000, annotated with the select GO term, while, the Reference Set is the percentage of genes represented in the microarray chip.

Conversely the down-regulated transcripts (**Fig. 36**) showed enriched classes belonging to organonitrogen compound metabolism, small molecule metabolic biosynthesis, and primary metabolic processes; and, translation activities and ribosome biogenesis.

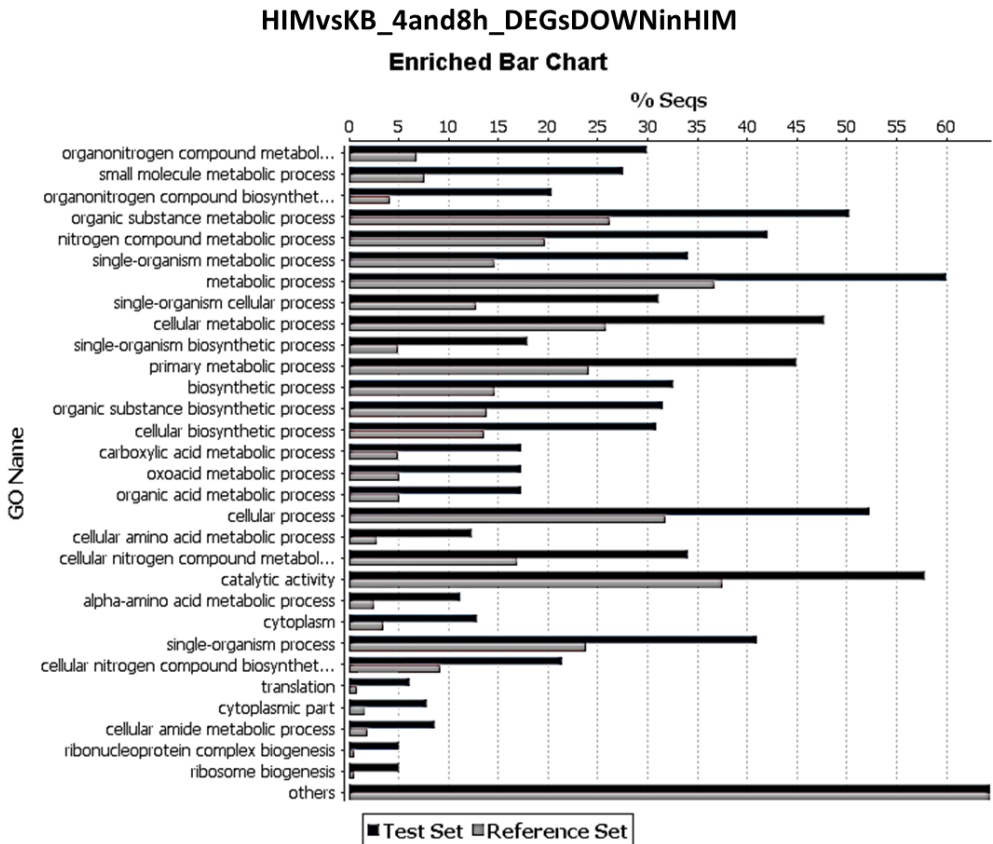


*Figure 36:* Functional enrichment analysis considering the GO term of the DEGs between HIM and KB at 4 and 8 hpi considering the DEGs down-regulated in HIM. The Test Set represents the percentage of the DEGs of Pst DC3000, annotated with the select GO term, while, the Reference Set is the percentage of genes represented in the microarray chip.

## 5. DISCUSSION

Plant pathogenic bacteria, such as *Pseudomonas syringae*, evolved different strategies to overcome the plant immune responses, to colonize the plant apoplast and then replicate aggressively to establish disease. The first phase of the infection requires different mechanisms carried out by the pathogen to adapt itself in the apoplast, a new hard environment characterized by low pH, hypo-osmotic pressure and poorness of nutrient [17]. Therefore, preliminary to the transcriptomic analyses, we investigated the adaptability of the different *Pseudomonas syringae* strains to low-nutrient conditions, in HIM medium.

As expected, the growth in minimal medium was slower than in the rich medium for all strains, with a growth rate strongly reduced after 12-16h, suggesting that some components in the minimal medium were likely depleted at that time, as already reported [18]. Moreover, the measured reduction of cell density was associated with the formation of cell aggregates, although with different timing and morphology for the different strains. For instance, formation of aggregates was particularly evident in biovars 1 and 3. These aggregates could be interpreted as an initial stage of biofilm formation, in response to stressful conditions. Indeed, cell aggregation was not observed in KB, where bacteria continued in a planktonic life-style, with continuous cell density increase up to the end of the experiment, after 48h. However, the influence of minimal medium in promoting aggregate formation are still under study.

Interestingly, cell aggregates formation also correlated with the up-regulation of genes encoding cyclic diguanylate (c-di-GMP) in the Psa strain CRA-FRU 8.43 (biovar3) grown in HIM. This signalling molecule has been reported to regulate biofilm formation, motility inhibition, switching regulation between the planktonic and sessile life-style and it is also a direct regulator of virulence factors [19, 20].

One fundamental event induced during bacterial colonization of the apoplast is the assembly of the *hrp*-encoded TTSS. As a matter of fact, *hrp*-gene expression is induced after infiltration of bacteria into plant leaves or in HIM, but is repressed in rich media, such as KB [21, 22, 23, 24]. In our experiments, *hrp* genes was occurred in HIM and not in KB within 8 hours after inoculum. This is in agreement with results reported by Xiao and associates (1992), who observed that *hrp* genes of *Pseudomonas syringae* pv. *syringae* were induced in the minimal medium (M63M) within 6 hours after inoculation and repressed in rich medium (KB). Our preliminary experiments on growth kinetics allowed us to best design the next microarray experiments aimed at investigating molecular bases of the variegated Psa virulence. In fact, we

decided to perform transcriptome analysis at 4 and 8 hours post-inoculum in minimal or rich medium based on the evidences that we gained that these conditions and timing maximize detection of *hrp* genes, thus empowering comparison of expression of virulence-related genes among biovars.

Growth in apoplastic-mimicking conditions (that is, in minimal medium) induced the major transcriptomic differences among the biovars. In particular, the strains belonging to the biovar 1 and 2 (J35 and KN2, respectively) showed an earlier gene modulation compared to other *Psa* strains, CRA-FRU 8.43 and V-13 (biovar 3). Moreover, the different biovars seem to activate two different primary virulence mechanisms, or the TTSS or the flagellum. Of note, the wide modulation of genes involved in TTSS regulation observed in the biovar 3 may explain at least in part the higher virulence of this biovar.

Thanks to increased availability of genomic data, it is becoming increasingly clear that genes encoding the flagellar components are always located on the bacterial chromosome and co-evolved with the rest of the genome, while the injectisome (TTSS)-encoding genes are often situated in virulence plasmids or pathogenicity islands. These elements described in the strains of the last *Psa* world-wide outbreak (*Psa* strains belonging to biovar 3) by Butler and associated (2013) [25], show a phylogenetic distribution independent from the respective species as they can be transferred among different bacteria in nature [26].

Considering the bacterial gene modulation observed in HIM, we notice that the *Pseudomonas syringae* strains presented a similar trend of down-regulation profiles, *i.e.*: GO terms belonging to translation processes, nitrogen compound metabolism, amino acids metabolism and nutrient assimilation classes. A similar negative regulation of nutrient assimilation was also reported in the work of Rico and Preston (2007) [27], in which *Pst* DC3000 appeared to use a narrow range of carbon and nitrogen sources when pre-inoculated in apoplast extracts or HIM. Those authors suggested that the nutrient limitation and the high stress suffered in HIM and in the apoplast extracts could lead to the alteration of the expression of genes involved in nutrient assimilation and thus limiting the adaptation of the microorganism to novel substrates. At variance, functional enriched analysis of genes up-regulated in HIM highlighted marked differences among biovars and strains, suggesting a more variegated reaction to nutrient-limiting conditions and therefore to the perception of plant apoplast. In particular, our data shows that *Psa* strains of biovar 3 (*i.e.*: CRA-FRU 8.43 and V-13) favour up-regulation of genes involved in the TTSS and production of effectors proteins, thus suggesting TTSS as the

---



primary virulence mechanism for these strains. Differently, Psa of biovar 1 and 2 exhibited preferred up-regulation of genes involved in the flagellum and cell locomotion. However, our analysis also highlighted differences within strains of the same biovar: for instance, despite both CRA-FRU 8.43 and V-13 strains (both of biovar 3) differentiate themselves from other Psa strains by showing enrichment of pathogenesis-related GO terms the extent of enriched terms related to this important process was higher in CRA-FRU 8.43 than in V-13. Similarly, the number of enriched GO terms (considering the up-regulated DEGs in HIM) related to iron transport and chelation was higher in CRAFRU 8.43 than in V13. As reported by Kim and coworkers (2009) [18,19], iron is a limiting nutrient in HIM and iron limitation plays an important role in inducing several virulence genes in Pst DC3000. Moreover, iron is also an essential element for bacteria since it is involved in the TCA cycle, electron transport chain, DNA synthesis and other crucial functions [28].

In CRA-FRU 8.43 we found up-regulated also classes of gene involved in the tryptophan synthesis, CoA-transferase activity, c-di-GMP binding suggesting possible virulence mechanism that could be involved in the biovar 3 pathogenicity. Indeed, tryptophan is the precursor of the anthranilate in the kynurenine pathways which could play a role in the regulation of virulence in *Pseudomonas aeruginosa* [29]. While, it has been established that the CoA-transferase activity is under the control of the HopZ1a effector, which is an essential pathogenic activity required to suppress: the host-plant secretory pathway and the cell-wall mediates defence mechanisms [30].

Considering the strains belonging to the other two biovars, we can observe some peculiar characteristics. In J35 was observed as up-regulated a class of GO terms related to the chemotaxis which is a pathway well studied in Pst DC3000. Indeed, it was observed that the fitness of Pst DC3000 within its host is dependent on the two main genes involved in the chemotaxis pathways *i.e.*: *che1* and *che2* [31]. The microarray analysis showed that KN2 strain modulated few primary virulence mechanisms mainly associated to the flagellum. Moreover, the functional enrichment analysis suggests modulation of different metabolic activities, compared to the other strain in response to apoplastic-mimic growth conditions, such as: cell-communication and carbohydrate metabolism. This is indicative of a primary mechanism rather focused on adaptation to the new environment than to pathogenic activities. Regarding to Pst DC3000 strain included in our study, our analysis indicates implication of an additional virulence mechanism involved in the regulation of programmed cell death in

response to growth in minimal medium. This observation is in agreement with previous reported in other pathovars such as *Ps phaseolicola* and *Ps syringae*, reporting modulation of genes to suppress the programmed cell death in plant, was observed also in other [32].

Future efforts should be devoted to detect the effect of the kiwifruit apoplast in the *Psa* transcription regulation and how the transcriptional profile of the *Psa* strains change from the epiphytic to the *in planta* environment. Indeed, it was observed that Pst DC3000 grew slightly better than *P. tabaci* and *fluorescens* in the tomato apoplast extracts [27], indicating the capacity evolved by Pst DC3000 to assimilate tomato metabolites able to increase its fitness, suggesting that the differences in apoplast composition could contribute to the host specificity [33]. Moreover, in a study conducted on *P. syringae* B728a recovered from leaf surface and apoplast it was observed that these two habitats played a crucial role in the transcriptional regulation and pathogen adaptation. Indeed, the epiphytic environment promotes the phenylalanine degradation which could be a mechanism to overcome the plant defence responses; while, the apoplast promotes the synthesis of secondary metabolites and possible phytotoxins [34].

Finally, our study revealed up-regulation of genes involved in transcriptional regulation as a core mechanism shared among the *Pseudomonas* strains, suggesting this process is strongly required for adaptation in a new hostile environment, as could be the one mimicked by the minimal medium.

Results presented in this work suggested a panel of different mechanisms that could be activated by different *Psa* biovars in the apoplast and provide sets of candidate genes that could be used as targets to develop new control strategies. Moreover, the bulk of expression data produced represents a valuable resource for future in-depth studies aimed at understanding the differences in virulence among biovars of this economically crucial bacterial species.

6. SUPPLEMENTAL RESOURCES

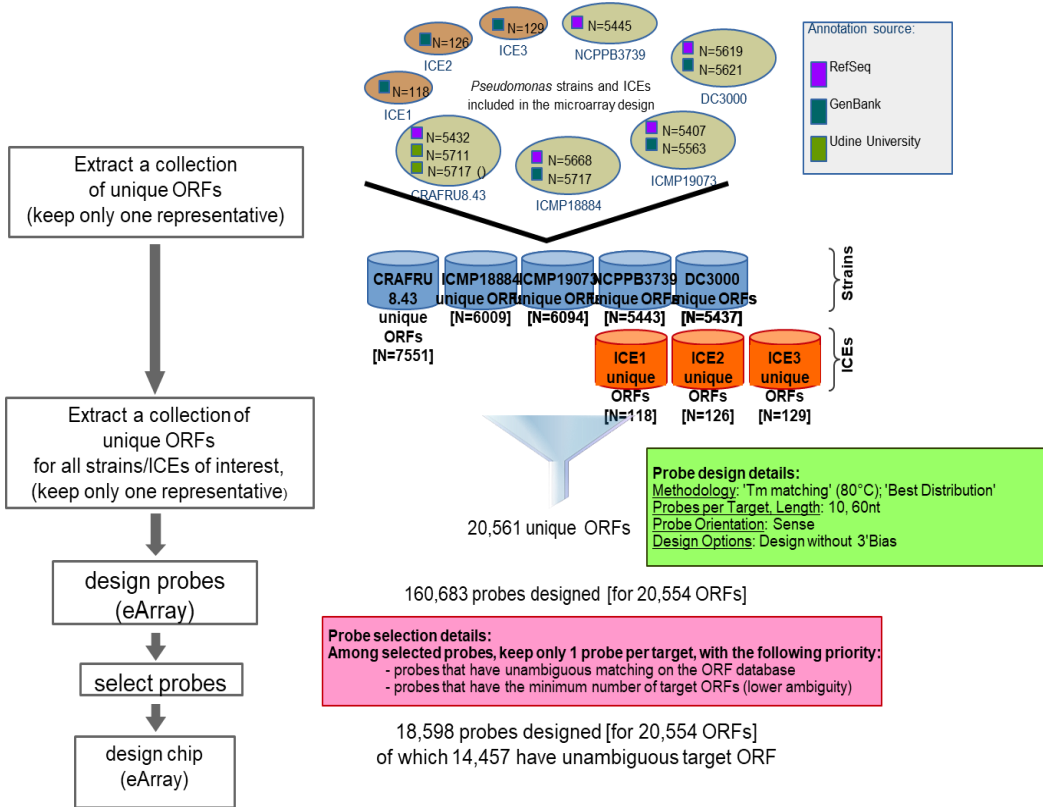


Figure 1: Flow-chart showing the procedure followed for the design of the multi-strain custom microarray.

List of the primers used in this chapter:

Gene	Primer Name	Sequence	TM
<i>rpoD</i>	rpODFORRT	GTTGCCCTTGCCGAATTGTT	60
<i>rpoD</i>	rpODREVRT	CATCACGTACGCACAACACTGC	62
<i>hprW</i>	hrpWFOR	GCCGACAAGTCGATGGGTAA	62
<i>hprW</i>	hrpWREV	TCGTTCTCACCCAGGTTAC	62
<i>hrpC</i>	hrpCFOR	TCCAGACGTTTACGCGCATC	62
<i>hrpC</i>	hrpCREV	GGCTGCAGTGATGAGACTGA	62

## 7. REFERENCES

- 1 Takashi, F. and Hiroyuki, S. (2106) Genome analysis of the kiwifruit canker pathogen *Pseudomonas syringae* pv. *actinidiae* biovar 5. *Scientific Report*, 6:21399, DOI: 10.1038/srep21399
- 2 Zupeng, W. *et al.* (2017) Whole transcriptome sequencing of *Pseudomonas syringae* pv. *actinidiae*-infected kiwifruit plants reveals species-specific interaction between long non coding RNA and coding genes. *Scientific Report*, 7: 4910, DOI:10.1038/s41598-017-05377-y
- 3 Vanneste, J. L. *et al.* (2011) Detection of *Pseudomonas syringae* pv. *actinidiae* in kiwifruit pollen samples. *New Zealand Plant Protection*, 64: 246-251
- 4 Chang, J. H. Zipfel, C. He, S. Y. *et al.* (2016) Bacteria establish an aqueous living space in plants crucial for virulence. *Nature*, Vol 539: 524, 528, DOI:10.1038/nature20166
- 5 Lindgren, P. B. Peet, R. C. Panopoulos, N. J. (1986) Gene cluster of *Pseudomonas syringae* pv. "*phaseolicola*" controls pathogenicity of bean plants and hypersensitivity of nonhost plants. *Journal of Bacteriology*, vol. 168 no. 2 512-522, DOI: 10.1128/jb.168.2.512-522.1986
- 6 McCann, H. C. *et al.* (2010) Genomic analysis of the kiwifruit pathogen *Pseudomonas syringae* pv. *actinidiae* provides insight into the origins of an emergent plant disease. *Plos Pathogens*, 9(7): e1003503, DOI:10.1371/journal.ppat.1003503
- 7 He, S. Y. *et al.* (2003) Type III protein secretion in *Pseudomonas syringae*. *Elsevier Microbes and Infection*, 5:301–310, DOI: 1 0.1016/S286-4579(03)00032-7

- 8** McCann, H. C. *et al.* (2013) Genomic Analysis of the Kiwifruit Pathogen *Pseudomonas syringae* pv. *actinidiae* Provides Insight into the Origins of an Emergent Plant Disease. *PLoS Pathogens*, doi: 10.1371/journal.ppat.1003503
- 9** Marcelletti, S. *et al.* (2011) *Pseudomonas syringae* pv. *actinidiae* draft genomes comparison reveal strain-specific features involved in adaptation and virulence to Actinidia species. *PLoS ONE*, doi: 10.1371/journal.pone.0027297
- 10** Takashi, F. and Hiroyuki, S. (2106) Genome analysis of the kiwifruit canker pathogen *Pseudomona syringae* pv. *actinidiae* biovar 5. *Scientific Report*, 6:21399, doi: 10.1038/srep21399
- 11** Schumacher, J. *et al.* (2014) Differential secretome analysis of *Pseudomonas syringae* pv. tomato using free-gel MS proteomics. *Frontiers in Plant Science*, DOI: 10.3389/fpls.2014.00242
- 11** Rees-George, J. *et al.* (2010) Detection of *Pseudomonas syringae* pv. *actinidiae* using polymerase chain reaction (PCR) primers based on the 16S–23S rDNA intertranscribed spacer region and comparison with PCR primers based on other gene regions. *Plant Pathology*, 59, 453–464, DOI: 10.1111/j.1365-3059.2010.02259.x
- 12** Murray, G. and Mansfield, J. (1999) Early events in host-pathogen interactions. *Elsevier Science*, DOI: biomednet.com/elecref/1369526600200312
- 13** Pfaffl, M. W. (2012) Quantification strategies in Real-time polymerase chain reaction. Chapter 3 of *Quantitative Real-time PCR in Applied Microbiology* edition by Martin Filion, *Caster Academic Press*, ISBN: 978-1-908230-01-0
- 14** Simon, P. (2003) Q-Gene: processing quantitative real-time RT–PCR data. *Bioinformatics*, Volume 19, Issue 11, Pages 1439–1440, DOI: 10.1093/bioinformatics/btg157
- 15** Ramakers, C. Ruijter, J. *et al.* (2003) Assumption-free analysis of quantitative real-time polymerase chain reaction (PCR) data. *Neuroscience Letters*, Volume 339, Issue 1, DOI: 10.1016/S0304-3940(02)01423-4
- 16** Maere, S. Heymans, K. Kuiper, M. (2005) BinGO: a Cytoscape plugin to assess overrepresentation of Gene Ontology categories in biological networks. *Bioinformatics* 21, 3448-3449
- 17** Kim, J. B. *et al.* (2009) Effect of the iron concentration on the growth of *Pseudomonas syringae* and the expression of virulence factors in *hrp*-inducing minimal medium. *Applied and Environmental Microbiology*, p. 2720–2726, DOI: 10.1128/AEM.02738-08

- 18** Kim, J. B. *et al.* (2010) Complex response to culture condition in *Pseudomonas syringae* pv. *tomato* DC3000 continuous cultures: the role of iron in cell growth and virulence factor induction. *Biotechnology and Bioengineering*, Vol. 105, No. 5, DOI: 10.1002/bit.22609
- 19** Cotter, P. A. and Stibitz, S. (2007) c-di-GMP-mediated regulation and biofilm formation. *Current Opinion in Microbiology*, Volume 10, Issue 1, Pages 17-23, DOI: 10.1016/j.mib.2006.12.006
- 20** Tamayo, R. Pratt, J. T. Camilli, A. (2007) Roles of cyclic diguanylate in the regulation of bacterial pathogenesis. *Annu Rev Microbiol*, 61:131–148, DOI: 10.1146/annurev.micro.61.080706.093426
- 21** Brown, I. R. *et al.* (2001) Immunocytochemical localization of HrpA and HrpZ supports a role for the Hrp pilus in the transfer of effector proteins from *Pseudomonas syringae* pv. *tomato* across the host plant cell wall. *Molecular Plant-Microbe Interactions*, Volume 14, Number 3, Pages 394-404, DOI: 10.1094/MPMI.2001.14.3.394
- 22** Hu, W. *et al.* (2001) Immunogold labeling of Hrp pili of *Pseudomonas syringae* pv. *tomato* assembled in minimal medium and in planta. *Molecular Plant-Microbe Interaction*, Volume 14, Number 2, Pages 234-24, DOI: 10.1094/MPMI.2001.14.2.234
- 23** Preston, G. M. (2000) *Pseudomonas syringae* pv. *tomato*: the right pathogen, of the right plant, at the right time. *Molecular Plant Pathology*, Volume 1, Issue 5, Pages 263–275, DOI: 10.1046/j.1364-3703.2000.00036.x
- 24** Xiao, Y. *et al.* (1992) Organization and environmental regulation of the *Pseudomonas syringae* pv. *syringae* 61 hrp cluster. *Journal of bacteriology*, Volume 173, Issue 6, Pages 1734-1741
- 25** Butler, M. I. (2013) *Pseudomonas syringae* pv. *actinidiae* from recent outbreaks of kiwifruit bacterial canker belong to different clones that originated in China. *Plos One*, 8(2): e57464, DOI: 10.1371/journal.pone.0057464
- 26** Diepold, A. and Armitage, P. (2015) Type III secretion system: the bacterial flagellum and the injectisome. *Royal Society Publishing*, DOI: 10.1098/rstb.2015.0020
- 27** Rico, A and Preston, G.M. (2008) *Pseudomonas syringae* pv. *tomato* DC3000 uses constitutive and apoplast-induced nutrient assimilation pathways to catabolize nutrients that are abundant in the tomato apoplast. *Molecular Plant-Microbe Interaction*, Volume 21, Number 2, Pages 269-282, DOI: 10.1094/MPMI-21-2-0269
-

- 28** Cornelis, P. (2010) Iron uptake and methabolism in pseudomonads. *Appl Microbiol Biotechnol* (2010) 86: 1637 doi: org/10.1007/s00253-010-2550-2
- 29** Bortolotti, P. *et al.* (2016) Tryptophan catabolism in *Pseudomonas aeruginosa* and potential for inter-kingdom relationship. *BMC Microbiology*, 16:137, DOI: 10.1186/s12866-016-0756-x
- 30** Lee, A. H. Y. *et al.* (2012) A Bacterial acetyltransferase destroys plant microtubule networks and blocks secretion. *Plos Pathogens*, 8(2): e1002523, DOI: 10.1371/journal.ppat.1002523
- 31** Clarke, C. R. *et al.* (2016) Comparative genomics of *Pseudomonas syringae* pathovar *tomato* reveals novel chemotaxis pathways associated with motility and plant pathogenicity. *PeerJ*, 4:e2570, DOI: 10.7717/peerj.2570
- 32** Jamir, Y. *et al.* (2003) Identification of *Pseudomonas syringae* type III effectors that can suppress programmed cell death in plant and yeast. *The Plant Journal*, 37: 554,565, DOI: 10.1046/j.1365-313X.2003.01982.x
- 33** Xin, X. F. *et al.* (2016) Bacterial establish an aqueous living space in plants crucial for virulence. *Nature*, Volume 539, DOI: 10.1038/nature20166
- 34** Yu, X. *et al.* (2013) Transcriptional responses of *Pseudomonas syringae* to growth in epiphytic versus apoplastic leaf sites. *PNAS*, DOI: 10.1073/pnas.1221892110

## **8. ACKNOWLEDGEMENT**

Dr Marco Scortichini to provide us the strains used in this study. Dr Firrao to share with us the genomic information about the CRA-FRU 8.43 strain. Dr Teresa Colombo to curate the bioinformatic design of the custom microarray and Dr Nicola Vitulo to curate the statistical data analysis of the microarray data.

## Chapter 3: The LuxR solos PsaR3 in

### *Pseudomonas syringae* pv. *actinidiae* biovar 3

#### 1. ABSTRACT

The quorum sensing (QS) involving the perception of *N*-acylhomoserine lactones (AHLs) by specific LuxR receptors is the best understood signal exchange in proteobacteria. It has the function to mediate the expression of virulence factors and to regulate the behaviour of bacterial community and the interaction with the hosts depending on bacterial community density. During the last 15 years, the studies on the QS revealed that the mechanism requires two partner proteins *i.e.*: a member of the LuxI family, responsible for AHL synthesis, and the cognate LuxR AHL-sensor transcription regulator, responsible for AHL perception and gene transcription regulation. However, some proteobacteria possess LuxR proteins lacking the cognate LuxI synthase, and thus named LuxR “solos”. Despite the knowledge on the LuxI/LuxR system, the role and the characteristics of the LuxR solos in many proteobacteria have not been elucidated yet. *Pseudomonas syringae* pv. *actinidiae* (Psa) possesses three LuxR solos, namely PsaR1, PsaR2 and PsaR3, the role of which is still unclear. In this work, we focused on PsaR3 and using a bioinformatic approach we defined its localization on the plasmid, its organization in a cluster of conserved genes. Moreover, we demonstrated, that it is specific of Psa biovar 3. Then, to elucidate the potential role of PsaR3 in Psa gene regulation and virulence mediation. Therefore, we characterized a mutant of Psa biovar 3 impaired in PsaR3, in terms of *in vitro* growth and gene expression, in different conditions, including the addition of kiwifruit leaf extract. Such analyses revealed that PsaR3 could play a role in the regulation of the function and composition of the cellular membrane as well as the regulation of cellular transporters that could participate in the virulence of Psa. Moreover, in line with the effect of the kiwifruit leaf extract, PsaR3 could be involved, at least in part, in inter-kingdom signalling communication.



## 2. INTRODUCTION

Since bacteria usually live associated with other different microorganisms and eukaryotic hosts, they evolved a mechanism to monitor and communicate to each other. This communication process was discovered 23 years ago and is called quorum sensing (QS) [1]. The QS controls a plethora of bacterial processes, such as: bioluminescence, sporulation, competence, antibiotic production, biofilm formation and virulence factors. It consists in the detection of population density through cell-cell communication via small diffusible molecules. The canonical QS in the Gram-negative bacteria is composed by two main actors, *i.e.*: a LuxI auto-inducer synthase that synthesizes acyl-homoserinelactones (AHLs) and a LuxR-type receptor, that senses the signal molecule, once it exceeds a certain threshold then promoting or repressing the expression of several genes or operons [2]. The LuxR-type receptor is about 250 amino acids in length and is divided into two domains, which are an amino-terminal AHL binding domain and a carboxy-terminal domain containing a helix-turn-helix (HTH) DNA-binding motif [3] for transcriptional regulation. However, some LuxR-type receptors have been shown to lack a cognate LuxI synthase, and thus have been called LuxR orphans or LuxR solos [4]. The LuxR solos could recognize AHL signal molecules, produced by neighbouring bacteria or other bacterial signal molecules like pyrones [5], or they could be involved in interkingdom communication through the recognition of signal molecules derived from plants as hypothesized for OryR, a LuxR solos of *Xanthomonas campestris* [6]. The last years have shown an increase in LuxR solos functional characterization studies, in particular regarding QscR in *Pseudomonas aeruginosa* and SdiA in *E. coli* [7, 8]. However, the signal molecules as well as the function of many LuxR solos still remain to be elucidated. *Pseudomonas syringae* pv. *actinidiae* possesses three LuxR solos namely PsaR1, PsaR2 and PsaR3, which have been shown to play a role in diverse Psa virulence traits (e.g.: *in planta* growth, motility, lipase secretion) [9]. Moreover, it was established that Psa does not produce AHL, thus opening the question regarding the signal molecules perceived by these three sensors. It has been proposed that LuxR solos PsaR2, which belongs to a sub-family of plant-associated bacteria (PAB) LuxR solos may respond to plant signal molecules. On the other hand, PsaR1 and PsaR3, which share higher similarity with canonical LuxR receptors might be involved in the recognition of AHLs produced by neighbouring bacteria, non-AHL bacterial signal molecules. However, it cannot be ruled out a possible role of PsaR1 and PsaR3 in mediating inter-kingdom signal communication as well.

To elucidate possible differences between the three Psa LuxR solos, we performed a bioinformatics analysis which revealed peculiar characteristics of PsaR3, *i.e.*: the biovar 3 specificity and the plasmid localization of its encoding gene. Since these characteristics could account for the higher virulence of biovar 3 we characterized Psa mutant impaired in PsaR3, both at phenotypical and molecular levels.

### 3. MATERIALS AND METHODS

#### 3.1 BACTERIAL STRAINS

In this work, we used a *Pseudomonas syringae* pv. *actinidiae* strain belonging to the biovar 3, called CRAFRU 10.22 isolated in *Actinidia chinensis*-HORT16A plants in Latina in 2008 and its corresponding PsaR3-impaired mutant ( $\Delta$ *psaR3*). Both strains were, kindly provided by Dr V. Venturi (International Centre for Genetic Engineering and Biotechnology ICGEB, Trieste). The construction of the  $\Delta$ *psaR3* mutant was described previously by Patel and colleagues [9].

#### 3.2 BIOINFORMATIC ANALYSIS OF PsaR3 LuxR solos

Protein multiple sequence alignment was performed using CLUSTALW 2.1 (<http://www.ebi.ac.uk/Tools/msa/clustalw2/>, January 2015) using Psa LuxR protein sequences retrieved from the draft genome of Psa, reference strain ICMP18884 ([https://www.ncbi.nlm.nih.gov/genome/185?genome\\_assembly\\_id=282936](https://www.ncbi.nlm.nih.gov/genome/185?genome_assembly_id=282936)). PsaR3 genomic localization and biovar specificity was achieved by NCBI-BLAST analysis (<https://blast.ncbi.nlm.nih.gov/Blast.cgi>). Biovar specificity was further confirmed by PCR analysis. The *psaR3* cluster organization as well as the intergenic region sequence were searched in the Pseudomonas Genome DB (<http://www.pseudomonas.com/>). The prediction of *cis*-acting elements in the cluster intergenic region, was performed using the Virtual Footprint Software (<http://www.prodoric.de/vfp/>) selecting “all items” parameter in the “Position Weight Matrix” section.

### 3.3 IN VITRO BACTERIAL GROWTH ASSAY

CRAFRU 10.22 growth was monitored in the rich medium, King's B (KB) and in the minimal *hpr*-inducing medium (HIM). Medium composition is described in the section 3.2 of the chapter 2. Both media were also further supplemented with 1% of kiwifruit leaf extract. Briefly, leaves of *Actinidia deliciosa* plants cultivated in growth chamber under controlled conditions were collected and the crude leaf extract was obtained using a juice extractor and then centrifuged to remove the debris and sterilized by filtration using a 0.2 µm-filter.

Single colonies of Psa CRAFRU 10.22 and  $\Delta$ *psaR3* mutant grown on KB agar were used to inoculate liquid KB broth. Bacterial cultures were incubated over-night at 28°C with shaking (200 rpm). Three-ml aliquots of cell suspension were centrifuged and washed three times in KB or HIM. Then the bacterial suspensions were adjusted with fresh medium to get a final OD<sub>600</sub> of 0.2 in HIM and 0.02 in KB in a final volume of 20 ml in 100-ml flasks. When required, kiwifruit leaf extract at a final concentration of 1% was added to the flasks. Bacterial suspensions were incubated at 28°C with shaking (200 rpm) and the OD<sub>600</sub> was monitored every 4 hours over 48 hours using a spectrophotometer.

### 3.4 GENES EXPRESSION ANALYSIS BY REAL-TIME qPCR

Real-time qPCR analyses were performed on samples harvested at 4 and 24 hours post-inoculation (hpi) of Psa CRAFRU 10.22 and  $\Delta$ *psaR3* mutant grown in HIM supplemented or not with kiwifruit leaf extract as described above (section 3.3.1.). Total RNA from bacterial cultures was extracted using the Spectrum Plant Total RNA Kit (Sigma Aldrich); and quantified using Nanodrop (Thermo Fischer). Then, 2 µg of total RNA were treated with TURBO DNase (Ambion) to remove the contaminant DNA and 10 µl of treated RNA was retro-transcribed using the SuperScript III Reverse Transcriptase (Invitrogen). The cDNA obtained was diluted to obtain a final amount of 20 ng. The primers, specific for each selected gene, were prepared at a stock concentration of 200 mM and the reaction was performed using the GoTaq PCR Master MIX (Promega) in the Proflex PCR System (Applied Bio-system) instrument. Two genes, encoding the sigma factor RpoD and a transaldolase were used as internal reference genes for relative expression calculation [10]. Specific primers were designed to amplify a small portion of the cDNA of interest using the NCBI primer blast tool (<https://www.ncbi.nlm.nih.gov/tools/primer-blast/>) and the quality of the primers was evaluated using Melting DNA Hybrid project PCR tool and DNA-hybridization program

([http://promix.cribi.unipd.it/cgi-bin/promix/melting/melting\\_main.exe?GRUP=0](http://promix.cribi.unipd.it/cgi-bin/promix/melting/melting_main.exe?GRUP=0)). The Real-time qPCR reaction cycle was set up as follow:

50°C x 2 minutes  
 95°C x 5 minutes  
 95°C x 30 seconds  
 60°C x 30 seconds  
 72°C x 20 seconds

} 40 cycles

The Proflex software (Applied Bio-system) automatically sets up a threshold for the amplification curve and gives back the Ct for each sample. The relative expression values (Mean Normalized Expression, MNE) of the target genes and the standard errors were calculated using Pfaffl and Simon equation [11, 12]. The LingRegPCR program (<http://www.hartfaalcentrum.nl/index.php?main=files&fileName=LinRegPCR.zip&description=LinRegPCR:%20qPCR%20data%20analysis&sub=LinRegPCR>) [13] was used to calculate the efficiency of the amplification reaction from the fluorescence data.

### 3.5 GENE EXPRESSION ANALYSIS BY MICROARRAY

CRAFRU 10.22 and  $\Delta psar3$  mutant were grown in HIM or HIM supplemented with kiwifruit leaf extract, as described in the 3.3.2 section; and harvested at 4 and 24 hpi ( $2.4 \times 10^9$  cells). Three biological replicates for each strain in each condition were collected and used for microarray analysis. Total RNA was extracted from the samples using the Spectrum Plant Total RNA Kit (Sigma Aldrich) and quantified by Nanodrop (Thermo Fischer). RNA quality was evaluated using Agilent RNA 6000 Nano Kit (Agilent Technologies). Then the RNA was processed as described in the One-Color Microarray-Based Gene Expression Analysis Low Input Quick Amp WT Labeling (Agilent Technologies, August 2015). Following hybridization, the chips were scanned using Agilent G4900DA SureScan Microarray Scanner System with the Agilent Scan Control software and the data extrapolated using the Agilent Feature Extraction software.

In collaboration with Dr Nicola Vitulo (University of Verona), raw data were normalized, statistically evaluated and processed to obtain the fold changes of the expression in the different conditions. Briefly, the average and the standard deviations of the triplicate-probe present on the microarray chip were calculated, and the data were normalized using the non-parametric tests.

The list of Differentially Expressed Genes (DEGs) was created considering only the CRAFRU probes present on the chip, with a False Discovery Rate (FDR)  $FDR < 0.05$ , independently of the  $\log_2$ fold-change. Functional category enrichment analysis was performed using BinGO (<http://apps.cytoscape.org/apps/bin-go>, Maere S, Heymans K, Kuiper M (2005) BinGO: a Cytoscape plugin to assess overrepresentation of Gene Ontology categories in biological networks. *Bioinformatics* 21, 3448-3449). The comparison of DEGs in the different strains and/or conditions- was performed using the online software Calculate and Draw Custom Venn Diagrams (<http://bioinformatics.psb.ugent.be/webtools/Venn/>, 2017). The bar chart based on the enrichment in Gene Ontology (GO) terms of the DEGs was generated using Blast2Go tool (version 4.1 March 2017) setting a False Discovery Rate,  $FDR < 0.01$ .

## 4. RESULTS

### 4.1 CHARACTERIZATION OF PSAR3-ENCODING GENE: LOCALIZATION AND SPECIFICITY

To establish the similarity of the PsaR sensors among the Psa strains, and in particular among the Psa biovars, we performed a NCBI Blast Nucleotide analysis ([https://blast.ncbi.nlm.nih.gov/Blast.cgi?PROGRAM=blastn&PAGE\\_TYPE=BlastSearch&LINK\\_LOC=blasthome](https://blast.ncbi.nlm.nih.gov/Blast.cgi?PROGRAM=blastn&PAGE_TYPE=BlastSearch&LINK_LOC=blasthome)) considering each Psa LuxR sequence separately and all Psa genomes present in public databases. The analysis highlighted that PsaR3-encoding gene was found only in the genome of Psa strains belonging to the biovar 3 (**Fig. 1**) and was localized on the plasmid.

Sequences producing significant alignments:

Select: [All](#) [None](#) Selected:0

Alignments								Download	GenBank	Graphics	Distance tree of results	⚙
	Description	Max score	Total score	Query cover	E value	Ident	Accession					
<input type="checkbox"/>	<a href="#">Pseudomonas syringae pv. actinidiae strain CRAFRU 14.08 plasmid unnamed, complete sequence</a>	1557	1557	100%	0.0	100%	<a href="#">CP019733.1</a>					
<input type="checkbox"/>	<a href="#">Pseudomonas syringae pv. actinidiae strain CRAFRU 12.29 plasmid unnamed, complete sequence</a>	1557	1557	100%	0.0	100%	<a href="#">CP019731.1</a>					
<input type="checkbox"/>	<a href="#">Pseudomonas syringae pv. actinidiae strain NZ-47 plasmid pPsa22180a, complete sequence</a>	1557	1557	100%	0.0	100%	<a href="#">CP017010.1</a>					
<input type="checkbox"/>	<a href="#">Pseudomonas syringae pv. actinidiae strain NZ-45 plasmid pPsa20586, complete sequence</a>	1557	1557	100%	0.0	100%	<a href="#">CP017008.1</a>					
<input type="checkbox"/>	<a href="#">Pseudomonas syringae pv. actinidiae ICMP 18708 plasmid, complete sequence</a>	1557	1557	100%	0.0	100%	<a href="#">CP012180.1</a>					
<input type="checkbox"/>	<a href="#">Pseudomonas syringae pv. actinidiae ICMP 18884 plasmid, complete sequence</a>	1557	1557	100%	0.0	100%	<a href="#">CP011973.1</a>					

Figure 1: Output of the blastn analysis (megablast) performed with *psaR3* gene sequence using *Pseudomonas syringae* pv. *actinidiae* taxid:103796 as selected organisms.

To confirm the biovar 3 specificity of PsaR3, observed *in silico*, we analysed experimentally the presence of *psaR3* gene in two strains belonging to biovar 3, *i.e.*: CRAFRU 10.22 and V-13, and two strains belonging to biovar 1 and 2, *i.e.*: J35 and KN2, respectively. The PCR analysis (**Fig. 2**) confirmed that PsaR3-encoding gene is present only in biovar 3 strains.

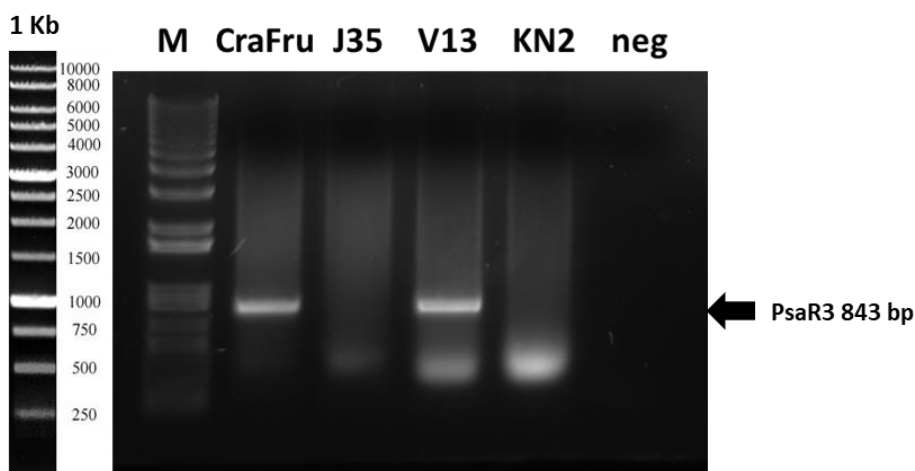


*Figure 2:* PCR analysis of PsaR3-encoding gene in different strains of Psa. PCR was performed using specific primers for *psaR3*. PCR products were separated on a 1% agarose gel and visualized with SybrSafe. M= marker (1 Kb), Neg= negative control.

Since in the canonical QS system (LuxR/I), both genes are found successively in the genome, we analysed the genes surrounding *psaR3* on the plasmid of Psa biovar 3. The analysis highlighted that *psaR3* was in a cluster containing different genes encoding: the anthranilate synthase components I and II (ASI and ASII) on one hand, and a phenyl-acetate-CoA ligase (PheCoA ligase), an acetyl transferase, a putative transcriptional regulator, a reductase NADPH dependent, a lipase (**Fig 3**) on the other hand. Moreover, these coding sequences were separated by a non-coding DNA sequence (intergenic region), which could play a role as bi-directional promoter for the regulation of the expression of cluster genes (**Fig. 3, b**).

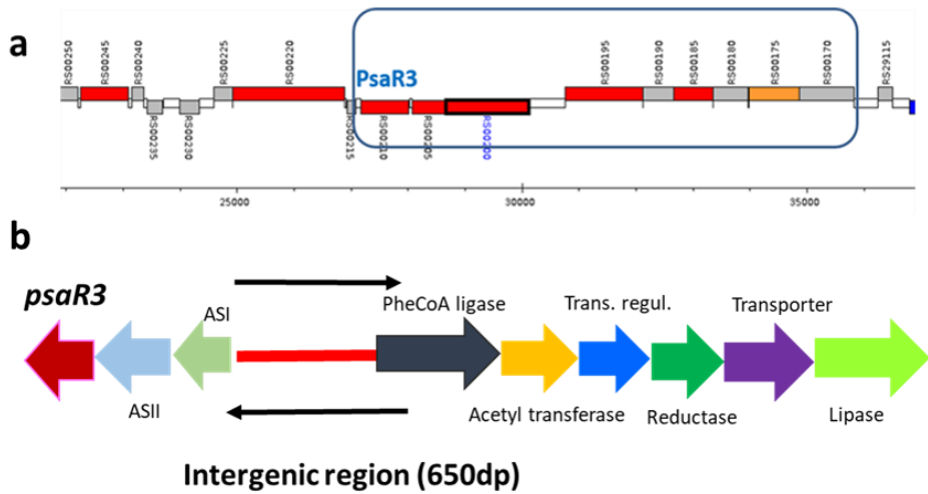


*Figure 3:* Organization of the gene cluster containing the PsaR3-encoding gene. a) schematic representation of the plasmid portion where the *psaR3* gene is located, obtained from the Pseudomonas Genome Database (<http://www.pseudomonas.com/>). b) schematic representation of the genes and the intergenic region present in the putative *psaR3*-cluster. The black arrows indicate the possible orientations for the intergenic region to function as putative promoter.

Given the biovar 3 specificity of the *psaR3* gene, we hypothesized a role of these elements in the higher virulence of the biovar 3. Moreover, considering the localization of the gene on the plasmid of Psa biovar 3 and thus the lateral gene transfers as a possible mechanism for the inheritance of one or more genes of the cluster, we performed a bioinformatic analysis to find other microorganisms containing a *psaR3*-like gene. The result of the analysis (**Table 1**) revealed that different *Pseudomonas* species and pathovars possess a sequence *psaR3*-like, although localized on their chromosome. The genes showing the highest sequence identity (96-100%), with *psaR3* belong to *Pseudomonas syringae* species, while the genes showing a lower similarity (around 60%) were present in strains related to *Pseudomonas fluorescens*. Interestingly, in all strains displaying PsaR3-encoding gene, such gene was always surrounded by the same genes as found in PsaR3 cluster. As mentioned above, we hypothesized that this intergenic region (non-coding DNA sequence), always present in the cluster, between the ASI- and PheCoA ligase-encoding genes (**Fig. 3, b**) could play a role as transcriptional promoter considering both orientations. We thus performed a bioinformatics analysis on the sequence retrieved from Psa V-13 (ICMP 18884) strain, to determine the presence of possible *cis*-acting



elements, either in the sense or in the antisense orientation (**Table 2**) using the Virtual FootPrint Software.

Strains with PsaR3-like	Localization	Host	% Identity
<i>Pseudomonas syringae</i> pv. <i>actinidiae</i>	Plasmid	<i>Actinidia deliciosa/chinensis</i>	--
<i>Pseudomonas syringae</i> pv. <i>pisi</i>	Chromosome	<i>Pisum sativum</i>	99
<i>Pseudomonas savastanoi</i> pv. <i>glycinea</i>	Chromosome	<i>soybean</i>	99
<i>Pseudomonas cornofaciens</i> pv. <i>porri</i>	Chromosome	<i>Allium ampeloprasum</i> var. <i>porrum</i>	96
<i>Pseudomonas amygdali</i> pv. <i>lachrymans</i>	Chromosome	<i>Cucumis sativus</i>	100
<i>Pseudomonas syringae</i> pv. <i>cunninghamiae</i>	Chromosome	<i>Cunninghamia lanceolata</i> Hook	100
<i>Pseudomonas syringae</i> pv. <i>broussonetiae</i>	Chromosome	<i>paper mulberry</i> ( <i>Broussonetia kazinoki</i> × <i>B. papyrifera</i> )	99
<i>Pseudomonas amygdali</i> pv. <i>tabaci</i>	Chromosome	<i>almond</i> ( <i>Prunus amygdalus</i> )	100
<i>Pseudomonas amygdali</i> pv. <i>aesculi</i>	Chromosome	<i>Buckeye and Horse-chestnut trees</i> (Genus <i>Aesculus</i> )	100
<i>Pseudomonas amygdali</i> pv. <i>myricae</i>	Chromosome	<i>Myrica trees</i>	100
<i>Pseudomonas camabina</i>	Chromosome	<i>Camnabis sativa</i>	100
<i>Pseudomonas fluorescens</i>	Chromosome		62
<i>Pseudomonas brassicacearum</i>	Chromosome	<i>Brassica napus</i>	60
<i>Pseudomonas chlororaphis</i>	Chromosome		63
<i>Pseudomonas kilonensis</i>	Chromosome		61

**Table 1:** List of bacterial strains showing a *psaR3*-like sequence in the genome. The strains with a PsaR3-like encoding gene showing a sequence identity with Psa sequence above 95% are highlighted in orange. Strains showing a lower *psaR3*-like sequence identity (around 60%) are highlighted in green.

Cis-acting element	Species	Start position	End position	Filament	Score	Sequence
AlgU (-35)	<i>P aeruginosa</i> (strain PAO1)	135	144	-	11.79	TGGAACCTCA
Anr_Dnr_40	<i>P aeruginosa</i>	275	288	-	12.38	TTGGCCGCTTCAA
CRE	CTGAGCTATTTAATAG	498	510	-	9.84	AAAAGTTTATTC
DegU	<i>B subtilis</i> (strain 168)	496	516	-	14.1	ATAAATAAAAGTTTATTTAC
DegU	<i>B subtilis</i> (strain 168)	501	521	+	13.92	ATAAACTTTTAATTATTTAC
DegU	<i>B subtilis</i> (strain 168)	493	513	+	12.51	AAAGTGAATAAACTTTTAAT
GcvA	<i>E coli</i> (strain K12)	252	256	-	10	CTAAT
IHF	<i>P aeruginosa</i> (strain PAO1)	75	82	-	9.67	CAAAGCGT
LasR	<i>P aeruginosa</i> (strain PAO1)	245	260	-	8.95	GTCGCTAATCAGCGAG
LasR	<i>P aeruginosa</i> (strain PAO1)	541	556	-	8.78	CTATTAATAGCTCAG
LasR	<i>P aeruginosa</i> (strain PAO1)	541	556	+	8.78	CTGAGCTATTAATAG
MetR	<i>E coli</i> (strain K12)	522	528	-	9.39	TGAAAAA
MetR	<i>E coli</i> (strain K12)	12	18	-	9.18	TGAACAA
OmpR	<i>E coli</i> (strain K12)	505	511	-	8.27	TAAAAGT
OmpR	<i>E coli</i> (strain K12)	455	461	+	8.04	TAAAAAG
OxyR	<i>E coli</i> (strain K12)	59	104	+	13.13	AATATAAAGCGCTTGACGCTT
RhIR	<i>P aeruginosa</i> (strain PAO1)	591	606	-	9.5	CTGCAATTACGCGCG
RhIR	<i>P aeruginosa</i> (strain PAO1)	396	411	-	9.22	CTTTAATTGCCTGTGG
RhIR	<i>P aeruginosa</i> (strain PAO1)	541	556	+	9.18	CTGAGCTATTAATAG
Spo0A (II)	CTGAGCTATTTAATAG	167	178	-	8.24	GATGTCGAACGT

**Table 2:** List of the putative *cis*-acting elements present in the intergenic region of the *psaR3* cluster. To identify the most significant *cis*-acting elements, a minimum score of 8 was chosen as a threshold. The *cis*-acting elements identified in sense orientation are highlighted in orange, while those identified in antisense orientation are highlighted in white.

The different putative *cis*-acting elements include motifs similar to: LasR and RhlR-regulated elements, two LuxR receptors involved in the QS mechanism of *Pseudomonas aeruginosa*. This suggested that intergenic region sequence, in both orientations, could be controlled by PsaR3 itself to regulate the gene-cluster. Moreover, the highest prediction score was observed for a sequence similar to the element regulated by DegU of *Bacillus subtilis*, a member of the two-component system (DegS/DegU), which plays an important role in the growth phase transition-, and is involved in the control of the expression of different bacterial cellular functions.

## **4.2 EVALUATION OF THE PUTATIVE FUNCTION OF PSAR3 IN Psa GROWTH AND IN THE EXPRESSION OF THE GENES BELONGING TO ITS CLUSTER**

We attempted to characterize the role of PsaR3 at phenotypical and molecular levels using a Psa mutant impaired in *psaR3*. Moreover, although PsaR3 does not display the canonical features of a plant-associated bacteria LuxR solos, strongest candidate as putative sensors for host plant recognition [9], but considering its peculiarity compared to canonical LuxR solos, we also considered a putative role for PsaR3 in the perception of signal(s) present in the kiwifruit leaf extract.

### **4.2.1 Psa GROWTH KINETICS**

To elucidate the role of PsaR3 and to identify the mechanisms, which could be regulated by the sensor, we monitored the growth of the wild-type strain (WT) CRA-FRU10.22 and the  $\Delta$ *psaR3* mutant impaired in *psaR3* in different media *i.e.*: HIM and KB, both supplemented or not with kiwifruit leaf extract. The two strains showed a similar growth pattern in rich medium (KB). Moreover, the addition of kiwifruit leaf extract did not seem to influence bacterial growth of both strains. In these conditions, both bacterial strains started the exponentially phase at 8 hpi until 24 hpi, when they reached the plateau phase without showing any substantial differences (**Fig. 4**).

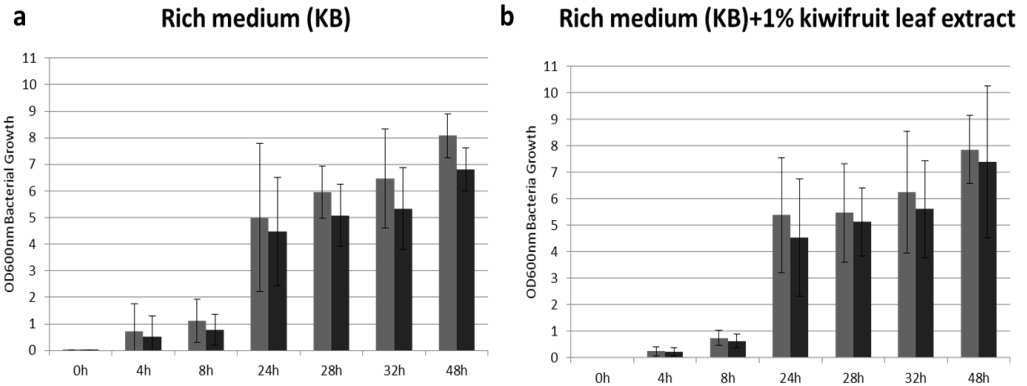


**Figure 4:** Growth curves of Psa strains CRAFRU 10.22 wt (grey) and  $\Delta psar3$  mutant (dull grey) in rich medium (a) and rich medium supplemented with kiwifruit leaf extract (b), at 28°C. The x-axis reports the OD<sub>600</sub> values and the y-axis reports the time points of the analysis.

Conversely, in minimal *hrp*-inducing medium (HIM), a medium that mimics the apoplastic conditions, the two strains showed a different growth kinetics, (**Fig. 5, a**). As expected, both strains hardly reached OD<sub>600</sub>=1, thus showing slower growth than in the rich medium due to the lack of nutrients. Surprisingly, for both strains we observed a strong drop of OD, occurring after 40 hpi for the wild-type strain and after 44 hpi for the  $\Delta psar3$  mutant but in a lower extent. The presence of the kiwifruit leaf extract in the medium anticipated the drop of OD, which occurred after only 24 hpi in the wild-type, and after 40 hpi in the  $\Delta psar3$  mutant (**Fig. 5, b**).

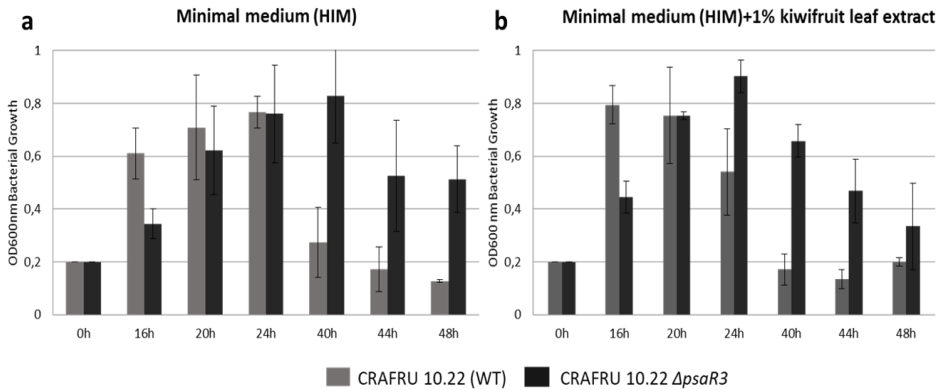


**Figure 5:** Growth curves of Psa strains CRAFRU 10.22 wt (grey) and  $\Delta$ psaR3 mutant (dull grey) in minimal medium (a) and minimal medium supplemented with kiwifruit leaf extract (b), at 28°C. The x-axis reports the OD<sub>600</sub> values and the y-axis reports the time points of the analysis.

The strong decrease in OD values, observed in the wild-type strain in HIM, was correlated with the presence of numerous macroscopic cell aggregates. However, according to a higher OD detected in the same medium the aggregates observed in the  $\Delta$ psaR3 mutant appeared to be less and/or smaller (**Fig. 6, a**). We could thus assume that the presence of such aggregates accounted for the OD decrease, due to the difficulty in reading the OD, and that PsaR3 plays a role in cell aggregate formation.

Interestingly, we also observed an effect of kiwifruit leaf extract on floc formation in the wild-type strain in which they appeared smaller than the aggregates observed in HIM alone (**Fig. 6**). By contrast, kiwifruit leaf extract did not seem to affect the macroscopic characteristics of the aggregates in the  $\Delta$ psaR3 mutant. These results suggest a possible effect of the kiwifruit leaf extract in Psa cell aggregate formation, likely mediated by the PsaR3 receptor.

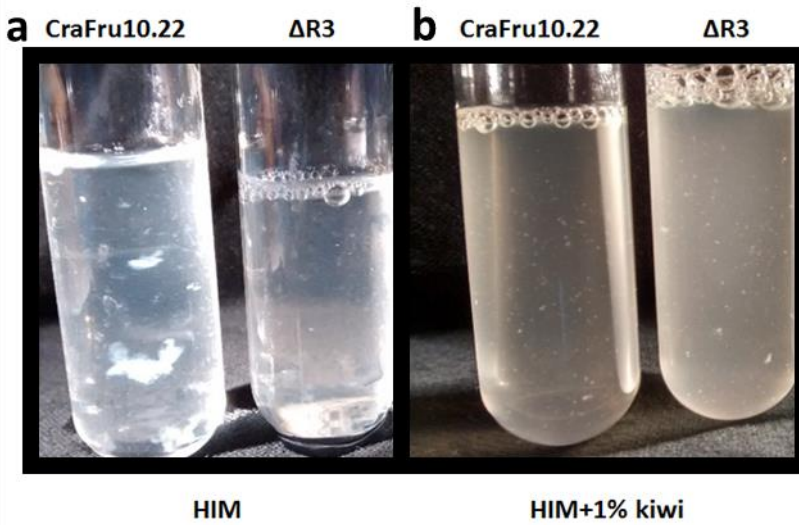


*Figure 6:* Macroscopic observation of the cell-aggregates formed in minimal medium (HIM) in absence (a) or presence (b) of kiwifruit leaf extract in CRAFRU10.22 wild-type strain (CraFru10.22) and  $\Delta psr3$  mutant ( $\Delta R3$ ). The pictures were taken at 40 hpi.

## 4.2.2 TARGETED EXPRESSION ANALYSIS OF THE GENES BELONGING TO PsaR3 CLUSTER

### 4.2.2.1 EXPRESSION EVALUATION OF THE GENES IN SENSE ORIENTATION

We evaluated the modulation of two genes present in the cluster in sense orientation, namely the genes encoding the PheCoA ligase and the lipase, in CRAFRU 10.22 wild-type strain and in  $\Delta psr3$  mutant both grown in HIM or HIM supplemented with 1% kiwifruit leaf extract. Expression was then analysed at 4 and 24 hpi.

To obtain reliable results and to avoid false positives due to the possibility of house-keeping gene modulation dependent on the presence of kiwifruit leaf extract, we used two house-keeping genes, *i.e.*: RpoD- and trans-aldolase-encoding gene [10].

The PheCoA ligase-encoding gene in the wild-type strain showed a slight modulation in HIM either at 4 or at 24 hpi, while the transcript level in the  $\Delta psr3$  mutant strongly increased at 24

hpi in the same condition (**Fig. 7**). Conversely, while the level of PheCoA ligase-encoding gene transcript was higher in the wild-type strain grown in presence of kiwifruit leaf extract, the latter had no effect on PheCoA ligase expression in  $\Delta psar3$ . It is worth notice that similar results were obtained with both house-keeping genes.

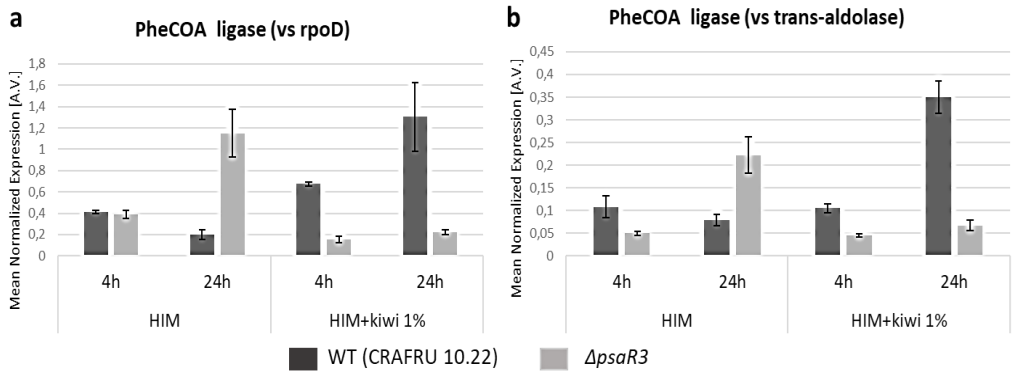


*Figure 7:* Expression of the PheCoA ligase-encoding gene, in CRAFURU 10.22-WT (dull grey) and in  $\Delta psar3$  mutant (light grey). Samples were taken at 4 and 24 hpi in HIM or HIM supplemented with kiwifruit leaf extract. The analysis was performed by Real-time qPCR using *rpoD*- (a) or *trans-aldolase*- (b) encoding genes as house-keeping genes.

The last gene of the *psar3*-cluster encodes a putative lipase. In the wild-type strain the lipase was only slightly regulated in HIM, either at 4 or 24 hpi. However, the addition of kiwifruit leaf extract in the medium strongly induced the expression of the gene (**Fig. 8**). By contrast, such strong induction observed in response to kiwifruit leaf extract was lost in the  $\Delta psar3$  mutant.

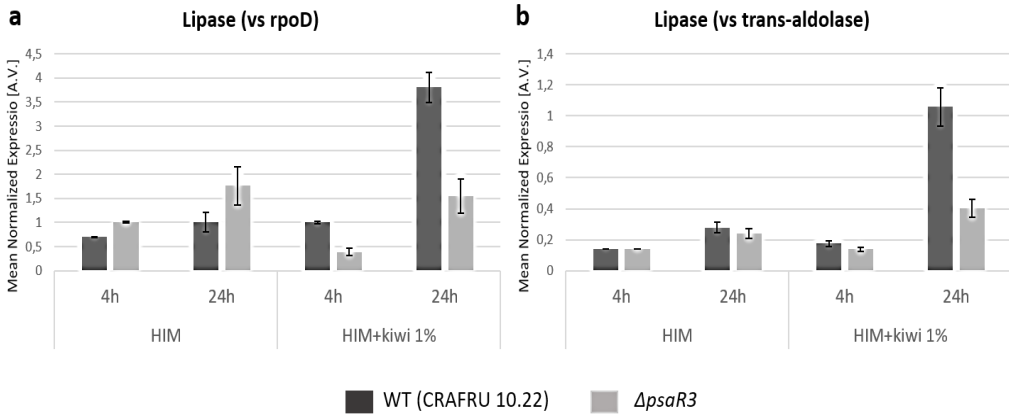


**Figure 8:** Expression of lipase-encoding gene, in CRAFUR 10.22-WT (dull grey) and in the  $\Delta psar3$  mutant (light grey). Samples were taken at 4 and 24 hpi in HIM or HIM supplemented with kiwifruit leaf extract. The analysis was performed by Real-time qPCR using rpoD- (a) or trans-aldolase- (b) encoding genes as house-keeping genes.

Overall, these results suggest that the genes located in sense orientation in *psaR3*-cluster were responsive to the addition of kiwifruit leaf extract, likely in a *PsaR3*-dependent manner.

#### 4.2.2.2 EXPRESSION EVALUATION OF THE GENES IN ANTISENSE ORIENTATION

We considered two genes in anti-sense orientation, namely ASI- and *PsaR3*-encoding genes. The ASI-encoding gene is strongly induced in the  $\Delta psar3$  mutant at 24 hpi in HIM but, the presence of kiwifruit leaf extract decreased its transcript level. Conversely, the ASI-encoding gene in the wild-type strain was not modulated, regardless the time point or growth conditions. These results thus suggest that this gene could be negatively regulated *PsaR3*.

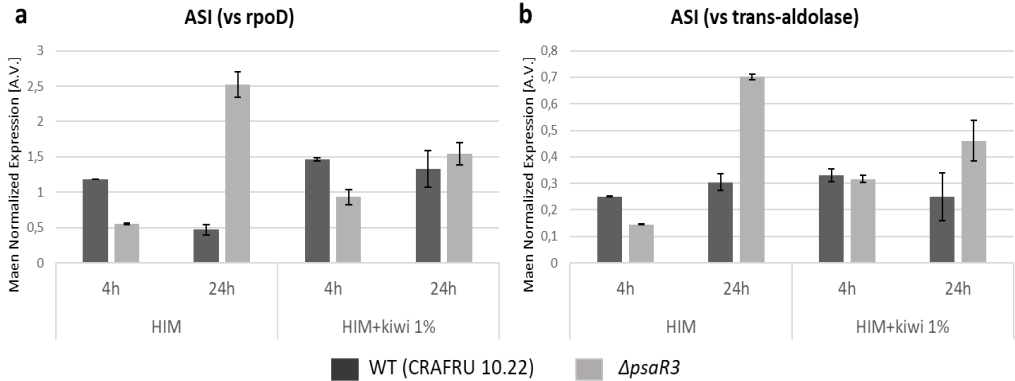


**Figure 9:** Expression ASI-encoding gene, in CRAFRU 10.22-WT (dull grey) and in the  $\Delta$ psaR3 mutant (light grey). Samples were taken at 4 and 24 hpi in HIM or HIM with kiwifruit leaf extract. The analysis was performed by Real-time qPCR using rpoD- (a) or trans-aldolase- (b) encoding genes as house-keeping genes.

PsaR3-encoding gene showed an expression level higher in the wild-type than in the  $\Delta$ psaR3 mutant, confirming the presence of the mutation at post-transcriptional level (**Fig. 10**). Moreover, the addition of kiwifruit leaf extract increased the level of *psaR3* transcripts only in the wild-type strain. This result suggests that the expression of this gene could be regulated by the presence of kiwifruit leaf extract.

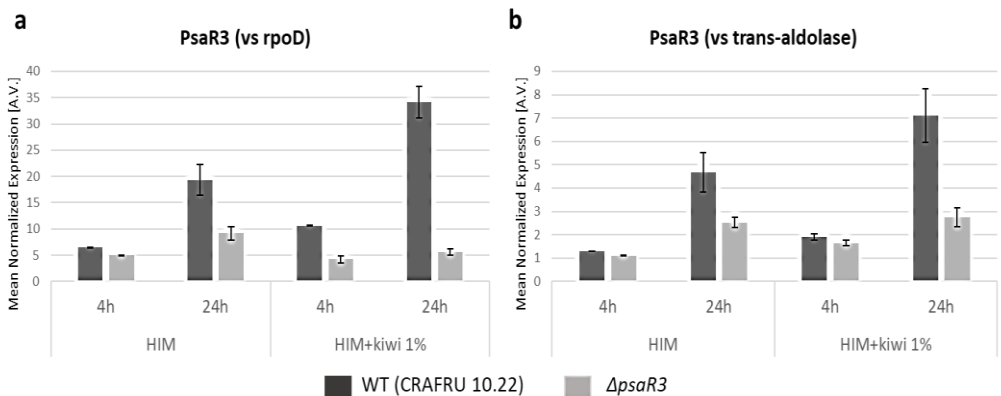


**Figure 10:** Expression of PsaR3-encoding gene, in CRAFRU 10.22-WT (dull grey) and in the  $\Delta$ psaR3 mutant (light grey). Samples were taken at 4 and 24 hpi in HIM or HIM supplemented with kiwifruit leaf extract. The analysis was performed by Real-time qPCR using RpoD- (a) or trans-aldolase- (b) encoding genes as house-keeping genes.



### 4.3 TARGETED EXPRESSION ANALYSIS OF *PsaR1* and *PsaR2* AND GENES INVOLVED IN BACTERIAL VIRULENCE

LuxR solos could regulate their own expression as well as the expression of other LuxR solos, as reported for QscR, LasR and RhlR, three LuxR of *Pseudomonas aeruginosa* [7]. Therefore, we evaluated the expression level of *psaR1* and *psaR2* in CRAFRU 10.22 (wild-type) and the  $\Delta$ *psaR3* mutant to establish whether their expression could be dependent on *PsaR3* and regulated by kiwifruit leaf extract.

In the wild-type strain *psaR1* resulted more expressed than in the  $\Delta$ *psaR3* mutant at 24h in HIM (**Fig. 11**), considering, both housekeeping genes. Its expression further increased following the addition of kiwifruit leaf extract at either 4 or 24 hpi.

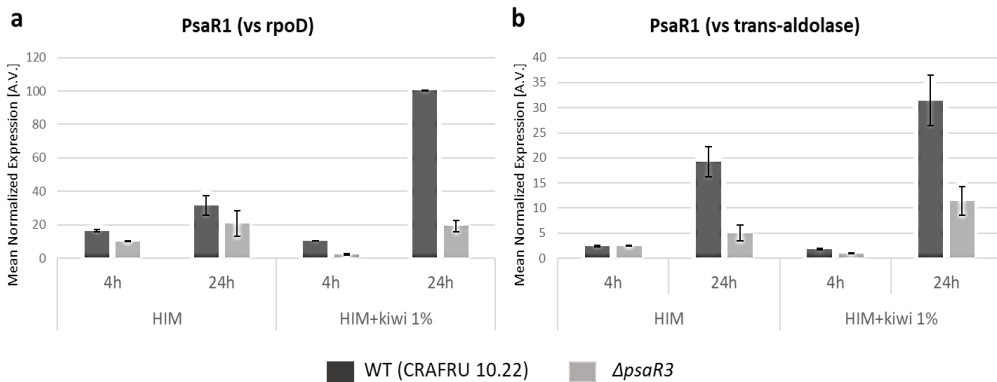


**Figure 11:** Expression of *PsaR1*-encoding gene, in CRAFRU 10.22-WT (dull grey) and in the  $\Delta$ *psaR3* mutant (light grey). Samples were taken at 4 and 24 hpi in HIM or HIM supplemented with kiwifruit leaf extract. The analysis was performed by Real-time qPCR using RpoD- (a) or trans-aldolase- (b) encoding genes as house-keeping genes.

No significant differences in *psaR2* expression was observed between wild-type and  $\Delta$ *psaR3* mutant strains in HIM alone (**Fig. 12**). However, the level of *psaR2* transcript strongly increased in the wild-type strain in presence of kiwifruit leaf extract at 24 hpi but such increase was impaired in the  $\Delta$ *psaR3* mutant (**Fig. 12**). These results suggest that the expression of both *psaR1* and *psaR2* could be regulated by kiwifruit leaf extract in a *PsaR3*-dependent manner.

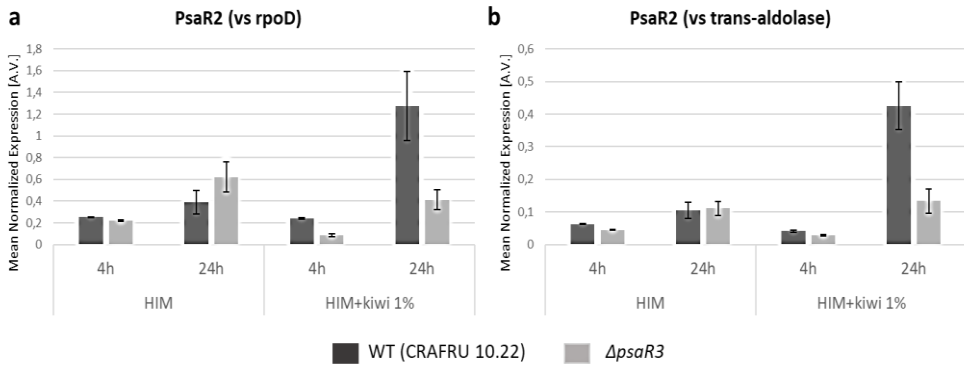


**Figure 12:** Expression of PsaR2-encoding gene, in CRAFRU 10.22-WT (dull grey) and in the  $\Delta psar3$  mutant (light grey). Samples were taken at 4 and 24 hpi in HIM or HIM supplemented with kiwifruit leaf extract. The analysis was performed by Real-time qPCR using RpoD- (a) or trans-aldolase- (b) encoding genes as house-keeping genes.

On the other hand, to evaluate a putative role of PsaR3 in the regulation of genes involved in bacterial virulence, we considered two well-known virulence-related genes, previously reported in literature.

First, the gene *hrpA1*, encoding a helper protein of the TTSS [14], was highly expressed either in the wild-type or in the  $\Delta psar3$  mutant in minimal medium at 4h (Fig. 13) and its expression decreased at 24 hpi. Moreover, *hrpA1* expression was further induced in the wild-type following the addition of the kiwifruit leaf extract, suggesting that this gene is responsive to host signal(s), as proposed in the literature [9, 14]. Interestingly, such strong increase was impaired in the  $\Delta psar3$  mutant, suggesting a possible direct or indirect regulatory role of PsaR3 in this mechanism.

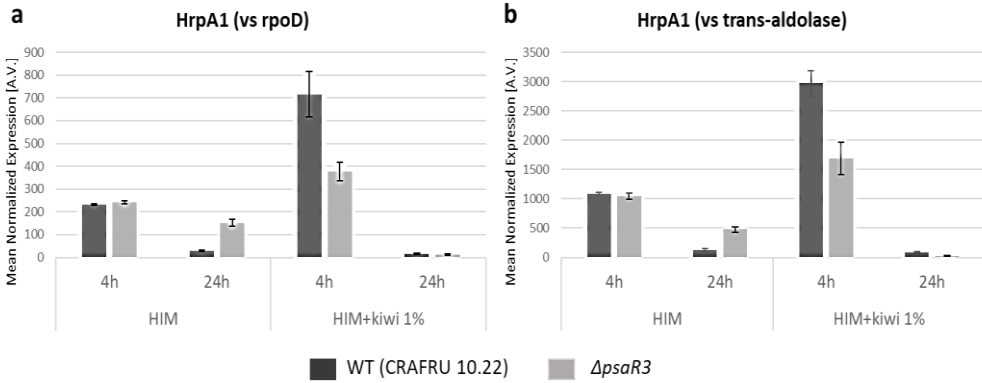


**Figure 13:** Expression of HrpA1-encoding gene, in CRAFURU 10.22-WT (dull grey) and in the  $\Delta$ psaR3 mutant (light grey). Samples were taken at 4 and 24 hpi in HIM or HIM supplemented with kiwifruit leaf extract. The analysis was performed by Real-time qPCR using RpoD- (a) or trans-aldolase- (b) encoding genes as house-keeping genes.

Another class of genes involved in the virulence of *Pseudomonas* phytopathogenic strains are the siderophore-encoding genes. Kim and colleagues, [15, 16] demonstrated that the virulence of *Pseudomonas syringae* pv *tomato* DC3000 is dependent to the amount of iron present in the minimal medium. Moreover, the gene *citM* encoding for a citrate transporter playing a role as siderophore, was shown to be fundamental for the growth of a strain of *Pseudomonas savastanoi* pv. *savastanoi* in olive plants [17]. We thus analysed the expression of the homologue *citM* in Psa in the different conditions. The **Fig 14** shows that *citM* was expressed at 24 hpi only in the wild-type strain grown in minimal medium supplemented with kiwifruit leaf extract, indicating an expression likely dependent on Psa3 and responsive to plant signal molecule(s) present in kiwifruit leaf extract.

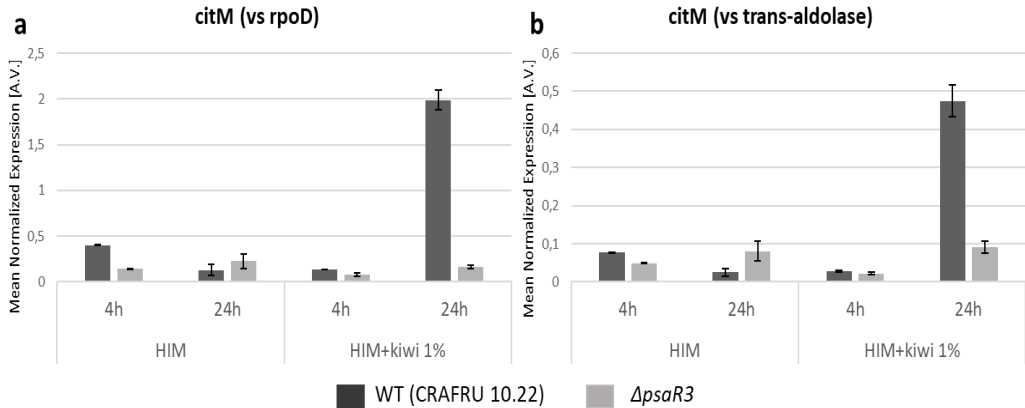


**Figure 14:** Expression of CitM-encoding gene, in CRAFRU 10.22-WT (dull grey) and in the  $\Delta psar3$  mutant (light grey). Samples were taken at 4 and 24 hpi in HIM or HIM supplemented with kiwifruit leaf extract. The analysis was performed by Real-time qPCR using RpoD- (a) or trans-aldolase- (b) encoding genes as house-keeping genes.

## 4.4 LARGE-SCALE TRANSCRIPTION PROFILE ANALYSIS OF CRAFRU 10.22 WILD-TYPE AND $\Delta Psar3$ MUTANT STRAINS

### 4.4.1 STATISTICAL OVERVIEW OF THE MICROARRAY DATA

Subsequently to Real-time qPCR analyses, we performed a large-scale gene expression analysis; using the microarray described previously (chapter 2), but considering only the probes corresponding to the genes present in the genome of CRA-FRU. The analysis was carried out with CRA-FRU 10.22 wild-type and  $\Delta psar3$  mutant strains, to identify the different pathways potentially regulated by Psa3. The two strains were cultivated in HIM supplemented or not with kiwifruit leaf extract and harvested at 4 and 24 hpi. The statistical analysis of the three biological replicates of each strain in each condition showed a clustering based on the time points of harvest, *i.e.*: 4 and 24 hpi (**Fig. 15**). Since one biological replicate of the  $\Delta psar3$  mutant grown in HIM for 24h clustered with the samples collected at 4h, we decided to exclude this sample from the analysis to ensure a good statistical robustness.

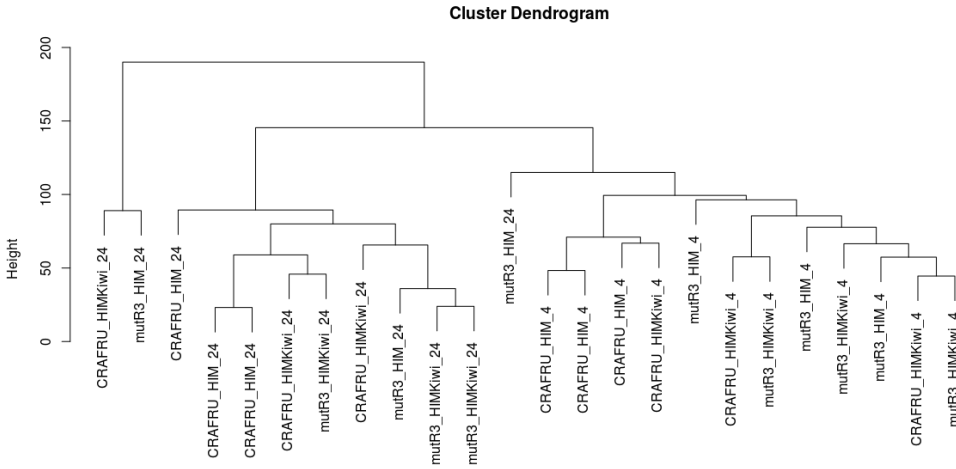


*Figure 15:* Cluster dendrogram of the microarray experiment. CRAFRU= CRAFRU 10.22 (WT); mutR3= CRAFRU 10.22  $\Delta$ *psaR3* mutant; HIM= HIM medium; HIMkiwi= HIM medium supplemented with kiwifruit leaf extract; 4= 4 hpi, 24= 24 hpi.

The dendrogram suggested that the bacterial transcriptome was influenced mainly by the time of the analysis. The mutation in the *PsaR3* receptor and the presence of kiwifruit leaf extract added into the medium seemed to play only a minor role.

#### 4.4.2 GENERAL OVERVIEW OF DIFFERENTIAL EXPRESSED GENES IN BOTH STRAINS

According to a likely transient modulation of genes differentially expressed in minimal conditions, such as *hrpA1* induction, we considered genes as differentially expressed, the ones showing a modulation, with a False Discovery Rate (FDR)  $<0.05$  regardless of the  $\log_2$ -FoldChange of their transcript level between 4 and 24 hpi. Thus assuming that at 24hpi was returned to a basal level. We thus identified 2100 genes and 1318 genes modulated in CRAFRU 10.22 wild-type in HIM and HIM supplemented with kiwifruit leaf extract, respectively. By contrast, the  $\Delta$ *psaR3* mutant showed 1000 genes modulated in HIM and 2438 in HIM supplemented with kiwifruit leaf extract (**Fig. 16**) In all conditions, the portion of the genes up- or down- regulated was around 50%.

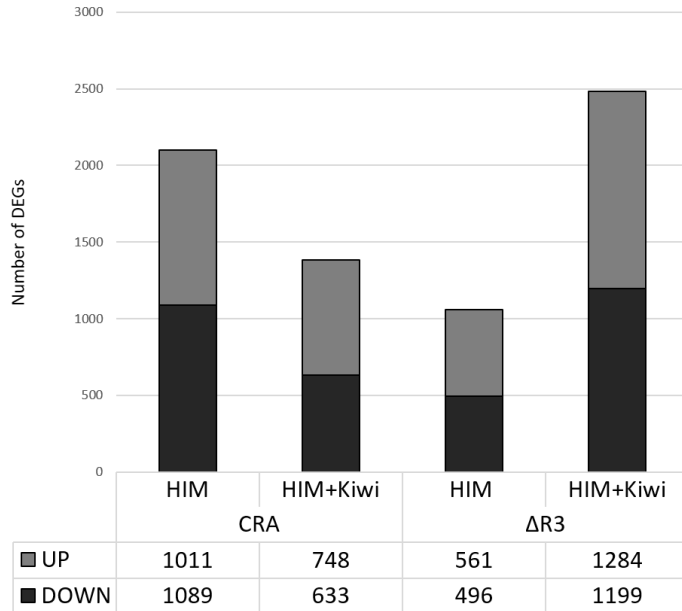


*Figure 16:* Number of genes up-regulated (grey) and down-regulated (black) between 4 and 24 hpi in CRAFRU 10.22 wt (CRA) and in the  $\Delta psar3$  mutant ( $\Delta R3$ ) in HIM and HIM supplemented with kiwifruit leaf extract.

This preliminary analysis suggested that the presence of kiwifruit leaf extract in the medium could decrease the number of DEGs in the wild-type CRA-FRU 10.22 strain, whereas it seemed to increase the number of modulated genes in the  $\Delta psar3$  mutant.

The diverse lists of DEGs obtained were further analysed to identify common, strain-, or condition- specific genes and the results obtained were represented as a Venn diagram (**Fig. 17**). Overall, we identified 553 common DEGs, *i.e.*: the genes modulated either in CRAFRU 10.22 wild-type or in the  $\Delta psar3$  mutant in both growth conditions. The genes uniquely modulated in the wild-type strain were 513 in HIM and 87 in HIM supplemented with kiwifruit leaf extract. On the other hand, the genes uniquely modulated in the  $\Delta psar3$  mutant were 123 in HIM and 812 in HIM supplemented with kiwifruit extract. These results, suggested that kiwifruit leaf extract could regulate Psa gene expression, with a particular effect observed in the  $\Delta psar3$  mutant. It is worth mentioning that two strains shared only 33 DEGs

in HIM and DEGs number increased to 131 in the presence of kiwifruit leaf extract in the medium.

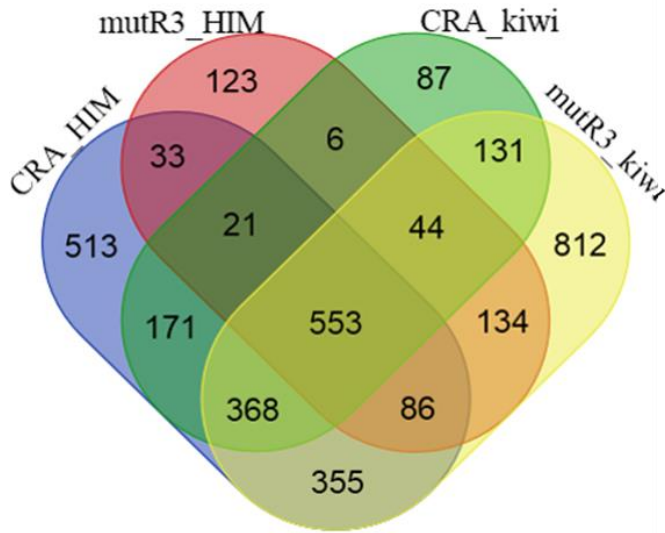


*Figure 17:* Venn diagram of the common or specific DEGs. CRA\_HIM= CRAFRU 10.22 wt in HIM, mutR3\_HIM=  $\Delta psar3$  mutant in HIM, CRA\_kiwi= CRAFRU 10.22 wt in HIM supplemented with kiwifruit leaf extract, mutR3\_kiwi=  $\Delta psar3$  mutant in HIM supplemented with kiwifruit leaf extract

In total, 1113 DEGs were commonly modulated between 4 and 24 hpi in the CRAFRU 10.22 wild-type strain grown in HIM or in HIM supplemented with kiwifruit leaf extract (**Fig. 18**), with around 50% of up-regulated genes and 50% of down-regulated genes (**Fig. 19**). Moreover, we observed more genes regulated only in HIM alone, with 987 HIM-specific genes, whereas only 268 genes were uniquely modulated in HIM supplemented with kiwifruit leaf extract. In the latest condition, we also observed more up-regulated than down regulated genes. It is worth noting that only 1 gene was commonly regulated in both HIM and HIM supplemented with kiwifruit leaf extract but showing an opposite regulation.

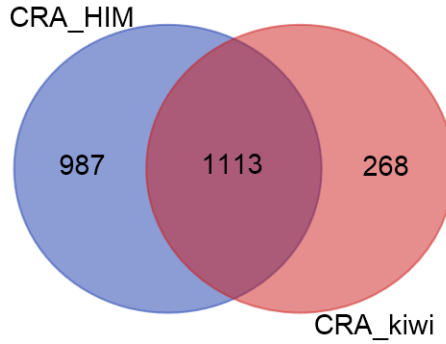


*Figure 18:* Venn diagram of the DEGs of CRAFRU 10.22 wt in HIM and HIM supplemented with kiwifruit leaf extract.

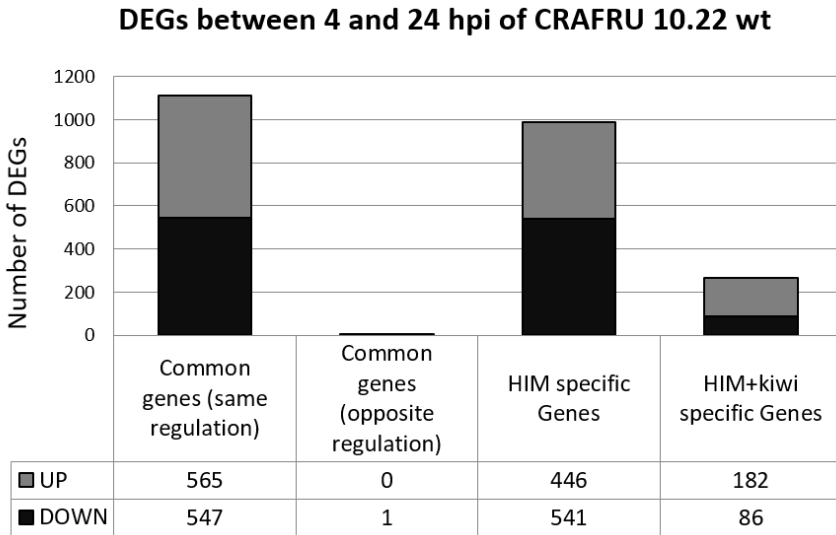


*Figure 19:* Number of up- and down- regulated genes between 4 and 24h of CRAFRU 10.22 wt in HIM and HIM supplemented with kiwi leaf extract.



The same analysis performed with the DEGs identified in the  $\Delta psar3$  mutant between 4 and 24 hpi in the different media showed that the major number of DEGs was modulated specifically in the presence of kiwifruit leaf extract, with a total of 1666 DEGs in HIM supplemented with kiwifruit leaf extract against 827 common DEGs and only 183 HIM-specific DEGs (**Fig. 20**). Among all common or condition-specific DEGs we observed about 50% of up-regulated and 50 % of down-regulated genes (**Fig. 21**). None of the common DEGs showed an opposite regulation between the two media.



Figure 20: Venn diagram of the DEGs of  $\Delta psar3$  mutant in HIM and HIM supplemented with kiwifruit leaf extract.

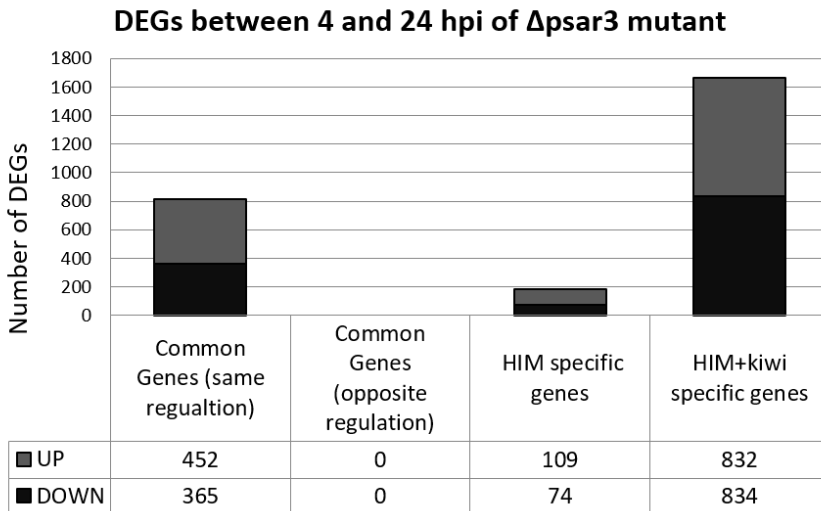


Figure 21: Number of genes up- and down regulated between 4 and 24 hpi of  $\Delta psar3$  mutant in HIM and HIM with kiwi leaf extract.

The analysis of DEGs between 4 and 24 hpi in HIM, comparing CRAFRU 10.22 wild-type and  $\Delta psar3$  mutant strains showed 1407 DEGs specifically modulated in CRAFRU 10.22 wild-type, with 45% of up-regulated genes and 55% of down-regulated genes (Fig. 22, 23). Most of the common DEGs were regulated in the same way.

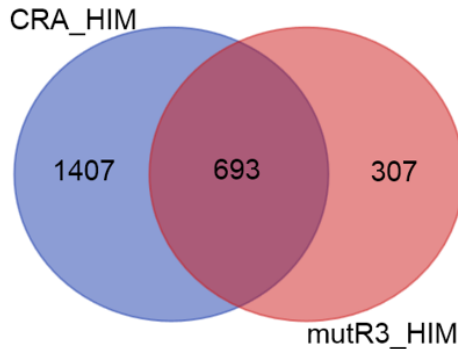


Figure 22: Venn diagram showing common and specific DEGs between CRAFRU 10.22 wt and  $\Delta psar3$  mutant in HIM.

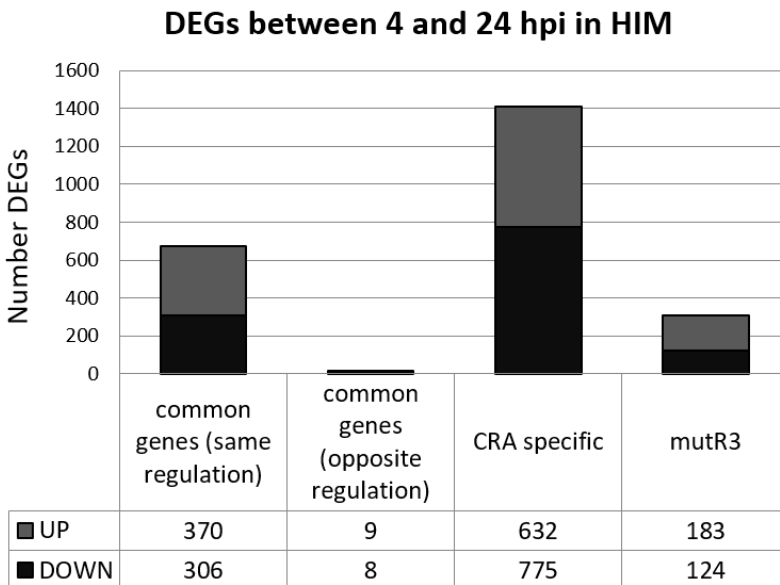
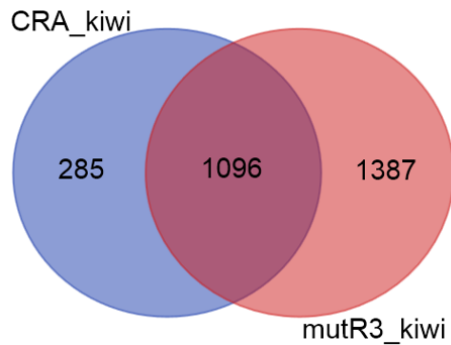


Figure 23: Number of genes up- and down regulated between 4 and 24 hpi of CRAFRU 10.22 wt and the  $\Delta psar3$  mutant in HIM.

Comparing the CRAFRU 10.22 wild-type and the  $\Delta psr3$  mutant, both grown in minimal medium supplemented with kiwifruit leaf extract, we found 1096 DEGs shared by the two strains, 285 DEGs specifically modulated in the CRAFRU 10.22 wild-type and 1387 DEGs specifically modulated in the  $\Delta psr3$  mutant (**Fig. 24, 25**). Among the common DEGs, three genes showed an opposite regulation between the two strains, while the other 1093 showed the same regulation, with 50% up-regulated genes and 50% of down-regulated genes. By contrast, 217 DEGs out of 285 specifically modulated in the wild-type strain were positively regulated, while the  $\Delta psr3$  mutant showed 50% of up-regulated and 50% of down-regulated specific DEGs genes.



*Figure 24:* Venn diagram of the DEGs of CRAFRU 10.22 wt and the  $\Delta psr3$  mutant in HIM supplemented with kiwifruit leaf extract.

### DEGs between 4 and 24 hpi in HIM with kiwifruit leaf extract

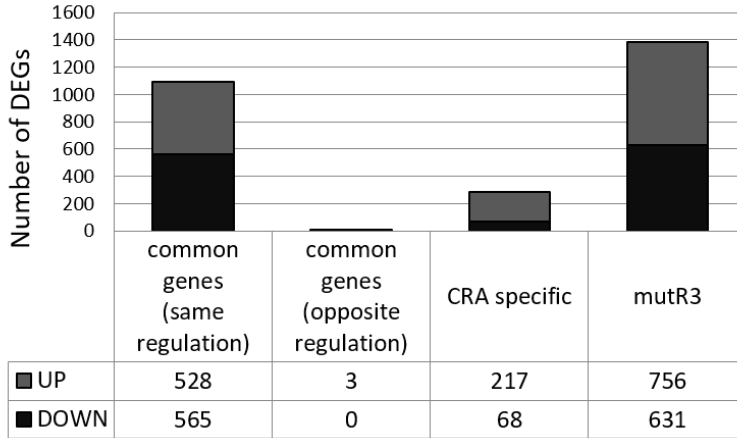


*Figure 25:* Number of up- and down- regulated genes between 4 and 24 hpi in CRAFRU 10.22 wt and  $\Delta psr3$  mutant strains in HIM supplemented with kiwifruit leaf extract.

### 4.3.3 FUNCTIONAL CATEGORY ENRICHMENT IN WILD-TYPE AND $\Delta$ PsaR3 MUTANT STRAINS IN THE DIFFERENT CONDITIONS

The statistical enrichment analysis was performed to identify the functional classes influenced by the addition of the kiwifruit leaf extract and/or by PsaR3. The analysis was performed using the BInGO (Cytoscape) software considering the DEGs between 4 and 24 hpi identified in CRAFRU 10.22 wild-type and  $\Delta$ psaR3 mutant strains in the two conditions. The different categories with  $FDR < 0.05$  were positively represented in the plots considering the value expressed as “1/adjusted p-value”.

The analysis of DEGs in HIM showed a significant enrichment in genes belonging mainly to classes related to pathogenesis, motor activity, and TTSS more enriched classes (**Fig. 26 and 27**).

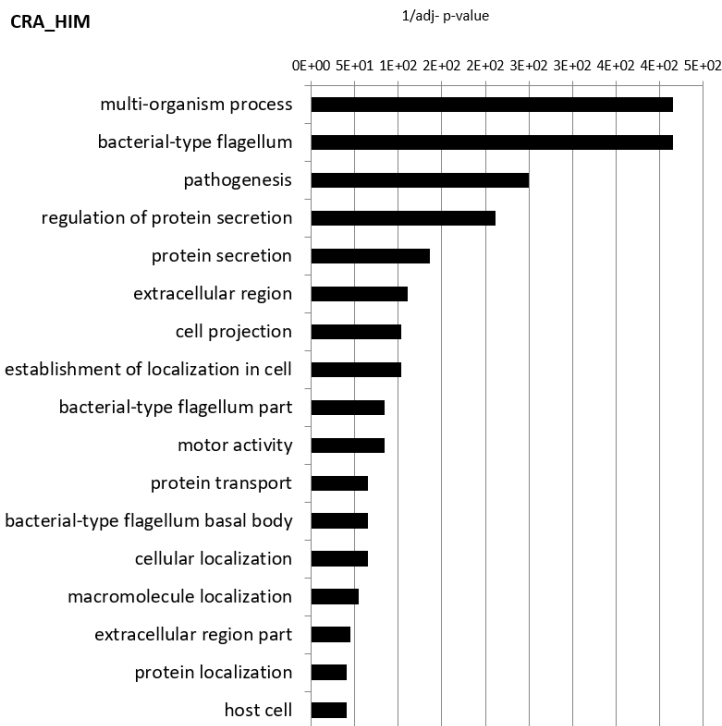


*Figure 26:* GO categories overrepresented in DEGs modulated in CRA-FRU 10.22 wild type strain grown in HIM between 4 and 24 hpi. GO category enrichment was analysed using BInGO

In addition to the above-mentioned GO categories, which were statistically more enriched compared to the wild-type strain, other functional classes were found to be regulated in the *psaR3* mutant grown in HIM alone, including categories related to sigma-factor activity and transcription regulation, in line with the mutation in the *PsaR3*, as well as electron transport chain and ubiquinone biosynthesis process involved in the energetic pathway. By contrast, the functional category related to host cell invasion, enriched in the wild-type strain was not significantly enriched in the  $\Delta$ *psaR3* mutant (**Fig. 27**).

Considering the GO terms enriched in the wild-type strain grown in HIM supplemented with the kiwifruit leaf extract, the statistical analysis revealed functional classes, not observed in minimal medium alone, such as: iron-transport siderophore, vitamin binding, sucrose, starch, glucan and amino acids metabolic process (**Fig. 28**). Moreover, we could notice categories related to sigma-factor activity and transcriptional regulation, which were enriched only in the  $\Delta$ *psaR3* mutant when bacteria were grown in HIM only.

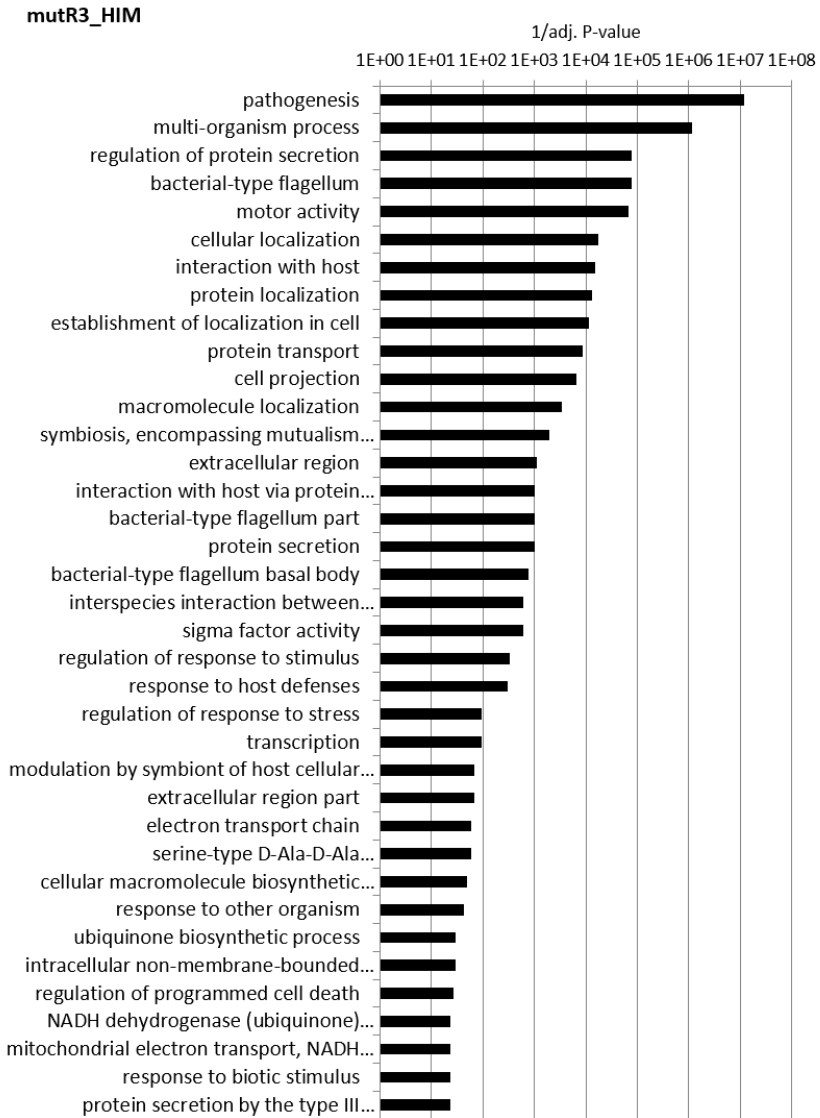


*Figure 27:* GO categories overrepresented in DEGs modulated in  $\Delta$ *psaR3* mutant strain grown in HIM between 4 and 24 hpi. GO category enrichment was analysed using BinGO.

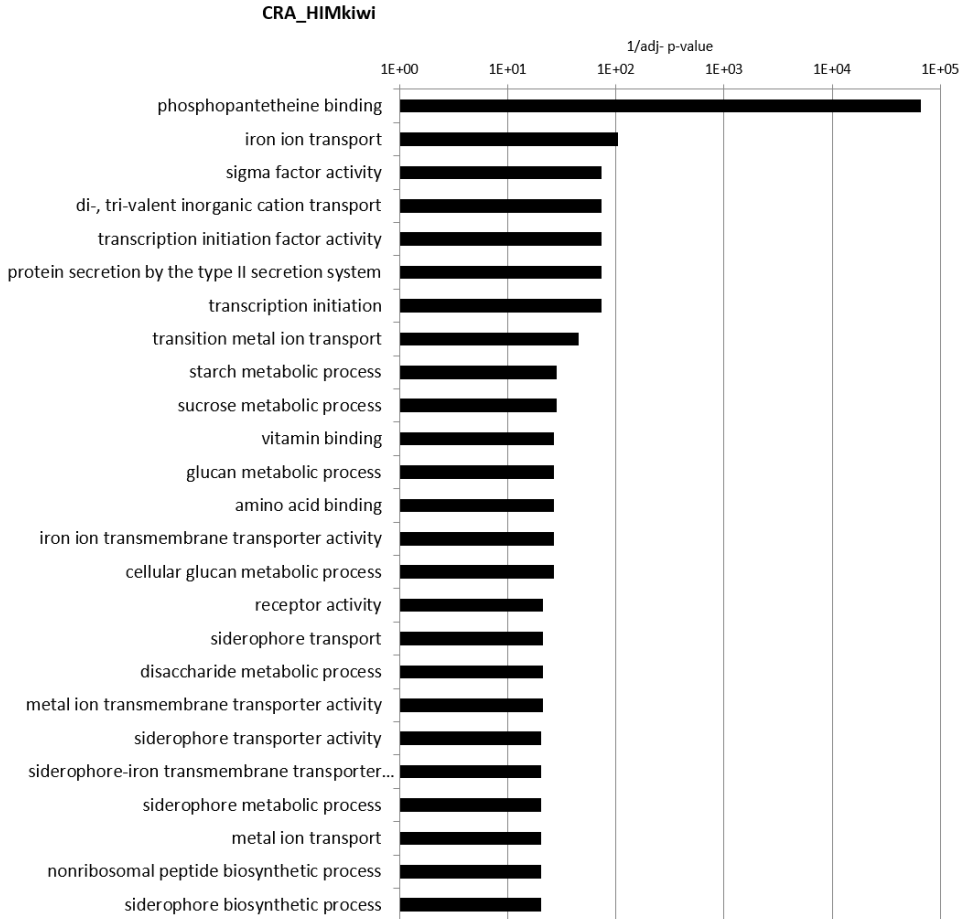


*Figure 28:* GO categories overrepresented in DEGs modulated in CRAFRU 10.22 wild type strain grown in HIM supplemented with between 4 and 24 hpi. GO category enrichment was analysed using BinGO.



In the  $\Delta psar3$  mutant grown in the minimal medium supplemented with the kiwifruit leaf extract the enriched classes were related to sigma-factor activity and transcription regulation activity as observed in the minimal medium alone, but also to the interaction with host as well as the category related to iron metal transporter (**Fig. 29**).

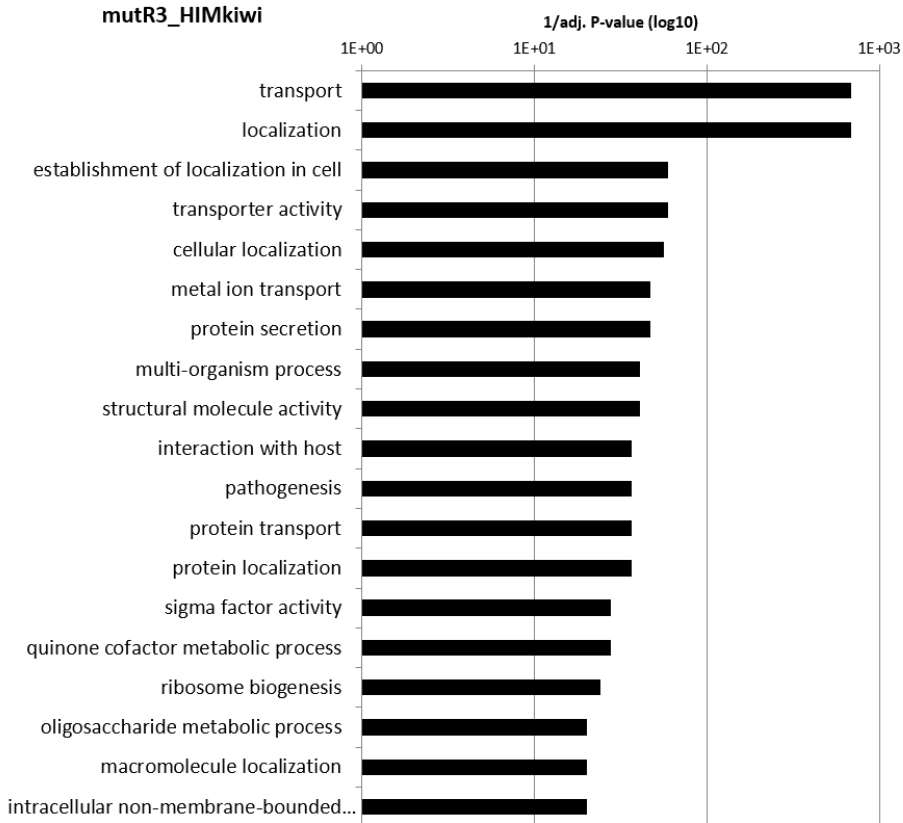


*Figure 29:* GO categories overrepresented in DEGs modulated in  $\Delta psar3$  mutant strain grown in HIM supplemented with between 4 and 24 hpi. GO category enrichment was analysed using BinGO.

The differential expression analyses were also performed considering the DEGs between the wild type strain and the  $\Delta psr3$  mutant, both grown in the minimal medium to evaluate the genes modulated specifically in absence of Psr3 and genes showing an opposite regulation between 4 and 24 hours in both strains (**Fig. 30**).

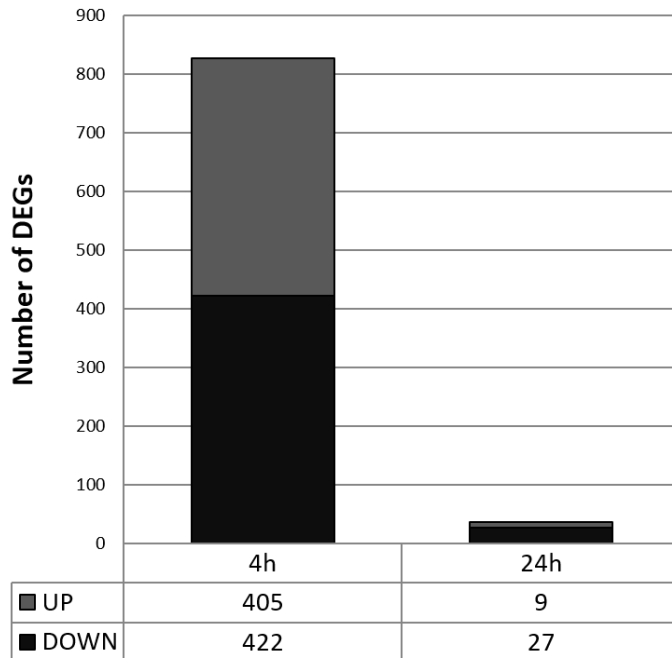


*Figure 30:* Number of DEGs between CRAFRU 10.22 wt and the  $\Delta psr3$  mutant between 4 and 24 h of growth in HIM.

The analysis highlighted 405 up-regulated genes and 422 down-regulated genes at 4 hpi, but only few DEGs at 24 hpi with 9 up-regulated and 27 down-regulated genes. We thus further considered only the time point 4 hpi to perform GO enrichment analysis. Such analysis showed that the genes positively regulated in the mutant belonged to functional categories related to the host-interaction process mediated by TTSS, motility such as the flagellum, and mechanisms involved in pathogenesis and necrosis (**Fig. 31**).

## HIM 4h UP

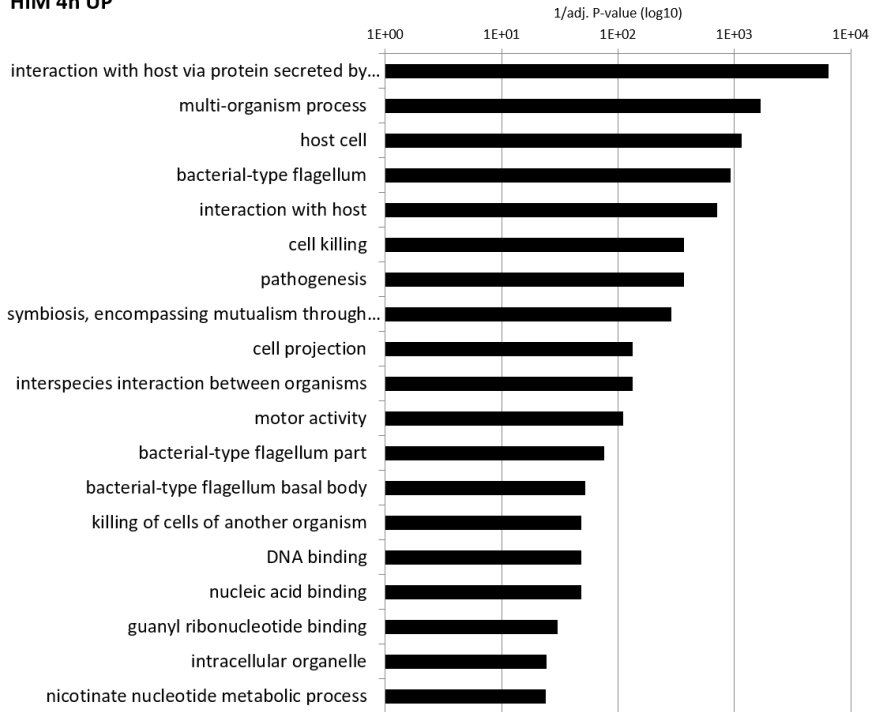
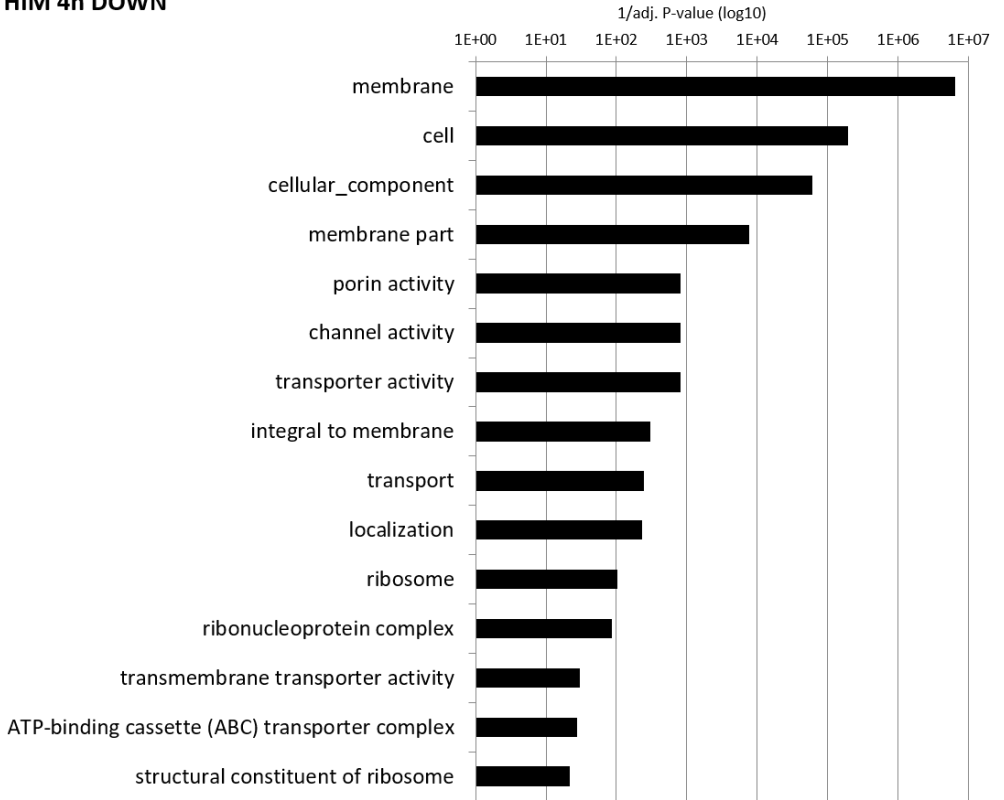


Figure 31: GO categories overrepresented among DEGs up-regulated in the  $\Delta psar3$  mutant grown in HIM at 4 hpi. GO categories enrichment was analysed using BinGO.

By contrast among the genes negatively regulated in the  $\Delta psar3$  mutant in comparison with the wild-type strain, we found categories related to cellular membrane component, transport and ribosomal activity (Fig 32).

## HIM 4h DOWN



*Figure 31:* GO categories overrepresented among DEGs down-regulated in the  $\Delta psaR3$  mutant grown in HIM at 4 hpi. GO categories enrichment was analysed using BinGO.

## 5. DISCUSSION

*Pseudomonas syringae* pv. *actinidiae* is characterized by three putative LuxR receptor-like proteins lacking a cognate LuxI synthase [9] and for which the function and the inducing signal molecule(s) have not been elucidated yet. The bioinformatic analysis on PsaR receptors highlighted that PsaR3 is localized on the plasmid and that it is specific of the strains belonging to the Psa biovar 3, further confirmed experimentally. Moreover, PsaR3-encoding gene was found to be localized within a cluster including genes encoding the anthranilate synthases component I and II, a phenyl-COA ligase, an acetyl transferase, a lipase, a putative reductase a transporter assuming that their expression could be regulated by the PsaR3 whether this protein plays a role as transcriptional regulator. An Interesting hypothesis about the cluster is that PsaR3 could promote the transcription of anthranilate synthase which could be a substrate for the production of a signal molecule that leads the PsaR3 activation, thus following a mechanism similar to as observed for the PQS in *P. aeruginosa*. Moreover, in *Pseudomonas* and *Xylella fastidiosa* genes encoding the anthranilate synthase and phenyl-CoA ligase are belonging to a cluster similar to that observed in the case of PsaR3 [17]. In this case the anthranilate produced could be used as substrate of phenyl-CoA ligase [18]. The molecules could be secreted thanks to a transporter, which is present in the PsaR3 cluster, thus regulating the Psa QS PsaR3-dependent.

Recently it was reported that in *Photorhabdus luminescens* and *Photorhabdus asymbiotica*, insect-larvae pathogenic bacteria, the two LuxR solos like receptors, *i.e.*: PauR and PluR, cannot sense AHL molecules but other endogenous product named photopyrones (PPYs), dialkylresorcinols (DARs) and cyclohexanediones (CHDs) used in the cell-cell communication mechanism. Following signal recognition, the receptors activate the transcription of the cognate *pcfABCDEF* operon causing the cell clumping concurring to increase the *Photorhabdus* pathogenicity [19].

The intergenic region presented in the cluster could be targeted (directly or indirectly) by PsaR3 and thus function as bi-directional promoter. The production of secondary metabolites in *Giberella fujikuroi*, like gibberellic acid, is under the control of a bi-directional promoter in a gene cluster [20].

The bioinformatic analysis to evaluate the putative promoter-role of the intergenic region contained in the *psaR3* cluster highlighted the presence of *cis*-acting elements regulated by transcription factor, binding the HTH motif, of other organism, such as: LasR, RhlR, DegU

and OryR of *P. aeruginosa*, *Bacillus subtilis* and *Escherichia coli* respectively; supporting the hypothesis that this region could play a role as bi-directional transcriptional promoter of the genes contained in the gene-cluster, probably activated by PsaR3, which could participate in the transcriptional regulation of Psa and thus likely playing a crucial role in the virulence of Psa.

In *Pseudomonas syringae*, the filamentous machinery of the TTSS is called the Hrp pilus in which the major structural protein is encoded by *hrpA* [21]. The HrpA1-encoding gene showed a high expression level in minimal medium at 4 hpi in the wild-type and it was further induced by the kiwifruit leaf extract, supporting the hypothesis of the role of a kiwifruit signal(s) in triggering the Psa virulence. Moreover, the higher level of the expression in the wild type in presence of the kiwifruit leaf extract, not observed in the case of the  $\Delta$ *psaR3* mutant, suggested that the PsaR3 could be responsible of the plant-signal recognition likely increasing the transcription level of genes involving in the TTSS formation which was already induced by HIM in a *psaR3*-independent manner as confirmed also by the microarray data.

The effect of the kiwifruit leaf extract was also appreciate considering the gene expression analysis of PsaR1- and PsaR2- encoding genes that showed an increase in the amount of the transcript for both putative receptors in relation with the presence of kiwifruit leaf extract in the medium. Moreover, such increase was observed in the wild-type, suggesting that PsaR3 could be involved in the regulation mechanism of the other two LuxR-like solos receptor validating its importance in regulating the high virulence of the biovar 3. As already mentioned, this kind of mutual regulation among the LuxR receptor was described also for the LasR-RhlR of *P. aeruginosa* [22]. However, to demonstrate a mutual regulation among the PsaR receptors also helpful to elucidate the role of the PsaR3 specific of the biovar 3 it would be useful to perform the *in-vitro* expression of these proteins and test their activity against a library of AHLs and plant derived molecules.

The expression level of the genes encoding the lipase, the pheCoA ligase and *psaR3* increased in presence of kiwifruit leaf extract, showing a possible role of the extract in the regulation of these genes. It is well known that the LuxR proteins can regulate the expression of neighbouring genes, in general LuxI synthases [23]; behaviour that we could observe also for PsaR3 which seems regulate the expression of the genes belonging to its cluster maybe recognizing a kiwifruit signal(s).

Moreover, the minor expression level in the mutant in comparison with the wild-type suggests a role of PsaR3 in the expression regulation that could be mediated by the kiwifruit leaf extract. The *ASI* is the only gene in the cluster showed differential modulation in the  $\Delta$ *psaR3* mutant suggesting that this gene could be either directly or indirectly repress by PsaR3 or not be regulated by the putative receptor.

The data obtained partly elucidates the role of kiwifruit leaf extract and PsaR3 in the gene-cluster regulation, suggesting another hypothesis for which PsaR3 could bind the intergenic region to promote the transcription of the genes in both orientations. In *P. aeruginosa*, LasR a LuxR-type protein, controls the transcription of *pqsH* a flavin-dependent monooxygenase involved in the PQS system, implying that LasR takes part in the control of the PQS system [24]. Moreover, LasR activates the transcription of *rhIR* and some virulence genes. RhIR forms a complex with the butanoyl-homoserine-lactone (BHL) *i.e.*: RhIR/BHL which is involved in the gene-regulation mechanisms and in the binding of the promoter region of *hcnABC* cluster encoding a Hydrogen Cyanide Synthase (HCN) which allows the growth of the pathogen in microaerophilic conditions [25] which is important for the survival of the pathogen within in its host.

#### **-Other possible regulators of cluster transcription**

In *Listeria monocytogenes* the orphan DegU, a response regulator of the two component system (DegU/DegS) belongs to NarL family, controls the transcription of genes involve in the motility and virulence of the pathogen as well as the biofilm formation [26]. However, this *cis*-acting element does not rule out a direct regulation by PsaR3 since annotated as NarL (with 37% of identity and 52% of positives match with NarL of *L. monocytogenes*). In *E. coli*, OxyR a LysR-type transcriptional regulation, is activated by the formation of a intramonomeric disulfide bridge in its LysR-domain which change the OxyR DNA-binding specific and thus activating the transcription of genes encoding peroxide-detoxifying enzymes like catalase, allowing the pathogen to overcome the host defence mechanisms [27].

Interestingly, the presence of genes encoding the anthranilate synthases component I and II in the *psaR3*-cluster suggests that their transcription activation could be mediated by *psaR3* receptor, thus leading the anthranilate synthesis which could activate a QS mechanism similar

to that observed in *Pseudomonas aeruginosa*, which is involved in increasing its virulence and which precursor of the PQS it is indeed the anthranilate [17].

To further elucidate the role of PsaR3 or kiwifruit extract in the Psa virulence, we evaluated through gene expression analysis either in small scale or in large scale their effect on the CRAFRU 10.22 and  $\Delta$ *psaR3* mutant. The phytopathogenic bacteria activate different strategies to suppress the defence responses of the host plant like the injection of a large number of virulence effector proteins using the TTSS within few hours from the host infection [21].

### **-Possible function of PsaR3**

Usually iron is poorly available in the eukaryotic hosts, so bacterial pathogens have evolved different strategies to scavenge this element, such as siderophores, heme uptake or utilization of host-iron binding proteins. Indeed, iron strongly affects the expression of bacterial virulence genes thus playing an important role in mediating host-pathogen interaction and ensuring bacterial infection. For instance, in *P. aeruginosa* iron is involved in biofilm formation and in the expression of virulence factors in a dose-dependent manner, *i.e.*: a low level of iron activates biofilm formation, extracellular DNA release and PQS mediated QS [28]. The level of available iron is directly associated to the expression of virulence genes also in *Pseudomonas syringae* pv. *tomato* [15, 16]. Moreover, Matas and associated (2012) [29] demonstrated that, in *Pseudomonas savastanoi* pv. *savastanoi*, the *citN* gene, encoding a citrate transporter involved in iron-uptake through siderophores, is fundamental for pathogen growth in the host, thus participating in the virulence of the pathogen. Interestingly, in Psa, we observed that the expression of *citM* was induced by kiwifruit leaf extract in a PsaR3-dependent manner in the poor HIM, which does not contain iron, thus suggesting a relationship between PsaR3 and iron availability regulation. Moreover, CitM-encoding gene was not directly found as differentially expressed in the microarray analysis. The more general class of citrate transporters was identified as enriched among up-regulated genes in the wild-type strain grown in minimal medium in presence of kiwifruit leaf extract. This supports the hypothesis that kiwifruit leaf extract could influence the iron availability which uptake could be regulated by PsaR3 and thus triggering the Psa virulence. Conversely, the functional category related to transport activity was down-regulated in the  $\Delta$ *psaR3* mutant grown in HIM, further supporting that these genes could be positively regulated by PsaR3, following the perception of some kiwifruit signal molecule(s).

---



The growth of Psa in HIM, which mimics the apoplasmic conditions, highlighted a phenotype of cell aggregation, characteristic of the growth in hostile conditions (poor nutrient availability and low pH) compared with the growth in a rich medium. This is in line with Wasim and associates [30], who reported that in *Azospirillum brasilense* the flocculation and cell-aggregation phenotype were promoted under stressful poor nutritional conditions, like an excess of reducing equivalent (high C/N ratios) and prolonged stationary phase. In the same way *P. aeruginosa* was shown to form cell aggregates during its infection process, in response to the poor energetic resources available in host environment. [31]. In *Xylella fastidiosa*, cell aggregation behaviour is an important virulence mechanism because the bacterial cell-clusters blocks the passage of nutrients from the roots to the leaves of the host plant [32].

Interestingly, cell aggregate formation was qualitatively different in the  $\Delta$ *psaR3* mutant, thus suggesting that this phenotype could be partially regulated by PsaR3. Accordingly, microarray analysis highlighted that the functional category related to “cellular membrane function” was down-regulated in the  $\Delta$ *psaR3* mutant grown in HIM supporting a direct or indirect role of PsaR3 in the regulation of genes involved in aggregate formation. Such a role for QS system was previously reported for the LasR/LasI system in *Pseudomonas aeruginosa*. The latest controls the expression of the tyrosine phosphatase TpbA that inhibits the expression of *pel* genes, an operon involved in extracellular matrix biosynthesis, thus allowing cell-aggregate formation [33]. In *Vibrio cholera*, the LuxR-like protein LuxO, activates the transcription of four small RNAs that prevent the binding of the ribosome to *hapR* mRNA, encoding the QS master regulator, leading to biofilm dispersion [34]. In *Xanthomonas campestris* the two-component system (TCS), RpfC/RpfG, controls biofilm dispersion, according to the formation of cell aggregate by the mutant *rpfC/rpfG* mutant grown in L medium, while the wild type grows planktonically under the same condition [35]. Interestingly, it was proposed that RpfC/RpfG may act through the perception of the diffusible signal factor (DFS), which could be a plant signal. Moreover, *R. leguminosarum* forms cell aggregates using cellulose microfibrils formed upon contact with root exudates [36]. In the same manner, the presence of kiwifruit leaf extract in the medium strongly affected the visible aspect of Psa cell-aggregates, which were smaller and more dispersed, thus suggesting that this phenotype could be regulated by kiwifruit signal(s). However, since the effect of kiwifruit leaf extract was similar in both Psa wild-type and  $\Delta$ *psaR3* mutant strains, this would be correlated to PsaR3, which in this case would play a role independent of plant signal recognition.

## 6. SUPPLEMENTAL RESOURCES

### List of primers used in this chapter:

Gene	Primer Name	Sequence	TM
<i>psaR3 (gene)</i>	psaR3FOR	ATGGATACGTACAACCTCACG	58
<i>PsaR3 (gene)</i>	psaR3REV	TTATATCCGGCCCGTTTGAT	58
<i>rpoD</i>	rpODFORRT	GTTGCCCTTGCCGAATTGTT	60
<i>rpoD</i>	rpODREVRT	CATCACGTACGCACAACCTGC	62
<i>transaldolase</i>	transaldolaseFOR	TGACCATCAGCACCGAGTT	58
<i>transaldolase</i>	transaldolaseREV	GCAGACAGCAGCGCTTCC	60
<i>pheCOA ligase</i>	pheCOAFOR	TGCGACACGGTAATCGCCAAAT	62
<i>pheCOA ligase</i>	pheCOAREV	TCAGCGAGGTCCTCGACCA	62
<i>lipase</i>	LipaseFOR	GTCGAGGGAGCTGGACATGT	64
<i>lipase</i>	LipaseREV	TGGCGCTGAAGAAGTTTCGAG	62
<i>anthranilate synthase comp I</i>	ASIFOR	CAACATGGACACCGCCATCG	64
<i>anthranilate synthase comp I</i>	ASIREV	GCAGTCTGCGAGGCCAAGG	64
<i>psaR3</i>	PsaR3FORRT	CAGCCACATCCTCACTCGCT	64
<i>psaR3</i>	PsaR3REVRT	TCCAACGGGTGATCGAAGTG	64
<i>psaR1</i>	PsaR1FORRT	GCTCCGTGAACCTTGAAGTGCT	64
<i>psaR1</i>	PsaR1REVRT	TTGGCGACGCCGAGCTTTGA	64
<i>psaR2</i>	PsaR2FORRT	GCGTGAACGCGAGTGCCTGA	64
<i>psaR2</i>	PsaR2REVRT	AACGCGGTTTTTGCGCCCA	64
<i>hrpA1</i>	hrpA1FOR	TGATGCACAAGCCAAGGCCA	62
<i>hrpA1</i>	hrpA1REV	TTCTTTGCCGCGCTGGATGG	62
<i>citM</i>	citMFOR	CTCAGCCCGCTGGTGCCTT	64
<i>citM</i>	citMREV	TACATGCTGCTATAGAACGGGA	64

## 7. REFERENCES

- 1 Subramoni, S. Venturi, V. (2009), LuxR-family ‘solos’: bachelor sensors/regulators of signalling molecules. *Microbiology Journal*, doi: 10.1099/mic.0.026849-0
- 2 Patankar, A. V. and Gonzales, J. E. (2009), Orphan LuxR regulators of quorum sensing. *FEMS Microbiology Review*, doi: 10.1111/j.1574-6976.2009.00163.x
- 3 Nasser, W. and Reverchon, S. (2007), New insights into the regulatory mechanisms of the LuxR family of quorum sensing regulators. *Analytical Chemistry Journal*, doi: 10.1007/s00216-006-0702-0

- 4** Fuqua, C. (2006), The QscR Quorum-Sensing Regulon of *Pseudomonas aeruginosa*: an orphan claims its identity. *Journal of Bacteriology*, doi: 10.1128/JB.188.9.3169-3171.2006.
- 5** Brachmann, A. O. *et al.*, (2013), Pyrones as bacterial signaling molecules. *Nature Chemical Biology*, doi: 10.1038/nchembio.1295
- 6** Zhang, L. *et al.* (2007), A proline iminopeptidase gene upregulated in planta by a LuxR homologue is essential for pathogenicity of *Xanthomonas campestris* pv. *campestris*. *Mol. Microbiology*, doi: 10.1111/j.1365-2958.2007.05775.x
- 7** Venturi, V. (2006), Regulation of quorum sensing in *Pseudomonas*. *FEMS Microbiology Review*, doi: 10.1111/j.1574-6976.2005.00012.x
- 8** Hudaiberdiev, S. (2015), Census of solo LuxR genes in prokaryotic genomes. *Front Cell Infect Microbiol.*, doi: 10.3389/fcimb.2015.00020
- 9** Patel, H. K. *et al.* (2014), The Kiwifruit Emerging Pathogen *Pseudomonas syringae* pv. *actinidiae* Does Not Produce AHLs but Possesses Three LuxR Solos. *Plos One*, doi: 10.1371/journal.pone.0087862
- 10** Rees-George, J. *et al.* (2010) Detection of *Pseudomonas syringae* pv. *actinidiae* using polymerase chain reaction (PCR) primers based on the 16S–23S rDNA intertranscribed spacer region and comparison with PCR primers based on other gene regions. *Plant Pathology*, 59, 453–464, doi: 10.1111/j.1365-3059.2010.02259.x
- 11** Pfaffl, M. W. (2012) Quantification strategies in Real-time polymerase chain reaction. Chapter 3 of *Quantitative Real-time PCR in Applied Microbiology* edition by Martin Filion, *Caster Academic Press*, ISBN: 978-1-908230-01-0
- 12** Simon, P. (2003) Q-Gene: processing quantitative real-time RT–PCR data. *Bioinformatics*, Volume 19, Issue 11, Pages 1439–1440, doi: 10.1093/bioinformatics/btg157
- 13** Ramakers, C. Ruijter, J. *et al.* (2003) Assumption-free analysis of quantitative real-time polymerase chain reaction (PCR) data. *Neuroscience Letters*, Volume 339, Issue 1, doi: 10.1016/S0304-3940(02)01423-4
- 14** Collmer, A. *et al.* (2000) *Pseudomonas syringae* Hrp type III secretion system and effector proteins. *PNAS*, doi: 10.1073/pnas.97.16.8770
- 15** Kim, J. B. *et al.* (2009) Effect of the iron concentration on the growth of *Pseudomonas syringae* and the expression of virulence factors in *hrp*-inducing minimal medium. *Applied and Environmental Microbiology*, p. 2720–2726, doi: 10.1128/AEM.02738-08

- 16** Kim, J. B. *et al.* (2010) Complex response to culture condition in *Pseudomonas syringae* pv. tomato DC3000 continuous cultures: the role of iron in cell growth and virulence factor induction. *Biotechnology and Bioengineering*, Vol. 105, No. 5, doi: 10.1002/bit.22609
- 17** Palmer, G. C., Jorth, P. A., & Whiteley, M. (2013). The role of two *Pseudomonas aeruginosa* anthranilate synthases in tryptophan and quorum signal production. *Microbiology*, <https://doi.org/10.1099/mic.0.063065-0>
- 18** McCann, H. C., *et al.* (2013). Genomic Analysis of the Kiwifruit Pathogen *Pseudomonas syringae* pv. *actinidiae* provides insight into the origins of an emergent plant disease. *PLoS Pathogens*, <https://doi.org/10.1371/journal.ppat.1003503>
- 19** Brameyer S. *et al.* (2014) Dialkylresorcinols as bacterial signaling molecules. *PNAS*, doi: 10.1073/pnas.1417685112
- 20** Malonek, S. *et al.* (2005) Functional characterization of two cytochrome P450 monooxygenase genes, P450-1 and P450-4, of the gibberellic acid gene cluster in *Fusarium proliferatum* (*Gibberella fujikuroi* MP-D). App. in Env. Microb., doi: 10.1128/AEM.71.3.1462-1472.2005
- 21** Cornelis, G. R. and Gijsegem F. V. (2000), Assembly and function of Type III Secretion System. *Annu. Rev. Microbiol.*
- 22** Medina, G. *et al.* (2003) Transcriptional regulation of *Pseudomonas aeruginosa* rhIR, encoding a quorum-sensing regulatory protein. *Microbiology*, doi: 10.1099/mic.0.26282-0
- 23** Wai-Leung, N. and Bassler, B. L. (2009), Bacterial quorum-sensing network architectures. *Annu. Rev. Genet.*, doi: 10.1146/annurev-genet-102108-134304
- 24** Lee, J. Lianhui, Z. (2014) The hierarchy quorum sensing network in *Pseudomonas aeruginosa*. *Prot. Cell*, doi: 10.1007/s13238-014-0100-x
- 25** Pessi, G. Haas, D. (2000) Transcriptional Control of the Hydrogen Cyanide Biosynthetic Genes hcnABC by the Anaerobic Regulator ANR and the Quorum-Sensing Regulators LasR and RhIR in *Pseudomonas aeruginosa*. *Journal of Bacteriology*, doi: 10.1128/JB.182.24.6940-6949.2000
- 26** Gueriri, I. *et al.* (2008) The DegU orphan response regulator of *Listeria monocytogenes* autorepress its own system and is required for bacterial motility, virulence and biofilm formation. *Microbiology*, doi: 10.1099/mic.0.2008/017590-0

- 27** Teramoto, H. *et al.* (2013) OxyR acts as a transcriptional repressor of hydrogen peroxide-inducible antioxidant genes in *Corynebacterium glutamicum* R. *The FEBS Journal*, doi: 10.1111/febs.12312
- 28** Wiens, R. J. *et al.* (2013) Iron-regulated expression of alginate production, mucoid phenotype, and biofilm formation by *Pseudomonas aeruginosa*. *MBio*, doi: 10.1128/mBio.01010-13
- 29** Matas, M. I. *et al.* (2012) Identification of novel virulence genes and metabolic pathways required for full fitness of *Pseudomonas savastanoi* pv. *savastanoi* in olive (*Olea europaea*) knots. *New Phytologist*, doi: 10.1111/j.1469-8137.2012.04357.x
- 30** Wasim, M. *et al.* (2009) Alkyl hydroperoxide reductase has a role in oxidative stress resistance and in modulating changes in cell-surface properties in *Azospirillum brasilense* Sp245. *Microbiology*, doi: 10.1099/mic.0.022541-0
- 31** Kragh, K. N. *et al.* (2016) Role of multicellular aggregates in biofilm formation. *MBio*, DOI: 10.1128/mBio.00237-16 Number 2, Pages 269-282, doi: 10.1094/MPMI-21-2-0269
- 32** Newman, K. L. *et al.* (2003) Use of a green fluorescent strain for analysis of *Xylella fastidiosa* colonization of *Vitis vinifera*. *Appl. Environ. Microbiol.*, 69, 7319–7327
- 33** Ueda, A. and Wood, T. K. (2009) Connecting quorum sensing, c-di-GMP, Pel polysaccharide, and biofilm formation in *Pseudomonas aeruginosa* through tyrosine phosphatase TpbA (PA3885). *PLoS Pathog.*, doi:10.5:e1000483
- 34** Zhao, X. *et al.* (2013) Posttranscriptional activation of a diguanylate cyclase by quorum sensing small RNAs promotes biofilm formation in *Vibrio cholerae*. *Mol Microbiol*, 89:989-1002.
- 35** Dow J. M., *et al.* (2003) Biofilm dispersal in *Xanthomonas campestris* is controlled by cell–cell signaling and is required for full virulence to plants. *PNAS*, 100:10995-11000.
- 36** Cava, J. R. *et al.* (1989) *Rhizobium leguminosarum* CFN42 genetic region encoding lipopolysaccharide structures essential for complete nodule development on bean plants. *J. Bacteriol.* 1989, 171, 8–15.

# **Chapter 4: Inter-kingdom signalling via PsaR3 between the kiwifruit pathogen *Pseudomonas syringae* pv. *actinidiae* and its host plant**

## **1. ABSTRACT**

Some experimental evidence suggested that a sub-family of LuxR proteins could sense signal molecules derived from plants. This indicates the presence of an inter-kingdom signalling communication system between bacteria and plants that could participate in host recognition and virulence triggering. In the previous chapter we showed that PsaR3, a LuxR solus protein of *Pseudomonas syringae* pv. *actinidiae* is specific of the biovar 3 and it could be necessary for the expression of relevant, virulence-associated genes. Moreover, we showed that it could be involved in the recognition or transduction of kiwifruit plant signal(s). In this chapter, we focused the attention on the PsaR3 receptor with three main approaches: *i*) first of all, we studied putative PsaR3-targeted sequences either in presence or not of kiwifruit leaf extract in the growing rich and minimal media, using the luciferase assay. These experiments allow us the identification of some kiwifruit leaf extract fractions able to increase the target promoter activity and that would be probably contain the signal likely recognized by PsaR3; *ii*) a RNAseq analysis of a Psa strain overexpressing the PsaR3 receptor, in an inducible manner, in two different conditions *i.e.*: rich media or a minimal medium supplemented with kiwifruit leaf extract, to identify genes modulated by *psaR3*-overexpression and by the perception of the plant host signal(s); *iii*) finally, developed a reliable protocol to produce and purify this receptor protein, for subsequent identification of its possible ligands and the target-sequence by DNA-binding assay.

## **2. INTRODUCTION**

The most common QS in Gram-negative bacteria consists of a LuxI-family synthase in charge of the synthesis of AHL signals which interact at quorum concentration with their cognate LuxR-family receptors: those act as transcription factors regulating the transcription

of several genes or operons [1]. AHLs present different structures, such as different acyl chain lengths (from 4 to 20 carbons) with diverse oxidation state of the C3 on the acyl chain.

Several studies on AHL-mediated QS, reported that the majority of plant associated bacteria (PAB) use QS for the regulation of virulence-associated pathways and to promote their growth within their hosts [2-5]. Other studies indicate that the plant can respond to bacterial AHLs with the regulation of plant genes showing different phenotypes [6-9]. *Arabidopsis thaliana* exposed to C6-HSL showed different levels of auxin and cytokinin in addition to growth defects [9]. Plants can also interfere with bacterial pathogenicity by producing low molecular weight compound which act as antagonist or agonist of bacterial AHLs [10-12]. QS-AHLs systems are composed of *luxI/luxR* encoding genes located closely to each other in the bacterial chromosome. As already mentioned in previous chapters, LuxR receptors not associated to LuxI –synthase, have been named LuxR solos.

They present the same modular structure of the LuxR receptors that is: an *N*-terminal domain and an DNA-binding helix-turn-helix (HTH) domain situated in the *C*-terminal region. The DNA-binding HTH domain binds gene promoter regions carrying conserved motifs (*lux*-box) [13, 14]. Some LuxR solos can recognize exogenous AHLs such as the QscR in *Pseudomonas aeruginosa* and SdiA in *Salmonella enterica* and *Escherichia coli* [15-17], while, other LuxR solos can respond to endogenous signals which are not AHLs such as photopyrones (PPYs) or dialkylresorcinols (DARs) in the case of *Photorhabdus* spp. [18]. Moreover, a sub-family of LuxR solos present in PABs evolved the capacity to recognize and respond to signal molecule(s) derived from plants [19, 20] as demonstrated for XccR of *Xanthomonas campestris* pv. *campestris*, OryR of *Xanthomonas oryzae* pv. *oryzae*, PsoR of *Pseudomonas fluorescens*, XagR of *Xanthomonas axonopodis* pv. *glycines* and NesR of *Sinorhizobium meliloti*. XccR regulates the transcription of the neighbouring *pip* gene (a proline immunopeptidase) and recognizes a crucifer compound not yet identified [21]. OryR is involved in the modulation of several virulence genes, motility genes and of the neighbouring *pip* gene and it responds to a plant signal [22]. XagR involved in the negative regulation of adhesion via *yapH* in response to a plant compound(s) which increases the spread of the pathogen within its host [23].

*Pseudomonas syringae* pv. *actinidiae* presents three LuxR solos, namely PsaR1, PsaR2 and PsaR3 among which PsaR3 shows some interesting features such as biovar 3 specificity, the plasmid localization and its location into a gene-cluster that could regulate Psa virulence as

described in the previous chapter. Moreover, the gene-cluster contains an intergenic region that could play a role as bi-directional transcriptional promoter and could be regulated by PsaR3 itself, according with the predicted presence of *cis*-acting elements putatively regulated by LuxR-family proteins. In this chapter we focused the attention on the activity of this putative promoter and its possible regulation by PsaR3 revealing *i*) that this LuxR solos mediates the transcriptional modulation of direct or indirect target and *ii*) that PsaR3 could take part in the Psa recognition of a kiwifruit signal thus mediating an inter-kingdom communication and likely playing a crucial role in the high virulence of biovar 3.

Based on some results obtained in the previous chapter that shows a possible regulation of the iron uptake likely mediated by PsaR3 we also considered the regulative region of the citrate transporter-encoding gene (*citM*) as a putative target sequence of PsaR3.

Finally, to elucidate better the transcriptional regulation role of this protein and the pathway(s) influenced by PsaR3, we performed a RNA-seq analysis on a Psa strain overexpressing *psaR3* under the control of arabinose-inducible promoter.

### 3. MATERIALS AND METHODS

#### 3.1 BACTERIAL STRAINS, CULTURE CONDITIONS AND CONSTRUCTS

*Pseudomonas syringae* pv. *actinidiae* strains CRA-FRU 10.22 and J35 were grown in King's B broth or HIM with or without kiwifruit leaf extract at 28 °C.

The total DNA of Psa strain CRAFRU 10.22 was extracted from a cell-suspension using the Ultra Clean Microbial DNA isolation Kit (M Bio laboratories) for the cloning of *psaR3* coding gene and the two putative PsaR3-targeted promoter regions (intergenic region and *citM* promoter).

- pBAD24 vector which express the *psaR3* and *psaR3*-His $\delta$ tag under the control of the arabinose-inducible promoter (Para) was constructed by cloning the full-size *psaR3*, and the *psaR3*-His $\delta$ tag in the pBAD24 using XmaI/XbaI as restriction enzymes.

- PBBI-MCS5-Terminator-RBS-lux vector which express the *lux*-operon situated in front of the *citM* promoter was constructed by cloning 700 bp upstream of the *citM*-coding sequence region using EcoRI/XhoI as restriction enzymes.

- PBBI-MCS5-Terminator-RBS-lux vector which express the *lux*-operon situated in front of the intergenic region which was cloned in both orientations (contig132:11289-11917 from the



Psa genome) was constructed by cloning the mentioned region in sense and antisense orientation using EcoRI/XhoI as restriction enzymes.

Correct constructs of all vectors was confirmed by DNA sequencing. The vectors were transformed in Psa strains CRA-FRU 10.22 or J35 by electroporation.

### 3.2 *cis*-acting elements ANALYSIS OF THE *citM* PROMOTER REGION

The *cis*-acting elements analysis of the 700 bp upstream of the putative *citM* coding sequence, was performed using the Transcription Factor Binding Site (TFBS) software of the genome2d suite (<http://genome2d.molgenrug.nl/index.php/tfbs-search> December 2016).

### 3.3 LUCIFERASE ASSAY

The luciferase assay was performed to test the activity of the *citM* promoter or the putative promoter activity of the intergenic region located in the cluster, in response to PsaR3 production. Experiments were carried out with Psa strains CRA-FRU 10.22 or J35 transformed either with pBAD24::*psaR3* and PBBI-MCS5::*promcitM*::lux or with pBAD24::*psaR3* and PBBI-MCS5::*intergenicregion*::lux. The same strains carrying the pBAD24::empty vector and PBBI-MCS5::*promcitM*::lux or with pBAD24::empty vector and PBBI-MCS5::*intergenicregion*::lux were used as negative controls. Single colonies of Psa CRA-FRU 10.22 transformed with the above mentioned constructs grown on KB agar (amp100/genta40) were used to inoculate KB broth (amp100/genta40) and incubated with shaking (200 rpm) over-night at 28°C. Then 1 ml aliquot of cell suspension was used to inoculate a fresh KB broth (amp-100/genta40) and incubated with shaking (200 rpm) for 4-6 hours at 28°C. Then 3 ml aliquot of cell suspension was centrifuged and washed three times in KB or HIM. Bacterial suspensions were adjusted to a final OD<sub>600</sub> of 0.2 in 3 ml final volume of KB (amp100/genta40) and HIM (amp100/genta40) and 160 µl of each culture were aliquoted into a 96-wells plate (black plates, clear bottom Corning Costar® plate). The 96-wells plate was incubated at 28 °C with shaking in the TECAN Spark machine, reading the OD and the luciferase signal every 15 minutes. After 1.5 hours, 10 µl (5%) of kiwifruit leaf extract was added and after 30 minutes 20 µl of arabinose at final concentration of 1 or 0.1% were added in each well (to induce the production of PsaR3) to obtain a plate with 200 µl of final volume in each well. In summary, bacteria were subjected to the following conditions: KB, KB plus kiwifruit leaf extract, HIM and HIM plus kiwifruit leaf extract with 1% arabinose, 0.1% arabinose, or without arabinose. Then 96-wells plate was incubated at 28 °C with shaking in

the TECAN machine, the OD and the luciferase signals were read every 15 minutes for 16 hours. Each condition was tested in triplicate and the luciferase assay was performed at least three times for each strain and each vector tested.

### **3.4 KIWIFRUIT LEAF EXTRACT HPLC SEPARATION AND TEST**

The total kiwifruit leaf extract (50 ml) obtained as described in the previous chapter (section 3.3.1 chapter 3) was treated with Ethyl-acetate (20 ml) to separate the hydrophobic phase from the aqueous phase. The treatment was performed 3 times in order to obtain a good phase separation. The two phases were further separated by HPLC (in collaboration with Jannis Brehm, LMU University).

The hydrophobic phase was further separated in fractions using the C18 HPLC column in a continuous step which started with 80% acetonitrile/20% ammonium acetate pH 6.5 and finished with 30% acetonitrile/70% ammonium acetate pH 6.5; fractions were collected every 2.5 minutes in a final volume of 1.7 ml.

The hydrophilic phase was further separated in fractions using the HILIC HPLC column in a multi-step gradient which started with 80% acetonitrile (with 10mM ammonium acetate)/20% water and finished with 75% water/25% acetonitrile (with 10mM ammonium acetate). The step gradient changed every 2.5 minutes increasing the amount of water by 5% and collecting 1.7 ml of column elution.

Every collected fraction was concentrated using the speed-vac to evaporate the solvent and resuspended in 200 µl of methanol for the hydrophobic fractions or 200 µl of 50% methanol and 50% water for the hydrophilic fractions; then 10 µl of each fraction was tested by luciferase assay.

### **3.5 RECOMBINANT PsaR3 PRODUCTION AND PURIFICATION**

#### **3.5.1 CELL CULTURE**

Since previous attempts to purify recombinant PsaR3 from *E. coli* were unsuccessful, we chose to work in Psa CRA-FRU 10.22. A single colonies of Psa CRA-FRU 10.22 pBAD24::*psaR3*-His<sub>6</sub>tag grown on KB agar (amp100) was used to inoculate KB broth (amp100) and incubated with shaking (200 rpm) over-night at 28°C. Over-night cultures were used to inoculate 1 L KB broth (amp100) at OD<sub>600</sub>=0.4-0.5. The cultures were grown at 28 °C with shaking (200 rpm) for 2 hours. Protein production was induced by adding 0.1% of

arabinose (final concentration). Bacterial cells were collected 5 hours post-induction and treated for protein extraction.

### 3.5.2 PROTEIN EXTRACTION

Bacterial pellets were resuspended in the cold Lysis Buffer (0.2 bacterial weight/ml lysis buffer) **Tab. 1**. The suspension was treated in the “Break-Killer-Machine” with a pressure of 1.36 KBar at 4°C for 3 times, in order to break the bacterial cells and release the proteins in solution. Then the suspension was centrifuged at 5000 rpm x 20 min at 4°C.

The suspension without cellular debris was ultra-centrifuged at 45000 rpm x 1h:20min and then the protein (cytosol fraction) was purified using the Ni-NTA Agarose (Qiagen).

**Table 1: Lysis Buffer**

Final conc.		Vi for 50mL	Ci
50mM	Tris/HCl pH 8.0	5ml	0.5M Tris/HCl pH 8.0
5%	Glycerin	5ml	50%
10 mM	MgCl <sub>2</sub>	1ml	0.5M MgCl <sub>2</sub>
0,5 mM	PMSF	0.1 ml	250 mM PMSF
1mM	DTT	0.5M	DTT
10 ng/ml	DNase		DNase
		38.8 ml	H <sub>2</sub> O

### 3.5.3 PROTEIN PURIFICATION

1 ml of Ni-NTA agarose was washed twice with 40 ml ddH<sub>2</sub>O and equilibrated with 40 ml of Lysis Buffer plus 20 mM Imidazole. The cytosol suspension was incubated with the equilibrated Ni-NTA at 4°C for 1 h in continuous rolling. The suspension was putted in the column and start to collect each fraction. The column was washed for 4 times with 10 ml Wash Buffer plus 40 mM Imidazole (**Tab. 2**) and then 6 elution steps were performed with 1 ml of Elution Buffer (250 mM Imidazole) **Tab. 3**. The presence of the protein in the different elution steps was checked by SDS-Page (12% acrylamide) and Comassie staining.

**Table 2: Wash buffer**

Final conc.		V for 100 mL	Stock solution
50 mM	Tris/HCl pH 7.5	10ml	0.5M Tris/HCl pH 7,5
10%	Glycerin	20 ml	50%
500 mM	NaCl	10 ml	5 M
40 mM	Imidazole	272.16 mg	Directly add powder
2 mM	$\beta$ -MeOH	13.90 $\mu$ l	$\beta$ -MeOH

**Table 3: Elution Buffer**

Final conc.		V for 10 mL	Stock solution
50 mM	Tris/HCl pH 7,5	1 ml	0.5M Tris/HCl pH 7,5
10%	Glycerin	2 ml	50%
500 mM	NaCl	1 ml	5 M NaCl
250 mM	Imidazole	1702 mg	Directly add powder
2 mM	$\beta$ -MeOH	2.78 $\mu$ l	$\beta$ -MeOH

### 3.6 RNASeq ANALYSIS TO IDENTIFY GENES REGULATED BY *PsaR3*

#### 3.6.1 CELL CULTURE

To highlight the transcriptional activity regulated by *PsaR3*, we performed a RNA-seq analysis using a *Psa* strain over-expressing *psaR3*. Single colonies of *Psa* CRA-FRU 10.22 pBAD24::*psaR3* and CRA-FRU 10.22 pBAD24::empty vector, used as a comparison, grown on KB agar (amp100) were used to inoculate KB broth (amp100) and incubated with shaking (200 rpm) over-night at 28°C. Cell suspensions were centrifuged and washed three times in KB or HIM. Bacterial suspensions were adjusted to a final OD<sub>600</sub> of 0.2-0.3 of 20 ml final volume of KB (amp100) and HIM (amp100) amended with 1 ml (5%) of kiwifruit leaf extract. The cell cultures were grown at 28°C for about 2 hours with shaking (200 rpm) and then induced by adding arabinose at final concentration of 0.1%. Bacterial cultures were collected 30 minutes from the arabinose induction and treated for RNA extraction.

### 3.6.2 RNA EXTRACTION

Bacterial pellet was resuspended in 1 ml ice-cold AE-Buffer (Tab. 4). The cell suspension was transferred into 2 ml tube and centrifuged at 5000 rpm x 2 min at 0°C. The supernatant was discarded and the cells were resuspended in 500 µl ice-cold AE-Buffer, in which was added 500 µl of Aqua-Phenol/Chloroform/Isoamylalcohol (P/C/I). The treated cells were vortexed really well, added 10 µl of 10% SDS solution, and vortexed again. The suspension was incubated for 30 min at 60°C in a thermomixer with shaking. The suspension was kept at 4°C over-night.

The suspension was centrifuged at 16100 rcf x 30 min at 0°C, then the supernatant was transferred into a Phase-lock-tube, in which were added 500 µl P/C/I and 50 µl 3M NaAc pH 5.2. The suspension was vortexed really well and centrifuged at 16100 rcf x 30 min at 0°C. The supernatant was transferred into a 2 ml tube, and added 2 ml 96% cold Ethanol, vortexed and precipitated at -80°C over-night.

The suspension was centrifuged at 16100 rcf x 40 min at 0°C, the supernatant was discarded, added 1 ml of 80% cold Ethanol (prepare it fresh, the ethanol adsorbs water from the air), vortexed really well and centrifuged at 161000 rcf x 10 min at 0°C. The supernatant was discarded and the previous step repeated. The remaining Ethanol was removed carefully and total RNA was dried for 60 min. Total RNA was solved in 100 µl of DEPC water. The RNA concentration and quality was determined using Nanodrop and Bioanalyser (Agilent RNA 6000 Nano Kit) respectively. Total RNA was processed for the DNase treatment and RNA-seq library preparation.

**Table 4: AE-BUFFER**

Final Conc.		Stock solution
20 mM	NaAc pH 5.2	3 M NaAc pH 5.2
1 mM	EDTA pH 8.0	0.5 M EDTA pH 8.0

### 3.6.3 DNase TREATMENT

40 µg per sample of total RNA were treated with 1 µl DNase at 37°C for 30 min in a 250 µl tube.

RNA	40 µg
DNase Buffer	10 µl
DNase	1 µl
H <sub>2</sub> O	up to 100 µl

1 µl of DNase was added after 30 minutes, mixed really well and putted the reaction at 37°C for 30 min.

The cleaning step was performed after the sample incubation as following describe. The solution was putted into a Phase-lock-tube and added 100 µl of P/C/I plus 10 µl of 3M NaAC pH 5.2; vortexed really well and centrifuged at 16100 rcf x 30 min at 0°C. The supernatant was transferred into a 2 ml tube, and added 2 ml 96% cold Ethanol, vortexed and precipitated at -80°C over-night. The suspension was centrifuged at 16100 rcf x 40 min at 0°C, the supernatant was discarded, added 1 ml of 80% cold Ethanol, vortexed really well and centrifuged at 161000 rcf x 10 min at 0°C. The supernatant was discarded and the previous step repeated. The remaining Ethanol was removed carefully and total RNA was dried for 60 min. Total RNA was solved in 100 µl of DEPC water. The RNA concentration and quality was determine using Nanodrop and Bioanalyser (Agilent RNA 6000 Nano Kit) reselectively. The treated RNA was used for the RNA-seq library preparation.

### 3.6.4 RNA-seq LIBRARY PREPARATION

5 µg of RNA were treated per sample with the Ribo-Zero rRNA Removal Kit for Gram-negative bacteria (Illumina). The RNA was analysed for integrity and quality and for determine its amount using the Bioanalyser (Agilent RNA 6000 Nano Kit). The library preparation was performed using the NEB Ultra II Directional RNA Library Prep Kit for Illumina (NEB) following the protocol for purified mRNA or rRNA depleted RNA as starting material. The library quality and amount was assessed on a Bioanalyzer (Agilent DNA 1000 Chip) and by Qubit Fluorometer analysis, respectively. The sequencing sample was prepared with 4mM of each prepared library in 120 µl final volume. The statistical data analysis and DEGs extrapolation were performed in collaboration with Dr Nicola Vitulo (University of Verona).

## 4. RESULTS

### 4.1 EVALUATION OF THE ABILITY OF PsaR3 TO INDUCE THE *citM* PROMOTER

The Real-time qPCR performed in the previous chapter showed that expression of *citM*, a putative citrate transporter probably involved in iron-uptake in Psa, was regulated by kiwifruit leaf extract in a PsaR3-dependent way. From this result, we hypothesized that the promoter region of *citM* can be targeted by PsaR3, and that the transcription could be triggered by molecule(s) contained in the kiwifruit leaf extract. To verify this hypothesis, we firstly performed an *in-silico* analysis on the 700 bp up-stream of the ATG of the *citM* coding sequence (**Table 5**) which revealed presence of *cis*-acting elements including motifs similar to those targeted by other bacterial LuxR-like transcriptional regulator. Such examples include OxyR of *E. coli* a LysR-type transcription factor that regulates expression of peroxide-detoxifying enzymes [24], SdiA, a quorum-sensing transcription regulator of *Salmonella enterica* sv. typhimurium and *E. coli*, involved in TTSS regulation and motility and chromosomal replication [25], RhIR of *Pseudomonas aeruginosa* which forms a complex with the butanoyl-homoserine-lactone (BHL) involved in gene-regulation mechanisms and allows pathogen growth in microaerophilic conditions [26]; MtrB, a response regulator of the two component system MtrA-MtrB in *Mycobacterium tuberculosis* involved in iron-uptake regulation [27].

TF	Query	Start	End	Strand	Score	Motif
<b>MtrB</b>	citr	587	602+		19,11	TCCGATGCTTGCTGATTTCTTGATGTGCACCCC TCTTGCGCCCCCACTCCACGTAA
<b>OxyR</b>	citr	8	45+		19,55	AGAGGTCTTGCTGCGCGAACTGGCGTCGCAG TTCAGT
<b>RhIR</b>	citr	18	34+		8,24	CTGCGCGAACTGGCGT
<b>SdiA</b>	citr	297	304+		15,01	CAACAATAATGGTGATTCCGATGCTTGCTG
<b>SdiA</b>	citr	386	400+		14,89	CCACAACGCTTGTGACAATAAAATTTGCGC

*Table 5:* The table reports the motif recognized by transcription factors LuxR-like in the putative *citM* promoter.

The responsiveness of the *citM* promoter to PsaR3 was investigated by luciferase assay as illustrated in **Fig. 1** in Psa strain CRA-FRU 10.22 was transformed with two different vectors, *i.e.* pBAD24 vector driving the expression of *psaR3* under the control of an arabinose-inducible promoter, and a vector in which the *citM* promoter region controls the expression of the lux-operon reporter. Using this system, PsaR3 expression is induced by adding arabinose in the culture medium, and if PsaR3 binds to the *citM* promoter, we can observe an increase of luminescence signal.

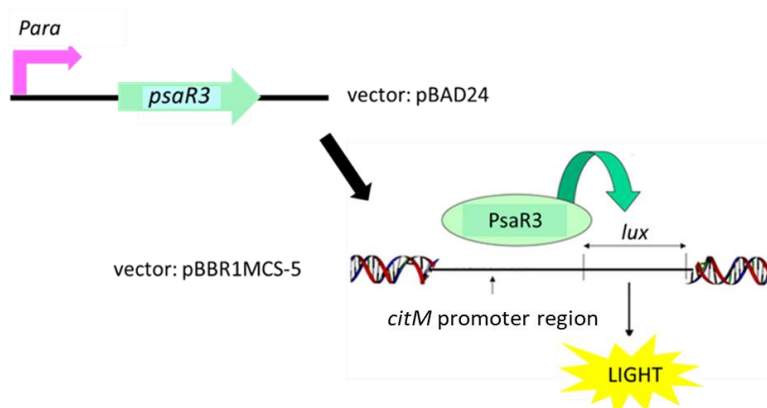


*Figure 1:* Draft that describe the luciferase assay in *Pseudomonas syringae* pv. *actinidiae* used to test the responsiveness of the *citM* promoter to PsaR3.

In Psa strain CRA-FRU 10.22, in rich medium the *citM* promoter activity was independent of the kiwifruit leaf extract or PsaR3 induction (**Fig, 2, a**), indicating that in this condition the *citM* promoter is not a target sequence for PsaR3 and it was not regulated by the kiwifruit leaf extract.



The same situation was also observed in the minimal medium with or without kiwifruit leaf extract or *PsaR3* induction (**Fig. 2, b**). It is worth to mention that the luminescence signal during the analysis was relatively low, suggesting a possible quenching activity in the system. However, it must be noted that the strain CRA-FRU 10.22 used for this analyses also contains an endogenous *PsaR3* that might interfere with the system. On the other hand, J35 is a *Psa* strain with a genome identity 99% of CRA-FRU 10.22 but naturally lacking *psaR3* and the *psaR3*-gene cluster.

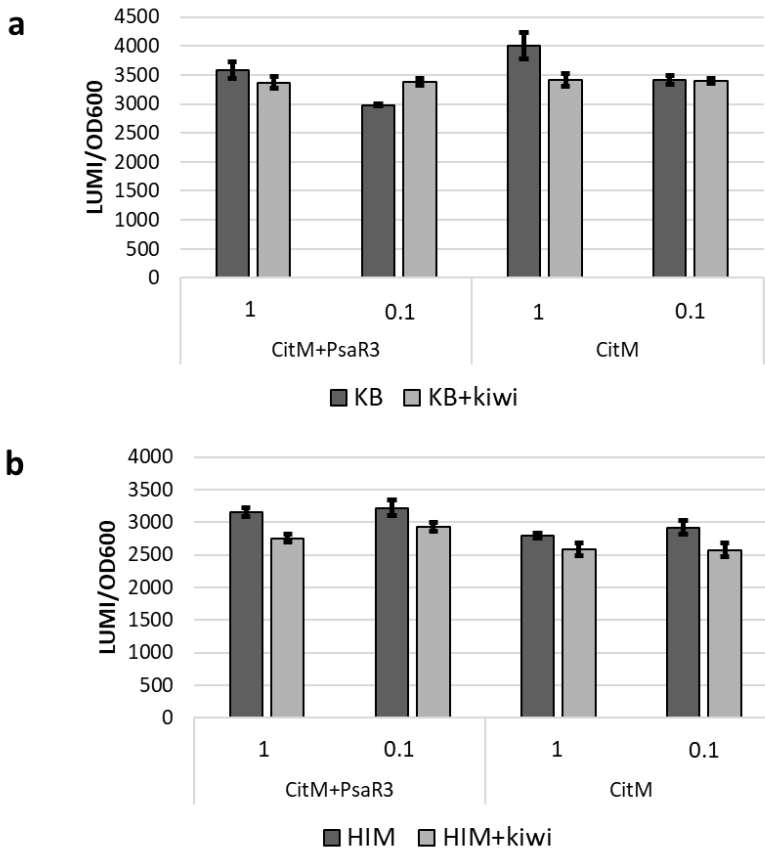


**Figure 2:** Plots showing the *citM* promoter activity expressed in luminescence/OD<sub>600</sub> 2 hours after *psaR3* induction with 1% and 0.1% of arabinose, in rich (a) and minimal medium (b) in CRAFRU 10.22 strain with both vector (CitM + *PsaR3*) with the pBAD24 empty vector (CitM) as negative control. The experiment was repeated four times and it is reported a representative experiment.

The promoter activity of *citM* was therefore tested also in J35. In rich medium, *citM* promoter was activated in absence of PsaR3 as revealed by the high luminescence signal (**Fig. 3, a**) in the negative control. Indeed, the luminescence signal decreased following PsaR3 induction, suggesting that PsaR3 could be a transcriptional repressor of this promoter and moreover, the activity of *citM* promoter was independent of the presence of the kiwifruit leaf extract.

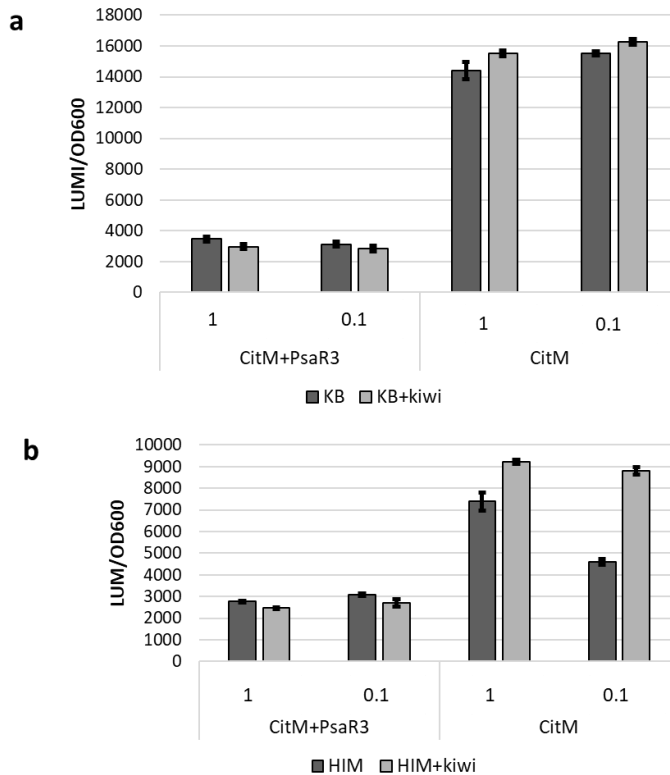


*Figure 3:* Plots showing the *citM*, promoter activity expressed in luminescence/OD<sub>600</sub>, 2 hours after *psaR3* induction with 1% and 0.1% of arabinose, in rich (a) and minimal medium (b) in J35 strain with both vector (CitM+PsaR3) and with the pBAD24 empty vector (CitM) used as negative control. The experiment was repeated four times and it is reported a representative experiment.

The putative *citM* promoter which was still induced also in minimal medium showed a decrease in the luminescence signal following the PsaR3 induction (**Fig. 3, b**). Moreover, the negative control shows also a further increase in the promoter activity due to the presence of

the kiwifruit leaf extract added into the medium. In this situation, PsaR3 seems to play a role as a transcriptional repressor.

## 4.2 EVALUATION OF THE INTERGENIC REGION AS A PUTATIVE BIDIRECTIONAL PROMOTER AND ITS RESPONSIVENESS TO PsaR3

As mentioned in the previous chapter, the PsaR3-encoding gene is localized in a gene cluster containing an intergenic region that could play a role as a bidirectional promoter. Moreover, an *in-silico* analysis revealed the presence of putative *cis*-acting elements recognized by LuxR-like transcription factors in both orientations, suggesting the possible regulation of this region by PsaR3 itself. The putative promoter activity of the intergenic region in both orientations and its responsiveness to PsaR3 were investigated by luciferase assay as described above.

We first tested the intergenic region in sense orientation, using two different concentrations of arabinose, *i.e.*: 1 and 0,1 %, to induce the expression of *psaR3*, **Fig. 4**. In rich medium, the promoter activity of the intergenic region in sense orientation was induced by kiwifruit leaf extract as revealed by the higher luminescence signal (**Fig. 4, a**), but seemed to be negatively regulated by PsaR3 since the activity was higher in the negative control. By contrast, in absence of kiwifruit leaf extract we did not observe any modulation of promoter activity by PsaR3 expression. The same situation was observed in minimal medium, *i.e.*: no response of sense promoter activity to PsaR3 induction, but strong activity in presence of kiwifruit leaf extract that was repressed following PsaR3 induction (**Fig. 4, b**). On the other hand, we observed strong differences in term of promoter activity of the intergenic region in the antisense orientation, in the different condition tested (**Fig. 4, c-d**). Indeed, the activity seemed strictly dependent on PsaR3 and moreover such promoter activity was responsive to the kiwifruit leaf extract but only in minimal medium, in which the addition of the extract induced a further increase of the antisense promoter activity (**Fig. 4, d**).

Such effect was not observed in rich medium (**Fig. 4, c**). It is worth to mention that the activity of the intergenic region in antisense orientation reach value of luciferase higher of which reached by the intergenic region in sense orientation. Together, these results clearly suggest PsaR3 leads to the regulation directly or indirectly of putative downstream promoters and some molecules present in the kiwifruit leaf extract could be recognized by the receptor.

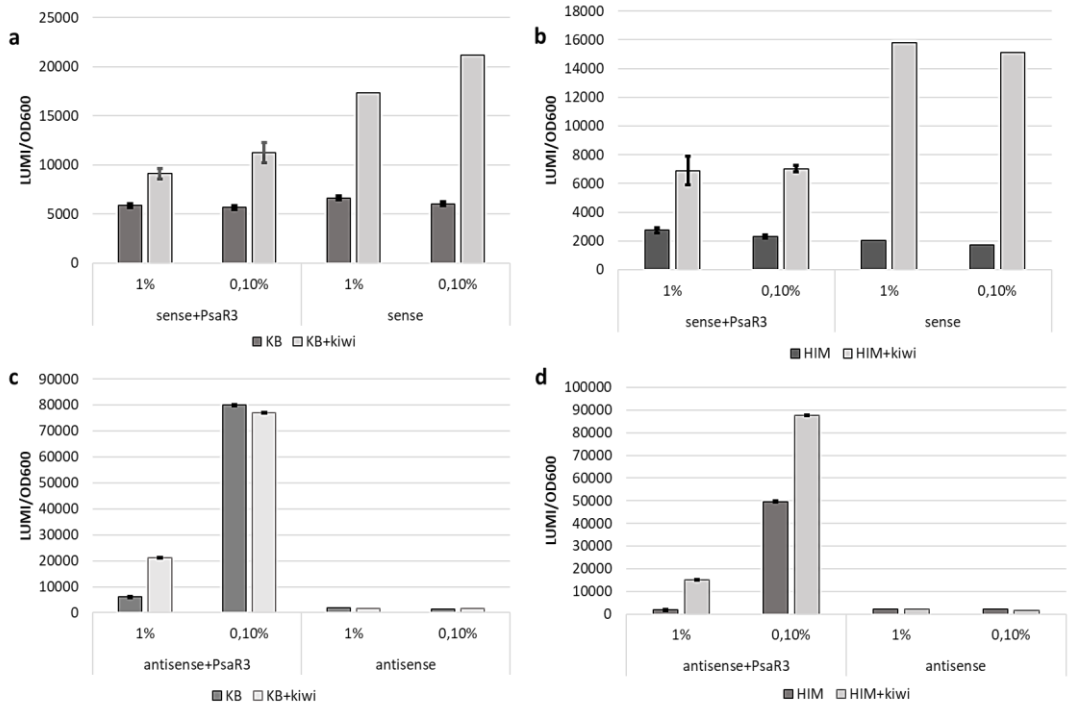


*Figure 4:* Plots showing the promoter activity expressed in luminescence/OD<sub>600</sub> of the intergenic region in sense orientation (a, b), and antisense orientation (c, d), 2 hours after psr3 induction with 1% and 0.1% of arabinose, in rich (a, c) and minimal medium (b, d) with and without kiwifruit leaf extract in CRA-FRU 10.22 strain. The experiment was repeated four times and a representative experiment is reported.

### **4.3 EFFECT OF DIFFERENT HPLC FRACTION OF KIWIFRUIT LEAF EXTRACT ON THE ACTIVITY OF THE “ANTISENSE” PROMOTER REGION**

The activity of the intergenic region in antisense orientation was strictly dependent on PsaR3 and increased when the kiwifruit leaf extract was added into the medium. The next hypothesis was the possibility that one or more molecule(s) present in the kiwifruit leaf extract could be sensed by Psa probably involving the PsaR3 receptor in the signal recognition, which further increase the promoter activity of the intergenic region in antisense orientation. Thus, for this purpose we evaluated the promoter activity of this region (following the PsaR3 induction) with different kiwifruit leaf extract fraction.

First of all, the aqueous phase of the kiwifruit leaf extract was separated from the hydrophobic phase using ethyl-acetate as organic solvent, and then the two phases were further separated by fractionation in HPLC columns. The plot in **Fig. 5** shows that none of the molecules from the hydrophobic fraction (from 1 to 22) was able to up-regulate the PsaR3-dependent promoter activity as observed with the total kiwifruit leaf extract. By contrast, the raw aqueous phase, not subjected to the HPLC separation yet, significantly increased the luminescence signal compared with the minimal medium alone (indicated with the red line), suggesting that the signal molecule recognized by Psa and able to interact directly or indirectly with PsaR3, could be present in these fractions.

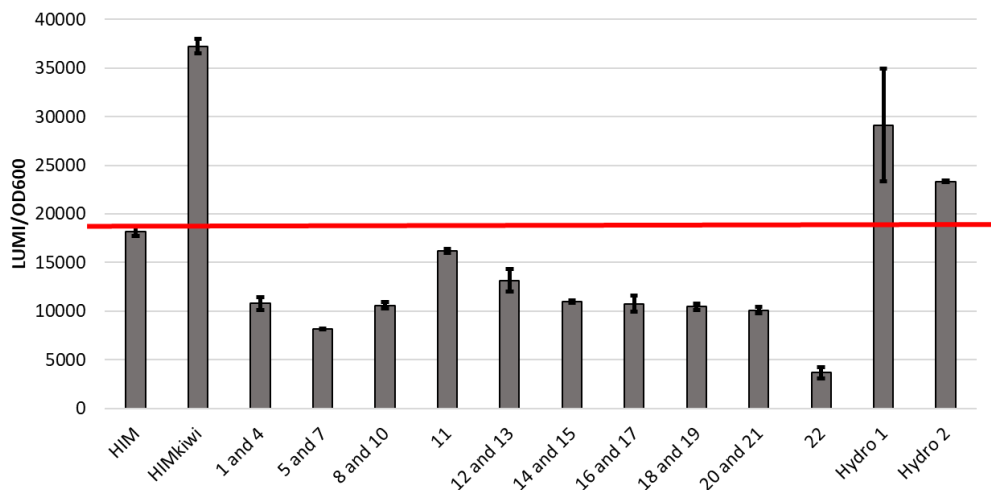


*Figure 5:* Plots showing the promoter activity expressed in luminescence/OD<sub>600</sub> of the intergenic region in antisense orientation, 2 hours after *psaR3* induction with 0.1% of arabinose, in minimal medium (HIM), minimal medium plus kiwifruit leaf extract (HIM kiwi), minimal medium plus the different HPLC hydrophobic fractions (1-22) and minimal medium plus the raw aqueous phases (hydro 1 and 2) derived from two extraction batches in CRA-FRU 10.22 strain. The experiment was repeated three times and a representative experiment is reported.

The aqueous phase was tested with the same method after HPLC separation. This analysis showed that there were some fractions (**Fig. 6**) in which the signal molecule(s) could be present. These “positive-signal” fractions were subjected to an accurate Mass Spectrometry analysis to identify the characterizing compounds (the analysis is in progress in collaboration with the Buchmann Institute for Molecular Life Sciences (BMLS), Goethe University, (Frankfurt)).

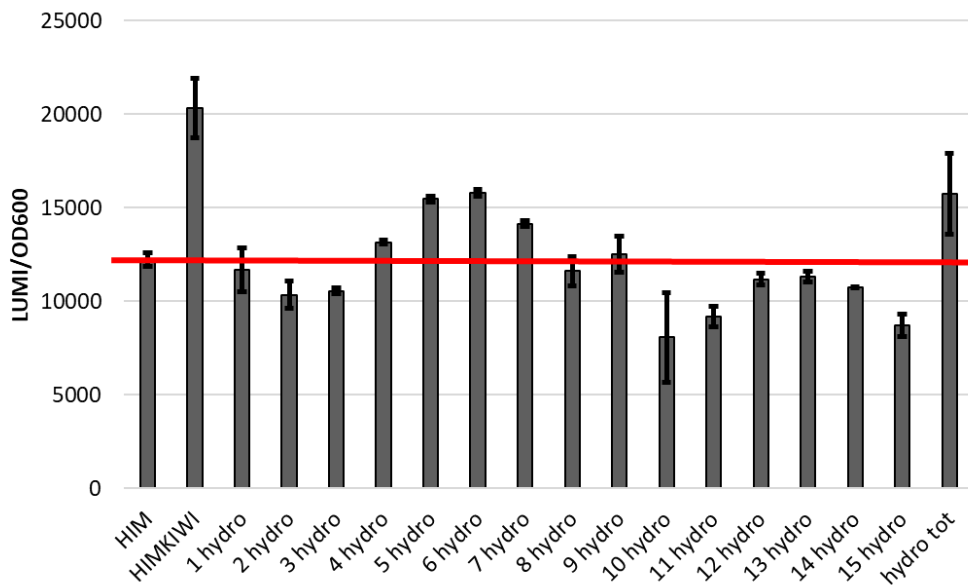


*Figure 6:* Plots showing the promoter activity expressed in luminescence/OD<sub>600</sub> of the intergenic region in antisense orientation, 2 hours after *psaR3* induction with 0.1% of arabinose, in minimal medium (HIM), minimal medium plus kiwifruit leaf extract (HIM kiwi), minimal medium plus the different HPLC hydrophilic fractions (1-15) and minimal medium plus the raw aqueous phases (hydro tot) in CRA-FRU 10.22 strain. The experiment was repeated three times and a representative experiment is reported.

Meantime, we performed several HPLC run of the raw aqueous phase of the kiwifruit leaf extract, with different wave-lengths of detection that is: 260 nm, which is the default wave-length of the HPLC analysis to detect aromatic compounds; 190 nm to detect the  $-C\equiv N$ ; 280 nm to detect  $-COOR$  or  $-C\equiv S$  and  $-C=O$  and 310 nm to detect  $-N=N$  and  $-ONO$ . The different UV spectra showed (**Fig. 7**) a big and wide peak in the first period of the analysis, corresponding to the collected fractions 1 and 2, probably due to the injection of the aqueous phase in the column, but also some interesting peaks corresponding to the eluted fractions from 5 to 10. This analysis suggests that a possible compound could be present in these fraction and it would be responsible to the activity observed in the luciferase assay.

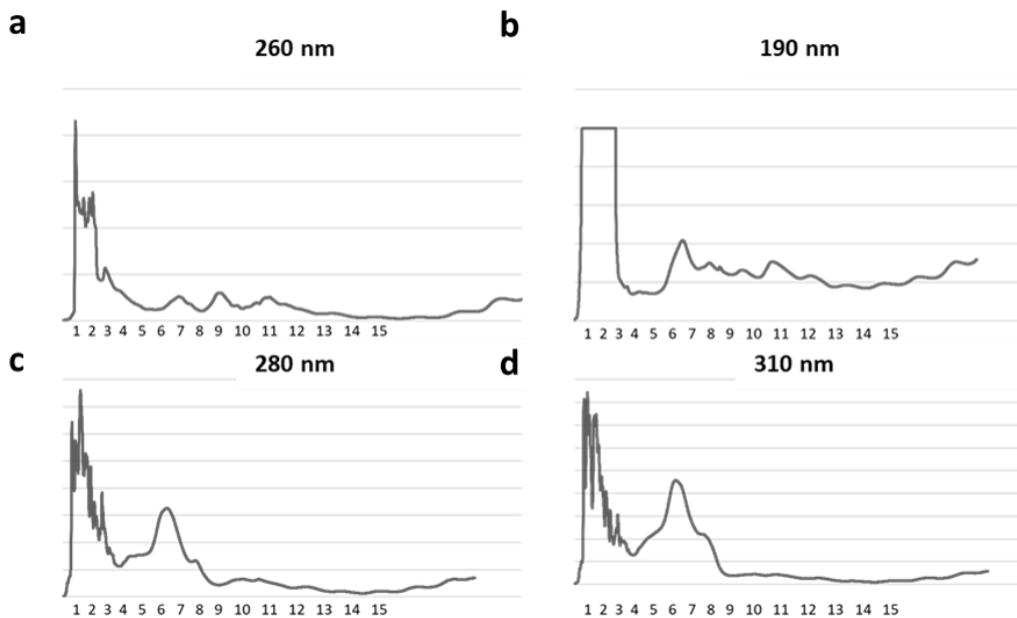


*Figure 8:* Plots showing the different UV spectrum (a=260 nm, b=190 nm, c=280 nm and d=310 nm) performed during the HPLC analysis of the raw hydrophilic phase of the kiwifruit leaf extract. The number from 1 to 15 (x-axis) corresponding to the fraction collected during the HPLC separation and collection.

#### 4.4 PRODUCTION AND PURIFICATION OF RECOMBINANT PsaR3

The main drawback in the production and purification of recombinant LuxR solos were their poor stability in absence of their ligand [28]. In our many attempts to purify the recombinant PsaR3 (*psaR3His<sub>6</sub>tag*) in *E. coli*, we initially tried several combinations of bacterial strains and post-induction time points, without any success, due to the degradation of the recombinant PsaR3His<sub>6</sub>tag (an example is reported in **Fig. 8**). Finally, we could set up a reliable protocol to obtain the recombinant PsaR3His<sub>6</sub>tag in the soluble fraction with a good purity by expressing the protein in Psa strain CRA-FRU 10.22. (**Fig. 9**).



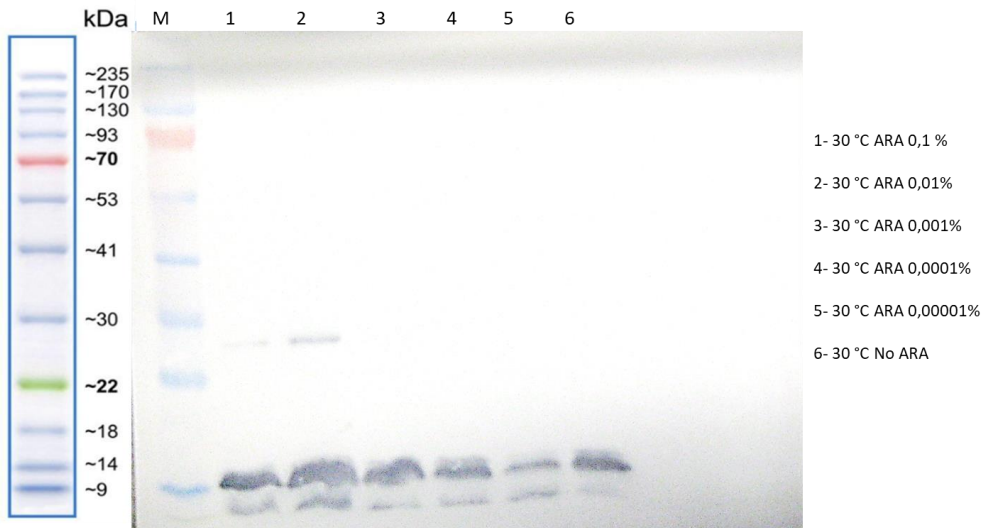


*Figure 8:* Western Blot of the SDS-PAGE (12% acrylamide) showing the recombinant Psar3His6tag produced in *E. coli* BL21 (total cell lysate). The blot is showing different *E. coli* sample using for the protein production, induced with different amount of arabinose and harvested 20 minutes post induction. The expected weight of the Psar3 is around 31 kDa calculated using the protein molecular weight calculate ([https://web.expasy.org/cgi-bin/compute\\_pi/pi\\_tool](https://web.expasy.org/cgi-bin/compute_pi/pi_tool)).

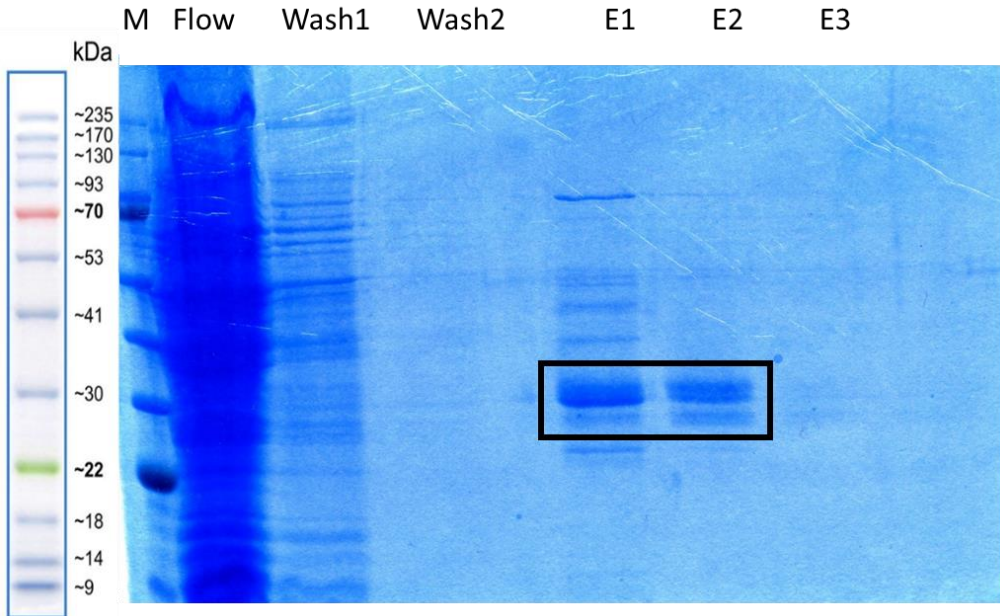


*Figure 9:* SDS-PAGE (12% acrylamide) with Coomassie staining showing the purified recombinant PsaR3His6tag produced in Psa CRA-FRU 10.22 from the cell-soluble fraction. The blot is showing different steps of wash and elution collected during the protein purification. M= marker, Flow=flow through, Wash 1 and 2= samples collected from the different washing steps performed during the purification; E1= elution 1, E2= elution 2, E3= elution 3.

#### 4.5 RNA-seq ANALYSIS TO IDENTIFY THE TRANSCRIPTOMIC PROFILES REGULATED BY PsaR3

Finally, we used another transcriptomic approach to investigate the possible transcriptional targets of PsaR3 and to define its role in the gene expression regulation, also considering the results obtained with the luciferase assay to set the experimental conditions and the harvest time-points. Indeed, the luciferase assay showed that the maximum in luciferase activity of the putative intergenic region-promoter was reached 2 hours after *psaR3* induction and rich and minimal medium, the last one supplemented with the kiwifruit leaf extracts, showed differences in promoter activity. Thus we performed a RNA-seq analysis, using CRA-FRU 10.22 strain carrying either the arabinose inducible promoter vector which leads the over-expression of *psaR3* gene following arabinose induction or the empty vector

used as a comparison in the analysis. The two strains were grown in rich medium or in minimal medium supplemented with the kiwifruit leaf extract and the sample for the analysis were harvested 30 minutes after arabinose induction. The data obtained from the sequencing were analysed in collaboration with Dr Nicola Vitulo (University of Verona).

#### 4.5.1 STATISTICAL OVERVIEW OF THE RNA-seq DATA

The statistical analysis showed that, for each condition analysed *i.e.*: KB or HIM supplemented with kiwifruit leaf extract (HIM-K), transcriptomic profiles following over-expression of *psaR3* clustered separately from those of the respective controls (**Fig. 10, 11**). The two figures show heat maps representing the DEGs between the strain that over-expressed *psaR3* and its negative control. The up-regulated genes are highlighted in red while in green are highlighted those down-regulated. Moreover, heat maps show that the results from the three biological replicates were reproducible despite that a biological replica is slightly different from the others.

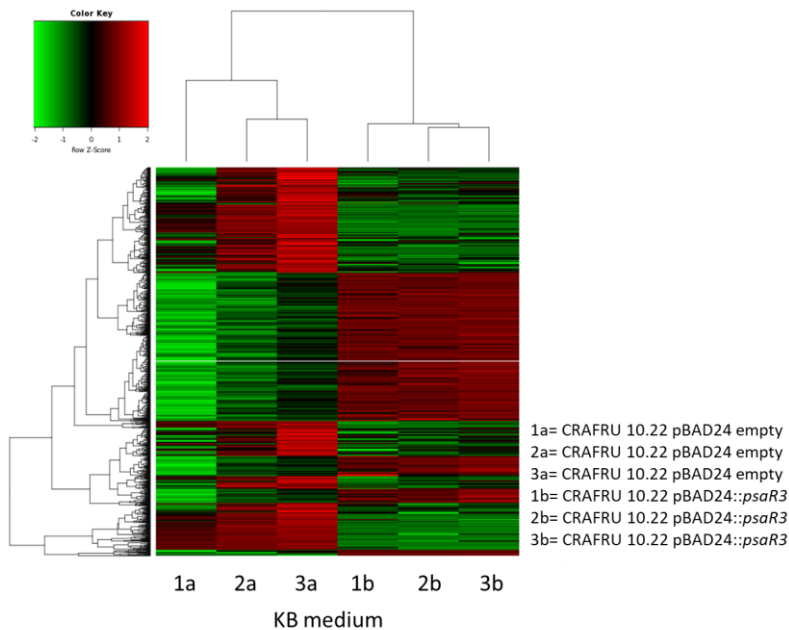


*Figure 10:* Hierarchical clustering and HeatMap of the DEGs ( $\log_2\text{FoldChange} > 1$  counts) of the different samples in rich medium (KB).

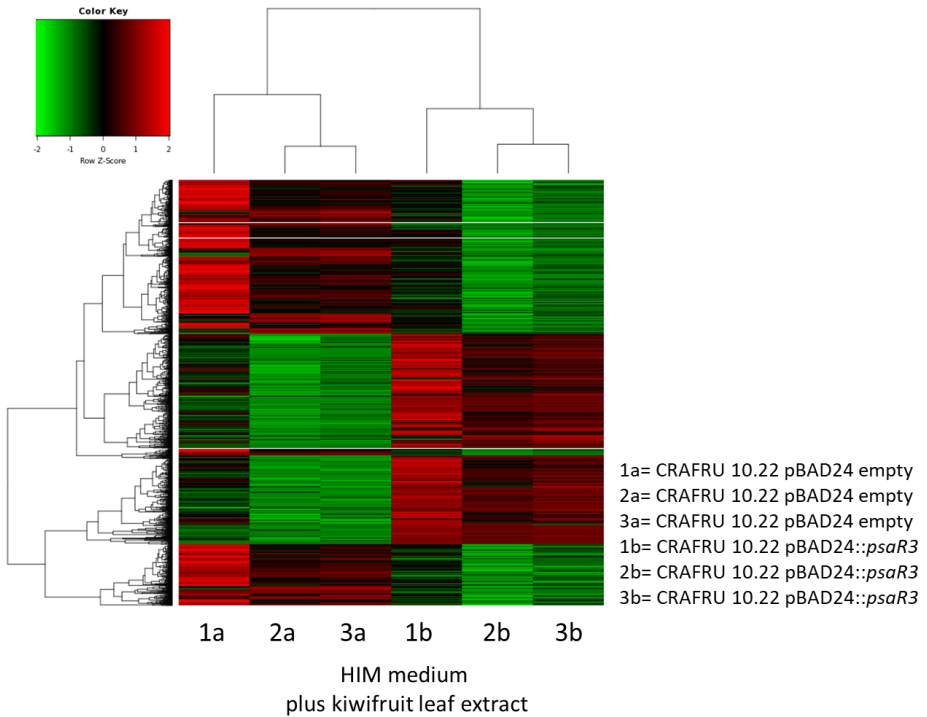


*Figure 11:* Hierarchical clustering and HeatMap of the DEGs ( $\log_2\text{FoldChange}>1$  counts) of the different samples in HIM medium plus kiwi fruit leaf extract.

#### 4.5.2 DEGs AMONG THE DIFFERENT CONDITIONS TESTED, A GENERAL OVERVIEW

The analysis of the DEGs between the CRA-FRU 10.22 strain over-expressing *psaR3* and its control (CRAFRU 10.22 with the pBAD24 empty vector) was performed considering the threshold of  $\log_2\text{FoldChange}>1$ . The Venn diagram shows the number of the DEGs in the different conditions tested (**Fig. 12**), and their overlapping. The DEGs, between the strains that overexpress *psaR3* and the negative control in HIM-K were 1896, among which 907 showed an up-regulation while and 989 were down regulated. Conversely, in KB were differentially modulated 1464 genes among which 755 were up-regulated while 709 were down-regulated. More in detail, the DEGs specifically regulated in HIM-K were 748 of which 314 were up-regulated and 414 were down-regulated; while the DEGs specifically regulated in KB were 316 of which 194 were up-regulated and 122 were down-regulated. The DEGs that showed a

negative regulation either in KB or in HIM-K were 564, while the common DEGs that showed a positive regulation in the both growing conditions tested were 550. The DEGs that showed an opposite regulation that is: positively regulated in HIM-K and negatively regulated in KB or vice versa were 23 and 11 respectively.

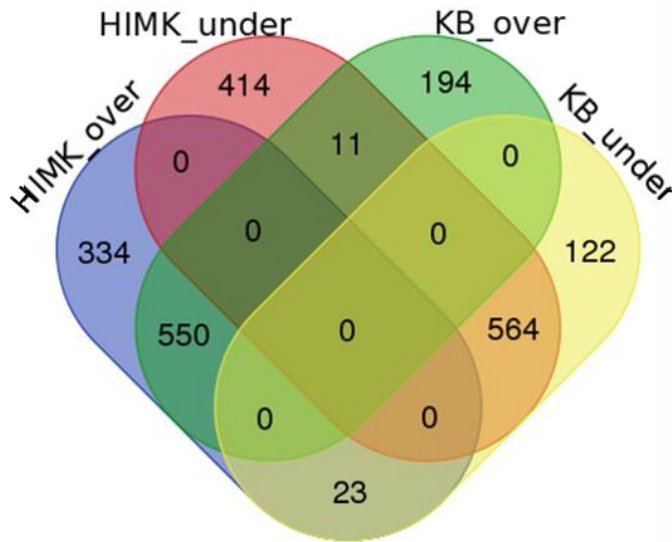


Figure 12: Venn diagram showing the specific and common DEGs positively and negatively modulated in the different conditions tested.

#### 4.5.3 FUNCTIONAL ENRICHMENT ANALYSIS OF THE DEGs BETWEEN *PsaR3*-DEPENDENT GENE EXPRESSION

The enrichment in functional categories of DEGs was performed to identify the functional genes categories influenced by *psaR3* over-expression in the two experimental conditions considered.

Interestingly, functional categories enriched among up-regulated genes in HIM-K were related to the pathogenesis, regulation of: secretion (also protein secretion mediated by TTSS), transport, cellular localization, and motility, DNA modification activity, interaction with host, repression of host mediated defence response, and the alginic acid metabolic process (**Fig. 13**).

DEGs UP HIMKiwi

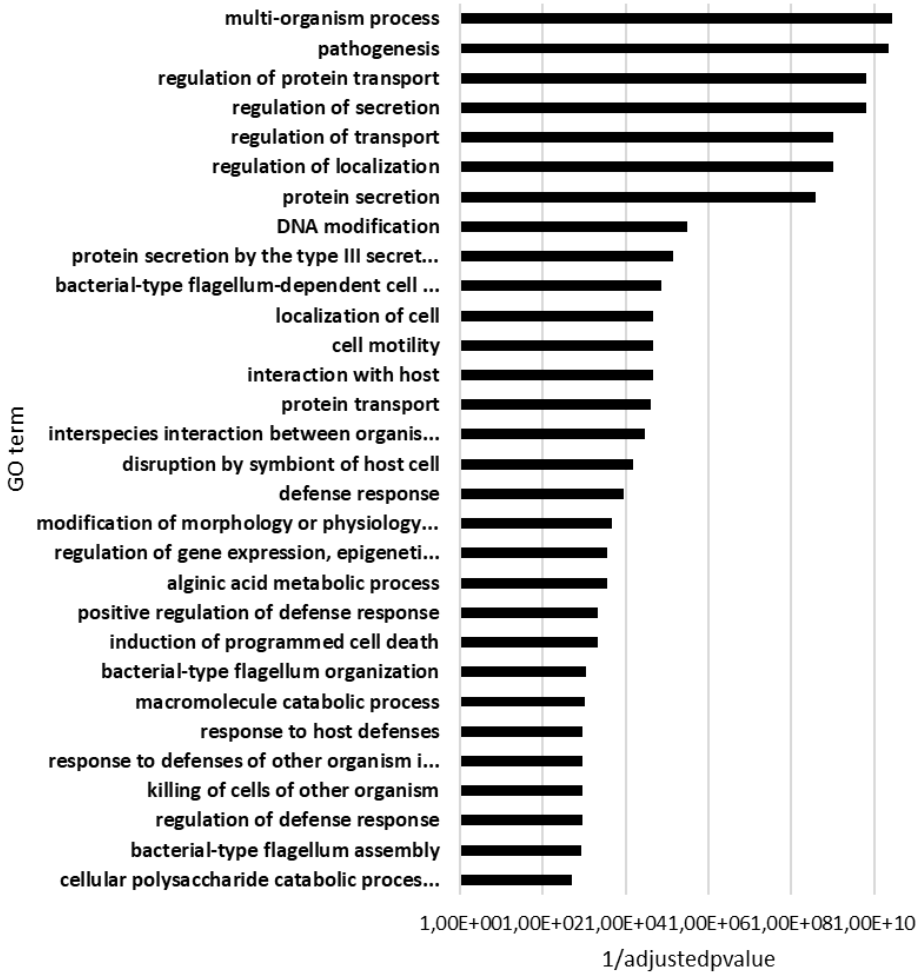
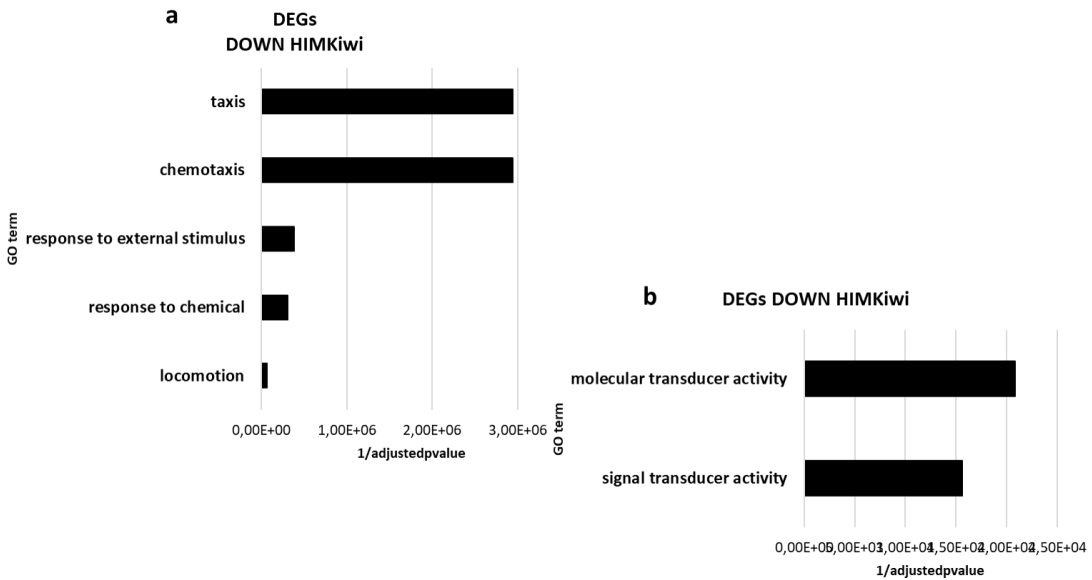


Figure 13: Enrichment in functional categories of the DEGs related to the biological process up-regulated in HIM plus kiwifruit leaf extract. Values are expressed as 1/adjustedpvalue.

Conversely, the functional categories classified as biological process down-regulated in HIM-K were related to chemotaxis, response to external stimuli and chemicals and locomotion (**Fig. 14, a**). While, the functional categories classified as molecular function showed down-regulated genes belonging to classes related to signal transduction and molecular transduction activity (**Fig. 14, b**).



*Figure 14:* Enrichment in functional categories related to the biological process (a) and molecular function (b) of the DEGs down-regulated in HIM plus kiwifruit leaf extract. Values are expressed as  $1/\text{adjustedpvalue}$ .

The functional categories belonging to the biological process up-regulated in KB were related to DNA modification and methylation, regulation of gene expression, cellular polysaccharide metabolic process and interesting we found the alginic acid metabolic process as well as highlighted considering HIM-K (**Fig. 15**).

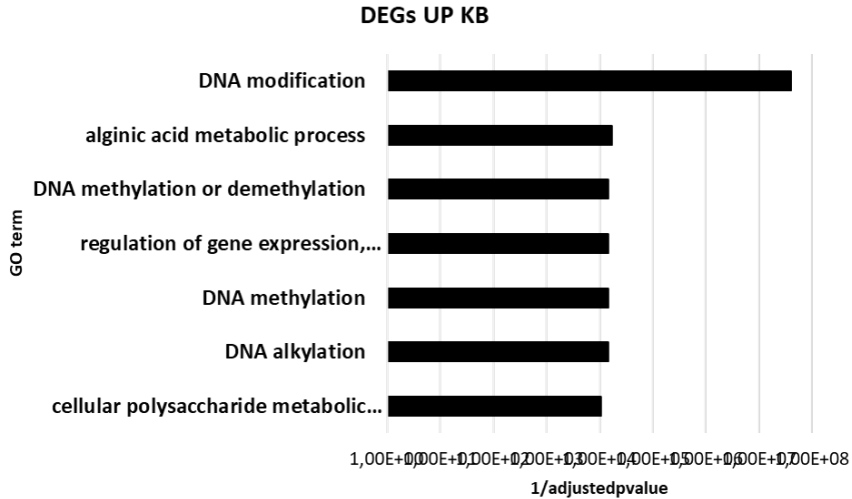


*Figure 15:* Enrichment in functional categories of the DEGs related to the biological process up-regulated in KB. Values are expressed as  $1/\text{adjusted p-value}$ .

The functional categories of biological process down-regulated in KB were related to cell communication and, as well as observed in HIM-K, chemotaxis process, locomotion, signalling, response to chemical and stimulus. Interestingly, classes as secretion (protein secretion TTSS mediated), regulation of transport, regulation of cellular localization, up-regulated in HIM-K, in this condition have been found down-regulated (**Fig. 16**).



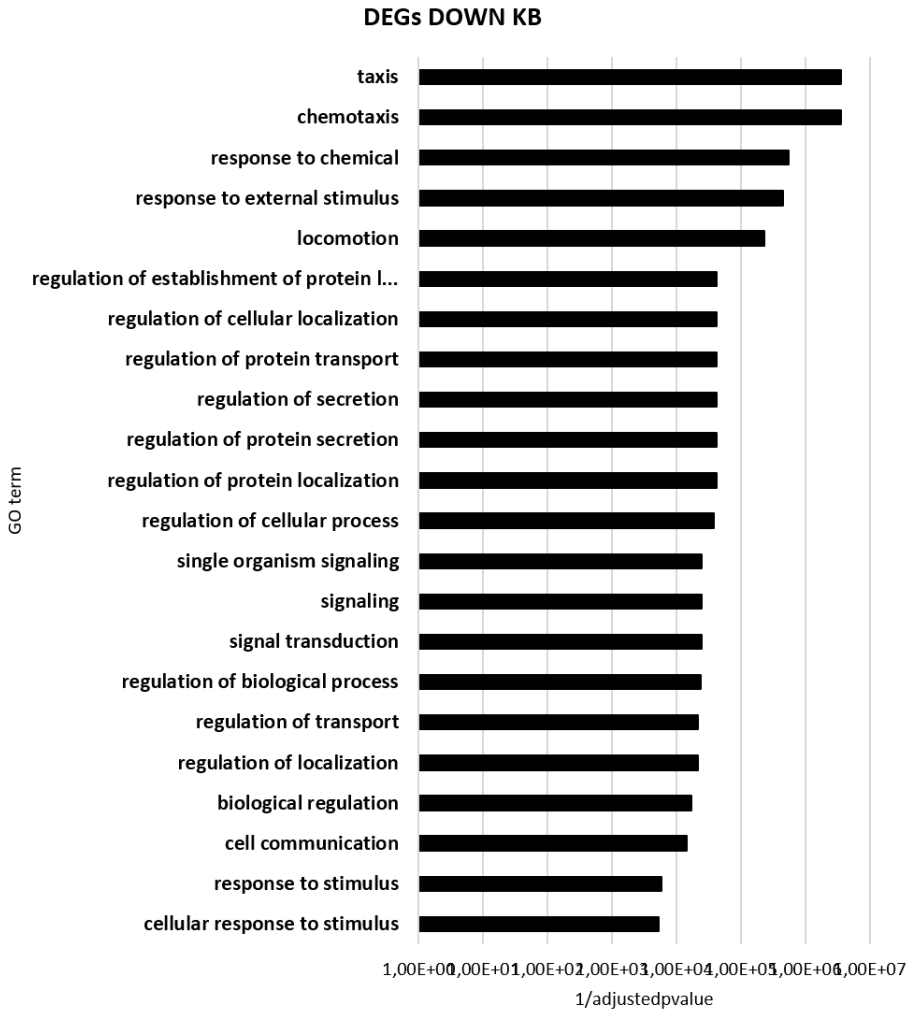


*Figure 16:* Enrichment in functional categories of the DEGs related to the biological process down-regulated in KB. Values are expressed as 1/adjusted pvalue.

Conversely, considering the DEGs down-regulated belonging to the functional categories named cellular component, we found that the two conditions tested showed the same classes (**Fig. 17**).

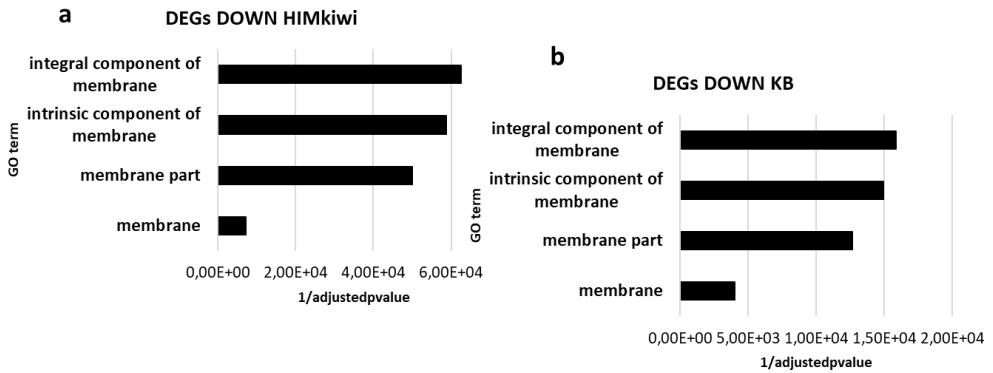


*Figure 17:* Enrichment in functional categories of the DEGs related to the cellular component down-regulated in HIM plus kiwifruit leaf extract (a) and KB (b). Values are expressed as 1/adjusted p-value.

#### 4.5.4 GENOMIC ISLANDS, OPERONS AND *psaR3*-CLUSTER MODULATION

The analysis of the RNA-seq data highlighted genes evaluated in previous chapters or genes belonging to a cluster or operons or gene islands.

In HIM-K we found up-regulated *citM*, *i.e.*: the citrate transporter found modulated considering the Real-time analysis but not modulated considering the microarray data (discussed in the previous chapter), and the *hrpA1*, more induced by the presence of the kiwifruit leaf extract in the medium, also not found in the microarray. Moreover, the genes belonging to the *psaR3*-cluster and also the *psaR3* gene itself (**Fig. 18**) resulted *psaR3* positively modulated. This result confirms the capacity of *PsaR3* to positively regulate the transcription of the genes in its cluster, and seems confirm our hypothesis in playing a role in the regulation of *citM* and *hrpA1*.

GeneName	LogFC	LogCPM	LR	p-value	P-adj	GeneDescription
IYO_RS00840	0,847254818	5,707703587	7,866709323	0,00503532	0,015997321	<b>citrate transporter</b>
IYO_RS06785	4,185174818	11,94684607	31,44487693	2,05E-08	1,80E-07	<b>HrpA1</b>
IYO_RS29525	5,419794796	7,601173515	45,39115997	1,61E-11	1,99E-10	<b>PsaR3 (LuxR solos)</b>
IYO_RS29530	5,545475657	5,732446989	180,9696666	2,98E-41	3,69E-39	<b>Anthranilate synthase component 2</b>
IYO_RS29535	5,876645933	7,129908647	225,5647596	5,53E-51	1,91E-48	<b>2-amino-4-deoxychorismate synthase</b>
IYO_RS29540	2,781930293	5,246419941	84,53103195	3,78E-20	9,19E-19	<b>Phenylacetate-coenzyme A ligase</b>
IYO_RS29545	3,163510177	4,49682715	72,31480484	1,83E-17	3,65E-16	<b>acetyltransferase</b>
IYO_RS29550	4,435580821	4,897577116	133,7790583	6,11E-31	3,21E-29	<b>transcriptional regulator</b>
IYO_RS29555	9,813785285	4,958036186	206,6063981	7,56E-47	1,66E-44	<b>2-amino-4-deoxychorismate dehydrogenase</b>
IYO_RS29560	6,20730735	4,924621792	174,1319319	9,26E-40	1,02E-37	<b>amino-acid metabolite efflux pump</b>
IYO_RS29565	7,213491383	5,877852627	208,7240477	2,61E-47	7,00E-45	<b>Lipase 1</b>

*Figure 18:* Transcriptional changes of *citM* (highlighted in green), *hrpA1* (highlighted in azure) and the genes belonging to the *psaR3*-cluster (highlighted in grey), in response to *psaR3*-overexpression in HIM-K. Each gene is indicated with a code in according to the gene nomenclature reported in the Pseudomonas Genome Database. LogFC= logFoldChange, LogCMP=log counts per million, LR=FoldChange ratio, p-value= p-value, p-adj= adjusted p-value

The *citM* and the genes belonging to the *psaR3*-cluster were found up-regulated also in KB (**Fig. 19**) highlighting the already mentioned capacity of PsaR3 to regulate the expression of the genes belonging to *psaR3*-cluster and a probable involvement in the modulation of the transporters involved in the iron up-take by siderophores like the citrate transporter recently proposed to take part in the iron-uptake in *Ps* *pv. tomato* [29].

GeneName	LogFC	LogCPM	LR	p-value	P-adj	GeneDescription
IYO_RS00840	1,492807	7,250481	9,103719	0,002551	0,010905	<b>citrate transporter</b>
IYO_RS29530	7,084788	5,974174	255,912	1,34E-57	7,17E-55	<b>Anthranilate synthase component 2</b>
IYO_RS29535	7,145501	7,552453	248,3638	5,90E-56	2,20E-53	<b>2-amino-4-deoxychorismate synthase</b>
IYO_RS29540	3,49873	5,246909	123,5732	1,04E-28	3,92E-27	<b>Phenylacetate-coenzyme A ligase</b>
IYO_RS29545	3,621061	4,13099	93,09594	4,98E-22	1,25E-20	<b>acetyltransferase</b>
IYO_RS29550	5,588789	4,731561	179,3971	6,56E-41	5,38E-39	<b>transcriptional regulator</b>
IYO_RS29555	9,646411	4,897443	202,7928	5,13E-46	6,36E-44	<b>2-amino-4-deoxychorismate dehydrogenase</b>
IYO_RS29560	6,540531	4,76483	193,8522	4,59E-44	4,72E-42	<b>amino-acid metabolite efflux pump</b>
IYO_RS29565	7,242764	5,464181	239,2953	5,60E-54	1,35E-51	<b>Lipase 1</b>

*Figure 19:* Transcriptional changes of *citM* (highlighted in green) and the genes belonging to the *psaR3*-cluster (highlighted in grey). in response to *psaR3*-overexpression in KB. Each gene is indicated with a code in according to the gene nomenclature reported in the Pseudomonas Genome Database. LogFC= logFoldChange, LogCMP=log counts per million, LR=FoldChange ratio, p-value= p-value, p-adj= adjusted p-value

The DEGs analysis highlighted the presence of the genes situated in adjacent loci predicted as genomic islands (GIs) in the Psa reference strain ICMP18884 (V-13). Genes contained in two GIs were strongly up-modulated both in HIM-K and KB (**Fig. 20, 21**). Some interesting genes belonging to the Type I restriction modification system which is considered a primitive immune system in bacteria as a defence mechanism against the invading genomes [30], a gene probably involved in the toxin-antitoxin system (TA system) [31].

CHAPTER 4

GeneName	logFC HIMkiwi	logFC KB	Gene description	Predicted
IYO_RS00025	11,4615174	5,699777125	N-6 DNA methylase	Genomic Island from IYO_RS00015 to IYO_RS00210
IYO_RS00030	10,83752042	11,2573525	type I restriction endonuclease subunit S	
IYO_RS00035	5,148317609	12,27344331	Type-1 restriction enzyme R	
IYO_RS00040	3,386775889	9,070526609	YD repeat-containing	
IYO_RS00045	9,265408293	10,80818036	restriction endonuclease subunit M	
IYO_RS00050	8,418567813	9,6867904	hypothetical protein	
IYO_RS00055	7,960048545	9,14775893	transposase	
IYO_RS00060	7,623249453	8,018867486	transposase	
IYO_RS00065	7,944039003	8,395422057	hypothetical protein	
IYO_RS00070	5,528863337	5,786950523	MULTISPECIES: hypothetical protein	
IYO_RS00075	3,938591369	4,666688691	hypothetical protein	
IYO_RS00080	9,560999857	9,458096487	hypothetical protein	
IYO_RS00085	4,245335061	5,206733155	chromosome partitioning	
IYO_RS00090	3,837252401	5,160215998	Chromosome-partitioning Spo0J	
IYO_RS00095	5,025783512	6,171215141	recombinase family	
IYO_RS00100	3,074168707	3,279613317	hypothetical protein	
IYO_RS00105	5,836849929	6,882878154	DNA-binding	
IYO_RS00115	2,765756639	5,982707652	Uncharacterised	
IYO_RS00130	3,254387899	3,949600846	type I restriction enzymeP M	
IYO_RS00145	3,245308662	4,252525587	type I restriction enzymeP M	
IYO_RS00155	4,917404264	5,57790779	Type-1 restriction enzyme R	
IYO_RS00160	3,872034399	5,163665372	metal-dependent hydrolase	
IYO_RS00165	4,211282821	5,152823863	hypothetical protein A3SM_05794	
IYO_RS00170	8,908241782	8,024663049	MULTISPECIES: hypothetical protein	
IYO_RS00175	8,045158857	7,664854579	toxin-antitoxin system antitoxin TIGR02293 family	
IYO_RS00180	8,041555644	7,109773648	haloacid dehalogenase	
IYO_RS00185	4,935946934	5,87728851	hypothetical protein	
IYO_RS00205	2,146331122	2,738447505	ATP-dependent DNA helicase	

Figure 20: Transcriptional changes of genes belonging to a genomic island (predicted in Psa strain ICMP18884) in response to *psaR3*-overexpression in HIM-K and KB. Each gene is indicated with a code in according to the gene nomenclature reported in the Pseudomonas Genome Database.

GeneName	logFC HIMkiwi	logFC KB	Gene description	Predicted
IYO_RS00855	5,726904746	6,31076556	DNA methylase	Genomic Island from IYO_RS00855 to IYO_RS00885
IYO_RS00860	2,915876996	3,726971571	hypothetical protein	
IYO_RS00865	4,911439294	6,252313315	hypothetical protein	
IYO_RS00875	8,887099738	9,005175758	RES domain-containing protein	
IYO_RS00880	3,431808363	4,725336541	toxin-antitoxin system antitoxin TIGR02293 family	
IYO_RS00885	5,703382629	8,981129799	Acetylornithine deacetylase	

Figure 21: Transcriptional changes of genes belonging to a genomic island (predicted in Psa strain ICMP18884) in response to *psaR3*-overexpression in HIM-K and KB. Each gene is indicated with a code in according to the gene nomenclature reported in the Pseudomonas Genome Database.

Conversely we found genes located in GIs strongly down-regulated in both HIM-K and KB (**Fig. 22 and 23**). Among those, there are genes encoding 2OG-Fe(II) oxygenase superfamily, involved in post-translational hydroxylation mechanism proposed as a novel regulatory mechanism in bacteria [32], a gene encoding an antitoxin; two genes encoding IS21 and IS66 family transposases.

GeneName	logFC HIMkiwi	logFC KB	Gene description	Predicted
IYO_RS03545	-0,750550975	-2,461992329	2OG-Fe(II) oxygenase superfamily	Genomic Island from IYO_RS03535 to IYO_RS03780
IYO_RS03555	-0,884468529	-2,521239751	sulfotransferase	
IYO_RS03560	-0,935467456	-2,714624105	clavamate synthase	
IYO_RS03585	-3,979866282	-4,746480404	Antitoxin	
IYO_RS03595	-1,225417907	-0,980768775	MULTISPECIES: hypothetical protein	
IYO_RS03630	-2,605728293	-2,345204251	type III chaperone	
IYO_RS03635	-1,289163585	-0,921722969	type III effector 3	
IYO_RS03745	-5,269034899	-3,661307106	IS21 family transposase	

*Figure 22:* Transcriptional changes of genes belonging to a genomic island (predicted in Psa strain ICMP18884) in response to *psaR3*-overexpression in HIM-K and KB. Each gene is indicated with a code in according to the gene nomenclature reported in the Pseudomonas Genome Database.

GeneName	logFC HIMkiwi	logFC KB	Gene description	Predicted
IYO_RS05210	-1,584038011	-2,028119585	class I SAM-dependent DNA methyltransferase	Genomic island from IYO_RS05175 to IYO_RS05280
IYO_RS05245	-4,455889935	-3,594508221	IS66 family transposase	
IYO_RS05275	-2,004163996	-0,875670351	HAD superfamily hydrolase	
IYO_RS05280	-1,661291153	-1,551135256	UDP-glucose 6-dehydrogenase	

*Figure 23:* Transcriptional changes of genes belonging to a genomic island (predicted in Psa strain ICMP18884) in response to *psaR3*-overexpression in HIM-K and KB. Each gene is indicated with a code in according to the gene nomenclature reported in the Pseudomonas Genome Database.

Finally, the DEGs analysis highlighted also the presence of a putative operon up-regulated in both HIM-K and KB which contain genes involved in antibiotic synthesis and transport (**Fig. 24**).

GeneName	logFC HIMkiwi	logFC KB	Gene description	Predicted
IYO_RS03790	2,986389968	5,341856129	MFS transporter	putative operon for non-ribosomal antibiotic biosynthesis and transport
IYO_RS03795	1,047108415	1,884327437	antibiotic synthesis	
IYO_RS03800	8,169512075	7,737972412	Tyrocidine synthase 3	

*Figure 24:* Transcriptional changes of genes belonging to a putative operon (predicted in Psa strain ICMP18884) in response to *psaR3*-overexpression in HIM-K and KB. Each gene is indicated with a code in according to the gene nomenclature reported in the Pseudomonas Genome Database.

The results obtained confirm a role of PsaR3 as transcriptional regulator, involved in the regulation of genes as well as GIs and operons. Moreover, they highlight, the capacity of the receptor to regulate the expression of the genes belonging in the *psaR3*-cluster.

## 5. DISCUSSION

LuxR solos protein can regulate expression of virulence genes, biofilm formation, cell motility, and moreover, it was observed that some of them could recognize plant signals and probably trigger pathogen virulence [19, 33]; *Pseudomonas syringae* pv *actinidiae* genome contains three putative LuxR solos protein [34], among them, PsaR3 is especially interesting because it presents some peculiar characteristics, such as it is biovar 3-specific, it is located in a plasmid and it belongs to a conserved gene cluster, leading to the hypothesis of a possible role in controlling gene expression within the cluster, as well as in the higher virulence of the biovar 3 upon plant signal recognition. Moreover, the *psaR3*-cluster is conserved in other bacteria such as other *Pseudomonas* and *Xylella fastidiosa*, thus suggesting an evolutionary importance [35].

### - Possible role of the PsaR3 and kiwifruit extract

The dual luciferase assay showed that PsaR3 probably plays a role as transcriptional repressor on *citM*-promoter in J35 strain. Conversely, the same analysis on the CRA-FRU 10.22 did not show any difference in *citM*-promoter activity and the luciferase signal was well below that observed using J35 strain. EsaR, a LuxR-type protein of *Pantoea stewartii* functions as transcriptional receptor in absence of the ligand [36] suggesting a similar behaviour for PsaR3 in J35 strain. A regulation of the *citM*-promoter by PsaR3 was expected based on the *cis*-acting elements analysis which revealed several sites recognized by LuxR-like proteins as mentioned in the result section such as: OxyR [24], SdiA, [25], RhlR [26]; MtrB [27]. Indeed, the RNA-seq showed that *citM* is up-regulated, in CRA-FRU 10.22, as already observed with the Real-time qPCR analysis discussed in the previous chapter, following the *psaR3*-overexpression either in KB or in HIM-K, suggesting that PsaR3 could have a role in the regulation of this gene. However, the regulation mechanism is still unclear. Probably, the endogenous PsaR3 present in CRA-FRU 10.22 could interfere with the luciferase assay, or the induction of *psaR3*-overexpression could have had a quenching effect on the luminescence. Beside the absence of PsaR3 in the J35 strain, other strain-specific differences might interfere with the system: the different strain and biovars of Psa have shown diverse molecular and biochemical phenotypes in many respects across our experiments, thus the overall regulatory network controlling iron uptake could obviously be complex to dissect.



The intergenic region in sense orientation showed that the activity of this putative promoter is enhanced by the presence of the kiwifruit leaf extract and reduced following PsaR3 induction, suggesting also in this case that PsaR3 could decrease the promoter activity as already observed for *citM* in J35 strain. Conversely, the intergenic region in antisense orientation was activated following PsaR3 induction and the kiwifruit leaf extract further increased its activity (in minimal medium). These experiments suggest that, PsaR3 could participate in Psa recognition of a kiwifruit signal(s), mediating an inter-kingdom signalling communication and thus regulate the expression of diverse genes. Some LuxR solos of PAB were already suggested as possible sensors for the presence of the host-plant. PsoR of *P. fluorescence* is produced in *E. coli* only in presence of rice or wheat leaves macerate but not with the cucumber in the medium indicating that PsoR could bind a plant molecule(s) specific either of rice or wheat that has not been elucidated yet [37]. XagR, a LuxR homologues of *Xanthomonas axonopodis* pv. *glycines* can be stabilized if the media contains the soyabean leaf macerate, and this receptor is also produced in the soyabean leaves inoculated with the pathogen and contributing to its virulence [23]. OryR was expressed in *E. coli* grown in media containing infected xylem sap recovered from rice about 10 days after infection [22]. However, based on the luciferase assay in KB, the promoter activity of the intergenic region in antisense orientation was strongly increased following the PsaR3 induction but unaffected by the presence of the kiwifruit leaf extract, thus suggesting that this receptor could also mediate the response to an endogenous non-AHLs ligand that might be produced in rich medium. In *Photorhabdus luminescens* and *Photorhabdus asymbiotica*, insect-larvae pathogenic bacteria, the two LuxR solos like receptors, *i.e.*: PauR and PluR, sense endogenous photopyrones (PPYs), dialkylresorcinols (DARs) and cyclohexanediones (CHDs) thus mediating the cell-cell communication [18]. It is also well known that poor nutrient media, such as HIM, can activate some aspects of bacterial pathogenicity. Thus the pathways activated by starvation in the apoplast, perception of the host, and QS signals can be highly interconnected and need further elucidation.

Finally, the luciferase assay data indicate that the compound sensed by Psa probably through the PsaR3 receptors seems to be present in the hydrophilic fraction, indicating a possible polar site in the molecule(s), although the nature of the molecule is still unknown. In the literature there are some indications about possible LuxR solos ligands, for example, recently it has been established that SdiA of *E. coli* is able to sense a phospholipid molecule

called 1-octanoyl-rac-glycerol (OCL) a precursor for membrane biogenesis found in prokaryotes and eukaryotes [38]. Moreover, salicylic acid, a phytohormone implicated in the plant immunity signal network, could also be recognized as Diffusible Signal Factors (DFS) and activate the QS mediated by LuxR in plant pathogen bacteria. *Xanthomonas oryzae* pv. *oryzae* (*Xoo*) uses the plant-immune hormone, salicylic acid (SA) to activate its virulence through to a DFS QS machinery at least partially dependent on OryR [39]. It is therefore possible that Psa may sense plant molecules and activate gene expression in a PsaR3-dependent manner. In this respect the MS analysis on-going on of the “positive-fractions” could help us to elucidate the nature of these molecules.

#### **- RNA-seq: PsaR3 transcriptional regulator**

The RNAseq data showed that the expression of several genes is influenced following *psaR3*-overexpression. Indeed, an interesting enriched class of genes up-regulated in KB and HIM-K following the *psaR3*-overexpression was the “alginic-acid metabolic process” suggesting that PsaR3 could be involved in the regulation of the alginate production and thus biofilm formation. The formation of a slime composed prevalently by alginic acid in *Pseudomonas aeruginosa* was found important for protection against antimicrobials and host defence mechanism [40]. In *E. coli*, the *luxS*/autoinducer-II, a LuxR *sdia* homologues, was found involved in the alginic-matrix formation [41]. Another example of protein belonging to the LuxR family involved in the extracellular matrix formation is the CsgD protein, which regulates the formation of curli fibers and biofilm as well as the cellulose production in *E. coli* and *Salmonella* [42]. Interestingly, the involvement of the PsaR3 in the formation of cell-aggregates was also observed in the previous chapter, thus highlighting a possible connection between PsaR3 and extracellular matrix formation. In *E. chrysanthemi* pv. *zeae* it was reported that an AHLs signal could induce the formation of cell-aggregates of different sizes based on the growing media [43].

PsaR3 could regulate directly or indirectly some GIs, as suggested by the experimental data. One GI, found up-regulated by *psaR3*-overexpression in both condition tested, contained some genes involved in the Type I restriction system and in the toxin-antitoxin system. The Restriction-Modification System (R-M system) is usually known as the primary immune bacterial system against invading genomes. R-M systems are classified mainly into four different types, based on their subunit composition, sequence recognition,

cleavage position, cofactor requirements and substrate specificity. The Type I enzyme consists of a hetero-oligomeric protein complex that acts as either restriction or modification enzyme. This R-M system was observed for the first time in *E. coli* involved in the cleavage of the unmethylated phage  $\lambda$  DNA [44] and subsequently also in *Helicobacter pylori*, *Streptococcus pneumoniae*, and *Staphylococcus aureus*. Our findings, suggest that in Psa, PsaR3 could play a role in the regulation of the immune bacterial system and thus protect Psa against phage infection.

The toxin-antitoxin (TA) system are small genetic elements composed by a toxin and its cognate antitoxin-encoding genes. The first TA system, *ccdA/ccdB*, was discovered several years ago [31]. Bacterial species that contains dozens of TA systems either in the plasmid or in the chromosome are *Mycobacterium tuberculosis* and *Nitrosomonas europaea* [45]. The TA system is composed by the toxin, always a protein and the antitoxin that can be either a protein or a small RNA (RNAs) [46-50]. The expression of the already mentioned CsgD a LuxR-type transcriptional regulator involved in biofilm formation and cellulase production is controlled by MqsR/MqsA toxin/antitoxin (TA) system. MqsR/MqsA reduces the expression of several stress response genes such as: *csgD*, *rpoS*, *mqsRA*, controls the shift from planktonic phase to biofilm formation through CsgD [51]. This mechanism suggests a possible feed-back loop of reciprocal regulation between the TA system and PsaR3, as *psaR3*-overexpression induces genes encoding the TA system in Psa in both condition tested while TA system could regulate *psaR3* expression, as observed for CsgD, and thus control biofilm or planktonic phase through PsaR3.

PsaR3 over-expression was followed also by the up-regulation of a putative operon involved in the non-ribosomal antibiotics synthesis and transport. *Bacillus subtilis* can produce several antibiotics which vary in the synthesis mechanism, such as: polyketides, aminosugars, phospholipids. Some researches suggest different roles for *B. subtilis* antibiotics other than the classical anti-microbial functions, for instance, non-ribosomally produced lipopeptides are involved in biofilm formation and swarming, while; lantibiotics function as pheromones in QS [52]. Interestingly to mention, CarR, a LuxR-type protein of *Erwinia carotovora*, regulate the production of carbapenem antibiotic in a AHLs dependent way [53], suggesting that PsaR3 could lead to the production of antibiotics in Psa through the regulation of this putative operon.

The genes belonging to the *psaR3*-gene cluster were found positively modulated by PsaR3, thus confirming also the Real-time qPCR data discussed in the previous chapter. These

data all together strongly highlighted that PsaR3 could be involved in the regulation of the genes in the cluster and might lead to the synthesis of endogenous signal molecules which could bind PsaR3, following a QS mechanism similarly to what already found in *Pseudomonas aeruginosa* [54]. Indeed, in *P. aeruginosa* and *Xylella fastidiosa* genes involved in the anthranilate synthase and phenyl-COA ligase (enzymes involved in the quinolone biosynthesis in Pa), were found associated in a cluster similar to the *psaR3*-cluster; and in the case of Psa the anthranilate could play a role as a substrate for phenyl-COA ligase [55] and the molecule could be secreted by the transporter presented in the *psaR3*-cluster and thus regulate a possible QS PsaR3-dependent.

Another aspect highlighted by the RNAseq data but also by the luciferase assay, is that some genes and pathways are influenced also by the presence of the kiwifruit leaf extract added into the medium. Interestingly, the TTSS-mediated secretion activity was up-regulated only in HIM-K following PsaR3 expression, suggesting that all these elements could be connected together. In *Pseudomonas syringae* the GacA/S Two Component Signal Transduction (TCST) system is found directly or indirectly involved in the virulence mechanism including toxin production, extra-polysaccharide matrix formation, TTSS and its effectors [56]. Moreover, the Gac system is activated in the host apoplast by a combination of signal such as: low pH, low osmolarity, lack of nitrogen source and complex carbon [57]. It was also reported that GacA/S controls the AhlIR/R (LuxI/R homologous) QS system essential for the regulation of the intercellular host tissue maceration, and epiphytic fitness, because it controls the extra-polysaccharide matrix formation and the swarming motility in different environments in *Pseudomonas syringae* pv. *tomato* [58, 59], thus showing a connection between the regulation of pathogen virulence, apoplast environment and QS. An apoplastic-mimicking environment as already described for the HIM medium, suggests that the Gac system of Psa could be activated, and thus controls the PsaR3-mediated QS and then playing a role in the modulation of the Psa virulence probably triggered also through the recognition of a kiwifruit signal(s).

Finally, the availability of a purified PsaR3 recombinant protein now allows to plan experiments: *i*) to identify its putative endogenous and/or exogenous (derived from a kiwifruit) ligand(s), thus investing the involvement of this receptor in the inter-kingdom signalling and possibly triggering the virulence in Psa and *ii*) identify the direct PsaR3 targeted sequence through DNA-binding assays [38, 60].

---

## 6. SUPPLEMENTAL RESOURCES

### List of primers used in this chapter:

Gene	Primer Name	Sequence	TM
citM promoter	CitrfwEcoRI	ATAGAATTCTGGAGGCAGAGTTCTTGCTG	68
citM promoter	CitrrvXhoI	GCGCTCGAGGGGAATACTCCAGACGTAATACG	68
<i>psaR3</i>	PsaR3fwXmaI	GCGCCCGGATGGATACGTACAACCTCACG	58
<i>psaR3</i>	PsaR3rvXbaI	GCTTCTAGATTATATCCGGCCCGTTTGAT	58
intergenic region <i>psaR3</i> -cluster sense	interregionsensfwEcoRI	ATAGAATTCAAATACGTCCACGCACA	56
intergenic region <i>psaR3</i> -cluster sense	interregionsensrvXhoI	GCGCTCGAGCGGGTCATAGTGCTTCTTA	56
intergenic region <i>psaR3</i> -cluster antisense	interregionantfwEcoRI	ATAGAATTCGGGTCATAGTGCTTCTTA	56
intergenic region <i>psaR3</i> -cluster antisense	interregionantrvXhoI	GCGCTCGAGAAATACGTCCACGCACA	56
<i>psaR3</i>	PsaR3HISPBAD24fwXmaI	GCGCCCGGAGGAGATATACCATGGGC	58
<i>psaR3His6tag</i>	PsaR3rvXbaIHISTAGCterm	GCTTCTAGATTAATGGTGGTGGTATGATGATCCGGCCCGTTTGAT	56

## 7. REFERENCES

- 1 Fuqua, C. Parsek, M. R. and Greenberg, E. P. (2001), Regulation of gene expression by cell-to-cell communication: acyl-homoserinylactone quorum sensing. *Annu. Rev. Genet.*, doi:10.1146/annurev.genet.35.102401.090913
- 2 Cha, C. *et. al.* (1998), Production of acyl-homoserinylactone quorum sensing signals by gram-negative plant-associated bacteria. *Mol. Plant Microbe Interact.* doi:10.1094/MPMI.1998.11.11.1119
- 3 Gonzalez, *et. al.* (2013), The interkingdom solo OryR regulator of *Xanthomonas oryzae* is important for motility. *Mol. Plant Pathol.*, 211–221. doi:10.1111/j.1364-3703.2012.00843.x
- 4 Gonzalez, J. E., and Marketon, M. M. (2003), Quorum sensing in nitrogen-fixing rhizobia. *Microbiol. Mol. Biol. Rev.* doi:10.1128/MMBR.67.4.574-592.2003
- 5 Ferluga, S. *et. al.* (2007), A LuxR homologue of *Xanthomonas oryzae pv. oryzae* is required for optimal rice virulence. *Mol. Plant Pathol.* doi:10.1111/j.1364-3703.2007.00415.x
- 6 Mae, A., *et. al.* (2001), Transgenic plants producing the bacterial pheromone N-acyl-homoserinylactone exhibit enhanced resistance to the bacterial phytopathogen *Erwinia carotovora*. *Mol. Plant Microbe Interact.* doi:10.1094/MPMI.2001.14.9.1035

- 
- 7 Toth, I. K., *et. al.* (2004), Potato plants genetically modified to produce N-acylhomoserinelactones increase susceptibility to soft rot *Erwinia*. *Mol. Plant Microbe Interact.*, doi:10.1094/MPMI.2004.17.8.880
- 8 Schenk, S. T., *et. al.* (2012), Arabidopsis growth and defense are modulated by bacterial quorum sensing molecules. *Plant Signal. Behav.*, doi:10.4161/psb.18789
- 9 Schikora, A., *et. al.* (2011), N-acyl-homoserinelactone confers resistance toward biotrophic and Hemibiotrophic pathogens via altered activation of AtMPK6. *Plant Physiol.*, doi:10.1104/pp.111.180604
- 10 Degrassi, G., *et. al.* (2007). *Oryza sativa* rice plants contain molecules which activate different quorum sensing N-acylhomoserinelactone biosensors and are sensitive to the specific AiiA lactonase. *FEMS Microbiol. Lett.*, doi:10.1111/j.1574-6968.2006.00624.x
- 11 Keshavan, N. D., *et. al.* (2005). L-Canavanine made by *Medicago sativa* interferes with quorum sensing in *Sinorhizobium meliloti*. *J. Bacteriol.*, doi:10.1128/JB.187.24.8427-8436.2005
- 12 Teplitski, M., *et. al.* (2004), *Chlamydomonas reinhardtii* secretes compounds that mimic bacterial signals and interfere with quorum sensing regulation in bacteria. *Plant Physiol.* doi: 10.1104/pp.103.029918
- 13 Choi, S. H., and Greenberg, E. P., (1991), The C-terminal region of the *Vibrio fischeri* LuxR protein contains an inducer-independent lux gene activating domain. *PNAS*, doi:10.1073/pnas.88.24.11115
- 14 Stevens, A. M., and Greenberg, E. P., (1997), Quorum sensing in *Vibrio fischeri*: essential elements for activation of the luminescence genes. *J. Bacteriol.* 179, 557–562.
- 15 Chugani, S. A., *et. al.* (2001), QscR, a modulator of quorum-sensing signal synthesis and virulence in *Pseudomonas aeruginosa*. *PNAS*, doi:10.1073/pnas.051624298
- 16 Ahmer, B. M. (2004), Cell-to-cell signalling in *Escherichia coli* and *Salmonella enterica*. *Mol. Microbiol.* doi:10.1111/j.1365-2958.2004.04054.x
- 17 Yao, Y., *et. al.* (2006). Structure of the *Escherichia coli* quorum sensing protein SdiA: activation of the folding switch by acyl-homoserinelactones. *J. Mol. Biol.*, doi:10.1016/j.jmb.2005.10.041
- 18 Brameyer S. *et al.* (2014) Dialkylresorcinols as bacterial signaling molecules. *PNAS*, doi: 10.1073/pnas.1417685112
-

- 19** Gonzalez, J. F. and Venturi, V., (2013), A novel wide spread interkingdom signalling circuit. *Trends Plant. Sci.*, doi:10.1016/j.tplants.2012.09.007
- 20** Venturi, V. and Fuqua, C., (2013), Chemical signalling between plants and plant pathogenic bacteria. *Annu. Rev. Phytopathol.*, doi:10.1146/annurev-phyto-082712-102239
- 21** Zhang, L., *et al.*, (2007), A proline iminopeptidase gene upregulate in planta by a LuxR homologue is essential for pathogenicity of *Xanthomonas campestris* pv. *campestris*. *Mol. Microbiol.* doi:10.1111/j.1365-2958.2007.05775.x
- 22** Ferluga, S., and Venturi, V., (2009), OryR is a LuxR-family protein involved in interkingdom signaling between pathogenic *Xanthomonas oryzae* pv. *oryzae* and rice. *J. Bacteriol.* 191, 890–897. doi:10.1128/JB.01507-08
- 23** Chatnaparat, T. *et al.*, (2012), XagR, a LuxR homolog, contributes to the virulence of *Xanthomonas axonopodis* pv. *glycines* to Soybean. *Mol. Plant Microbe Interact.* doi:10.1094/MPMI-01-12-0008-R
- 24** Maddoks, S. E. and Oyston, P. C. F. (2008), Structure and function of the LysR-type transcriptional regulator (LTTR) family proteins. *Microbiology*, doi: 10.1099/mic.0.2008/022772-0
- 25** Ahmer, B. M. *et al.*, (1998), *Salmonella typhimurium* encodes an SdiA homolog, a putative quorum sensor of the LuxR Family, that regulates genes on the virulence Plasmid. *J. Bacteriol.*, vol. 180 no. 5 1185-1193
- 26** Pessi, G. Haas, D. (2000) Transcriptional Control of the Hydrogen Cyanide Biosynthetic Genes hcnABC by the Anaerobic Regulator ANR and the Quorum-Sensing Regulators LasR and RhIR in *Pseudomonas aeruginosa*. *Journal of Bacteriology*, doi: 10.1128/JB.182.24.6940-6949.2000
- 27** Zhart, T. C. and Deretic, V. (2000), An essential two-component signal transduction system in *Mycobacterium tuberculosis*. *J. Bacteriol.*, doi: 10.1128/JB.182.13.3832-3838.200024
- 28** Zhang, R. G. *et al.* (2002) Structure of a bacterial quorum-sensing transcription factor complexed with pheromone and DNA. *Nature*, doi: 10.1038/nature00833
- 29** Jones, A. M, and Wildermuth M. C. (2011), The phytopathogen *Pseudomonas syringae* pv. *tomato* DC3000 has three high-affinity iron-scavenging systems functional under iron limitation conditions but dispensable for pathogenesis. *J. Bacteriol*, doi: 10.1128/JB.00069-10
- 30** Vasu, K and Nagaraja V., (2013), Diverse Functions of Restriction-Modification Systems in addition to cellular defense. *MMBR*, doi:10.1128/MMBR.00044-12.

- 
- 31 Unterholzner S. J. *et al.* (2013), Toxin anti-toxin systems biology identification and application. *MGE*, doi:10.4161/mge.26219
- 32 Staalduinen L. and Jia Z. (2015), Post-translational hydroxylation by 2OG/Fe(II)-dependent oxygenases as a novel regulatory mechanism in bacteria, *Frontiers in Microbiology*, doi: 10.3389/fmicb.2014.00798
- 33 Patel, H. K. *et al.* (2014), The Kiwifruit Emerging Pathogen *Pseudomonas syringae* pv. *actinidiae* Does Not Produce AHLs but Possesses Three LuxR Solos. *Plos One*, doi: 10.1371/journal.pone.0087862
- 34 McInthosh, M. *et al.* (2008) Competitive and cooperative effects in Quorum-Regulated galactoglucan biosynthesis in *Sinorhizobium meliloti*. *J. Bacteriol.*, doi: 10.1128/JB.00063-08
- 35 Palmer, G. C., Jorth, P. A., & Whiteley, M. (2013). The role of two *Pseudomonas aeruginosa* anthranilate synthases in tryptophan and quorum signal production. *Microbiology*, <https://doi.org/10.1099/mic.0.063065-0>
- 36 von Bodman, S. B. Majerczak, D. R. and Coplin, D. L. (1998) A negative regulator mediates quorum-sensing control of exopolysaccharide production in *Pantoea stewartii* subsp. *stewartii*. *PNAS*, 95(13): 7687–7692.
- 37 Subramoni, S. *et al.* (2011) Bacterial subfamily of LuxR regulators that responds to plant compounds. *Applied and environmental microbiology*, doi: 10.1128/AEM.00183-11
- 38 Nguyen Y, *et al.* (2015) Structural and mechanistic roles of novel chemical ligands on the SdiA Quorum-Sensing transcriptional regulator. *MBio*, doi: 10.1128/mBio.02429-14
- 39 Xu, J. *et al.* (2015), Phytohormone-mediated interkingdom signaling shapes the outcome of rice-*Xanthomonas oryzae* pv. *oryzae* interaction, *BMC Plant Biology*, doi: 10.1186/s12870-014-0411-3
- 40 Bjarnsholf, T. *et al.*, (2009), *Pseudomonas aeruginosa* biofilms in the respiratory tract of cystic fibrosis patients. *Paediatric Pulmonology*, doi: 10.1002/ppul.21011
- 41 Laverty, G. *et al.*, (2014), Biomolecular mechanisms of *Pseudomonas aeruginosa* and *Escherichia coli* biofilm formation. *Pathogens*, doi: 10.3390/pathogens3030596
- 42 Brombacher E. *et al.* (2006), Gene Expression Regulation by the Curli Activator CsgD Protein: Modulation of Cellulose Biosynthesis and Control of Negative Determinants for Microbial Adhesion. *J. Bacteriology*, doi: 10.1128/JB.188.6.2027-2037.2006
- 43 Hussain, M. B. B. M., *et al.*, (2008), The acyl-homoserine lactone-type quorum-sensing system modulates cell motility and virulence of *Erwinia chrysanthemi* pv. *zoeae*.
-



*Journal of Bacteriology*, doi:10.1128/JB.01472-07

- 44** Tock, M. R., and Dryden, D. T. F., (2005), The biology of restriction and antirestriction. *Curr. Opin. Microbiol.* doi: 10.1016/j.mib.2005.06.003
- 45** Ogura T., and Hiraga S., (1983) Mini-F plasmid genes that couple host cell division to plasmid proliferation. *PNAS*, doi: org/10.1073/pnas.80.15.4784
- 46** Kawano, M. *et. al.*, (2007) An antisense RNA controls synthesis of an SOS-induced toxin evolved from an antitoxin. *Mol Microbiol*, doi.org/10.1111/j.1365-2958.2007.05688.x
- 47** Durand, S. *et. al.*, (2012) The essential function of *B. subtilis* RNase III is to silence foreign toxin genes. *PLoS Genet* doi: 10.1371/journal.pgen.1003181
- 48** Miki, T. *et. al.*, (1992) T. Control of segregation of chromosomal DNA by sex factor F in *Escherichia coli*. Mutants of DNA gyrase subunit A suppress letD (*ccdB*) product growth inhibition. *J Mol Biol* doi:10.1016/0022-2836(92)91024-J
- 49** Schumacher, M. A. *et. al.* (2009) Molecular mechanisms of HipA-mediated multidrug tolerance and its neutralization by HipB. *Science*, doi.org/10.1126/science.1163806
- 50** Winther, K. S. Gerdes, K. (2011) Enteric virulence associated protein VapC inhibits translation by cleavage of initiator tRNA. *PNAS* doi: 10.1073/pnas.1019587108
- 51** Soo, V. and Wood, T. K. (2013) Antitoxin MqsAr represses curli formation through the master biofilm regulator CsgD. *Scientific Reports*, doi: 10.1038/srep03186
- 53** Stein, T (2005) *Bacillus subtilis* antibiotics: structures, syntheses and specific functions. *Molecular Microbiology*, doi: 10.1111/j.1365-2958.2005.04587.x
- 53** McGowas, S. *et. al.*, (1995), Carbapenem antibiotic production in *Erwinia carotovora* is regulated by CarR, a homologue of the LuxR transcriptional activator. *Microbiology*, doi: 10.1099/13500872-141-3-541
- 54** Palmer, G. C., *et. al.*, (2013), The role of two *Pseudomonas aeruginosa* anthranilate synthases in tryptophan and quorum signal production. *Microbiology*. doi: org/10.1099/mic.0.063065-0
- 55** McCann, H. C., *et. al.*, (2013), Genomic Analysis of the Kiwifruit Pathogen *Pseudomonas syringae* pv. *actinidiae* Provides Insight into the Origins of an Emergent Plant Disease. *PLoS Pathogens*, doi: 10.1371/journal.ppat.1003503
- 56** Chatterjee, A. *et al.* (2003) GacA, the response regulator of a twocomponent system, acts as a master regulator in *Pseudomonas syringae* pv. *tomato* DC3000 by controlling regulatory

RNA, transcriptional activators, and alternate sigma factors. *Mol. Plant Microbe Interact*, doi: 10.1094/MPMI.2003.16.12.1106

**57** Rahme, L.G. *et al.* (1992) Plant and environmental sensory signals control the expression of hrp genes in *Pseudomonas syringae* pv. *phaseolicola*. *J. Bacteriol*, doi: 10.1128/jb.174.11.3499-3507.1992

**58** Monier, J. M. and Lindow, S. E. (2003) Differential survival of solitary and aggregated bacterial cells promotes aggregate formation on leaf surfaces. *PNAS*, doi: 10.1073/pnas.2436560100

**59** Quinones, B. *et al.* (2005) Quorum sensing regulates exopolysaccharide production, motility, and virulence in *Pseudomonas syringae*. *Mol. Plant Microbe Interact*, 10.1094/MPMI-18-0682

**60** Mittler, G. Butter, F. and Mann, M. (2009) A SILAC-based DNA protein interaction screen that identifies candidate binding proteins to functional DNA elements. *Genome Research*, doi: 10.1101/gr.081711.108

## **8. ACKNOWLEDGEMENT**

PD Dr Ralf Heermann to participate actively into this project and to give me the possibility to work in his lab, Dr Nicola Vitulo to curate the statistical data analysis of the RNAseq data, Jannis Brehm to curate the HPLC kiwifruit extract fractionation.

## Conclusions and future perspectives

In this thesis, several approaches were undertaken to elucidate the molecular basis of Psa pathogenicity. Thanks to an in-house designed microarray chip, I studied the transcriptomic profiles of *Pseudomonas syringae* pv. *actinidiae* biovars (1, 2 and 3) revealing a panel of different mechanisms activated by different Psa strains in conditions that mimic the plant apoplast environment (minimal medium). This work provided some interesting hypotheses and sets of candidate genes that could be functionally explored to understand the differences in virulence among biovars of this economically important bacterial species. Moreover, the bulk of expression data produced represents a valuable resource for future in-depth studies aimed at identification of crucial bacterial targets, to develop new control strategies against this - and possibly other - bacterial diseases. Further studies could be conducted to investigate the transcriptomic differences occurring in the shift from the epiphytic to the endophytic bacterial phases, to elucidate the mechanism operating in Psa to overcome plant defence responses.

The study on the role of PsaR3 and its involvement in Psa virulence revealed some interesting features of this receptor such as: *i*) Psa biovar 3 specificity, *ii*) location on a plasmid, specific to the strain belonging to biovar 3 strains and *iii*) the existence of a gene cluster consistently associated to PsaR3. The transcriptomic analyses of PsaR3 mutant and overexpressing strains suggested that PsaR3 could participate in the transcriptional regulation of genes involved in biofilm formation, iron uptake, TTSS-mediated protein secretion and thus could probably be involved in the high virulence of the biovar 3. Moreover, PsaR3 can regulate the transcription of the genes situated in its cluster (*psaR3*-cluster), suggesting that this cluster could serve to the synthesis of a signal molecule possibly sensed by PsaR3, as observed in other bacterial models. This work highlighted the complex interconnections among different bacterial responses to environmental stimuli and host perception, and opens the way to further investigations to identify the molecular signal(s) controlling virulence-related behaviours.

The study on the putative promoter activity of the intergenic region located in the *psaR3* cluster suggested that this region could indeed promote transcription of genes in the *psaR3*-cluster, and is likely regulated by PsaR3. Moreover, the experimental analysis of the promoter activity of the intergenic region revealed that a signal contained in the kiwifruit leaf

extract could be sensed by Psa, possibly involving the PsaR3 receptor, thus triggering Psa response to plant perception.

In the end, the availability of a purified PsaR3 recombinant protein now allows to plan experiments: *i*) to identify its putative endogenous and/or exogenous ligand(s), especially those derived from the kiwifruit plant, thus investigating the involvement of this receptor in the inter-kingdom signalling and possibly in Psa virulence, and *ii*) identify the sequences directly targeted by PsaR3 through DNA-binding assays.

The clarification of the communication mechanisms between plants and pathogens would be very useful to develop new strategies for interfering with the first steps of bacterial infection, thus developing alternative control measures for plant disease control.